

THÈSE DE DOCTORAT

SELF-STRATIFYING FLAME RETARDANT COATINGS FOR PLASTICS

Présentée et soutenue publiquement à

L'UNIVERSITÉ DES SCIENCES ET TECHNOLOGIES DE LILLE

École doctorale Sciences de la Matière, du Rayonnement et de l'Environnement

Pour obtenir le grade de

DOCTEUR

Spécialité : Chimie des Matériaux

Par

Agnès Beaugendre

Ingénieur diplômé de l'École Nationale Supérieure de Chimie de Mulhouse
Master Formulation des systèmes Colloïdaux et Polymères de l'Université de Haute-Alsace

Thèse dirigée par

Prof. Maude Jimenez et Dr. Mathilde Casetta

Soutenue le 29 Novembre 2017 devant la Commission d'Examen composée de :

Prof. Sophie Duquesne	ENSC Lille	Présidente du jury
Prof. Christelle Delaite	Université de Haute-Alsace	Rapporteur
Prof. Baljinder Kandola	Université de Bolton	Rapporteur
Dr. Samuel Devisme	Arkema	Examineur
Dr. Vincent Rerat	Dow Corning	Invité
Prof. Maude Jimenez	Université Lille 1	Directrice de thèse
Dr. Mathilde Casetta	Université Lille 1	Co-Encadrante de thèse

PhD THESIS

SELF-STRATIFYING FLAME RETARDANT COATINGS FOR PLASTICS

PhD defended at

UNIVERSITÉ DES SCIENCES ET TECHNOLOGIES DE LILLE

École doctorale Sciences de la Matière, du Rayonnement et de l'Environnement

To obtain the grade of

DOCTEUR

Specialty: Materials Sciences

By

Agnès Beaugendre

Graduated Engineer of École Nationale Supérieure de Chimie de Mulhouse
Master Degree Formulation of Colloidal Systems and Polymers, Université de Haute-Alsace

PhD thesis supervised by

Prof. Maude Jimenez and Dr. Mathilde Casetta

Defended on November, 29th 2017 in front of the following dissertation committee:

Prof. Sophie Duquesne	ENSC Lille	Committee chair
Prof. Christelle Delaite	University of Haute-Alsace	Rapporteur
Prof. Baljinder Kandola	University of Bolton	Rapporteur
Dr. Samuel Devisme	Arkema	Examiner
Dr. Vincent Rerat	Dow Corning	Guest
Prof. Maude Jimenez	University of Lille 1	Thesis Director
Dr. Mathilde Casetta	University of Lille 1	Thesis Co-Supervisor

Acknowledgments

The work presented in this manuscript has been carried out within the UMET laboratory (CNRS UMR-8207), headed by Pr. Alexandre Legris, in the ISP-R₂F team (“Ingénierie des Systèmes Polymères – Reaction and Resistance to Fire”) led by Pr. Serge Bourbigot. I would like to thank them for giving me the opportunity to join their laboratory, work on this innovative project and achieve this PhD.

First and foremost, I would like to thank my supervisors, Maude Jimenez and Mathilde Casetta, and the members of the project, Sophie Duquesne, Séverine Bellayer, Stéphanie Degoutin and Christel Pierlot for offering me the chance to work on this project and including me into their team. I appreciate the time they spent to train me, the advice, suggestion, expertise and scientific knowledge they shared. I am grateful for the confidence they placed in me, which was deeply rewarding. I also thank the ANR (Agence Nationale de la Recherche) for funding the STIC project (ANR- 14-CE27-0010) and the competitiveness cluster MATIKEM to support this work.

I am very grateful to Prof. Sophie Duquesne who agreed to chair the jury, and also to Prof. Christelle Delaite, Prof. Baljinder Kandola, Dr. Samuel Devisme and Dr. Vincent Rerat who accepted to take on their time, to bring their expertise as reviewers of this manuscript and to be part of the jury.

I also would like to acknowledge Ahmed Addad and Séverine for always providing me help, advices and well-chosen remarks regarding electronic microscopy, and also Johan, Pierre, Gregory Stoclet, Myriam Moreau and Raphael Lebeuf for their expertise on different apparatus and techniques I used.

I express my heartfelt thanks to the R₂FIRE team: Maude, Mathilde, Sophie, Gaëlle, Fabienne, Séverine, Serge, Fanny, Pierre, Johan and Michel for their kindness and help when needed, for the good time we spent, talk we had and for their zest for life. I am truly indebted to Brigitte, who is far more than the kindest secretary I have ever met. My time spent in the office 10 wouldn't have been the same without her. Further, I would like to thank everyone in the lab

for the wonderful easy-going atmosphere we shared: Ben, Morgane, Hirako, Laurie, Roland, Tata, Sophie, Gizem, Charlotte, Elodie, Chi, Sarah, Alexis, Maryem, Pauline, and those who already left, Dr. Ben, Bebert and Renaud, you were my mentors when I arrived, and also Andrea, Anil, Matthieu, Regis, Mathieu C., Sayed, Marion. Some members of the laboratory have not been named yet because they have become more than colleagues; they are now real friends with whom sharing time after work is precious. Audrey, you managed to complete a real challenge and earned by far the golden cup for your support, your presence, for giving me the motivation every day and for being more than a friend and a roommate. Nittaya, you are one of the strongest person I have ever met, thank you for sharing your kindness, experience and lifestyle. Sawsen, sharing our adventures, run sessions, breaks and part of life was a gift. Nico, you have been more than supportive and helpful and even more since it began before we met. Thank you for your good (and bad) mood, your honesty, your musical culture and creativity. Adi, the Edimbra' guy, your support was unbeatable. Charlotte, the baby is all yours!

Thank you to the interns who also worked in the project and help me a lot during their training period: Sarah, you were perfect and Ganga.

It was a pleasure to work with people always available to provide support while I completed my work, laugh and share a part of their experience. It has been a considerable help. I wish all the best in your future endeavors, and your encouragement are much appreciated.

Last but not least, I would like to thank all the people who have been listening to me talking about my PhD (sometimes a lot) without knowing exactly what I was really talking about. Thanks to all in my family and especially my siblings who have been more than supportive for me: *Marie & Lou'*, *Sis' (petite tête)* and *Syl'*. Thanks to my friends: Mimie, Margot, Bibou, Arli, LiLy, LyLi, Ninette, Rominou, Billy, Belynda, Mon Roi, Ma Loute, AL, Mike, Olivier, Stéph, Marmotte, Nico. Thank you to Émilien for his contagious vibe of energy and goodness, for his love and patience.

For the great moments we have already had together and hopefully the ones to come, I will always be grateful.

Georgie

Table of content

Acknowledgments	7
Table of content	9
Abbreviations	14
General introduction	17
Chapter I: Theoretical aspects of the project	25
I-1 Introduction.....	26
I-2 Approaches to flame retard plastics	26
I-2-1 Bulk treatment.....	26
I-2-2 Reactive approach	27
I-2-3 Surface treatments	28
I-3 Examples, issues and current solutions associated to flame retardant surface treatments	29
I-3-1 Intumescent coatings	29
I-3-2 Layer-by-layer process.....	30
I-3-3 Sol-gel treatments	32
I-3-4 Plasma treatments.....	33
I-3-5 Issues and current solutions associated to surface treatments.....	34
I-3-6 Conclusion	35
I-4 Self-stratifying coatings.....	36
I-4-1 Introduction	36
I-4-2 Historical background.....	37
I-4-3 The concept	37
I-4-4 Degree of stratification.....	40
I-4-5 Evaluation of stratification	41
I-4-6 Factors affecting self-stratification.....	43
I-4-7 Experimental aspect of self-Stratification	47
I-4-8 Models to build self-stratifying systems.....	54
I-4-9 Promising self-stratifying coatings.....	61
I-4-10 Conclusion	68

I-5 Conclusion and strategy	69
Chapter II: Materials and methods	73
II-1 Raw materials	74
II-1-1 Substrate.....	74
II-1-2 Resins and solvents.....	74
<i>Resins.....</i>	<i>74</i>
<i>Solvents</i>	<i>77</i>
II-1-3 Fillers with specific FR properties.....	77
II-2 Coatings processing	79
II-2-1 Formulation	79
II-2-2 Application.....	80
II-2-3 Curing procedure: Optimization of the crosslinking process	80
<i>II-2-3-1 Differential Scanning Calorimetry (DSC).....</i>	<i>81</i>
<i>II-2-3-2 Investigation of the epoxy-amine conversion rate.....</i>	<i>83</i>
II-3 Physico-Chemical characterizations.....	86
II-3-1 Solubility measurements: Hansen’s Three-Dimensional Solubility Parameters	86
II-3-2 Surface properties	87
<i>II-3-2-1 Contact Angle measurements.....</i>	<i>87</i>
<i>II-3-2-2 Adhesion measurements.....</i>	<i>88</i>
<i>II-3-2-3 Color changes measurements.....</i>	<i>89</i>
II-3-3 Thermal study: Thermo-Gravimetric Analyses (TGA)	90
II-3-4 Chemical analysis.....	92
<i>II-3-4-1 Fourier Transform Infrared spectroscopy (FTIR)</i>	<i>92</i>
<i>II-3-4-2 Raman spectroscopy</i>	<i>93</i>
II-3-5 Microscopic analyses	93
<i>II-3-5-1 Sample preparation</i>	<i>94</i>
<i>II-3-5-2 Electronic microscopy.....</i>	<i>94</i>
II-3-6 Fire testing methods and characterization of the mode of action of materials during combustion	96
<i>II-3-6-1 Limiting oxygen index (LOI)</i>	<i>97</i>
<i>II-3-6-2 UL-94.....</i>	<i>97</i>
<i>II-3-6-3 Mass loss calorimeter (MLC).....</i>	<i>98</i>
<i>II-3-6-4 Characterization of the solid residues</i>	<i>100</i>
<i>II-3-6-5 Pyrolysis-gas chromatography- Mass spectrometry (Py-GCMS).....</i>	<i>101</i>
<i>II-3-6-6 Pyrolysis combustion flow calorimeter (PCFC)</i>	<i>102</i>
II-4 Accelerated ageing testing	104

II-4-1 Ageing under UV-rays exposure	104
II-4-2 Ageing under temperature and relative humidity conditions.....	105
II-5 Conclusion	106
Chapter III: Design of self-stratifying coatings.....	107
III-1 Introduction.....	108
III-2 Prediction of stratification	109
III-2-1 Solubility parameters – Hansen approach	109
III-2-1-1 Hansen solubility spheres.....	110
III-2-1-2 Prediction of the compatibility between resin binary mixtures.....	114
III-2-1-3 Conclusion.....	117
III-2-2 Surface energy approach.....	118
III-2-3 Conclusion	121
III-3 Self-stratification on polycarbonate substrate	121
III-3-1 Stratification of binary blends	121
III-3-1-1 Stratification of unfilled epoxy/silicone blends ¹⁴²	122
III-3-1-2 Stratification of unfilled epoxy/fluoropolymer blends ¹⁵²	126
III-3-1-3 Stratification of pigmented binary blends of thermoplastic and thermoset resins.....	130
III-3-1-4 Stratification of pigmented binary blends of thermoplastic and thermoset resins.....	137
III-3-1-5 Comparison between experimental and theoretical models.....	141
III-3-1-6 General conclusion on binary blends.....	141
III-3-2 Stratification of ternary blends.....	143
III-3-2-1 Stratification study	143
III-3-2-2 Conclusion.....	147
III-4 Conclusion	147
Chapter IV: Fire performances and ageing resistance of epoxy/silicone and epoxy/fluoropolymer self-layered coatings	151
IV-1 Introduction: State of the art on flame retardancy	153
IV-1-1 What about a fire?	153
IV-1-2 Thermal degradation of polymers.....	154
IV-1-3 Mode of action of FR additives.....	155
IV-1-3-1 Overview of the FR's mode of action.....	155

IV-1-3-2 Flame retardant characteristics of iron oxide.....	157
IV-2 Fire performances of the self-stratifying coatings applied on PC.....	159
IV-2-1 Development and evaluation of the FR properties of the epoxy/silicone and epoxy/fluoropolymer coatings applied on PC.....	159
IV-2-1-1 Fire retardancy of the PC coated with unfilled epoxy/silicone or epoxy/fluoropolymer coatings..	159
IV-2-1-2 Fire retardancy of the PC coated with iron oxide-filled epoxy/silicone or epoxy/fluoropolymer coatings.....	163
IV-2-1-3 Comprehension of the mode of action.....	168
IV-2-1-4 Conclusion.....	191
IV-2-3 Proposed mode of action of the epoxy/silicone coating	193
IV-3 Impact of ageing on film properties and fire performances of self-stratifying coatings applied on PC.....	195
IV-3-1 Ageing of polycarbonate	195
IV-3-2 Ageing of polycarbonate coated with unfilled epoxy-based self-stratifying system	198
IV-3-3 Ageing of polycarbonate coated with the epoxy-based self-stratified FR system after incorporation of iron oxide particles	202
IV-3-4 Conclusion	204
IV-4 Conclusion.....	205
General conclusion	209
Outlooks.....	213
List of Figures, Tables and Equations	219
References.....	225
Appendix.....	241
Résumé/ Abstract	266

Abbreviations

ATR	Attenuated total reflectance
BDP	Bisphenol-A bis(diphenyl phosphate)
BSE	Back scattered electrons
BuAc	Butyl acetate
C	Overlap volume of Hansen spheres/ Carbon element
CaCO₃	Calcium carbonate
CIE	Commission international de l'éclairage
DETA	Diethylene triamine
DGEBA	Bisphenol A diglycidyl ether
DMSO	Dimethyl sulfoxide
DSC	Differential scanning calorimetry
DTG	Derivative thermogravimetry
EDX	Energy dispersive X-ray spectroscopy
EPMA	Electron probe microanalyser
FE	Fluoro ethylene
Fe₂O₃	Iron oxide particle
FR	Flame retardant/retarded
FTIR	Fourier transformation infrared
FTT	Fire testing technology
HRR	Heat release rate
HSP	Hansen solubility parameters
IO	Iron oxide
LbL	Layer by layer
LOI	Limiting oxygen index
MIBK	Methyl isobutyl ketone
MLC	Mass loss cone
MLR	Mass loss rate
MTM	Methyltrimethoxy silane
NC	Non classified
PC	Polycarbonate
PCFC	Pyrolysis combustion flow calorimeter

PDMS	Polydimethylsiloxane
pHRR	Peak of HRR
RDP	Resorcinol bis(diphenyl phosphate)
SEM-EDX	Scanning electron microscopy
SiO₂	Silicon dioxide
SMLR	Specific mass loss rate
STIC	Self-stratifying intumescent coatings
T_g	Glass transition temperature
TGA	Thermogravimetric analysis
THR	Total heat release
TOF	Time of flame out
T_{pHRR}	Time to pHRR
T/RH	Temperature/ Relative humidity
TTI	Time to ignition
UV	Ultraviolet
V	Overlap factor
VE	Vinyl ether
WDS	Wavelength-dispersive spectroscopy
ΔE	Color difference
γ	Surface tension
γ₁₂	Interfacial tension between component 1 and 2
γ^d	Dispersive part of the surface tension
γ^p	Polar part of the surface tension

General introduction

Fire risk in buildings structures is directly related to combustible materials such as plastics, and even to common non-combustible materials such as steel which loses its strength under intense conditions – a fact unfortunately demonstrated by the tragic collapse of the twin towers in New York, USA on 11 September 2001.

In 2016, the International Association of Fire and Rescue Services (CTIF) reported that 195,000 deaths per year are caused by fire.¹ Despite these figures, plastics and textiles, which heavily contribute to the development and propagation of fire, are growing in popularity in a large number of applications including building and construction, automotive, electrical and electronic fields. The production of plastics is actually dominated by China, Europe and North American Free Trade Agreement (NAFTA) countries: it regularly increases for more than 50 years and reached 250 MT in 2013 (Figure 1).

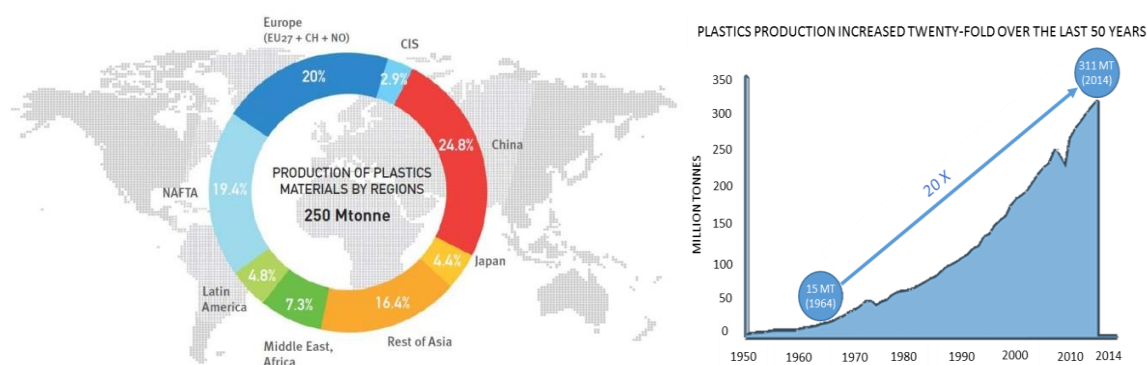


Figure 1. 2013 World production of plastic materials (thermoplastics and polyurethanes)² and Growth in Global Plastic Production 1950-2014³

Moreover, fire safety regulations become more stringent to try to reduce fire hazards. This fire issue leads governments and companies to invest heavily in effective flame retardant (FR) treatments, which might be able to retard the ignition of plastics and/or decrease flame spread, thereby preventing fire hazards, loss of life and damage to property. In order to provide durable fireproof properties to plastic based materials, various approaches have been developed (Figure 2).

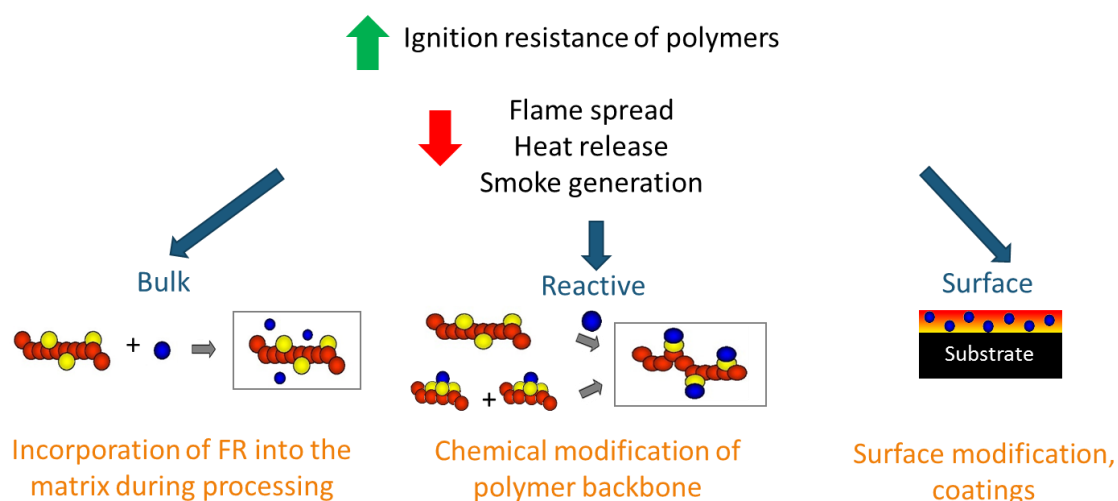


Figure 2. The different approaches to fire retard a polymeric matrix

The first one involves the incorporation of FR additives into the bulk polymeric matrix during processing. This technique is low cost and fast and thus widely used: the global flame retardant chemicals market, primarily driven by technological advancements in fire safety solutions and regulations, keeps increasing (Figure 3). However high loadings (up to 65 wt.%) are needed to bring efficient FR properties to the material. As a consequence, intrinsic properties (such as strength and elastic modulus) can be impacted and migration of fillers to the surface can also occur over time, leading to a decrease of the fire performances.

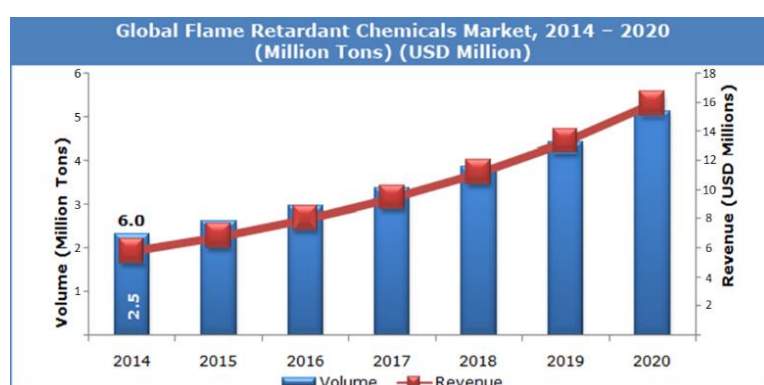


Figure 3. Global flame retardant chemicals market between 2014 and 2020⁴

The second approach, usually rather expensive and hard to upscale, consists in the chemical functionalization of the polymer backbone by FR units. Such modifications however depend on the matrix to be flame retarded, and this can lead to a change in the morphology and

physical properties of the bulk polymer (melting point, density...). Last, but not least, the third approach involves surface modification. This concept is quite new (2012) and allows concentrating the fireproof properties at the surface of the material, where fire starts, without interfering with the bulk properties of the polymer. The UMET-R₂FIRE group has been the first to propose the concept consisting in efficiently protecting polymer matrices (Polypropylene, Polyamide and Polycarbonate) by solvent based or waterborne intumescent coatings⁵⁻⁷, and some of them are now being manufactured.⁸ However, long-term protection performance of these coatings under exposure to environmental conditions (UV rays, moisture, chemicals...) is compromised because of the loss of adhesion or of some of their intrinsic properties, which reduce their efficiency over time.

To overcome these drawbacks, the setup of a functional coating requires the application of three different layers, each of them having a specific role: a primer to enhance the adhesion of the coating onto the substrate, an intermediate functional layer (e.g. with fire retardant properties) and a protective topcoat to avoid or limit ageing. However, these multilayered systems require multiple formulations, complex application and curing procedures which not only contribute to environmental waste generation and pollution, but also use excessive amount of energy until a solid film has been produced.⁹ Finally, the interlayer adhesion is often an issue. This is why the eco-concept of self-stratification has been developed in the frame of STIC project. This approach can overcome the major disadvantages mentioned above by allowing the formation, in one step, of complex multilayer systems or gradient coating structures which spontaneously stratify after application onto a substrate. The properties of the resulting system are gathered in one coating composition (optimized surface and adhesion properties) while reducing the processing steps, emission of solvents, production costs and also interlayer adhesion failures (Figure 4).

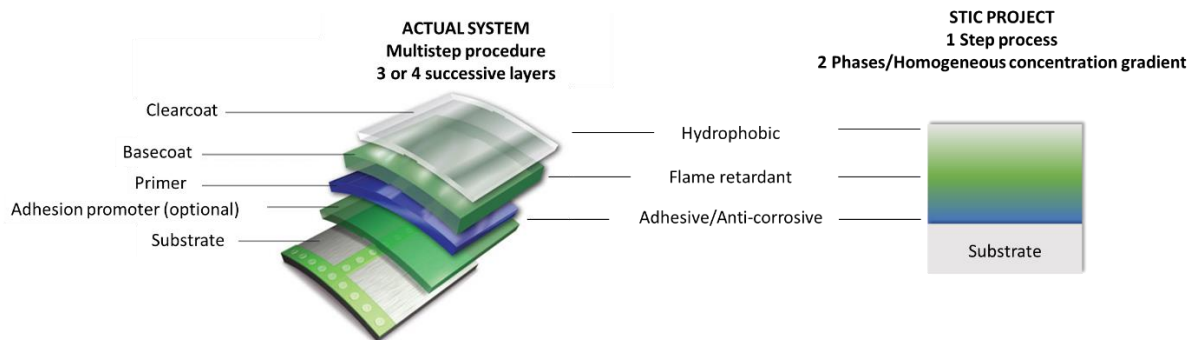


Figure 4. Flame retardant self-stratifying coatings concept (STIC Project)

The interest for self-stratifying coatings has been kept quite constant over the last decade: around 50 papers and a dozen of patents are dedicated to the subject (Figure 5). Self-stratifying mixtures have a multitude of potential applications that have not been widely explored yet. To date, this concept has been applied in specific coatings fields (automotive, self-healing, for corrosion- and weather-resistant applications⁹⁻¹², etc.) but it has never been considered for fire retardant purpose. No paper dealing with fire retardant self-stratifying coatings has been published up to now, although a large panel of chemical substances, including pigments, can act as flame retardants. It thus opens the door to a real challenge in this field, while favoring an industrial eco-efficient development of products.

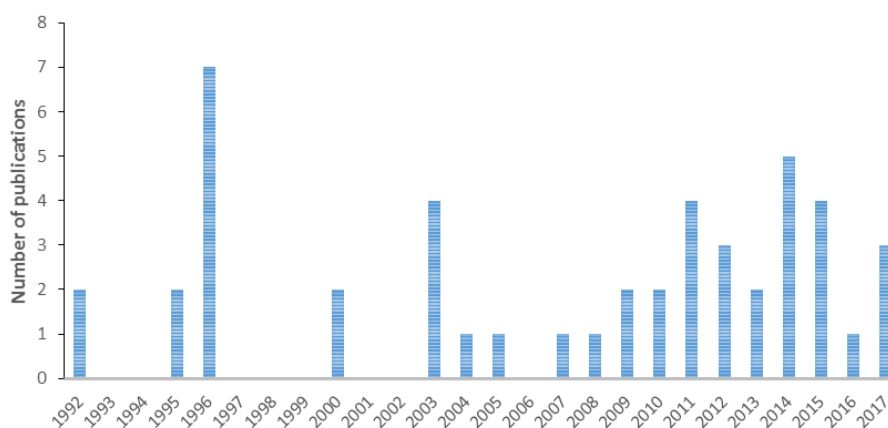


Figure 5. Number of publications from 1992 to 2016 including "self-stratifying", "self-stratification" or "self-layering" terms (Scopus April 2017)

Aim of this PhD thesis is thus to establish a proof-of-concept on formulating model self-stratifying flame retardant coatings which can overcome (i) adhesive, (ii) flame retardant and (iii) weathering issues.

Polycarbonate (PC) is selected as the substrate of choice for the study because of an increased demand from automotive, electronics and packaging industries. Moreover, PC represents a good illustration of the actual bulk treatment's limits to fire retard a polymeric matrix: the use of some halogenated compounds (the most commonly used FR for PC) is now banned in some countries¹³, and the addition of phosphorous-based FR lowers the mechanical properties of the polymer and leads to its yellowing under temperature or humidity conditions. Finally, although the introduction of specific non-halogenated additives (for example polymethylphenylsilsesquioxane spheres¹⁴), even in small amounts, mechanical resistance issue still remains.

The main objective of this PhD thesis is to obtain a perfect stratification giving rise to two well distinct and homogeneous layers on polycarbonate, or at least a coating in which the phase separation leads to a stratification characterized by a homogeneous concentration gradient more or less pronounced in the film thickness. Aim is to design one thin (< 150 μm) self-stratifying fire retardant system showing good adhesion to PC, resistance to UV and moisture, and having equivalent or better fire performances than a multilayered coated PC.

This manuscript is organized into four parts. The first chapter gives an overview of the existing pathways to fire retard plastics substrates, and more particularly on the current issues and solutions associated to fire retardant surface treatments.

The second chapter is devoted to the description of materials and methods which have been used and developed to complete the study. Theoretical considerations to predict the stratification of a coating composition are also discussed.

On the basis of theoretical considerations and a literature review, specific resin systems have been selected and tested to develop self-stratifying coatings on polycarbonate. The influence of a set of factors (solvents, fillers, crosslinking induced by a curing agent...) on the stratification level during the film forming process is studied in the third chapter.

The influence of the incorporation of specific flame retardant fillers in two successful self-stratifying systems, based on epoxy/silicone and epoxy/fluoropolymer combination, is then deeply examined. Fire performances are evaluated, and particular attention is given to the understanding of the mode of action of the additive in the coating. The final goal is to reach better or at least equivalent FR properties than a multilayered FR system. Finally, the last chapter deals with the impact of two type of ageing conditions (T/UV and T/RH) both on the end-use properties of the most successful fire retarded systems and on their fire performances. To complete the manuscript, a general conclusion is drawn and proposals for future studies on the subject are given.

Chapter I: Theoretical aspects of the project

The worldwide consumption of plastics rises considerably by 9 % each year, reaching around 230 billion tons per year. Due to their good properties, such as light weight, low processing costs and high strength, polymeric materials play an important role in many fields such as packaging, building, automotive, clothing, etc. Unfortunately, one of the major limitations of plastics is their inherent flammability: polymers exhibit poor fireproofing performance and thus need to be modified to prevent or delay fire spread.

The aim of this first chapter is to present the different methods to flame retard polymeric materials, emphasizing the approaches by surface treatment. The different strategies existing in the literature to fireproof a polymeric material will be described, and the advantages, drawbacks and issues associated to these different treatments will be discussed.

As the objective of this PhD thesis is to manage to fire retard plastic materials by designing novel kinds of coatings (i.e. self-stratifying coatings), particular attention will be given to the self-layering approach and a literature review on current developments of these coatings will be presented.

I-1 Introduction

Fire risks are inherent in combustible building materials such as plastics, and even in popular non-combustible materials such as steel which lose their strength in intense heat – a fact unfortunately demonstrated by the tragic collapse of the twin towers in New York, USA on 11 September 2001. Moreover, with the increasing trend of more stringent fire safety regulations, demands for reduction of the fire hazard posed by highly combustible materials such as plastics have gained importance in recent years. These issues lead many companies (building, furniture, transportation...) to invest heavily in effective flame retardant treatments, which might be able to prevent or retard the ignition of these materials and/or decrease flame spread, thereby preventing fire hazards, loss of life and damage of property. Various types of approach to fire retard plastic materials have been investigated up to recently and are commonly used in various domains such as electrical and electronics, building construction and transportation. The present chapter reviews the different approaches which exist to fire retard plastic matrices, and the actual issues encountered by their use. Particularly, the use of surface treatments, their problems and current solutions associated will be developed in a second part. Finally, a literature review based on the self-stratifying approach will be proposed.

I-2 Approaches to flame retard plastics

The following section describes the three main approaches commonly used to fire retard a polymeric matrix: (i) the bulk, (ii) the reactive and the (iii) surface pathway. The main advantages and drawbacks of these techniques are also discussed.

I-2-1 Bulk treatment

The “bulk approach” involves the blending of the polymer with fillers, stabilizers or active species, extruded or processed (Figure 6).¹⁵ This approach is mostly a low cost and fast technique, which however tends to some limits: the loading of FRs needed to be effective is usually high (up to 65 wt.% for cable and wire for example), which can lead to a significant influence on the intrinsic properties of the materials such as strength and elastic modulus. In

addition, the migration of the additives from the bulk to the surface of the polymer can form a non-uniform compound after a while. Lastly, because of the weak interaction between the additives and the polymer matrix, “fragile” points can form in the matrix, decreasing the mechanical strength of the specimens.^{16, 17} And finally plastic producers intend to reduce the thickness of their samples, involving processing issues because of the high amount of FR additives. This can detrimentally influence processability, melt rheology, and in particular cases the strength and toughness of the composite. These limitations can be mitigated by judicious formulation such as surface treatment of the fillers, the use of processing aids and the combination with other conventional FRs.

The earliest FRs used for synthetic polymers were halogenated derivatives, based on the discovery of halogenated hydrocarbons and waxes. In 2010, metal compounds corresponded to 56 % of the FR substances used, followed by inorganic and organic phosphorus compounds. Indeed, in recent years, environmental considerations concerning the use of halogen-based systems have paved the way for the increased use of phosphorus-based FR as alternatives to these compounds. Furthermore, this has generated active research to identify novel FR based on phosphorus (and also possible synergistic combinations with compounds of other fire inhibiting elements) and with several inorganic nanofillers (e.g. phyllosilicates and carbon nanotubes).¹⁸ In response to the pressure to develop environmentally friendly coatings, silicon-containing fillers have also been explored as their addition in a relatively small amount can significantly enhance fireproofing properties of a material.¹⁹⁻²⁴

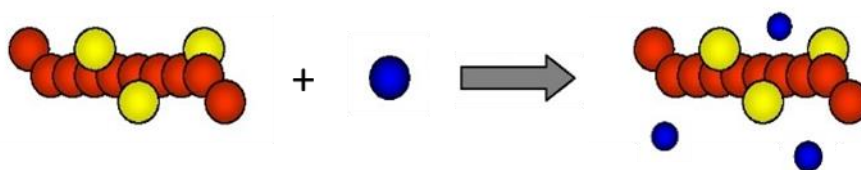


Figure 6. Bulk treatment approach to fire retard a polymeric matrix

I-2-2 Reactive approach

The second and very efficient approach consists in the chemical modification of the polymer backbone using for example functionalized monomers (Figure 7).²⁵ Such modifications, usually rather expensive, however depend on the matrix to be fire retarded. These changes can also

lead to a modification in morphology and physical properties of the bulk polymer (melting point, density...). Finally, the upscaling is not easy with most thermoplastic polymers and thus is not commonly used.

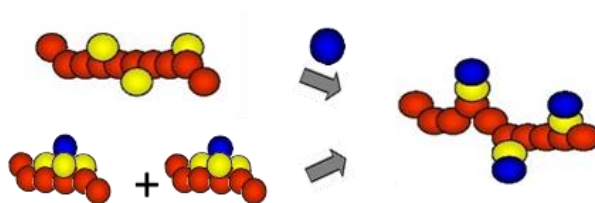


Figure 7. Reactive approach to fire retard a polymeric matrix

I-2-3 Surface treatments

The third approach mostly involves surface modification and allows concentrating the fireproofing properties where it is the most needed, i.e. onto the polymer surface (where the flammability takes place). It is commonly used to protect some substrates (e.g. wood²⁶, steel²⁷, textile²⁸) against fire, but it is quite a recent concept to fire retard plastic matrices. This approach allows overcoming the issues posed by the bulk or reactive methods: desired final properties can be reached without affecting the properties of the bulk materials.

Functionalization of surfaces has always been a common industrial process for a wide range of applications, from cosmetics to anti corrosion coatings. New processes and functions are more and more developed to enhance actual properties in response to economic and environmental challenges. Surface treatment processes are wide and use a large panel of technologies as:²⁹

- Plasma treatment (activation, plasma liquid deposition)
- Physical and Chemical Vapor Deposition (PVD and CVD)
- Etching (Dry or humid method, ion beam etching)
- Grafting of molecular function for specific applications (Radiation grafting, photografting)
- Nano structuration or texturing

- Sol-gel and Layer-by-Layer (LbL) process
- Powder deposition via electrostatic deposition
- Laser treatment for surface modification (patterning) and for metallic surfaces (pickling, alloys formation, doping)
- Application of a coating or varnish, Langmuir-Blodgett films, self-assembled monolayers
- Roughening, polishing, nanopolishing
- Biological methods (physical adsorption of biomolecules (e.g. proteins, peptides, drugs, lipids ...), chemical conjugation of biomolecules to surface groups, cell seeding and growth).

The most common surface treatments used in the fire retardancy field are described more precisely in the following part of this review. The issues and the solutions associated to each surface treatment are also discussed.

I-3 Examples, issues and current solutions associated to flame retardant surface treatments

Fire retardant coatings, varnishes and thin films can be used to fire protect inflammable materials such as wood³⁰, textile³¹ or polymers³²

Flame retardancy of polymeric matrices by thin film deposition is a very recent approach that is currently being developed in research institutes. Only few techniques indeed exist to allow the deposition of very thin films on polymer surfaces. In the next section, surface treatments of plastics in the fire retardant field are presented: intumescent coatings, layer-by-layer assembly (LbL), sol-gel coatings, plasma technologies.

I-3-1 Intumescent coatings

Intumescent systems were first reported by Gay-Lussac in 1821 to flame retard textiles.³³ Later on, it was stated that the ingredients of intumescence are mainly composed of an inorganic acid or a material yielding acidic species upon heating (e.g. phosphate), of a char former (e.g.

pentaerythritol) and of a blowing agent that decompose at the right temperature and at the right time to enable the blowing of the system (e.g. melamine).

Intumescent systems can be used as effective and promising coatings to form a physical barrier at the surface of the substrate to be protected. An insulating macro and microporous foam is built through action of heat, and can protect the substrate up to 2 hours in particular cases. When heated beyond a critical temperature (between 180 and 300 °C), the intumescent paint swells and turns into a foam which limits the heat transfers between the flame and the underlying substrate. Depending on the fire scenario, different kinds of matrices are used: acrylic for cellulosic and epoxy for hydrocarbon fire scenario.³⁴ Such paints are generally applied by spray, brushed or wire rod but require high precision to obtain a homogeneous protection. The aesthetic aspect is also the main drawback. Ageing properties are also a crucial point as these coatings can be used for both indoor and outdoor applications.

In the literature, it is reported that the application of a thin environmentally friendly intumescent coating on polycarbonate (thickness < 150 µm) can lead to excellent FR properties: a high Limiting Oxygen Index (LOI) value (58 vol.%), a V0 rating at UL-94 test and a low rate of heat release measured during mass loss calorimeter test were obtained.⁶ The substrate was flamed before coating deposition in order to optimize the adhesion, a key factor when such approach is used. Those promising results opened the door to a real breakthrough in the field of fire retarded polymers, whatever the thickness of the substrate. However, some weathering issues remained, leading to a loss of adhesion of the coating and thus to a decrease of the FR properties.³⁵

I-3-2 Layer-by-layer process

The Layer-by-Layer (LbL) technique was discovered in 1966 by Iler³⁶ and developed by Decher et al.³⁷ in the 90's. LbL technique consists in alternating deposition of oppositely charged materials (polyanions and polycations) with washing steps in between on a solid substrate. This leads to the formation of polyelectrolyte multilayer films whose thickness ranges from nanometer to micrometer (Figure 8). The properties of the deposited film thus arise from the structural arrangement of its constituents, their dynamics and the parameters chosen for the process.^{38 39-42}

This popular technique is widely used in various fields such as drug delivery and biomaterials^{43, 44}, anti-reflection⁴⁵, electrochromic^{46, 47}, oxygen barrier^{48, 49} and recently the technique was considered as a potential method to design flame retardant coatings.⁵⁰⁻⁵⁴ Indeed, in 2009, Grunlan's team opened the pathway to fire retard fabrics by developing, for the first time, a thin LbL organic-inorganic FR coating, based on branched polyethylenimine and laponite clay.⁵⁵ They demonstrated the possibility to create a FR coating through the use of a wet technique, and highlighted the improvements that can be achieved by using inorganic additives. The efficiency of replacing laponite by montmorillonite to reduce the flammability of polymers is also reported within the following years.^{53, 54, 56-58} These promising developments have led several groups of researchers to build up original LbL flame retardant coatings using various kinds of inorganic additives: polyhedral oligomeric silsesquioxanes (POSS)^{59, 60}, SiO₂⁶⁰⁻⁶², carbon nanotubes^{50, 63} and nanoparticles. These inorganic-based LbL coatings generally improve the fire performances thanks to the formation of a physical barrier protecting the substrate from heat and oxygen diffusion.

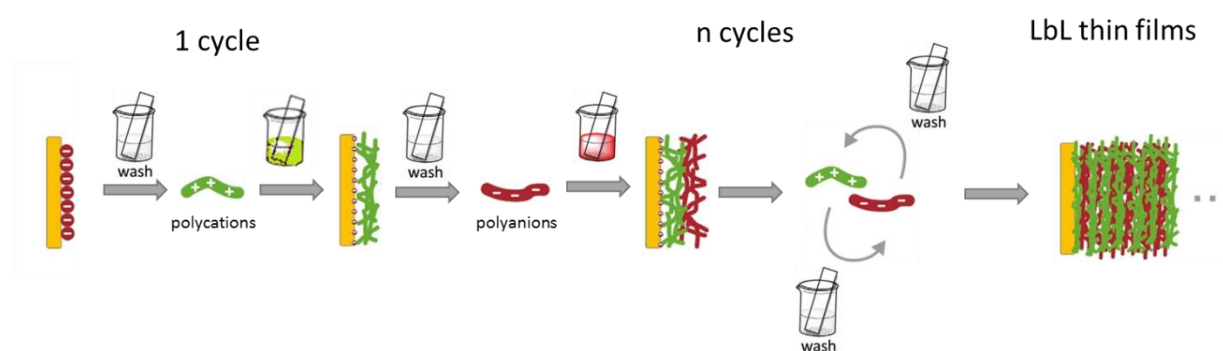


Figure 8. Schematic representation of Layer-By-Layer assembly: the different steps are repeated until the desired number of bilayers is obtained

K. Apaydin et al. investigated for the first time the use of LbL technique combined to flame retardants to decrease the reaction to fire of thin polymer plastics (polyamide 6,6, polyamide 6, PLA).⁶⁴ These results led a high number of laboratories to design new original FR coatings, particularly on fabrics (cotton, ramie, polyester, polyamide and acrylic), foams^{61, 63, 65-68} and films.⁵³ Carosio *et al.* deposited a LbL nanostructured coating made of SiO₂ nanoparticles which showed a great enhancement of the FR properties of PC: the incandescent melt dripping

during the FR test was suppressed on 0.2 mm PC films. Cone calorimeter tests were also promising: the time to ignition was increased and the heat release and total heat release rate were lowered.⁶⁹ UV-curable films on PC were also successful in suppressing the dripping, the smoke release and the particulate formation.⁷⁰

Finally, this technique offers several advantages (simplicity, deposition on surfaces of almost any nature and any shape, possibility to replace dipping by spraying,⁷¹ broad processing window, possibility to control numerous parameters (concentration, adsorption time and temperature, reagents)) but also some drawbacks (repeatability issues, contamination of rinsing and/or polyelectrolyte solutions during the multiple dipping, ageing and poor resistance to washing). Furthermore, it is noteworthy to notice that it is easier to fireproof fabric or foam materials because the FR coating can cover a greater surface in comparison to plastics such as polyamide 6 and polycarbonate films.⁶⁴

I-3-3 Sol-gel treatments

Sol-gel method is one of the simplest technique to design inorganic or hybrid organic-inorganic coatings from a solution.⁷² This technique is based on two successive reactions: hydrolysis of metal hydroxides (generally tetraethoxysilane (TEOS) or tetramethoxysilane) followed by the condensation of two metal hydroxides to form metal oxides species.

It presents numerous advantages such as low synthesis temperature (20-150 °C), easy coating of large surfaces, low thickness, high optical quality and assessment of high purity material.⁷³ This process is used in many fields such as superhydrophobic materials^{74, 75}, UV protection⁷⁶, luminescence⁷⁷, antimicrobial activity^{78, 79} and flame retardant textiles.^{80, 81}

As an example in the flame retardancy field, Alongi et al. succeeded to reduce the peak of heat release rate by 34 % and to increase the time to ignition by 74 % developing coatings containing inorganic precursor (TEOS/H₂O - 3: 1) onto cotton and polyester fabrics.⁸⁰ The sol-gel pathway is widely used to fire retard textiles, ceramic⁸², glass or wood⁸³⁻⁸⁵, but the method is not widespread for polymeric matrices.^{86, 87}

The quality of the prepared films however depends on the process parameters, of the technique used for the deposition and of the ambient conditions (hygrometry for example).

The repeatability can be poor and ageing can also be an issue, depending on the final application.

I-3-4 Plasma treatments

Plasma is an ionized gas constituted by charged particles, positive electrons and ions, which react at the surface of a material. In 1879, Crookes was the first to describe the fourth state of matter, also called “state of ionized gas”. Later on, in 1978, Langmuir introduced the term “plasma” to design some equipotential regions in discharge tubes containing a neutral electrically ionized gas. Indeed, more than 99 % of the visible matter in the universe is in the plasma state. With increasing energy input, the state of matter changes from solid to liquid to gaseous. If additional energy is then fed into a gas by means of electrical discharge, the gas will turn into plasma. When plasma comes into contact with solid materials like plastics and metals, its energy acts on the surfaces and changes important properties such as surface energy. In the manufacturing industry, such treatment allows increasing the adhesiveness and wettability of surfaces. This makes possible the use of new (even non-polar) materials and environmentally-friendly, solvent-free (VOC-free) paints and adhesives.

By varying the gas pressure, three common cold plasmas can be generated, e.g. low, subatmospheric and atmospheric pressure. These three processes exhibit various advantages and drawbacks including high maintenance costs, expensive vacuum systems and the impact of the environment.

Up to recently, low pressure plasma processes have been widely used to improve the fire properties of a large range of polymers such as plastics⁸⁸⁻⁹⁰ and fabrics (cotton^{91, 92}, silk^{93, 94}, polyacrylonitrile⁹⁵ ...). The use of plasma polymerization to improve the fire properties of plastics started in 1999 in our team.⁸⁹ By depositing about 50 µm of tetramethyldisiloxane-based coating onto polyamide 6 (3 mm), a decrease of 30 % of the heat release rate compared to pristine polyamide 6 was observed. Similar improvements were obtained later by Schartel et al. by depositing hexamethyldisiloxane-base coating (thickness < 10 µm) onto polyamide 6.6 (3 mm). However in that case, the time to ignition was shortened in the cone calorimeter test.

Recently, and due to the limitations of this process, another plasma method operating at atmospheric pressure such as plasma jet and dielectric barrier discharge plasma was developed. It exhibits many advantages such as continuous treatment, cost effective process and line speed and its effectiveness in the fire retardant field was demonstrated to fire retard textile and plastic substrates.^{92, 96} Plasma-Enhanced Chemical Vapor Deposition (PECVD) has also been used to fire retard polyamide 6 and polycarbonate substrates (0.5 mm): a significant increase in the time to ignition (+ 143 %) was registered in cone calorimeter after coating deposition due to the formation of a high-performance barrier layer at the surface of the substrate.⁹⁷ However, this technique requires high processing times to obtain very thin films.

I-3-5 Issues and current solutions associated to surface treatments

To provide durable fire retardancy to a material through its surface and to overcome the major drawbacks (e.g. adhesion and ageing issues), at least three different coatings or treatments bringing different functional properties (e.g. adhesive, fire retardant and hydrophobic properties) are usually needed. Indeed, exposure to long-term environmental conditions can cause the coating to lose some of its properties, thus reducing its effectiveness over time.^{98, 99} Because fire safety requirement is throughout the entire life of a building structure, which may last many tens of years, it is important to investigate the long-term protection performance of FR coatings under exposure to environmental conditions (UV rays, moisture, water, chemicals...). Degradation occurs as the result of environment-dependent chemical or physical attacks, often caused by a combination of degradation agents, and may involve several chemical and physical mechanisms.

To avoid such degradation, a topcoat is usually necessary. Moreover, plastics have chemically inert and nonporous surfaces with low surface tensions, which makes the bonding difficult to conduct with coatings, adhesives, inks and other substrates. Surface treatments allow improving this bonding prior to coating, laminating or printing by increasing surface energy and wettability. Flame treatment is a well-established, low cost and rapid method to improve adhesion.¹⁰⁰ It was for example used by our team to develop the concept consisting in efficiently protecting polymer matrices (e.g. Polypropylene, Polyamide and Polycarbonate) by solvent based or waterborne intumescent coatings.⁵⁻⁷ For higher and longer lasting treatment, corona or atmospheric plasma with variable chemistries can be used.¹⁰¹ Finally, the adhesion

properties of coating/substrate interface can also be improved by means of a primer layer, whatever the substrate.

The application of such multilayered systems/treatments usually require complex formulation, application and processing steps which not only contribute to environmental waste generation and pollution, but also use excessive amount of energy until a solid film has been produced.

Thus, considering those issues, it would be highly desirable to reduce the number of layers to a minimum, providing the equivalent or better overall performance of the current systems, forming multilayered paint films from a single coat system. One solution could be the use of the self-stratifying approach to design new FR coatings. Indeed, self-stratifying coatings are promising coating systems based on incompatible polymer blends which can produce polymer/polymer laminate: a complex multi-layer or gradient coating structure is formed from one single coat, providing an undercoat and finishing coating in one step process. The preferential distribution of concentration through the film thickness greatly eliminates the interfacial adhesion failure without compromising the advantages of a multi-layer system, and thus favors an industrial eco-efficient process.¹⁰²⁻¹⁰⁴ Finally, this concept constitutes a great possible versatile process for a broad range of applications and could thus favor the development of new products, taking into account the reduction of solvent and labor cost. Powder, waterborne and solventborne coating systems have the ability to stratify. A literature review about self-stratifying coatings is proposed in the next part of this chapter.

I-3-6 Conclusion

This part has evidenced why it is necessary to improve the reaction to fire of polymeric materials and which strategies (bulk and surface treatment) were suitable to flame retard them. The limitations of bulk treatment led us to consider the surface treatment approach. Among the surface treatments described, one surface approach has drawn our attention: the deposition of a coating onto the surface to bring flame retardant protection to polymeric matrices. This technique presents several advantages such as simplicity, universality, ability to be implemented at industrial scale, preservation of the intrinsic properties of the material to be protected, etc. As the aim is to avoid a multi-step treatment (primer/coating/topcoat), the

self-stratifying approach, never considered in the flame retardancy field until now, has been chosen in this PhD thesis. The following part of the manuscript is devoted to the description of the self-stratifying coatings.

I-4 Self-stratifying coatings

I-4-1 Introduction

A common three layer coating system consists of a primer and a topcoat with an intermediate coating whose composition depends on the desired properties (Figure 9). The primer brings corrosion resistance and enhances adhesion of the coating to the substrate, while the topcoat provides the aesthetic aspect, the durability, scratch and chemical resistance. To overcome the drawbacks generated by the complex formulation for each layer, the longtime application and curing procedures, the new effective and economical concept of self-layering coatings has been developed to reduce the number of layers while providing a coating with equivalent or better performance than a multilayered system. This approach allows a one-step formation of complex multi-layer or gradient coating structures which, after application onto a substrate, spontaneously form two distinct layers, thus providing an undercoat and finishing coating in one step. During the film forming process, the coating separates spontaneously into two continuous adherent functional layers to form a thermodynamically stable layered coating.

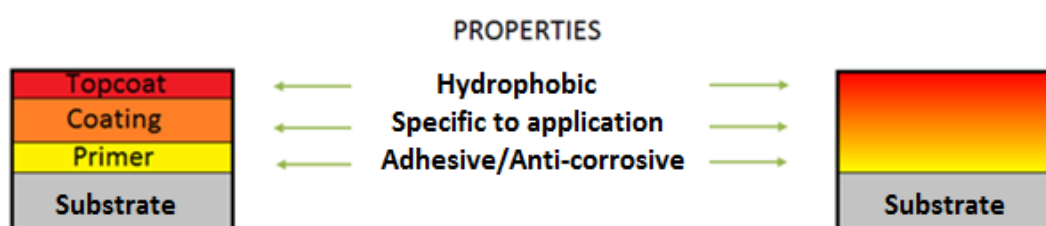


Figure 9. Self-stratifying approach

I-4-2 Historical background

About two decades ago, Funke and his collaborators published some work on self-stratifying coatings and introduced the concept of blending incompatible polymers to allow a one-step formation of complex multi-layer or gradient coating structures. They used a mixture of two powdered polymers applied on a metallic substrate and tried to minimize the free interfacial energy by heating both polymers above their melting temperature (T_m). From these results, they defined the characteristics necessary for a coating to spontaneously layer in terms of solubility parameters and by capillary rise test (combination of surface tension and viscosity measurements).¹⁰⁵ From those results, specific formulations for stratified powder coatings were patented.¹⁰⁶ Later on, the concept was applied to liquid solvent-based¹⁰⁷⁻¹¹¹ and waterborne^{112, 113} paints, with the use of selective coagulation, electrodeposition, substrate wetting or penetration processes to create specific driving forces for self-stratification. Verkholtantsev tested formulations based on liquid coatings from two polymers diluted in a common solvent. He succeeded to extend the theory that phase separation can occur as the solvent evaporates with subsequent layer formation, thus resulting in a film which has better overall performances than when the components are applied separately.^{9, 108}

Self-stratifying coatings provide major advantages including economic benefit, decreased time of processing (application of only one layer), no contamination between layers, improved interlayer bonding; thus, less chance of inter-layer adhesion failure is expected. The enhancement of adhesive properties to a substrate contributes to protection against corrosion (for metallic substrates), and to the upgrading of surface properties like the enhancement of chemical durability, ultraviolet and weather resistance. As a sustainable process, it helps reducing emissions and energy consumption.¹¹⁴

Up to now, these coatings have been developed for automotive applications¹⁰, self-healing coatings, weather-resistant or corrosion resistant solvent based coatings⁹, waterborne coatings¹¹⁵ and research works are still in progress to improve the process.^{114, 116, 117}

I-4-3 The concept

A coating system is formulated with a mixture of several chemical substances which are categorized as binder, volatile components, pigments and additives. The binder constitutes

the continuous film that allows the adhesion to the substrate whereas volatile components are liquid substances used to adjust the coating system to a suitable viscosity for application, allowing the film formation to occur. Pigments are insoluble solid particles which bring, among others, the color to the coating; additives such as catalysts, stabilizers, flow modifiers, etc. are added to the formulation to adjust the coating properties. During film formation, physical and chemical changes occur and the volatile components evaporate, therefore enabling the drying of the liquid coating mixture into a solid state film. During the evaporation process, entanglement of the polymer chains occurs, forming a tight-knit matrix. After film formation, further reactions like oxidation or crosslinking (e.g., two-component epoxies and urethanes) are required to generate a cross-linked film of higher molecular weight. The film formation process for a solventborne coating is depicted in Figure 10. For powdered coating systems, the powder melts upon heating, leading to the formation of a solid state film. The self-stratification occurs at this stage of the process.

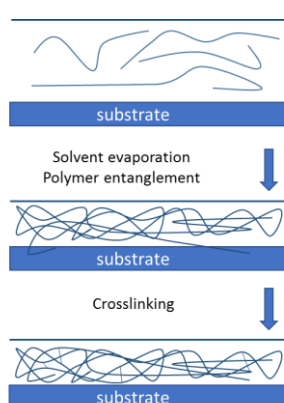


Figure 10. Film formation process for solventborne paint

Under certain conditions, the development of film-forming formulations based on a homogeneous mixture of incompatible polymers can lead to the formation of a polymer/polymer laminated structure. When phase separation takes place, it results in a fine heterophase polymer structure and liquid polymer blend compositions form non-homogeneous in-layer (self-stratified) coatings (Figure 11).¹¹⁸

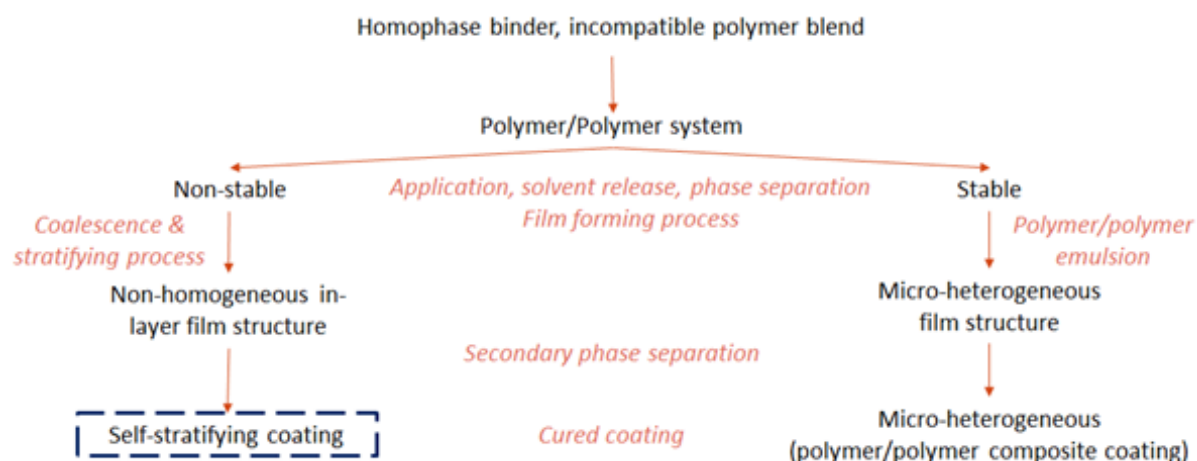


Figure 11. Steps of self-stratifying concept compared to common process¹¹⁸

Experimentally, to produce a homogeneous solution, two incompatible resins are dissolved in a common solvent or in a mixture of several solvents, and the coating is applied in a single step. The mixing of the incompatible resins must take place just before the application on a substrate since chemical and physical changes occur directly after the mixing. The separation thus occurs, followed by stratification forming a two-layer coating system. If the system is crosslinkable (blend of thermoplastic and crosslinkable resins), the molecular weight rapidly increases due to crosslinking reactions until the gel point is reached. A 3D network is then built which separates from the solution because of its increasing insolubility and decreasing swellability. The solution is expelled from the nets, and meanwhile it becomes poorer in crosslinkable species and richer in thermoplastic resin.¹⁰⁹

Self-stratification can be induced by physical and/or chemical changes occurring at one or more of the different stages of the process: (a) during solvent evaporation, (b) during heat and/or mass exchange, (c) during chemical reaction.⁹ The simplified process is illustrated in Figure 12. Finally, each layer performs a specific function: the lower layer promotes adhesion and protects the substrate while the upper layer brings an aesthetic aspect and provides protection against atmospheric conditions.¹¹⁹ The lower layer is also referred to as the basis resin, and the upper layer as the stratifying resin.

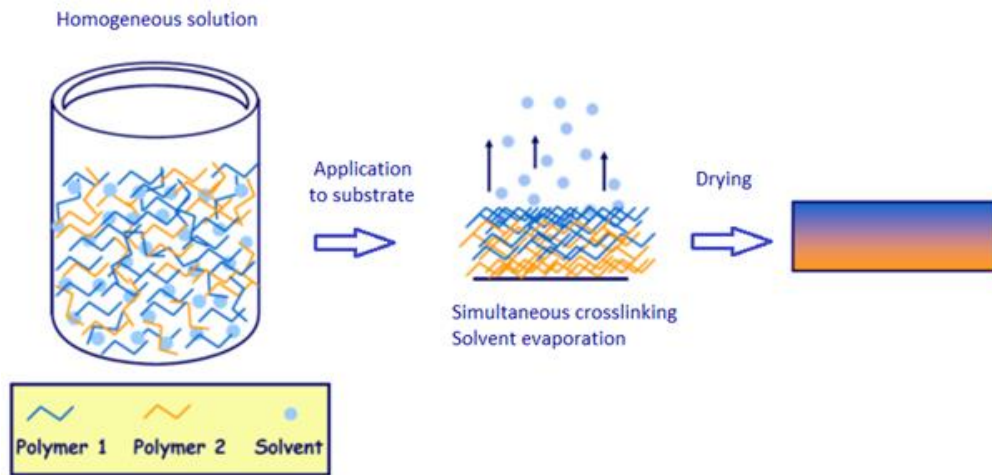


Figure 12. Film forming process with self-stratifying coatings¹²⁰

I-4-4 Degree of stratification

Mixtures of incompatible polymer blends can lead to different degrees of stratification after the film formation, that can be rated from I to IV (Figure 13). Film surface and cross-section analyses allow determining such classification.¹⁰⁹

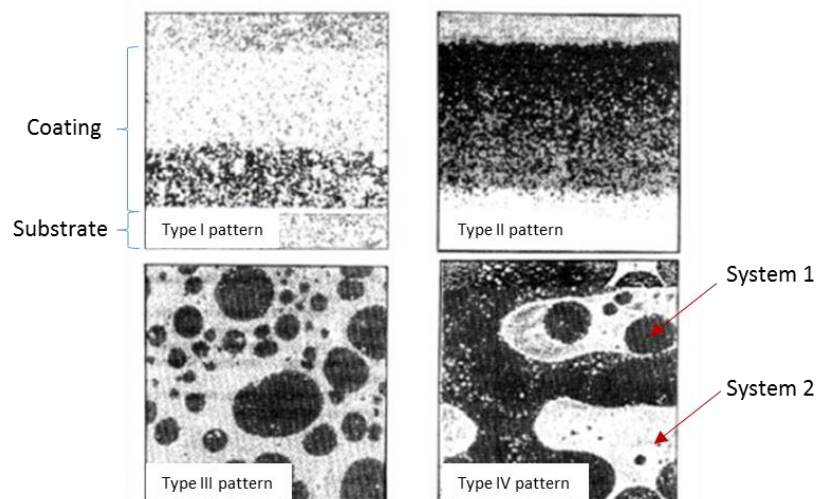


Figure 13. Type I to IV patterns defining the degree of stratification of a coating¹⁰⁹

The type I pattern is related to a perfect stratification. The mixture of incompatible polymers gives rise to two well distinct and homogeneous layers. The phase separation corresponding to a type II pattern leads to a stratification characterized by a homogeneous concentration gradient more or less pronounced through the film thickness. In the type III pattern, there is formation of isolated spherical particles of various diameters composed of only one resin, or of mostly one resin, dispersed in the continuous matrix of the other polymer. A concentration gradient of spherical particles can appear throughout the film thickness. Finally, the type IV pattern is composed of large islands or isthmus shaped regions very rich in one of the components or constituted of only that component. The coalescence of spherical particles can be responsible for the formation of the islands, which can exhibit, like in the previous pattern, a concentration gradient. However, it is important to notice that a 100 % degree of stratification can lead to a significant reduction of interlayer adhesion and thus to poor properties.¹¹⁹

I-4-5 Evaluation of stratification

Self-stratification in coatings can be expressed in terms of: (i) concentration (concentration difference in one resin between the base and top layers of the coating, or determination of the concentration in one selected polymer through the coating thickness), (ii) thickness (determination of the thickness of layers having distinct polymer structure or composition), (iii) properties (properties of both coating interfaces can be analyzed (hardness, chemical resistance, glass transition temperature ...)).¹²¹

Analysis of the stratification can be carried out with unpigmented and pigmented systems. Depending on the nature of the coating, layering can be evidenced by various characterization methods. Most evaluations can be performed by visual or microscopic examinations. The visual appearance of unpigmented films can reveal the layering: translucent or cloudy films generally indicate respectively compatibility or incompatibility, whereas color difference can be used with pigmented systems. Also, the occurrence of fine, medium or coarse structures refer to some extent to the degree of incompatibility. Irradiation of the sample with UV light might be an alternative for an easier analysis as it can lead to the discoloration of some binders.

Finally, in addition to be economically attractive, improved properties can be obtained if all the factors affecting the stratification can be controlled and adjusted.

The following sections will describe the theoretical and experimental aspects of the self-layering concept. As these different notions have already been reviewed in the article entitled: *Self-stratifying coatings : A review*¹²² from A. Beaugendre and al., published in *Progress in Organic Coatings* (2017), parts of the paper are incorporated in the manuscript. The first and last part of the article, not presented in this section, are available in the Appendix 1.

I-4-6 Factors affecting self-stratification

In this section, theoretical aspects of the self-layering process are covered by discussing the different parameters and mechanisms which can be responsible for the phenomenon. Among them, kinetic and thermodynamic conditions, and mechanisms based on gravitation, selective wetting, surface tension or phase contraction are detailed.

2.1. Theoretical aspect of self-Stratification

Self-stratification can be described as a phase separation directed in the coating axis, as a normal to the coating interfaces. This process needs some driving forces to achieve a phase separation during the film forming process.

2.1.1. Kinetic and thermodynamic conditions for stratification

Controlled kinetic and thermodynamic conditions are needed for the self-stratification to occur.

First, a phase separation in the polymer blend must occur, and the stratification process must precede the curing reaction (crosslinking); or the two phenomena must only partially overlap if the systems include a curing agent.

Thermodynamically, a polymer/polymer incompatibility must exist: the less polar component behaves as the stratifying component, and the more polar one as the binder for the base layer.

Fig. 10 illustrates the distribution of each resin in a self-stratifying coating according to its surface energy.

First, the interfacial tension between the base layer and the stratifying layer – λ_{12} –, should be large enough to avoid one phase being dispersed in the other phase during the film forming process. The intended base coat must also spontaneously wet the substrate, meaning that the interfacial tension between the base layer and the

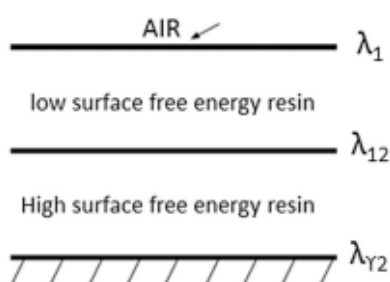


Fig. 10. Distribution of resins according to their interfacial tension in a self-stratified coating.

substrate – λ_{r2} – must be very low. Finally, the total surface and interfacial surface energy must be as low as possible.

Several mechanisms, described in the following part, can explain the self-stratification process.

2.1.2. Mechanisms of self-stratification

Intermolecular forces allow phase separation and the formation of a heterophase polymer structure via a diffusion process. However, these forces are unable to orientate the separated phases in an assigned direction, which is necessary for self-stratification. Thus, the binder needs a separate driving force which can be a surface tension gradient, a selective substrate wetting, contraction forces, etc.

Verkholantsev classified incompatible polymer blends according to the nature of binder to explain self-stratification mechanisms [21]:

- mixed polymer 'melts' (powder and solvent free paints with low volatile organic compounds (VOC)).
- binders based on a mixture of polymer dispersions (solvent or waterborne paints).
- solventborne paint compositions based on polymer-polymer emulsions (two-component paint).
- solventborne binders based on initially homophase solutions of incompatible polymer blends in volatile solvents, convertible into a heterophase state.

Different mechanisms of stratification were identified according to his work:

- Mechanism driven by gravitation.
- Selective wetting mechanism.
- Pigment wetting mechanism.
- Mechanism driven by surface tension gradients.
- Phase contraction mechanism.

Each mechanism will be described in the following paragraphs.

2.1.2.1. Mechanism driven by gravitation. This mechanism can concern systems a, b and c. In this case, the temperature of the system is above the melting temperature (T_m) of both polymers. In formulations without any curing agent, it leads to complete and sharp

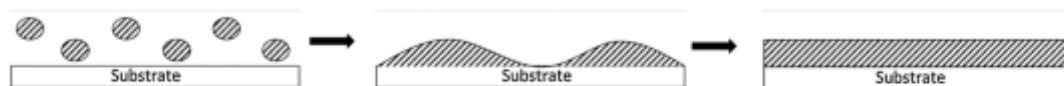


Fig. 11. Schematic representation of substrate selective wetting mechanism.

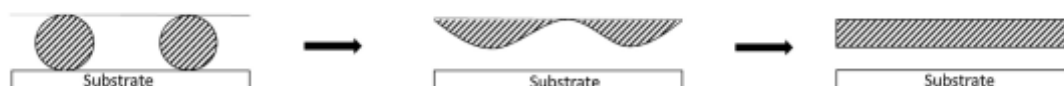


Fig. 12. Surface tension gradient mechanism (Marangoni effect) [21].

stratification or, in a process with curing agents, the curing reactions occur above T_m .

An expression for the velocity of sedimentation V_s of the dispersed phase particles, based on Stokes' law, states that:

$$V_s \propto \frac{\Delta\rho \cdot r^2}{\eta} \quad (1)$$

with $\Delta\rho$ the relative density of liquid polymers or phases of polymer/polymer emulsions (kg m^{-3}), η the viscosity of the phase concerned (Pa.s) and r the particle radius (m). The temperature of the system must be well above the T_m of both polymers even with a high $\Delta\rho$ value in order to ensure that the viscosity is low.

For example, a 80–100 μm film of an incompatible epoxy/vinyl resin blend with a plasticizer needs 1–3 h of heating at 120 °C for a complete stratification [21].

2.1.2.2. Selective substrate wetting mechanism. This mechanism can concern systems a, c and d. This process is due to the selective wetting of a substrate by one phase of a two-phase liquid system and is thus sensitive to the nature of the substrate (Fig. 11). Low volatile solvents, non-stable polymer/polymer emulsions and low viscosity of the stratifying phase are necessary for the stratification to occur. This mechanism is suitable to control adhesion durability and surface properties of thin coatings.

Thermodynamically, the spreading coefficient S can be defined by the relation:

$$S = \gamma_{sv} - (\gamma_{lv} + \gamma_{ls}) = W_a - W_c$$

With γ_{sv} , γ_{lv} and γ_{ls} representing respectively the free surface energy of the interface between the substrate and the vapor phase, between liquid and vapor phases and between liquid phase and substrate; W_a the work of adhesion and W_c the work of cohesion. Thus, according to this equation, spreading can occur if the adhesion between two liquids is greater than the cohesion in the liquid which is in the position for spreading, while spreading does not occur if the cohesion is greater than the adhesion. Consequently, if $S > 0$ then spreading occurs [26]. Since only large scale motion is of importance in spreading, only the free surface energies are involved.

When a coating is pigmented, selective pigment wetting mechanism can also occur. Pigments are dispersed in one of the resins (the basis or the stratifying resin depending on the desired application) prior to the mixing of the two media.

2.1.2.3. Pigment wetting mechanism. This mechanism can occur with systems a, c and d. For system "c", there is first a phase separation during the film forming process. The next step is a selective wetting of pigment particles with one of the polymer phase, followed by particle coalescence in order to form a gel structure. Finally, the contraction of structure with separation leads to a 'sandwich' structure.

2.1.2.4. Surface tension gradients mechanism. This mechanism can be applicable mainly to coatings of low viscosity, solvent based or thin-layer thermally curable assemblies [17]. The mechanism is illustrated in Fig. 12.

Two mechanisms can be distinguished: capillary flow and Benard cells.

2.1.2.4.1. Capillary flow. This mechanism can be applied to systems c and d composed of a blend of incompatible polymers, selected near the two-phase concentration region and diluted with specific solvents chosen according to their volatility and affinity for polymers. The coating has to be applied using a process promoting an intensive evaporation of solvents (like spraying). The phase separation thus would undergo a spinodal mechanism: the binder forms an interpenetration network of separated phases.

The driving force is a result of the non-uniform evaporation of solvents (the Marangoni Effect) and the stratification rate depends on the interfacial tension gradient, on parameters related to the structure of the system and on flow characteristics.

A criterion (D) predicts the direction of emulsification taking into account parameters of both phases (the viscosity η , the surface activity Δ and the concentration of surface-active species):

$$D_{w/o} = \frac{\eta_0}{\eta_w} \frac{\Delta_w}{\Delta_o} \frac{C_w}{C_o} \quad (2)$$

with w referring to the more polar phase and o to the less polar one. A 'polar-in-less polar' type emulsion forms when $D < 1$, and vice versa.

According to this equation, the stratifying phase should have a lower viscosity than the base phase, a higher phase volume and should contain a surface-active component (additive or modifier for example) to promote the stabilization of the interface. In this case, a low molecular weight polymer, a low-volatile solvent and a low total polarity favor stratification.

In Fig. 13, the capillary stratification mechanism is described. The volume content of the stratifying phase has to be higher than the base phase to avoid porosity in the dry polymer structure.

2.1.2.4.2. Benard cells. Systems b, c and d can be concerned by this mechanism. This process corresponds to the transportation of the lightest polymer particles to the top layer and is driven by surface tension gradient. It can be applied to the stratifying layer composed of a low viscous polymer/polymer emulsion (nucleogenic mechanism). In his overview of a European Community Research Project, Walbridge observed that the formation of Benard cells is essential for self-layering [9].

2.1.2.5. Phase contraction mechanism. This mechanism can concern systems c and d. Similarly to coalescence, phase contraction forces are due to the minimization of free interfacial energy in the liquid-gel systems by decreasing the interfacial surface. This mechanism occurs at the interfaces, with homophase or heterophase compositions, and provides efficient stratification. Fig. 14 shows a scheme of the mechanism.

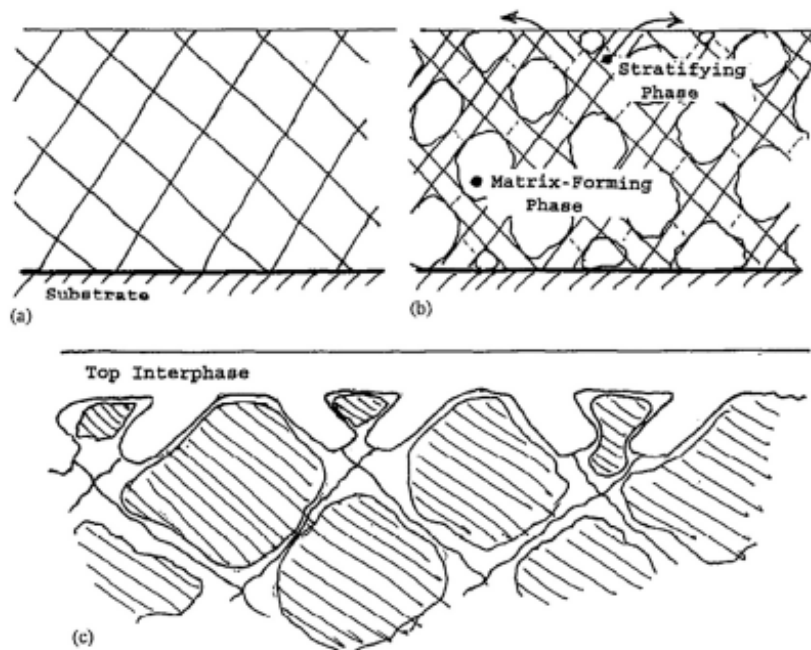


Fig. 13. Capillary stratification mechanism: (a) interpenetration networks; (b) capillary system, capillary flow and emulsification process; (c) top surface covered with a stratified phase [21].



Fig. 14. Phase contraction scheme [21].

The resultant polymer structure is dependent on the nature of the substrate, has a long-lasting heterophase gel structure and the stratifying phase has a low viscosity. This approach is described in Fig. 15

Interpenetrated networks are formed, showing that phases undergo different degrees of contraction, producing the driving force for phase separation. This mechanism depends on the volatility of solvents and on the composition of the system [(a) and (b)], and the driving force acts as a destination force if one phase is fixed on a substrate (selective wetting) or attached to the top interface (as a result of solidification of a dried surface layer).

If driven by phase contraction, the process is affected by several thermodynamic factors [1]:

- Polymer/polymer ratio.
- Thermodynamic affinity of the solvents used toward both polymer partners.
- The presence of compatibilizer, decompatibilizer or surface tension controller.
- Phase viscosities.
- Pigment Volume Concentration (PVC) level.
- Film thickness.

This mechanism is not easily feasible or is of low intensity if the viscosity increases too rapidly or if self-emulsification takes place in the early stage of the film forming process. Moreover, even if phase contraction forces are the most convenient to drive the process,

their generation requires a sufficient level of volatile components in organic formulations.

Two mechanisms of action can also take place simultaneously. For example, Fig. 16 describes a scheme of mechanism driven by both surface tension gradients and phase contraction depending on time evolution. In a first step, two liquid phases coexist generated by the phase decomposition process. Then, viscosity increases due, for a short period of time, to the formation of capillary structures, capillary flow, self-emulsification and contraction of phase structure, giving rise to the stratification. While the viscosity of both phases keeps increasing, the crosslinking process begins shortly after the end of the stratification. In fact, as it was mentioned previously, the stratification has to precede the crosslinking reactions. The formation of a heterophase structure occurs both during the stratification and the development of crosslinking reactions.

Among all the previously described stratification mechanisms, the one based on free surface tension is predominant: phase separation is driven by intermolecular forces and the formation of two homophases from a heterophase mixture occurs due to the minimization of the free energy of mixing. Some disagreements remain upon the importance of surface tension to drive phase separation. Miscibility could also explain the phenomenon adequately as the layering has to be induced by a particular polymer with a specific interface. The film-substrate interface can be directed by reactive chemistry and the film-air may be surface tension phenomena. In particular case, it was proven that the self-assembly can be driven by miscibility and diffusion parameters rather than by difference in surface tension [27].

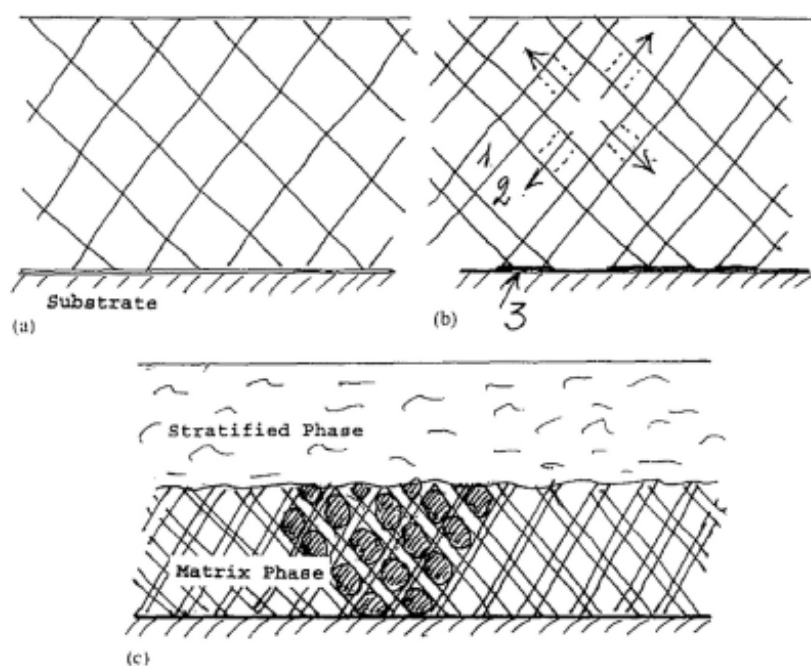


Fig. 15. Contraction stratification mechanism: (a) interpenetrating phase network, (b) prevailing contraction of the phase, (c) stratified structure. 1 and 2: polymer phases; 3: attachment to a substrate [21].

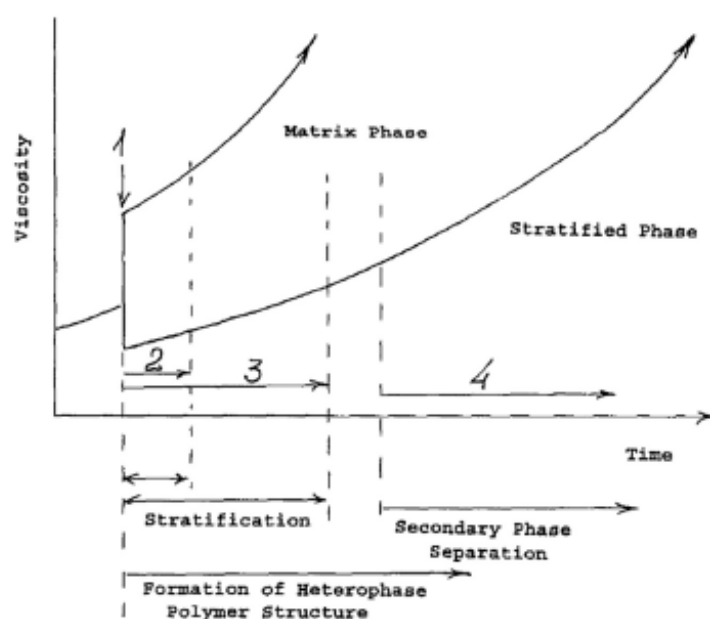


Fig. 16. Time-dependent transformation in phase decomposing liquid polymer films: 1, phase decomposition process produces two liquid phases; 2, capillary structure, capillary flow and self-emulsification; 3, contraction of phase structures; 4, development of crosslinking reactions [21].

However, these forces are not the only parameters that can impact the stratification process. The composition of the system, the melting temperature of polymers used, the rate of solvent

evaporation, the viscosity and the application methods, the film formation conditions, the film thickness. . . can also affect the stratification mechanism.

I-4-7 Experimental aspect of self-Stratification

The experimental parameters which can influence the self-stratification are reviewed in this part of the chapter: the characteristics of the materials composing the system, and more particularly the Hansen solubility parameters of the selected resins which allow to calculate a percentage of compatibility between two resin systems, the substrate and the processing conditions.

2.2. Experimental aspect of self-Stratification

2.2.1. The formulation of the coating

2.2.1.1. Resins. As mentioned previously, the resin choice is crucial for the stratification to occur and particularly its type, molecular weight, glass transition temperature, crosslinking rate and curing agent if applicable.

2.2.1.1.1. Molecular weight of polymers. Studies seem to establish that the higher the molecular weight the higher the degree of incompatibility, leading to better phase separation [1]. Indeed, a change in molecular weight influences the mutual solubility of polymers and thus the layering: a small change in molecular weight can induce drastic modification in mutual solubility between polymers [9].

The influence of the molecular weight of polymers was investigated by Vink using a chlorinated rubber resin (Alloprene R10) in combination with epoxy resins of different molecular weights (Epikote). He showed that the level of stratification improves with increasing molecular weight, and that the type of solvent also influences stratification (Table 2). The stratification ranking ranges from 1 to 6, 1 referring to optimum stratification (type I coating).

No stratification was observed with the epoxy resin having the lowest molecular weight (Epikote 828). This result is supported by a high overlap factor ($V = 96.2\%$). On the other hand, the degree of incompatibility increases for higher molecular weights and a well-stratified two-layer coating is obtained.

2.2.1.1.2. Glass transition temperature. From the Flory Huggins equation and considering that specific interactions between polymers (Eq. (3)), Toussaint assumed that a large difference in their T_g would favor phase separation because of differences in the polymer chain flexibility.

$$\frac{\Delta G_m}{RT} = \frac{\varphi_A}{N_A} \ln \varphi_A + \frac{\varphi_B}{N_B} \ln \varphi_B + \varphi_A \varphi_B \chi + \frac{\Delta G_H}{RT} \quad (3)$$

in which φ_A and φ_B are volume fractions of polymers A and B, N is the number of segments in a chain, χ the Flory interaction parameter which can be estimated from the solubility parameters, and ΔG_H is dependent on the enthalpy and entropy due to specific interactions like hydrogen bond formation. From this equation, it is assumed that a high Flory interaction parameter and low ΔG_H will favor the immiscibility of the polymers (free volume effect),

Table 2
Stratification of pigmented systems of Epikote/Alloprene R10 as a function of the type of epoxy and solvent [1].

Epikote (Molecular Weight [g mol^{-1}])	1st phase: Epikote/ Fe_2O_3 combination	2nd phase: Alloprene R10/ TiO_2 combination	Overlap factor V (%)	Stratification ranking ^c
	Solvent	Solvent		
828 (379)	MIBK	MIBK	96.2	6
1001 (900–1000)	MIBK	MIBK	40.2	2
1002 (1150–1400)	MEK	MIAC		2
1004 (1695–1890)	MIBK	MIBK	34.2	2
1004 (1695–1890)	MEK	MIAC	22.6	2/3
1007 (4760–8000)	MEK ^a	MEK	19.4	2
1009	MEK	MEK	22.3	1
1009	MEK	MIAC	22.6	1
1009	MEK/MIAC ^b	MIAC	22.6	1/2
1009	MEK/MIAC	MEK	22.6	2/3
1009	MEK/MIAC	MEK/MIAC	22.6	1

^a MEK = butanone.

^b MIAC = Methyl Isoamyl Ketone.

^c Ranking: 1 = optimum, 6 = no stratification.

initial molecular weight of polymers will play an important role in the retention of solvent. Indeed, solvent retention is even more pronounced when the extent of chain entanglement is high [17]. It is also interesting to notice that curing agents may enhance the compatibility of particular resin combinations and can provide efficient bonding between layers [1,10,14,28,29].

However, the addition of a crosslinking agent needs to be carefully controlled. Indeed, a too reactive catalyst can hinder thoroughly self-stratification because of the gelation of the system: the viscosity increases too rapidly impeding coalescence of the spherical particles of the separated phase into larger domains and their migration [8,28]. Vink and Bots suggested that, in some cases, the increase in viscosity due to solvent evaporation occurred at a much faster rate than the increase in molecular weight by the curing process, and thus deteriorate the resulting stratifying pattern [29]. Finally, the hardener can be incompatible with the uncrosslinked other resin [28,29].

Vink and Bots investigated this effect and figured out that the presence of a hardener, in general, did not enhance the degree of stratification (Table 3). Stratification was usually adversely affected (particularly with Euredur XE27 and XE200), which could be attributed to the effect of the hardener on resin incompatibility [29].

However, the effect of curing agent is strongly dependent on the resin used. For example, XE460 polyamine hardener has a positive effect on stratification in the Epikote 1001/Alloprene R10 system but, adversely, it affects the Epikote 1009/Alloprene R10 system (Table 4).

In some cases, the presence of chemical bonding between the top and bottom layers, though bridge with the crosslinker, was also evidenced [14]. During crosslinking, the decrease in mobility delays the phase separation process and can even lead to the formation of a three phase system [27].

Therefore, hardener can influence the stratification as it can affect both phase separation and compatibility of the system.

2.2.1.2. Solvent and rate of evaporation. A number of authors have demonstrated that self-stratification can be initiated by solvent evaporation [28,30–32].

Practically, binders for self-stratifying coatings are usually four component systems: two incompatible resins and two solvents

Table 3
Stratification of unpigmented formulation in the presence of hardener [29].

1st system		2nd system		Curing agent ^a	Stratification ranking ^b
Resin 1	Solvent 1 (Teb)	Resin 2	Solvent 2 (Teb)		
Epikote 828	THF (66 °C)	Alpex CK450	Heptane (98 °C)	None	1
				XE 26 or 40	1
				XE 90, 278 or H3	2
				XE 14	4
Epikote 1007	THF (66 °C)	Alloprene R10	Butyl acetate (126 °C)	XE 27 or 200	4
				None	2
Epikote 1004	Cyclohexane (81 °C)	Alpex CK450	Decane (174 °C)	XE 14, 26, 40, 90, 200, 278 or H3	6
				None	2
				XE 14 or 26	2
				XE 27, 40, 90, 200, 278 or H3	6

^a XE: Euredur (Schering), XE14: fast amine hardener; XE26: aliphatic polyamine; XE27: aliphatic etheramine; XE40: cyclo-aliphatic polyamine; XE90: polymercaptane; XE200: polyaminoamide; XE278: polyaminoimidazoline; H3 or Epikure H3: ketamine (Shell).

^b Ranking: 1 = optimum, 6 = no stratification.

Table 4
Stratification of systems of Epikote/Alloprene R10 as a function of type of hardener.

1st system: Epikote			2nd system: Alloprene R10		Curing agent ^a	Stratification ranking ^b
Epikote	Pigment	Solvent (Teb)	Pigment	Solvent (Teb)		
1001	Fe ₂ O ₃ /ZnPO ₄	MIBK (116 °C)	TiO ₂	MIBK (116 °C)	None	2
					XE 14	3
					XE 14/Fe ₂ O ₃	6
					XE460	1
1009	Fe ₂ O ₃	MEK (80 °C)	TiO ₂ (treated)	MIAK (144 °C)	None	1
					D L75 in MEK	1/2
					XE90	2
					XE460/Fe ₂ O ₃ in MEK or MIBK	5

^a XE460: Euredur 460, modified polyaminoamide adduct (Schering); DL75: Desmodur L75: aromatic polyisocyanates (Bayer).

^b Ranking: 1 = optimum, 6 = no stratification.

the solution before reaching concentration at which phase separation starts, the greater and the more spontaneous the stratification. Phase separation should occur immediately after the application of the coating onto a substrate as a result of solvent evaporation [33]. If properly controlled, primary phase separation produces liquid phase capable of self-stratification during the film forming process. As the solvent evaporates from the top surface, the particles are not uniformly concentrated across the vertical height of the film. The Peclet number Pe (in this case equal to the ratio between the evaporation rate and the particle diffusion rate) can describe this process: if the diffusion of one type of particle is dominant during drying, the resulting system is such that one component dries uniformly, while the other is carried by the downward interface. This results in segregation. A key aspect of this mechanism is that it is independent of orientation as gravity does not play any role. Experimentally this phenomenon can be observed through the controlled evaporation of water from drying films of two types of latex particles, each with a different particle radius.

In principle, it should be possible to obtain a stratified coating by preferential evaporation of one solvent in a mixture of two incompatible resins with two solvents. For that purpose, the solvent with the highest volatility must be a solvent for both resins while the solvent with low volatility must be a solvent for one of the resins and a non-solvent for the other resin. According to Vink, the rate of solvent evaporation should not be too high because the binders need sufficient time to separate and to form a layer before the system becomes too viscous. The critical value for the relative evaporation rate (considering *n*-butyl acetate = 1) appeared to be about 4–5: below 0.8, the evaporation rate is considered to be slow, medium from 0.8 to 3 and high above 3.0 [29].

On the contrary, Baghdachi et al. demonstrated that phase separation is not affected by solvent evaporation rate in a thermosetting polyurethane coating formulation, but largely kinetically controlled in common thermosetting systems [14].

2.2.1.3. Pigments. Pigments were first and foremost used for stratification detection, before being employed for upgrading the properties of the coating when well-chosen. Their absorbing properties, as well as their particle size and their affinity toward a medium are of high importance. Recent research works seem to establish that, depending on the type of substrate and on the desired final properties, aesthetic and anti-corrosive characteristics are favored. It is generally considered that "this type of coating, where only one layer (usually the lower layer) is pigmented, is encountered industrially especially in automotive applications and is often called 'base coat/clear coat' system" [10].

It has been reported that when well chosen, pigments have no negative effect on the stratification process and that the degree of phase separation is the same or is even better than in the case of pigment-free systems. They will essentially affect the visual appearance and the adhesion of the coating compared to unpigmented systems, depending mainly on their dispersion and on the wettability of the pigment [23]. From the most compiled papers, pigments well wetted in the phase in which they are dispersed remain in their original dispersion phase after the mixing of the two dispersions. However, Benjamin et al. showed that, under given conditions, the pigment can migrate through the whole film thickness of the coating and impair the stratification. It was thus suggested that pigments have not the same affinity with either the topcoat or the basis resin and need to be dispersed in the medium for which they have the higher affinity [8,10,24]. In particular cases, the migration of pigment toward the other medium, without affecting the stratification, have been evidenced [23].

The addition of a second pigment is difficult but has been achieved by Benjamin and his collaborators on metallic substrates using a silane coated titanium dioxide pigment located in a fluorinated polyether [10]. It was found that the addition of TiO₂ to systems showing a high level of stratification with a single pigment

has an unfavorable effect on the paint (low level or no stratification).

Vink studied deeply the binary mixture of Epikote 1001/Alloprene R10 with the incorporation of a pigment in each phase (Table 5). He showed that pigments generally stay in their dispersion phase. It seems that stratification is better when only one pigment is incorporated into the system (formulation n°6–stratification ranking = 1/2) compared to the bi-pigmented systems (formulation 2–5–stratification ranking = 2). While investigating the different factors influencing stratification, he figured out that its degree can even be enhanced by a particular pretreatment of the pigment with an adhesion promoter. Moreover, he demonstrated that the effect of the promoter depends both on its type and on the system studied. For example, a silane promoter has a non-negligible influence on the Epikote 1001/Alloprene R10 system compared to the Epikote 1001/Laroflex MP45 one: the nature of interaction between the adhesion promoter and the resin is clearly of importance [29].

Finally, pigment density and gravity do not impart the process [8,10,29], and particles with rather different sizes are necessary for a good stratifying system, but not for color stability [9]. Moreover, it was shown that in a two-pigments system, the difference in particle size is critical which, afterward, led to the conclusion that all factors which are known to affect the floating process will also affect the stratification process [29].

2.2.1.4. Other additives. Additives are not widely used in self-stratifying coatings since the majority promotes the compatibility of both resins instead of disfavoring it. Moreover, it can be noticed that additives which prevent from cell formation inhibit the layering [9].

Decompatibilizers are sometimes used to substantially accelerate the phase separation process with moderate or negligible influence on the composition of equilibrium solutions. Silicon or fluorinated oligomers (i.e. oligomers or polymers) are particularly employed because of their immediate incompatibility with conventional resins [22]. Also called stratification promoters, they bring higher gloss and scratch resistance to the coating, but also give poorer protective properties [11]. Silicone based modifiers have negative effect on the permeability and insulation properties of both homophase and heterophase matrix coatings (probably by inducing a rougher polymer structure) [21].

Wetting and dispersing agents are mainly concerned. Leveling agents do not modify the film aspect but deteriorate the level of phase separation: type I coatings tend to become type II coatings with the addition of this type of additive [8]. Flow control agents and surface active agents were proven to cause the same damage on the resulting coating. Nevertheless, Disperbyk 300 and 307 surfactants have shown acceptable stratified pattern [29].

Dispersion aids are sometimes used when an anticorrosive barrier pigment is added, and an improved pigment separation was observed when silane modified TiO₂ is used as pigment. Usually, silane contains epoxy groups [24].

In Table 6, several examples of additives commonly used in coating formulations are presented. Their impact on the stratification in an acrylic/epoxy system is highlighted: in all case, the degree of stratification became worse [29].

Solubility parameters and surface tensions are critical parameters to take into account when dealing with stratification, and thus have to be determined for all the materials used in the paint formulation. The solubility behavior of chemicals is determined experimentally by the Hansen's solubility parameters.

2.2.2. Hansen's solubility parameters

The first study on the solubility parameters was performed by Hildebrand and Scott [34,35] to define the hydrogen and polar

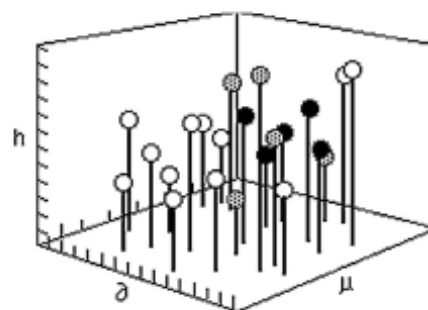


Fig. 17. A three dimensional box used to plot solubility information, δ = Hildebrand value, μ = dipole moment, h = hydrogen bonding value [36].

bonding. The main issue was to determine if hydrogen bonding significantly affects solvent retention or not. Solvents, polymers and resins, emulsifiers, pigments, plasticizers and dyes have been characterized according to this theory to determine solubility, mutual solubility and compatibility of polymers, resins and phases of pigment dispersion.

These experiments led to a new empirical concept which takes into account all the energies involved in the process: the Hansen solubility or the "three dimensional solubility" parameter (E), describing phenomena with an important solvent effect or where the materials involved can be characterized by their individual interactions with a series of solvents. A new aspect of solvent properties is studied and this method allowed predicting the paint behavior during the manufacturing and drying processes.

2.2.2.1. Crowley's approach. In 1966, Crowley introduced the first three dimensional system with axes given by the Hildebrand solubility parameter also called Hildebrand value δ , a hydrogen bonding parameter (h), and the dipole moment (μ). A scale representing each of these three variables is assigned to one of the edges of an empty cube (Fig. 17). Any point within the cube represents, in this way, the intersection of the three specific values. A small ball, supported on a rod, is placed at the intersection of values for each individual solvent. Each solvent is located within the cube and solubility tests are performed on individual polymers. A black ball means that the solvent dissolves the polymer; non-solvents are represented by white balls and partial solubility by a grey ball.

2.2.2.2. Hansen's approach. The 3D solubility parameters. The most widely accepted three component system is the three parameter system developed by Charles M. Hansen in 1966. He divided the total Hildebrand value into three parts: a dispersion force component, a hydrogen bonding component and a polar component.

His approach differs from the one of Crowley in two ways: (1) by using a dispersion force component instead of the Hildebrand value as the third parameter, and (2) by relating the values of all three components to the total Hildebrand value.

The solubility parameter was thus defined as the square root of the cohesive energy density [37]:

$$\delta = \left(\frac{e^0}{V_m} \right)^{1/2} \quad (4)$$

where $-e^0$ is the molar potential energy of the liquid and V_m is its molar volume. The solubility parameter unit is MPa^{1/2}.

The assignment of Hansen parameters is governed by an equation determining that the total cohesion energy E is given by the

Table 5
Stratification ranking of systems of Epikote 1001/Alloprene R10 in MIBK as a function of the type of pigment [29].

N	Epikote 1001/pigment	Alloprene R10/pigment	Stratification ranking ^a
1	Fe ₂ O ₃ , Bayferrox 140 M, 10%	Heliogen Blau, HB680, 5%	2/3
2	Fe ₂ O ₃ , Bayferrox 140 M, 20%	Heliogen Blau, HB680, 20%	2
3	Fe ₂ O ₃ , Bayferrox 140 M, 20%	Pigment Grün, Grün 6060, 20%	2
4	Heliogen Blau, HB680, 10%	Pigment Grün, Grün 6060, 20%	2
5	CrO ₂ , grün GN-M, 20%	TiO ₂ , Kronos LRK, 20%	2
6	CrO ₂ , grün GN-M, 20%	None	1/2

^a Ranking: 1 = optimum, 6 = no stratification.**Table 6**
Stratification of system Epikote 1009/Fe₂O₃–Alloprene R10/TiO₂ in MEK-MIAK as a function of additives.^a

Additive used in the 1st system (Epikote 1009/Fe ₂ O ₃)	Additive used in the 2nd system (Alloprene R10/TiO ₂)	Stratification ranking ^b
None	None	1
None	Lactimon or Byk 307	2
None	Byk 300	3
None	Disperbyk or Resiflow	4
Disperbyk	None, Lactimon or Byk 300	4
Disperbyk	Disperbyk or Resiflow	6
Byk 300	None, Lactimon or Byk 300	2/3
Byk 300	Disperbyk or Resiflow	4
Lactimon	None, Lactimon, Resiflow or Byk 300	4
Lactimon	Disperbyk	6
Resiflow	None, Lactimon, Byk 300 or Resiflow	6
Byk 307	None or Byk 307	2

^a Disperbyk: alkylammonium salt of polycarboxylic acid (dispersant Byk); Byk 300/307: polyether modified dimethylpolysiloxane, 52% in xylene/BuOH nad pure, respectively (surface active agents, Byk); Lactimon: alkylammonium salt of copolymer of polycarboxylic acid and polysiloxane (flow control agent, Byk); Resiflow W50: polyacrylate (flow control agent, Worlée).^b Ranking: 1 = optimum, 6 = no stratification.

sum of the individual energies (dispersive ΔE_d , polar ΔE_p and hydrogen bonding forces ΔE_h):

$$\Delta E = \Delta E_d + \Delta E_p + \Delta E_h \quad (5)$$

Dividing this equation by the solvent molar volume leads to an equality between the square of the total (or Hildebrand) solubility parameter and the sum of the squares of the Hansen dispersion, polar and hydrogen bonding components:

$$\frac{\Delta E}{V_m} = \frac{\Delta E_d}{V_m} + \frac{\Delta E_p}{V_m} + \frac{\Delta E_h}{V_m} \quad (6)$$

Or

$$\delta^2 = \delta_d^2 + \delta_p^2 + \delta_h^2 \quad (7)$$

Then, $\delta_d = \left(\frac{\Delta E_d}{V_m}\right)^{1/2}$, $\delta_p = \left(\frac{\Delta E_p}{V_m}\right)^{1/2}$, $\delta_h = \left(\frac{\Delta E_h}{V_m}\right)^{1/2}$ represent respectively the effects of the dispersion, polar and hydrogen bonding forces. In this way, for a given solvent, the three dimensional solubility parameter can be considered as a vector of δ_d , δ_p and δ_h and thus can be located in a three dimensional system with the dispersion axis, the polar axis and the hydrogen bonding axis constituting the axes of the system [38].

Charles Hansen also used a three-dimensional model to plot polymer solubility. He found that, by doubling the dispersion parameter axis, an approximately spherical volume of solubility would be formed for each polymer. This spherical volume can be described in a simple way: the coordinates at the center of the solubility sphere are located by means of three component parameters (δ_d , δ_p , δ_h), and the radius of the sphere is called the interaction radius (δ_a). Table 7 gives the Hansen parameters and interaction radius of several polymers.

2.2.2.3. *Thermodynamic background.* In thermodynamics, the free energy of mixing must be negative or equal to zero for the solu-

tion process to occur spontaneously. The free energy change for the solution process is given by the relationship:

$$\Delta G^M = \Delta H^M - T\Delta S^M \quad (8)$$

where ΔG^M is the free energy of mixing, ΔH^M is the heat of mixing, T is the absolute temperature, and ΔS^M is the entropy change in the mixing process. Hildebrand and Scott proposed an equation giving the energy of mixing for non-polar liquids:

$$\Delta E^M = \varphi_1\varphi_2(X_1V_{m1} - X_2V_{m2})(\delta_1 - \delta_2)^2 \quad (9)$$

in which φ_1 and φ_2 are volume fractions of solvent and polymer, X_1 and X_2 the molar fractions and V_{m1} and V_{m2} the solvent and polymer volumes. Respectively, according to this equation, it demonstrates that at constant composition, ΔE^M will be low when the solubility parameters of the liquids or polymers are close. Also, ΔE^M will be smaller for liquids of low molar volume.

Experimental approach: To determine the Hansen Solubility Parameters (HSP) of a liquid or polymer, the resin is mixed with up to 56 solvents of known solubility, with a concentration of solids between 10 and 60 wt.%. The solubility is determined after 24 h, 7 days and 4 weeks. The HSP consider specifically three parameters: the energy from dispersion forces δ_d (van der Waals), dipolar intermolecular forces δ_p (related to dipole moment) and hydrogen bonds δ_h between molecules. These parameters correspond to the coordinates of the solubility sphere of the material in the Hansen space. The center of the sphere is the HSP of the tested material and the radius defines the limits of non-dissolving solvents. The solubility parameter "distance" between two materials 1 and 2, Ra, is based on their respective partial solubility parameter components:

$$Ra^2 = 4(\delta_{d1} - \delta_{d2})^2 + (\delta_{p1} - \delta_{p2})^2 + (\delta_{h1} - \delta_{h2})^2 \quad (10)$$

The smaller Ra (thus the nearer two materials), the greater is the probability for the two materials to be compatible (to dissolve into each other). This equation was developed from plots of experi-

Table 7
Hansen Parameters and Interaction Radius of Polymers [39].

Type and trade name of polymers Polymer (trade name, supplier)	δ (MPa ^{1/2})			
	δ_d	δ_p	δ_h	R
Cellulose acetate (Celliclore [®] A, Bayer)	18.6	12.7	11.0	7.6
Chlorinated polypropylene (Parlon [®] P-10, Hercules)	20.3	6.3	5.4	10.6
Epoxy (Epikote [®] 1001, Shell)	20.4	12.0	11.5	12.7
Isoprene elastomer (Cerijflex [®] IR305, Shell)	16.6	1.4	-0.8	9.6
Cellulose nitrate (1/2 sec, H-23, H form)	15.4	14.7	8.8	11.5
Polyamide, thermoplastic (Versamid [®] 930, General Mills)	17.4	-1.9	14.9	9.6
Poly(isobutylene) (Lutonal [®] IC-123, BASF)	14.5	2.5	4.7	12.7
Poly(ethyl methacrylate) (Lucite [®] 2042, DuPont)	17.6	9.7	4.0	10.6
Poly(methyl methacrylate) (Rohm and Haas)	18.6	10.5	7.5	8.6
Polystyrene (Polystyrene LO, BASF)	21.3	5.8	4.3	12.7
Poly(vinyl acetate) (Mowilith [®] 50, Hoechst)	20.9	11.3	9.6	13.7
Poly(vinyl butyral) (Butvar [®] B-76, Shawinigan)	18.6	4.4	13.0	10.6
Poly(vinyl chloride) (Vilpa [®] KR, k=50, Montecatini)	18.2	7.5	8.3	3.5
Saturated polyester (Desmophen [®] 850, Bayer)	21.5	14.9	12.3	16.8

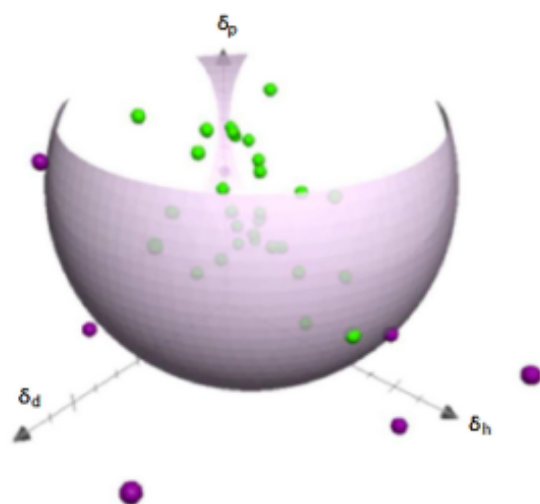


Fig. 18. 3D Hansen solubility sphere.

mental data [40]. Then, the Relative Energy Difference, RED, can be defined to determine the solubility space:

$$RED = \frac{Ra}{Ro} \quad (11)$$

If the RED number is equal to 0, there is no energy difference between the two materials. A RED number lower than 1 indicates a high affinity (system will dissolve) whereas a higher RED number indicates lower affinity (system will not dissolve). A RED number equal or close to 1 means the partial dissolution of the system.

In Fig. 18, the solute is represented by the sphere and the green (good solvent) and purple (non-solvent) balls represent solvents tested. All balls located inside the sphere represent the solvents that can dilute the solute according to this theory.

The ratio $\left(\frac{Ra}{Ro}\right)^2 = RED^2$ is a ratio of cohesion energies. This quantity is important to relate the Hansen solubility parameter approach to the theory of Huggins and Flory.

When the compatibility behavior of a given polymer towards solvents is determined, it also allows a comparison with other pre-selected materials. If two resins have their solubility spheres in the Hansen's space located in sufficiently distinct positions, then they are expected to be only partially compatible. As a matter of fact, the volume of the overlap region between the two solubility

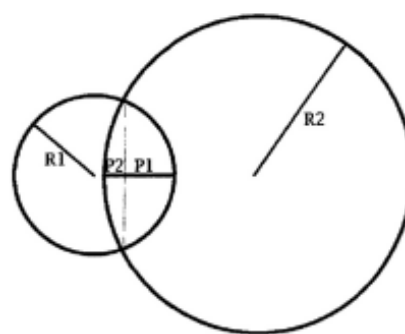


Fig. 19. Overlap between solubility spheres [10].

spheres can be used to predict the compatibility of resins, and thus the stratification.

The lower the common volume, the lower the expected compatibility. The volume of the overlap region can be calculated from the equation [10]:

$$C = \frac{1}{3} \pi [P_1^2 (3R_1 - P_1) + P_2^2 (3R_2 - P_2)] \quad (12)$$

C represents the overlap volume of the spheres, P_1 and P_2 the height of the sphere segments (Fig. 19), R_1 , R_2 the radii of the spheres (R_1 is the smaller sphere).

The overlap factor V allows to compare the relative sizes of the common volume between two resins (Fig. 20). It is expressed as a percentage of volume of the smaller sphere:

$$V = 100 \frac{C}{\frac{4}{3} \pi R_1^3} \quad (13)$$

For the stratification process to occur, it has been stated that $V < 80\%$ is necessary, but this condition is not sufficient to obtain stratification [29,38]. Thus, this model needs to be carefully considered when studying the compatibility between binary mixtures of polymers.

Different assumptions have been made to plot the Hansen solubility parameters. The Teas graph (Fig. 21) is one example of triangular planar graph based on the assumption that all materials have the same Hildebrand value. Solubility behavior is thus determined by the relative amounts of the three component forces

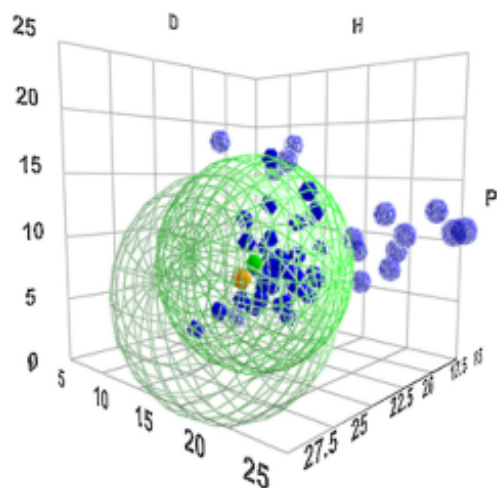


Fig. 20. Two Hansen solubility spheres in the Hansen space.

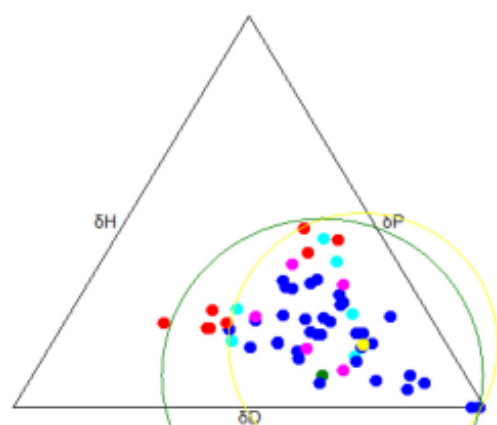


Fig. 21. Teas graph of Neocryl B875 (DSM).

contributing to the total Hildebrand value [36]. The Hildebrand solubility parameter (cohesive energy density) is also defined by:

$$\delta = \sqrt{\frac{\Delta H_v - RT}{V_m}} \quad (14)$$

with ΔH_v the heat of vaporization, V_m the molar volume in the condensed phase, R the gas constant and T the temperature.

Teas parameters (called fractional parameters) are mathematically derived from Hansen values and indicate the percent contribution of each Hansen parameter towards to the whole Hildebrand value:

$$f_d = \frac{f_d}{f_d + f_p + f_h} \quad f_p = \frac{f_p}{f_d + f_p + f_h} \quad f_h = \frac{f_h}{f_d + f_p + f_h} \quad (15)$$

In other words, if all three fractional parameters are added together, the sum will always be the same:

$$f_d + f_p + f_h = 100 \quad (16)$$

It has to be taken into account that Hildebrand values are not the same for all liquids. Consequently, the Teas graph remains an empirical system. Solvent positions were originally defined on the

graph according to Hansen values (using Eq. (1)), and subsequently adjusted to correspond to exhaustive empirical testing.

It is also interesting to notice that visual observations can be coupled with this model. Vink and T.L. Bots demonstrated that at $V > 90\%$, films are mostly translucent which is consistent with compatible resins. At $V < 90\%$, films are not translucent indicating incompatibility. Consequently, the structure appears to be dependent on the V value. Between 70 and 90%, a matt homogeneous structure is obtained, whereas at lower V value, the structure is much coarser [29].

2.2.3. The substrate

The substrate plays an important role in the self-stratifying process and particularly its surface tension. According to the literature, polymers, aluminum, glass and steel are the main substrates to be coated.

Toussaint focused her work on plastic substrates that have a lower surface energy than metals: polypropylene, poly(ethylene propylene diene monomer), poly(acrylonitrile)/butadiene styrene (TF60), polyphenylene oxide (Noryl) and polycarbonate (Lexan) with various commercially available binders [8].

Steel substrates have a high surface energy (41.3 mN m^{-1}) and need special treatment before the application of any coating to reduce the surface energy [41]. The adhesion to steel is also better when the polarity of the metal increases [42].

Abbasian et al. studied the stratification phenomenon of epoxy-acrylic coatings on aluminum and glass substrates and figured out that most of the stratified coatings were formed on glass substrates [28]. According to Carr theory, stratified coatings require a selective substrate wetted by one of the two resins, which means that the interfacial tension between the substrate and one of the polymers should be very low, and this polymer should also have a selective affinity with the substrate [6]. However, in terms of surface free energy, both aluminum and glass have a high surface free energy (57.8 and 28.9 mN m^{-1} respectively) and experimental results are not compatible with Carr theory. They concluded that there is a competition between enthalpic and entropic effects on adsorption and that the theory from thin films to thick films suffers from shortcomings. Although the minimum surface free energy is a non-negligible parameter for the stratification process, the entropy reduction of the polymeric chains has also to be taken into account since the large difference between two polymers strengthens the entropic effect. Fig. 22 shows different films obtained on aluminum and glass substrates.

In Fig. 22(a), the non-stratified system on aluminum plate shows a regular phase separated structure, as usually observed in incompatible mixtures, whereas on Fig. 22(b), the system developed for a glass substrate has stratified and shows a relatively thin stratified layer and a normal phase separated back layer. In Fig. 22(c), high stratification is exhibited without any normal phase separation in the lower layer.

2.2.4. The processing

2.2.4.1. Viscosity. Viscosity influences the stratification process since it has an impact on solvent evaporation, on pot life (thus on the crosslinking when there is a curing agent). If the viscosity is too high, the process will have problems to stratify properly.

2.2.4.2. Temperature. The processing temperature has an impact on the stratification process since it influences solvent evaporation and crosslinking rates (if a third component is involved in the formulation).

A high temperature favors solvent evaporation and accelerates crosslinking reactions. However, processing with a too high temperature will prevent stratification since phase separation has to take place before the film formation.

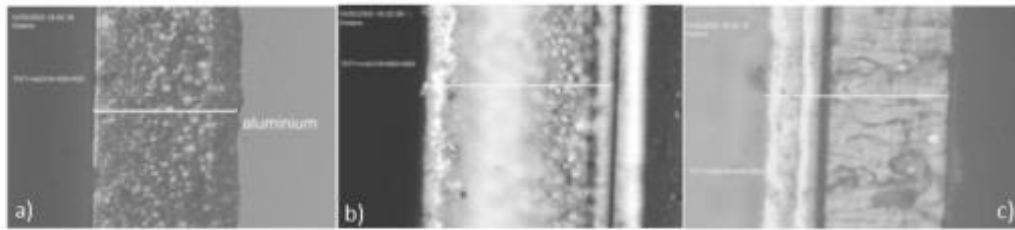


Fig. 22. Example of non-stratified coating on aluminum (a), of slightly stratified coating on glass (b) and highly stratified coating on glass (c)—glass on the right (800- μm film) [28].

I-4-8 Models to build self-stratifying systems

In order to predict whether a system of two polymers or resins in a solvent mixture will self-stratify, researchers have developed different models: the UNIFAC model and a model based on surface tension relationships.¹²³ Most of these models are commonly used by scientists. However, it has to be taken into account that a typical coating is a complex system made of many interactive and reactive components. Thus, the properties of the resulting coating are affected by numerous factors (interaction between coating ingredients, solvent evaporation, application method, storage, environmental conditions ...).¹¹⁴ Consequently, some authors have demonstrated that these models are not always reliable and need to be carefully considered.

The UNIFAC model aims at predicting phase behavior, vapor pressure, evaporation rate and surface tension for systems containing two polymers or resins in a solvent mixture. The second model predicts which system will give rise to self-stratification when the surface energy and the concentration relationship of the pure resins in solution are given.

3.1. UNIFAC model

Different systems of resins were used to establish this model: acrylic/acrylic, epoxy/acrylic and alkyd/acrylic resin combinations.

3.1.1. Theory

3.1.1.1. *Phase separation.* Phase separation analysis, also called liquid-liquid equilibrium, is divided in two parts: the detection of phase separation and the calculation of the phase separation point.

This model consists in checking if a matrix A is positive in a precise range of concentration. The matrix A represents the second derivative of the Gibbs free energy of mixing ΔG_{mix} , and is given by the equation:

$$A_{ij} = \frac{\partial^2 \Delta G_{mix}}{\partial x_i \partial x_j} \quad i, j = 1, 2, \dots, NC-1 \quad \text{where } \Delta G_{mix} = RT \sum_i^{NC} \ln(a_i) \quad (17)$$

with NC the number of components in the system, a_i the activity of the component i in the solution, which is equal to $x_i \omega_i$ (with x_i the

Table 8
Experimental (into brackets) and calculated concentrations to predict phase separation [41].

Epoxy/Acrylic Ratio	Phases	Solids (wt.%)	Epoxy resin (wt.%)	Acrylic resin (wt.%)	MIBK (wt.%)	Xylene (wt.%)
1:1	I	– (29)	– (10)	– (19)	– (26)	– (45)
	II	–	– (28)	– (2)	– (23)	– (47)
3:1	I	27.8 (30)	12.2 (15)	15.6 (15)	24.7 (25)	47.6 (45)
	II	32.0 (36)	32.0 (35)	0.0 (1)	24.3 (21)	43.7 (43)
5:1	I	27.3 (30)	12.4 (16)	14.9 (13)	24.8 (25)	47.9 (46)
	II	31.4 (33)	31.4 (33)	0.0 (0)	24.4 (22)	44.3 (45)
9:1	I	26.9 (30)	12.6 (28)	14.3 (2)	24.8 (20)	48.3 (50)
	II	30.8 (32)	30.8 (31)	0.0 (1)	24.4 (25)	44.8 (43)

I: Upper phase, II: Lower phase of the coating, "–" = no separation.

mole fraction of the component i and ω_i the activity coefficient of i).

The equilibrium condition is also expressed with the isofugacity criterion: $a_i^I = a_i^{II}$ with a_i^I and a_i^{II} the activity of the component i in phase I and phase II respectively.

An iterative procedure is then used to solve this N linear equation system (one for each component).

3.1.1.2. Evaporation rate. The evaporation rate is divided into two categories for its calculation: external factor and components

External factors take into account the environmental conditions: temperature, humidity, air velocity and surface geometry. Component factors include diffusion coefficient in air, vapor pressure, heat of vaporization and activity coefficient.

The mass transfer occurring during evaporation is caused by the difference between concentrations at equilibrium and bulk concentrations. Thus, the evaporation rate is expressed by:

$$R_i = k_i (y_i^{eq} - y_i^0) + y_i^{eq} \sum R_i \quad (18)$$

with y_i^{eq} the equilibrium concentration of component i , dependent on the vapor pressure of the pure component, y_i^0 the bulk concentration of component i in the vapor phase, k_i the mass transfer coefficient of component i dependent on the molecular weight (MW_i), on the diffusion coefficient in air of component i (D_i) and on the air velocity (\dot{V}_{air}) ($k_i = 46MW_i D_i^{0.58} \dot{V}_{air}^{0.68}$).

The differential balance then expresses the variation of evaporation: $dM_i = AR_i dt$ with dM_i the amount of component i evaporated during the time interval dt , and A the surface area of the film (constant). The total amount evaporated during dt is thus expressed as:

$$dM_t = Adt \sum R_i \quad (19)$$

To solve this equation, the total change of mass per time interval is defined as 1.0% of the initial weight and the equation is then solved numerically by iteration. The numerical iteration is stopped when the percentage of solvent is above 10%.

3.1.1.3. Surface tension. Equation for a non-ideal mixture has been used in the model. Numerical iteration (Newton-Raphson iteration) is also used with the thermodynamic equation:

$$\bar{A}_i \gamma_{mix} = A_i \gamma_i - RT \ln \left(\frac{x_i \bar{\omega}_i}{x_i^{surf} \bar{\omega}_i^{surf}} \right) \quad i = 1, 2, \dots, NC \quad (20)$$

with \bar{A}_i the partial molar surface area of component i in the mixture, x_i the molar fraction of component i in the bulk liquid phase, x_i^{surf} the mole fraction of component i in the surface layer, $\bar{\omega}_i^{surf}$ the activity coefficient of component i in the surface layer, $\bar{\omega}_i$ the activity coefficient of component i in the bulk liquid phase. Moreover, $\sum x_i^{surf} = 1$ and the surface area $A_i = CV_i^{1/3}$ with V_i the molar volume of component i , C a constant. γ_{mix} , x_1^{surf} , x_2^{surf} , ... x_{NC}^{surf} are solved numerically using the iteration method.

3.1.2. Experimental approaches to check the validity of the model

Different systems were used to confirm the accuracy of the model.

3.1.2.1. Phase separation. Phase separation was measured experimentally and calculated for each system. In Table 8, the theoretical and experimental concentration data for an epoxy/acrylic system in MIBK: xylene (7:13) are detailed at 25 °C using different ratios. The polymer concentration was set at 30 wt.-%.

Table 9
Experimental (into brackets) and theoretical percent solids at phase separation for different ratios of acrylic: PMMA [41].

System	Acrylic/PMMA ratio		
	1:4	1:1	4:1
Acrylic: PMMA 10	23(-) ^a	30(-)	91(-)
Acrylic: PMMA 40	10(13)	9(11)	18(11)
Acrylic: PMMA 65	8(10)	6(8)	12(7)

^a No separation observed experimentally.

Table 10
Composition of solvent mixtures used in Fig. 23(c).

Solvent mixture	Composition (wt.%)
S1: MIBK - Xylene	50:50
S2: MIBK - Xylene - Dowanol PM	50:30:20
S3: Xylene	100

After calculation, the model predicts that no phase separation occurs at a 1:1 ratio, which is not in accordance with experimental results. It can also be seen that the calculated phase separation is not as sensitive to the polymer concentration as experimentally observed. For the 3:1 and 5:1 ratios of epoxy: acrylic resins, experimental and calculated results are in acceptable agreement. For the 9:1 ratio, the calculated composition of phase I does not correspond to the experimental results.

The influence of the molecular weight of one polymer in a two polymer system was also studied. Different acrylic (MW = 40 000 g mol⁻¹)/PMMA (MW varied between 10 000 and 65 000 g mol⁻¹) blends were dissolved in butyl ethanoate at 25 °C. Calculated values and experimental measurements of the percent solids at phase separation are compared in Table 9.

Calculated and experimental data are in accordance except when PMMA has a too low molecular weight, no phase separation occurs. Calculations predict a minimum percent solids at phase separation for a 1:1 ratio of acrylic: PMMA 40 and 65. On the contrary, experimental results show that the percent solids at phase separation decrease with the increase of PMMA molecular weight.

To conclude, the UNIFAC model can be used to predict phase behavior of polymer-polymer-solvent systems, even when the two polymers have a slight molecular weight difference (not too high). However, the model does not predict that the percent solids at phase separation depends on the ratio of the polymers involved.

3.1.2.2. Evaporation rate. Several experiments were set up to illustrate the factors that can influence evaporation of solvent. Different epoxy/acrylic systems were used as examples. Evaporation profiles were drawn, they showed that:

- The drying time decreases slightly when molecular weight of the epoxy increases as shown in Fig. 23(a), where the type of epoxy resin (Epikote, see Table 2 was varied in the three epoxy/acrylic systems).
- In Fig. 23(b), it can be seen that the ratio of polymers involved has no real influence on the drying time.
- The drying time is very dependent on the selected solvent mixture as observed in Fig. 23(c). Solvents with a high vapor pressure evaporate faster than solvents with a low vapor pressure. The composition of the three solvent blends tested in Fig. 23(c) is detailed in Table 10.

Evaporation rate, phase separation and surface tension have been calculated for a large amount of systems containing an acrylic polymer (varying the type, molecular weight or ratio of the second polymer and varying the type of solvent mixture). The results

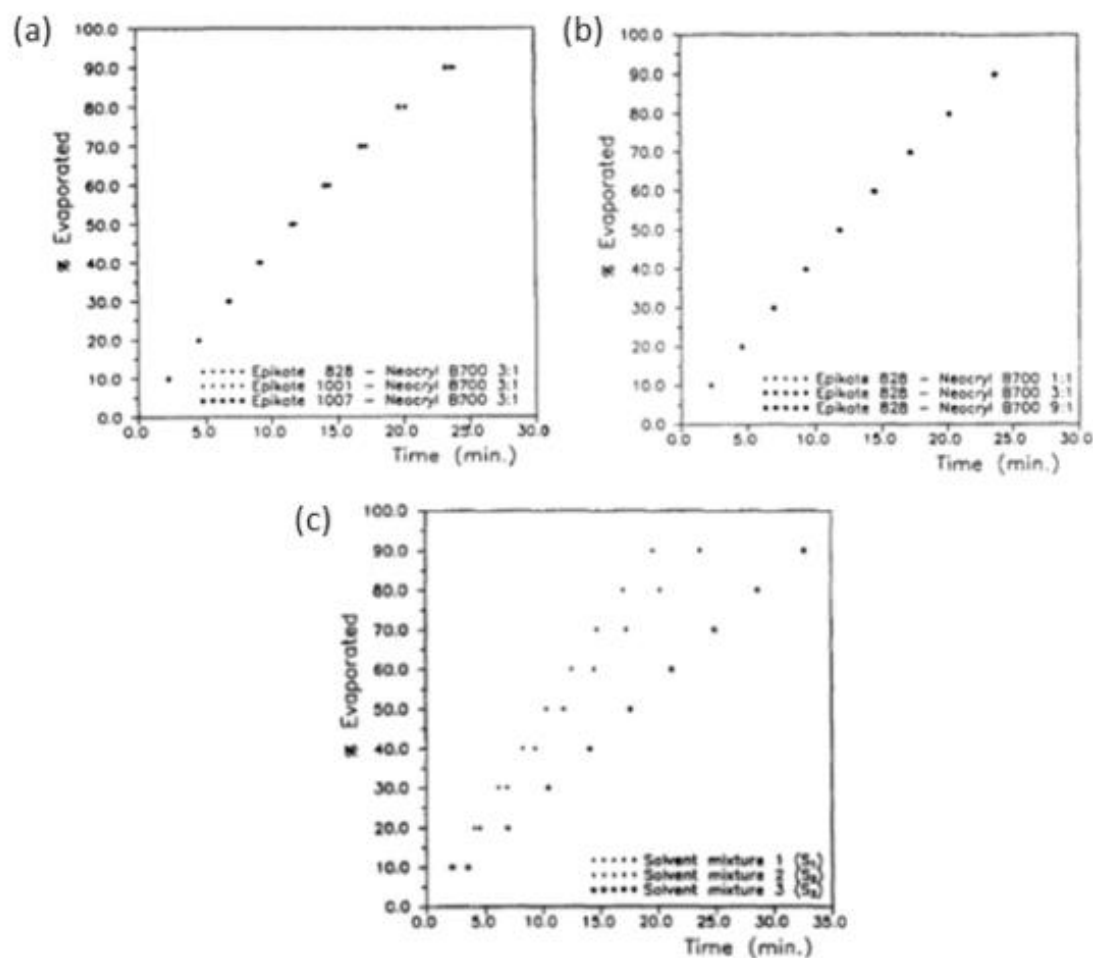


Fig. 23. (a) Blends of Epikote/Neocryl B700 at 3:1 ratio in MIBK/xylene; (b) Blends of Epikote 828/Neocryl B700 in MIBK/xylene at different polymer ratio; (c) Evaporation rate (%) vs. time (min.) for an epoxy/acrylic system (3:1 ratio) in different solvent mixtures (S1–S3) [41].

demonstrated that the UNIFAC model can estimate quite precisely the point of phase separation in a two polymer epoxy/acrylic type of system but not for an acrylic/alkyd system (calculations are not in accordance with experimental results).

3.2. Model based on surface energy

The work of Funke on self-stratifying powder coatings demonstrated that surface energy difference between two resins is the primary driving force for stratification [2]. Thus, some researchers tried to develop a model based only on surface free energy relationship of two polymer solution phases.

3.2.1. Theory

This model requires to know the surface energies and the interfacial surface tension of the two phases, and the surface energy of the substrate used. It is assumed that the concentrations of the two phases remain constant and that each phase contains predominantly one of the resin components. In reality there is a continuous variation of the surface tension while the solvent evaporates, but

it is assumed that the surface energy of the pure solid resin can be used as an approximation for the predictions.

When a phase is dispersed in another one, the coalescence is thermodynamically favored, unless particles are stabilized somehow, which leads to a decrease of interfacial area and thus of the surface energy of the system. For stratification to occur in a thin film, it can be stated that:

- The intended base coat component must spontaneously wet the substrate
- The total surface and interfacial surface tensions of the layer system must be as low as possible

Fig. 24 represents a scheme of the different layers of the coating and surface and interfacial tensions influencing the stratification process.

According to Young's equation:

$$\gamma_{s1} - \gamma_{s2} - \gamma_{12} \cos \theta = 0 \quad (21)$$

with γ_{s1} the substrate/resin 1 interfacial surface tension, γ_{s2} the substrate/resin 2 interfacial surface tension, γ_{12} the interfacial ten-

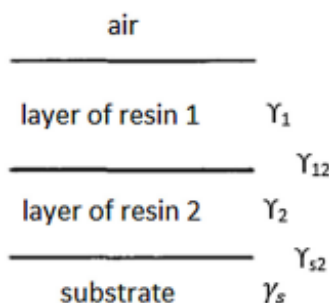


Fig. 24. Interfaces in a two-component coating film.

Table 11
Surface energy values for various substrates.

Substrate	γ^d (mN m ⁻¹)	γ^p (mN m ⁻¹)	γ^{total} (mN m ⁻¹)
Uncleaned steel	36.5	4.8	41.3
Acetone cleaned steel	28.7	15.6	44.3
Abraded steel	32	34	66
Aluminum foil	30.3	27.5	57.8
Polypropylene	25.6	7.1	32.7
Polypropylene oxide	32.0	11.2	43.2
Polycarbonate (Lexan)	35.6	10.7	46.3

sion between the two resins and θ the contact angle between the resin 2 and the substrate.

To follow the spontaneous wetting of the substrate, the surface energy of the system should decrease; thus:

$$\gamma_s - \gamma_{s2} - \gamma_{12} - \gamma_1 > 0 \quad (22)$$

with γ_s the surface energy of the substrate. The total surface and interfacial surface tension of the layer system must be as low as possible, which means that the required layer sequence is the most favorable when:

$$\gamma_{s1} + \gamma_{12} + \gamma_2 > \gamma_{s2} + \gamma_{12} + \gamma_1 \quad (23)$$

$$\gamma_{s1} - \gamma_1 - \gamma_{s2} + \gamma_2 > 0 \quad (24)$$

3.2.2. Experimental approaches to check the validity of the model

According to the Harmonic Mean method of Wu [44] and the Young's law, any surface energy can be calculated if contact angles of two reference liquids are known.

For an interface between two materials, Wu expressed the interfacial surface tension by the following relationship:

$$\gamma_{12} = \gamma_1 + \gamma_2 - \frac{4\gamma_1^d \gamma_2^d}{\gamma_1^d + \gamma_2^d} - \frac{4\gamma_1^p \gamma_2^p}{\gamma_1^p + \gamma_2^p} \quad (25)$$

with γ_1 and γ_2 the total energies of resins 1 and 2 respectively. This method is mostly used for the calculation of surface free energy for polymers with low surface free energy (up to 30–40 mN m⁻¹). Table 11 reports the results of surface energies calculated for various substrates.

Table 12
Theoretical and experimental surface free energy values on PC [8].

Resin 1	Resin 2	$\gamma_{s1} - \gamma_{s2} - \gamma_{12} \geq 0$	$\gamma_{s1} - \gamma_1 - \gamma_{s2} + \gamma_2 > 0$	$\gamma_s - \gamma_{s2} - \gamma_{12} - \gamma_1 > 0$	Theory	Exp.
Lumiflon LF 200	Plexigum M 890	-5.49	5.30	3.00	X	X
Lumiflon LF 200	Plexigum PM 381	0.49	3.03	8.97	✓	✓
Lumiflon LF 302	Plexigum M890	-2.92	4.19	2.69	X	X
Lumiflon LF 200	Desmolac 2770	0.003	0.85	8.51	✓	✓
Desmophen 4125	Lumiflon LF 200	0.69	7.16	12.81	✓	✓
Lumiflon LF 200	Synthacryl VSC 11	-5.30	5.48	3.19	X	X

Table 13
Commercial name and type of resins tested [8].

Resins	Type
Lumiflon LF 200	Fluorinated polyether
Lumiflon LF 302	Fluorinated polyether
Desmophen 4125	Epoxy resin
Plexigum M890	Thermoplastic acrylic
Plexigum PM 381	Thermoplastic acrylic
Desmolac 2770	Polyurethane
Synthacryl VSC 11	Thermoplastic acrylic

3.2.2.1. Prediction of stratification from solid resin surface energies.

To sum up, based on surface energy considerations, the three conditions to be satisfied for stratification to be theoretical assessed are:

$$\gamma_{s1} - \gamma_{s2} - \gamma_{12} \geq 0 \quad (26)$$

$$\gamma_{s1} - \gamma_1 - \gamma_{s2} + \gamma_2 > 0 \quad (27)$$

$$\gamma_s - \gamma_{s2} - \gamma_{12} - \gamma_1 > 0 \quad (28)$$

If the disperse and polar contributions of all components (the two pure resins and the substrate) are known, these conditions can be calculated and the prediction of stratification from solid resin surface energies is possible.

The results of calculated and experimental data are reported in Table 12 for six formulations coated on Lexan (a polycarbonate (PC)) [8]. The composition of the different resins is detailed in Table 13.

From Table 12, it can be seen that there is a good correlation between the predicted values given by the 3 conditions and the observations made from the experiments. These results suggest that this method can be used to predict stratification on PC. The same methodology was carried out on Teflon TF60, and among the three systems showing experimentally stratification, only one was confirmed by theoretical calculations. Results are presented in Table 14.

Thus, this model has to be used with care as theoretical calculations and experimental results do not always correlate. Indeed, this method does not take into account the influence of the solvent on surface energy, which could explain that the prediction is not valid for all systems. Moreover, since stratification occurs before the total evaporation of the solvent, this effect should be included in the model.

3.2.2.2. Prediction of stratification from solution surface energies.

The relationship between the surface tension and the resin concentration was measured experimentally and determined using the UNIFAC model. According to those results, the general form obtained is described by the equation:

$$\gamma_{mix} = \gamma_{sol} + A \exp(Bf) \quad (29)$$

with γ_{mix} the surface energy of the solution, γ_{sol} the surface energy of the solvent, f the weight fraction of the solvent and A, B two constants. A can be determined experimentally or using the relationship: $\gamma_r - \gamma_{sol}$ (for $f=0$) with γ_r the surface energy of the pure resin. This equation allows the determination of the total surface tension of a resin solution at any concentration.

Table 14
Surface free energy values on Teflon TF60 [8].

Resin 1	Resin 2	$\gamma_{s1} - \gamma_{s2} - \gamma_{12} \geq 0$	$\gamma_{s1} - \gamma_1 - \gamma_{s2} + \gamma_2 > 0$	$\gamma_s - \gamma_{s2} - \gamma_{12} - \gamma_1 > 0$	Theory	Exp.
Lumiflon LF 200	Plexigum M 890	-8.12	2.67	-7.19	X	X
Lumiflon LF 200	Plexigum PM 381	0.46	3.01	1.39	✓	✓
Lumiflon LF 302	Plexigum M890	-4.55	2.55	-7.50	X	X
Lumiflon LF 200	Desmolac 2770	-0.26	0.56	0.67	X	✓
Desmophen 4125	Lumiflon LF 200	-1.34	5.14	5.25	X	✓
Lumiflon LF 200	Synthacryl VSC 11	-8.00	2.78	-7.07	X	X

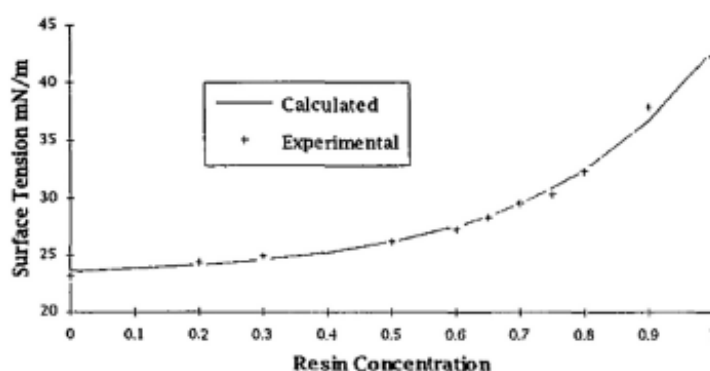


Fig. 25. Effect of resin concentration on surface tension of a blend of epoxy resin with MIBK [41].

As an example, Fig. 25 reports the calculated and experimental data of the effect of the resin concentration on surface tension of a blend of a Bisphenol-A epoxy resin with MIBK. Both data follow the same exponential trend: the higher the resin concentration, the higher the surface tension. The surface energy is dominated by the solvent or solvent mixture, except at high resin concentration where the addition of a small amount of solvent leads to an important decrease in the solution surface tension.

Then, in order to predict stratification, disperse and polar components of the surface tension must be known. It can be assumed that they vary in a similar way as the total surface energy. Polar and disperse contributions of the A coefficient are calculated from the following equations:

$$A^p = \gamma_r^p - \gamma_{sol}^p \quad (30)$$

$$\text{and } A^d = \gamma_r^d + \gamma_{sol}^d \quad (31)$$

The other constant of Eq. (29), B, is determined experimentally. From equations 30 and 31, and by assuming that there is no variation of concentration in the two phases, the prediction of the stratification can be determined by plotting the three conditions of stratification against resin concentration. Two examples are given in Fig. 26.

For the epoxy/acrylic system (Fig. 26(a)), all conditions are positive whatever the resin concentration. Stratification is thus predicted, which is in agreement with experimental data. For the second system (epoxy/fluorinated polyether resin) (Fig. 26(b)), the stratification is predicted up to 80% resin concentration. From this concentration, one of the three conditions becomes negative ($\gamma_{s1} - \gamma_{s2} - \gamma_{12}$): the model no longer predicts the stratification. This result can be explained by a reduction of movement between phases due to the high viscosity of the system.

According to the results obtained with both experimental and calculated data, the stratification process can be predicted – but with care – given the concentration dependence of the surface tension of resins in a solvent or solvent mixture. Several conclusions can be drawn from these results and particularly, mandatory conditions have to be fulfilled for the stratification to occur:

- The system should separate into two phases during the drying process.
- One polymer should be concentrated in one of the phases.
- The interfacial tension between the two liquid phases should be large enough to stop the second phase from being dispersed in the first phase.
- The total surface and interfacial energy of the required layer sequence must be as low as possible (the solvent mixture in the bottom phase has to have an affinity with the substrate and the polymer in the bottom phase is partly compatible with the substrate).

3.3. Model based on Hansen solubility parameters

A study performed by Vink and Bolt shows that although good stratification was obtained with resins having low overlap factors, other systems with the same characteristics did not stratify [29]. They tested systems containing an epoxy resin combined with different types of other resins in the presence of adhesion promoters (Table 15). For example, although the system Epikote 1001/Laroflex MP45 exhibits stratification with a V factor of 65.1, systems with lower V factor did not stratify (Epikote 1001/Neocryl B728).

This study also demonstrates that the adhesion promoter has an influence depending on the nature of interaction with the resin. In the case of the Alloprene R10 resin, depending on the adhesion promoter used, the level of stratification is ranked from 1 to 6.

The influence of the epoxy resin and solvents was also studied and a comparison was made between the overlap factor and the stratification level to see if Hansen theory correlates well or not with experimental results (Table 16). For the system Epikote 828/Alloprene R10, no stratification was observed, which correlates with the high V factor (96.2%). Moreover, well stratified films were obtained with lower V factors (40.2% and 22.6%), which is in accordance with Hansen theory.

Thus, as detailed in Section 2.2.2, Hansen solubility theory is not sufficient to predict stratification in a system, and has to be used with care.

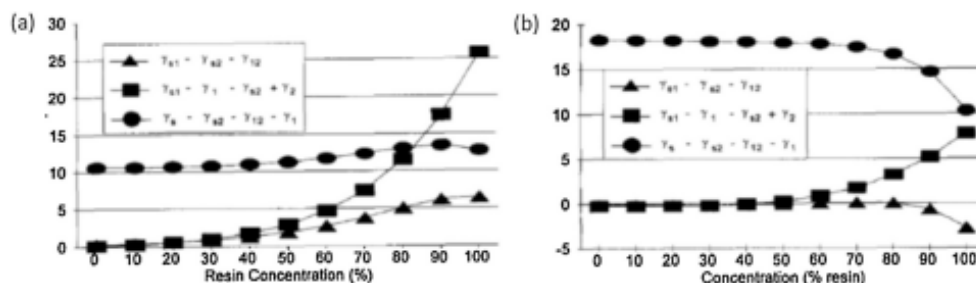


Fig. 26. Prediction of stratification (a) for a Bisphenol A epoxy/thermoplastic acrylic system in *n*-butyl acetate and (b) for a Bisphenol A epoxy/fluorinated polyether system [41].

Table 15

Stratification of combinations in MIBK of Epikote 1001/IBTMEO^a- treated Bayferrox 140M as first phase with physically drying binders containing TiO₂ (Kronos LKR, 10%) treated with adhesion promoters [29].

2nd phase		Overlap factor V (%)	Stratification ranking ^b
Resin	Silane (4%) ^c		
Vinylite VYHH	A189	83.8	4
	A174, A186, A187 or AMEO	83.8	6
Vinylite VAGH	A189 or AMEO	79.6	4
	A174, A186, A187	79.6	5
Laroflex MP45	AMEO	65.1	2
Neocryl B728	A174, A186, A187 or A189	65.1	3
	AMEO, A186, A189	42.9	5
Alloprene R10	A174 or A187	42.9	6
	AMEO	40.2	1
	A189	40.2	2
	A187	40.2	4
	A186	40.2	5
	A174	40.2	6

^a IBTMEO: isobutyl trimethoxy silane (Dynamit Nobel), A174: γ -methacryloxypropyl trimethoxy silane (Union Carbide); A186: β -(3,4-epoxycyclohexyl)ethyl trimethoxy silane (Union Carbide); A187: γ -glycidioxypropyl trimethoxy silane (Union Carbide); A189: γ -mercaptopropyl trimethoxy silane (Union Carbide); AMEO: γ -aminopropyl triethoxy silane (Dynamit Nobel).

^b Ranking: 1 = optimum stratification, 6 = no stratification.

Table 16

Stratification of pigmented system Epikote/Alloprene R10 as a function of the type of epoxy resin and solvent [29].

1st phase: Epikote/Fe ₂ O ₃		2nd phase: Alloprene R10		Overlap factor V (%)	Stratification ranking ^a
Epikote	Solvent	Epikote	Solvent		
828	MIBK	MIBK	MIBK	96.2	6
1001	MIBK	MIBK	MIBK	40.2	2
1004	MIBK	MIBK	MIBK	34.2	2
1007	MEK	MEK	MEK	19.4	2
1009	MEK	MEK	MEK	22.6	1
1004	MEK	MIAC	MIAC	22.6	2/3
1009	MEK	MIAC	MIAC	22.6	1
1009	MEK/MIAC	MIAC	MIAC	22.6	1/2
1009	MEK/MIAC	MEK	MEK	22.6	2/3
1009	MEK/MIAC	MEK/MIAC	MEK/MIAC	22.6	1

^a Ranking: 1 = optimum stratification, 6 = no stratification.

3.4. Model based on phase state diagram

Phase state diagrams can be used to predict the behavior of a multi-component system. In fact, such diagrams allow the representation of the composition of any blend of two or more components and to detect any change of composition [45]. A ternary phase diagram is used for two incompatible polymers in one common solvent, and a quaternary phase diagram for two incompatible components and two solvents.

Each point of the diagram corresponds to the state of the system as either a homophase solution, a metastable solution, which is about to separate into a heterophase blend, or a two-phase system. The principle of a phase diagram is illustrated in Fig. 27. The phase

separation process occurs when the point of composition crosses a binodal line, representing the border between stable homophase and non-stable heterophase systems. If the process is sufficiently low (near the equilibrium state), it generates particles of new phase (mechanism of nucleation and particle growth) and transforms the initial homophase blend into dispersed systems. However, if the process is fast or if there is a fast change in temperature, phase separation takes place when the point of composition reaches spinodal line. At this stage, phase separation occurs, creating structures belonging to the mutually penetrating phase networks [46].

In order to have an incompatible polymer blend to produce a self-stratifying coating, binders may be selected as an initial

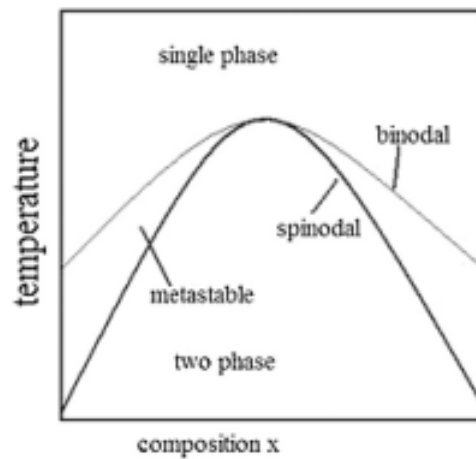


Fig. 27. Simplified phase diagram.

homophase system or as a two-phase liquid (a polymer/polymer emulsion).

Scientists from the Russian Academy of Science performed further investigations in this field, and developed an optical method to determine the location of the binodal and spinodal curves in the phase diagram of a stratifying liquid mixture. By using short laser pulses (light-induced phase transition), they quantitatively identified the limits of stability of a mixture with respect to stratification [47].

I-4-9 Promising self-stratifying coatings

Finally, a literature review on the most promising resin, solvent, additive and substrate combinations which have been developed up to recently to form self-layering compositions is proposed.

Since Funke introduced the concept of self-stratifying coatings [2], many scientists were involved in the design of such coatings and in the understanding of the involved in self-stratification.

The complexity of this process and the high number of influent factors generate a great amount of scientific papers, with sometime contradictory results. In those studies, the influence of a large range of commercially available and synthesized on the self-stratification process have been studied, as well as the effect of various curing agents (when the formulation includes a third component like polyisocyanate, polyamines. . .), substrates, pigments and solvents. Therefore, it is difficult to correlate the results of those studies and to draw general conclusions. Each factor needs to be carefully considered, taking into account the fact that its influence has not yet been fully elucidated and depends on the selected system.

Halogenated, epoxy, chlorinated rubber, vinylics, polyesters, alkyd, thermoplastic acrylics, non-reactive polyurethanes, siliconized polyether/alkyd/epoxy ester, thermosetting acrylics and fluorinated polyether resins have been carefully investigated lately to formulate self-stratifying coatings [48].

The most promising binary combinations, reported in the literature, are summarized in Table 17: typical basis resins with high free surface energy migrate to the substrate during the stratification process, and typical stratifying resins with low surface free energy migrate to the interface with air.

Interesting results were obtained with binary mixtures of thermoplastic and thermoset resins, and experiments led by Toussaint revealed that a blend of a thermoplastic and of a crosslinkable resin including a curing agent as a third component was the most successful system [8].

In the following part, promising resin combinations are detailed (binary blends, blends including a crosslinkable resin with the addition of a curing agent. . .) and the influence of a great number of parameters on the resulting stratification pattern is discussed.

Table 17
Typical resins exhibiting self-stratification [48].

Typical basis resins (high free surface energy: FSE >40 mJ/m ²)	Typical stratifying resins (low free surface energy: FSE <30 mJ/m ²)
Epoxy resins	Acrylic resins
Epoxy resins	Polysiloxane
Vinyl copolymers (VA/BA - EVA)	Fluorinated polyether
Melamine - MF/PF resins	Silicone oligomers
Polyester	PTFE
Polystyrene	Silicone-modified alkyd
Polyvinyl chloride	Polyesters resins
Polymethyl methacrylate	PET

4.1. Resins

The nature of the resin, as well as its combination with solvents, curing agent, pigments and additives have a non-negligible impact on the level of stratification. Commercially available resins are generally used to formulate the coating. Only few synthesized resins have been tested and patented but in both cases, high level of stratification can be obtained. Binary blends of resins, including or not a crosslinking agent, are reported in this section of the paper.

Regarding the bottom layer, epoxy resins have been preferably selected, in particular for metallic substrates, due to their uses in this commercial marketplace. They found wide uses in various industrial application fields such as surface coatings, laminates, adhesives, composites, etc. They possess excellent characteristics: hardness, mechanical and electrical resistance, durability, hydrophobicity, chemical resistance due to the secondary hydroxyl group, and resistance to abrasion, moisture, thermal shock and also weather resistance. Their usage cost is generally more important than that of other thermosetting polymers, and their thermal and flame resistance (which depend on the structure of the epoxy monomer, on that of the curing agent, and on the crosslink density if considered) need to be improved for many application areas [10,49–51].

Regarding the top layer, thermosetting acrylics and polyesters, polyurethanes, vinylics and other thermoplastic and thermosetting resins are the main resins that have been studied up to now. However, acrylics and fluoropolymers can be a choice of interest for coating applications requiring chemical resistance, thermal stability, low friction, resistance to UV degradation, durability and flexibility.

4.1.1. Binary blends of thermoplastic and non-crosslinked thermoset resins

Binary mixtures of thermoplastic and thermoset resins, and in particular mixtures based on halogenated, acrylic, vinylics, non-reactive polyurethanes and also silicone resins without the introduction of a hardener led to well stratified coatings [8,9,21,23,29,41].

4.1.1.1. Binary blends of thermoplastic resins. Toussaint et al. show that a combination of an halogenated resin (Lumiflon LF 200, ICI Resins) with either a vinylic (VMCH, Union Carbide), an acrylic (Plexigum PM 381, Röhm) or a non-reactive polyurethane (Desmolac D 2700 or D 4125, Bayer) results in a type II pattern. When the acrylic resin is blended with a non-reactive polyurethane (D 2770 or D 4125) or an halogenated resin (LF 200), the same pattern is obtained, as well as in the case of a blend based on a vinylic resin (VMCH) with either an halogenated (LF 200) or a non-reactive polyurethane (D 2770 or D 4125) [8]. It was demonstrated by Vink and T.L. Bots that a chlorinated rubber (Alloprene R10) with various

Table 18
Resulting pattern obtained from infrared studies on crosslinked unpigmented systems [10].

Resin 2	"Amine A"				Jeffamine D230				Versamid 115			
	Epikote				Epikote				Epikote			
	828	1001	1004	1007	828	1001	1004	1007	828	1001	1004	1007
Neocryl B-700	0	4	4	4	2	3	4	4	3	3	4	4
Neocryl B-804	0	2	4	4	0	3	4	4	3	3	4	4
Neocryl B-813	0	2	2	2	0	0	2	4	2	2	2	3
Crodaplast AC-550	0	0	2	2	0	0	2	4	0	0	0	2
Crodaplast AC-500	0	0	4	4	0	0	0	2	0	0	0	2
Neocryl B-728	0	2	2	0	0	0	0	2	0	2	3	3
Neocryl B-811	0	0	2	2	0	0	0	3	(2)	0	2	3

Stratification: 0 = no stratification; 4 = full stratification. Amine A = 4, 4-methylenebis(cyclohexyl) amine. Figures in parentheses indicate that some stratification had occurred but resin went to the substrate interface and the epoxy resin to the air interface systems.

Table 19
Separation of components on interfaces air/coating and coating/substrate (steel) of the upper and bottom surface of coating [42].

Resin 1	Resin 2	Phase	Share of acrylic resin (%)	Share of epoxy resin (%)	Adhesion of coating (Mpa)
Neocryl B700	Epidian 1	Top	91.2	8.8	<0.7
		Bottom	0.0	100.0	
Neocryl B700	Epikote 1001	Top	92.1	7.9	1.72
		Bottom	4.6	95.4	
Neocryl B700	Epidian 012	Top	100.0	0.0	2.82
		Bottom	0.0	100.0	

Table 20
Phase separation data for Epikote 1001/Lumiflon LF 200 obtained by ATR-FTIR [10].

Phase separation data for Epikote 1001/Lumiflon LF 200					
Ratio Epikote:Lumiflon	Phase	Epikote (%)	Lumiflon (%)	MiBK (%)	Xylene (%)
1:1	Top	40	0	30	30
	Bottom	11	31	29	29
3:1	Top	44	0	28	28
	Bottom	18	37	22	22
5:1	Top	46	0	27	27
	Bottom	8	42	25	25
9:1	Top	47	0	27	27
	Bottom	22	27	26	26

vinyl chloride copolymers (VMCC and VAHG) can also reach a type II pattern [29].

4.1.1.2. Blends of an epoxy resin with a thermoplastic. A wide range of epoxy resins have been tested up to now and they are still being studied. Type I or II patterns can be obtained with systems including an epoxy as the basis resin and one of the following resins as the topcoat resin: chlorinated rubbers (Alloprene R10, *Zeneca Resins*; Alpex CK450, *Hoechst*), thermoplastic or thermosetting acrylics (Crodaplast AC-500, *Croda Resins Ltd.*), vinyl chloride copolymers (Vinylite VMCC, VAHG from Union Carbide), chloro-sulfopolyethylene, fluoro-chloro copolymers, long oil alkyd (VAS 9223, *Resinous Chemicals*), fluoroethylene or vinyl ether copolymers, poly(isobutyl methacrylate) (Neocryl B700, *ICI Resins*), fluorinated polyethers (Lumiflon LF 200 or LF 916, *ICI Resins*), acrylic copolymers and nitrocellulose [29]. On the other hand, the combination of an epoxy (Epikote 828 or 1007) with a chlorinated rubber (Alpex CK450) exhibits a type I stratification when the system is not pigmented [10,29]. In this study, Vink et al. based the choice of resins in accordance with the overlap factors and on the Hansen solubility parameters and evaporation rates for solvents. In addition, it was recently shown that a blend of Bisphenol A epoxide (DGEBA, *Sigma Aldrich*) with a silicone resin (Phenyl silsesquioxane, *Dow Corning*) could lead to a type I pattern in the case of unpigmented systems [23]. Finally, formulations using Epikote 1001 and 1004 (*Shell UK Ltd.*) as basis resin exhibit improved stratification patterns compared to other grades of Epikote [10].

Those studies also show that without curing agent, the resulting paint film tends to be brittle and is of relatively low molecular weight, leading to poor chemical resistance. As a consequence, it is not possible to develop those systems for industrial applications. As mentioned previously, when a system crosslinks, the molecular weight increases, which favors the stratification process. Consequently, different assumptions have been made to explain the influence of the crosslinking of the thermosetting system and of the curing agent nature on the degree of stratification. The next part of this review is dedicated to the understanding of the role of the curing agent in coatings formulations.

4.1.2. Blend of thermoplastic and thermoset resins involving a curing agent

The incorporation of a compound in a thermoplastic/thermoset self-stratifying system can modify the resulting stratification pattern and this is particularly true for curing agents. As discussed in the first chapter, the crosslinking reaction might be a driving force in the stratification process and the effect of the curing agent is strongly dependent on its nature. Although it is agreed that the crosslinking reaction significantly affects stratification, the resulting coating also depends on the stratifying resin, and particularly on its surface energy. Some examples of systems comprising a curing agent are presented hereafter.

4.1.2.1. Epoxy based systems. During the stratification process, epoxy resins are usually cured with an amine curing agent (anhy-

driles are less common), while the stratifying resins do not take part in the crosslinking reaction. Such compositions are of interest for the coating industry as the presence of the thermoplastic resin can provide some elasticity to the brittle epoxy resin [10]. In a coating with a high degree of stratification, a small percentage of topcoat resin in the base layer can play the role of plasticizer, improving the elasticity of the base layer. For example, when an acrylic resin is used as topcoat resin and has a surface energy close to the one of the epoxy, the degree of stratification will be low.

- Epoxy/acrylic blends

Physical and chemical properties of the acrylic resin have a strong influence on the stratification process [20]. In an acrylic/epoxy system, it has been shown that a better separation is obtained with a low polar acrylic resin, and an epoxy resin with an epoxy number ranging between 0.11 and 0.21 [42]. The most effective separation has been achieved by Langer et al. with a mixture of a thermoplastic acrylic (a poly(isobutyl methacrylate), Neocryl B700 (DSM Neoresins+) of very low surface energy (33.1 mN/m^{-1}) and an epoxy resin (Epidian 012 and 0.21 [42]). The most effective separation has been achieved by Langer et al. with a mixture of a thermoplastic acrylic (a poly(isobutyl methacrylate), Neocryl B700 (DSM Neoresins+) of very low surface energy (33.1 mN/m^{-1}) and an epoxy resin (Epidian 012 and 0.21 [42]). The most effective separation has been achieved by Langer et al. with a mixture of a thermoplastic acrylic (a poly(isobutyl methacrylate), Neocryl B700 (DSM Neoresins+) of very low surface energy (33.1 mN/m^{-1}) and an epoxy resin (Epidian 012 and 0.21 [42]). The most effective separation has been achieved by Langer et al. with a mixture of a thermoplastic acrylic (a poly(isobutyl methacrylate), Neocryl B700 (DSM Neoresins+) of very low surface energy (33.1 mN/m^{-1}) and an epoxy resin (Epidian 012 and 0.21 [42]).

Benjamin et al. studied a large range of resins with different curing agents (Table 18). Table 18 The thermoplastic acrylic, Neocryl B700 of low surface energy and polarity reaches a type I pattern when combined with the epoxy Epikote 1004 and 1007 and three different hardeners [10]. Other thermoplastic acrylics, as Neocryl B875, give rise to the same stratified coating [8]. When mixed with an epoxy oligomer (particularly with Epidian 1, Epikote 1001 and Epidian 012, Shell and Chemical Company Organika-Sarzyna Poland), the thermoplastic exhibits as well a type I pattern but low adhesion on steel compared to other systems (Table 19) [42].

The use of a Schiff base epoxy resin instead of the commercial bisphenol-A resin, combined with poly(isobutyl methacrylate) can also lead to a high level of stratification [20]. Moreover, the epoxy resin has a high surface energy (52 mJ/m^2), which makes it a good candidate for steel substrate. The content of epoxy resin in the bottom layer was 100% and the top layer was containing more than 90% of the acrylic resin with led to a type I stratified coating.

- Epoxy/fluorinated polyether blends

A fluorinated polyether (Lumiflon LF 200) exhibits the highest level of stratification, when combined with three cured epoxy resins (Epikote 1001, 1004 and 1007) cured with a proprietary polyoxypropyleneamine curing agent. This result is similar to the studies of Benjamin et al. that reported high stratification for uncrosslinked systems. The basis layer of the coatings contains mainly the epoxy resin, whereas the upper phase could contain significant amount of both resins, even though the system is fully stratified (Table 20). Another grade, Lumiflon LF916, shows also a layering effect with Epikote 1001 and 1004 but has its best pattern with Epikote 1007. However, in the study, Epikote 1007 was set apart because of its high viscosity which could be an issue for processing and in particular for the dispersion of pigments [10].

Alyamaç, in her PhD thesis entitled "self-stratifying coatings", studied a blend of fluorinated acrylic copolymers and inorganic modified epoxy resin [52]. The fluorinated acrylic copolymers containing various acrylate and methacrylate groups were synthesized by free radical polymerization and the epoxide (DER 317, Dow Chemicals) was inorganically modified by tetraethyl orthosilicate and crosslinked by melamine formaldehyde resin. The concentration of fluorine near the air-film interface of the resulting coating was much more important than the one around the film-substrate interface, meaning that the acrylic copolymers containing fluorine

migrated to the top of the coating during the film formation. These investigations finally showed that an acrylic copolymer with low molecular weight and low surface tension improves the stratification process, and also that the synthesized epoxy resin (tetraethyl orthosilicate modified epoxy) exhibits stratification in this blend.

- Epoxy/other resins blends

It is interesting to note that a silicone-modified epoxy ether, Plastocryd SC-400 (Croda Resins Ltd.), exhibits a type II pattern with Epikote 1001, 1004 and 1007 cured with polyoxypropyleneamine curing agents. The combination with a long oil alkyd (VAS 9223) gives the same results with Epikote 1001, 1004 and also with Epikote 828 which has lower molecular weight.

Other combinations including a crosslinked epoxy resin were proposed by Vink. They include chlorinated rubbers, vinyl chloride copolymers, chloro-sulfopolyethylene, fluoro-chloro copolymers and nitrocellulose. The combination of an epoxy with a chlorinated, Epikote 1001/Alloprene R10 (Overlap factor $V = 40.2\%$), was chosen in accordance with the previous results. The combination Epikote 1001/Alloprene R10 with XE460 as curing agent showed the best stratification.

Soucek also proposed a formulation with an epoxy resin having epoxide end groups and an alkoxide oligomer (phosphate or ester end group) as the first phase, and a polymeric binder having a polymer derived from fluorinated vinyl-based monomer as the second phase [53,54]. The formulation includes a curing agent. Experimentally, the epoxy resin (DER 317) reacts with fatty acid (Pamolyn 380) to generate a multi-phase stratified coating wherein each individual phase (rich in a different polymeric binder) is separated from the other by a diffuse interface.

4.1.2.2. Polyurethane based blends. Thermosetting polyurethane coatings are of interest to develop sustainable self-stratifying systems coatings. Baghdachi et al. reached a high degree of stratification by synthesizing a thermoset polymeric organic coating composed notably of hydroxyl urethane dendrimer (or primary hydroxyl polyols, epoxy silsesquioxane fluorinated secondary hydroxyl containing polyols) and hexamethylene diisocyanate in combination with hydroxyl functional fluoroethylene alkylvinyl ethers (Lumiflon 200 and 910 from Asahi Glass Company). The formulation also contained a di-epoxy POSS (diglycidoxypropyl functionalized polyhedral oligomeric silsesquioxane) which after investigation could induce a reduction of mass mobility and transfer in the system by reacting with the crosslinker. This would thus favor stratification by forcing the immobilization of the materials in the system. They also investigated other homologous systems such as the combination of silicon containing analogs (linear epoxy functional polydimethylsiloxane resin) as a replacement for the diglycidoxypropyl POSS that resulted in stratified coatings [14]. Related formulations were filed by Baghdachi et al. and describe a process for preparing a self-stratifying coatings including a polyol, a silsesquioxane, a polyurethane dendrimer and a crosslinker for topcoat application [55], and this formulation was then extended to pigmented coatings by the addition of a pigment and a dispersive agent [56].

Yagci et al. also managed to design antimicrobial self-stratifying polyurethane coatings in which synthesized precursors (quaternary ammonium compounds) are bonded to the polymer network by addition of a polyisocyanate crosslinker [57].

4.1.2.2. Polyester resin based blends. Crosslinkable polyester resins (Desmophen A365, Desmophen 670 crosslinked with Desmodur N75, and Europox 7001 crosslinked with Jeffamine D230) were tested in combination with a fluorinated polyether (Lumiflon LF 200). This study confirmed the ability of the system to stratify: both

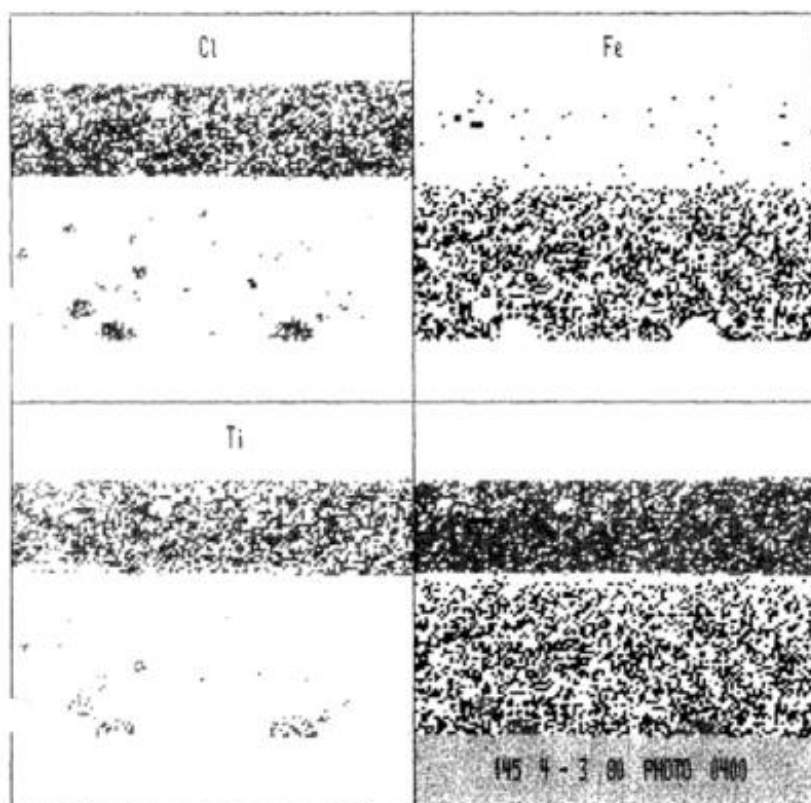


Fig. 28. EDX mapping through layer thickness [8].

Table 21
Formulation tested by Toussaint exhibiting stratification [8].

Material type	Commercial grade	Weight (g)
Fluorinated resin	Lumiflon LF 200	100
Pigment 1	TiO ₂	28
Thermosetting polyester resin	Desmophen 670	100
Pigment 2	Red iron oxide	44
Curing agent	Desmodur N75	51
Solvents	Xylene/diacetone alcohol 1/1 vol./vol.	38
	Xylene	27

pigmented and unpigmented formulations led to a type I pattern [8]. Table 21 shows an example of formulation, and its resulting stratification pattern are reported in Fig. 28.

According to those results, it is obvious that the intricacy of the process and the high number of resins tested in scientific papers generate a great number of results. Therefore, it is difficult to correlate them. At this point, it is obvious that the elaboration of a general model is quite complicated as the number of factors involved in the stratification process is high. The proposed theoretical models are thus not always reliable. Nevertheless, those various studies allows to postulate that the most efficient systems include a thermoplastic and a thermoset resin, and that in most cases, the crosslinking of the thermosetting resin can improve the stratification.

Other parameters than resins can also influence the self-stratification process: solvents, pigments, additives, and even the substrate or the processing conditions can play a role in favoring

or limiting this process. Their respective effects are detailed in the incoming part.

4.2. Solvents

As mentioned previously, a solvent with a high volatility and polarity should be used for the high surface energy resin (top layer), and a solvent with a low volatility and polarity is recommended for the low surface energy resins (bottom layer). Both pure solvent and solvent blends have been tested in research works [8,10,41].

Solvents are generally selected so that the solubility requirements of the resin are satisfied, and taking into account their respective Hansen solubility parameters. On an experimental level, xylene, and blends containing xylene, MIBK, 1-methoxy-2-propanol or butylacetate [8–10,29] are often chosen as solvents. Solvents are also used as viscosity regulators during the grinding process of pigments or to facilitate the spraying process [8].

Very few papers and patents are related to waterborne self-stratifying coatings. Experiments performed with commercial solutions and dispersion resins were not conclusive in providing self-stratified coatings [9]. Nevertheless, two formulations have been recently patented: (i) a waterborne organic silicon-acrylic acid self-stratifying coating (Table 22) [16]; and (ii) a UV-cured self-stratifying coating [15] which led to a commercial UV-hardenable clear lacquer UVHC 8558 (GE Bayer Silicones), based on 100% solid silicone acrylates and a water-based commercial lacquer (MB 9-744 from BASF Coatings) as reported by Berkau et al.

Table 22
Formulation of an aqueous silicone-acrylic self-stratifying paint [16].

Content (%)	Component
10–15	Organic silicone emulsion
50–60	Acrylic emulsion
5–10	Organic silicone modified acrylic emulsion
5–7	Fillers
5–7	Pigments
0.2–0.5	Thickener
2–3	Auxiliary agent
10–20	Water

A combination of commercial alkyd dispersion with an acrylic emulsion polymers was also proven to give rise to well layered coating through a mechanism comparable to that demonstrated in powder coatings, thus not influenced by the evaporation process [9].

The self-stratifying approach is sometimes used to design new coatings with preferential migration of additives, such as surfactants. For example, in latex emulsion, when water evaporates, surfactant molecules can either be driven to the film-air interface and thus affect surface properties or, on the contrary, migrate to the substrate-film interface to enhance adhesion [58].

Finally, self-stratified latex blends containing charged and neutral particles, with the neutral particles concentrated at the film/air interface, have also been recently reported with a process driven by the vertical flow of water during the formation of latex films [12]. The spontaneous vertical segregation between the two types of particles is limited to a difference in collective diffusivity, and not to the preferential agglomeration or to specific interactions between the particles and the film/substrate interface. During film formation, the top layer enriches itself in neutral particles whereas charges spheres escape from this layer, faster than their neutral analogue due to their mutual repulsion. In this type of stratification process, the solid content must not be too high and the drying time must be comprised between the characteristic diffusion time of the charged and the neutral particles.

4.3. Additives

Up to now, the addition of pigments have been widely studied in self-stratifying coating compositions. Few publications mention the incorporation of additives to self-stratifying systems, as reviewed in Section 2.2.1.4, since the majority have negative effect on stratification [8,29]. However, particular compatibilizers were proven to be successful.

4.3.1. Addition of one pigment

As mentioned in Section 2.2.1.3, the degree of phase separation is generally the same or even better in the case of pigmented systems, compared to pigment-free systems [8,24].

Titanium dioxide (TiO₂), red iron oxide, chromium oxide and zinc phosphate are the main pigments reported in the literature because of their inertness [10,24]: they show no particular influence on the stratification.

Depending on their properties and their affinity towards resins, pigments are primarily dispersed in a specific medium (base or top layer). It is shown that pigments usually stay in their dispersion phase.

This phenomenon was investigated by Toussaint, who concluded that pigments stay in their original dispersion phase because they are well-wetted by the respective binders. The desorption of the binder is difficult and very slow, if not inexistent [8].

Red iron oxide and zinc phosphate, usually dispersed in an epoxy resin, are mostly used on steel due to their anticorrosive properties. It was reported that for epoxy resins pigmented with these

two compounds, films showed similar stratification level as with unpigmented formulations [10,23,24]. The most promising systems consist in formulations of an epoxy (Epikote 1001) cured with polyoxypropyleneamine and combined with either a fluorinated (Lumiflon LF 200) or a thermoplastic acrylic (Neocryl B700). It was confirmed in those cases that pigments are located in the phase in which they were primarily dispersed (i.e. epoxy base layer). Another promising system recently studied is a combination of an epoxy resin with a silicone. In this specific case, it was evidenced that iron oxide did not remain in its original dispersing phase, and migrated toward the silicone medium without affecting the stratification [23]. Zinc phosphate exhibited the same behavior when blended in a particular solvent (Butylacetate: xylene, 1:1 ratio).

On the contrary, yellow iron oxide prevents resin stratification in an epoxy/acrylic system [24].

Pigments having aesthetic or weather-resistant properties are selected for the topcoat layer. As an example, titanium dioxide is usually blended within the thermoplastic resin and used for its mechanical, chemical, weather resistance properties and ease of detection by microscopic chemical analyses.

Further experiments were also carried out to determine whether or not gravity influences the final location of pigments inside the coating [10,29]. After the coating application, films were turned to the other side during drying and analyses showed that pigments were still located in their original dispersion phase.

Complementary experiments have shown that pigment density was not a driving force in the process [10]. In different studies, the preferential affinity of the pigment for one of the phases was confirmed.

Finally, Mackulin concentrated his work on self-stratifying latex resins and patented a coating based on a combination of two latexes: a base latex and a stratifying latex resin comprising hybrid latex particles of metal oxide nanoparticles [59]. This self-stratifying latex was intended to be used as an additive to base latex resins for enhancing the washability, UV absorbance or other characteristics.

4.3.2. Addition of more than one pigment

If several works prove that the addition of one pigment has no effect on the stratification process, however the addition of two or more pigments reveals contradictory results. Vink and Bots established that “the stratification is strongly dependent on the pretreatment of the pigment” [29]. Adding more than one pigment is thus challenging and a fundamental issue for industrials as pigments aim at both improving the resistance to weathering (decorative opaque pigment in the upper layer), and to corrosion (anticorrosive pigment in the lower layer in the case of steel substrate). In such systems, the pigments sometimes spread into both phases, even though the system is well-stratified. This point was demonstrated by Benjamin and his collaborators by dispersing zinc phosphate in the epoxy phase, and titanium dioxide into the other phase. The combination exhibited a good level of stratification before the addition of the second pigment, but this structure was not retained afterwards. In most cases, pigments were located through the whole film thickness or evidenced in some ways preferential affinity with one of the resins. Only two combinations gave rise to full stratification: a blend of an epoxy resin crosslinked with a polyoxypropyleneamine, and two different grades of thermoplastic acrylics [10].

At the opposite, in the BRITE project, Toussaint [8] designed three successful self-stratifying coatings with the addition of two pigments (one in each layer): blends of a fluorinated resin (Lumiflon LF 200) filled with TiO₂ with respectively one epoxy and two polyesters media (Eurepox 7001 cured with Jeffamine D230 and pigmented with Cadmium yellow; Desmophen 670 pigmented with Red iron oxide and cured with Desmodur N75, or Desmophen

A365 pigmented with Cobalt blue and cured with Desmodur N75), each combination containing specific solvent blends. In all cases, pigments remained in their original dispersion phase and a stratification type I was obtained.

Finally, Langer et al. also reported a type II pattern of self-stratifying coating for a mixture of Acrylic/TiO₂ and Epoxy/Red Iron oxide & Zinc phosphate [24].

4.3.3. Addition of an adhesion promoter

Other studies revealed that the negative effect of a second pigment can be counterbalanced by adding a specific adhesion promoter [8,10,29] that improves the interaction between the resin of the dispersing medium and the pigment, and thus prevents a possible exchange of pigment between the two phases. Particularly, a silane coupling agent (amino propyl triethoxy silane, AMEO) is often used. In that case, self-layering coatings containing two or three pigments exhibited a stratification level corresponding to a type II pattern [24]:

1. (Acrylic/TiO₂)/(Epoxy/Red Iron oxide & Zinc phosphate/dispersion aid silane with epoxy groups).
2. (Acrylic/Chrome oxide green)/(Epoxy/Natural lamellar iron oxide/dispersion aid).
3. (Acrylic/TiO₂)/(Epoxy/Natural lamellar iron oxide/dispersion aid).

Looking at these 4 systems described, systems containing zinc phosphate have higher adhesion strength than interlayer cohesion: interlayer cohesion was indeed found to be comparable to systems applied layer upon layer. Systems with natural lamellar iron oxide did not exhibit any pulling off of layers during pull off test, and showed very good adhesion to substrate. Considering anticorrosive properties (evaluated by salt spray chamber testing), only systems 1. and 2. exhibited good properties.

Other compatibilizers or dispersing agents have negative effects on the coating.

It was also noticed that the effect of a silane pretreatment on TiO₂ was dependent on the selected epoxy resin [29]. This statement was confirmed by Benjamin et al. who obtained a fully stratified coating by combining a fluorinated resin (Lumiflon LF 200) with two different grades of epoxy resin: in the systems Lumiflon LF 200/TiO₂ coated with AMEO, combined with either Epikote 1001 or 903/red iron oxide [10], the pigments remained in their dispersed phase. Since both the chlorinated rubber used in the BRITE Project [60] and Lumiflon contain chlorine, it was suggested but not confirmed that the AMEO may react with the C–Cl bond. Moreover, with Neocryl B700, a thermoplastic acrylic which does not contain any C–Cl bond, stratification was not good.

Other studies show that silicone and fluorine-containing oligomers used as additives can accelerate the stratification process with rather no influence [7,10,61]. For example, a mixture based on crosslinked epoxy (pigmented with titanium dioxide) and an acrylic resin modified with a silicone oligomer exhibits self-stratification, with the top surface enriched with acrylic and silicone components, while the bottom phase is composed of the epoxy resin and pigments. EDS experiments have proven that the top layer is almost free of pigments [1]. Silane adhesion promoter—for example AMEO (3-aminopropyltriethoxy silane)—has the ability to bond the inorganic TiO₂ to the organic resin [10].

To sum up, even if some aspects of the stratification mechanism remain unclear when several pigments are incorporated in the formulation, some general conclusions can be drawn:

- Pigments can be used either for stratification detection, or for their intrinsic properties (aesthetic, weathering resistance, corrosion resistance...).
- When well-chosen and dispersed in the right medium (e.g. for which they have the highest affinity), pigments have no negative effect on stratification, in some case, they can even enhance the process.
- The addition of more than one pigment is difficult but can be achieved with the incorporation of a coupling agent (particularly silane coupling agents).

4.4. Substrate

The film-substrate interface is of primary importance for the study of self-layering behaviors, and thus the choice of the substrate. Steel, plastics, glass and aluminum foil are the main substrates that have been studied up to recently.

4.4.1. Plastics substrates

Toussaint et al. applied binary blends of thermoplastic resins on various types of plastics: Poly(ethylene propylenediene monomer) (EPDM), Poly(acrylonitrile/butadiene styrene) (ABS), Teflon (TF60), Polyphenylene oxide (PPO), Polycarbonate (PC) [8].

On PPO, the highest degree of stratification was obtained by combining an halogenated resin (Lumiflon LF 200, *ICI Resins*) with either a non-reactive polyurethane (Desmolac 2770, *Bayer*) or a vinylic resin (VMCH, *Union Carbide*), or by combining an acrylic resin (Plexigum PM 381, *Röhm*) with a non-reactive polyurethane (Desmolac 4125, *Bayer*).

On Teflon, a type II pattern can be obtained with (i) a mixture of an halogenated resin (LF 200) with a vinylic resin (VMCH) and (ii) a non-reactive polyurethane (D 2779, D 4125 or D 2770) with an acrylic resin (PM 381).

On polycarbonate, the following combinations stratify: (i) a mixture of an halogenated resin (LF 200) with a vinylic resin (VMCH) or non-reactive polyurethanes (D 2770 or D 4125), (ii) an acrylic resin (PM 381) in combination with non-reactive polyurethanes (D 4125 or D 2770) or an halogenated resin (LF 200), (iii) a blend of a vinylic resin (VMCH) with a non-reactive polyurethane (D 2770) [8]. Recently, an epoxy/silicone system was demonstrated to give perfect layering on PC, with and without an amine curing agent [23].

4.4.2. Glass substrates

Vink and Bots studied different unpigmented systems applied on glass including an epoxy resin (Epikote 828 and 1007) combined with various resins: chlorinated rubbers (Alloprene R10, Alpex CK450), thermoplastic acrylics, vinyl chloride copolymers (Vinylite VMCC and VAHG), chloro-sulfopolyethylene, fluoro-chloro copolymers, acrylic copolymers and nitrocellulose. Systems which exhibited stratification are gathered in Table 23. The first system (Epikote 828/Alpex CK450) showed the highest level of stratification [29].

Abbasian et al. obtained a high level of stratification on float glass using a blend of epoxy (Araldite GT 7071, *Vantico Company*) and acrylic (Degalan AL23, *Roehm Co.*) resins, with the addition of a hardener (Aradur 2969CH) [28]. This stratification level was better than the one obtained on aluminum plates for the same formulation.

4.4.3. Metallic substrates

4.4.3.1. *Steel substrates.* Binary combinations of commercial acrylic and epoxy resins are successful on producing self-layering combinations on steel, more specifically the system containing a blend of methylmethacrylate and ethylacrylate copolymer (Paraloid B44) and epoxy oligomer (Epikote 1001) [31]. Amongst the systems

Table 23
Stratification of unpigmented formulations on glass substrate [29].

1st combination		2nd combination		Overlap factor V(%)	Ranking of stratification ^a
Resin	Solvent	Resin	Solvent		
Epikote 828	THF	Alpex CK450	Heptane	55.4	1
Alloprene R10	Toluene	Vinylite VMCC	Ethyl acetate	53.0	2
Alloprene R10	Toluene	Vinylite VMCC	DMF	53.0	2
Alloprene R10	Ethyl acetate	Vinylite VAHG	Acetone	39.6	2
Alloprene R10	Acetone	Vinylite VAHG	Diacetone alcohol	39.6	2
Alloprene R10	Butyl acetate	Vinylite VAHG	Diacetone alcohol	39.6	2
Epikote 1007	THF	Alloprene R10	Butyl acetate	19.4	2

tested, this formulation exhibits the highest adhesion to steel (4.2 MPa) after pull-off test (EN 24624:1992 standard with PosiTest Pull-off adhesion Tester) but low stratification compared to systems described in Table 19, also applied on steel. On the contrary, Neocryl B700 (IBMA) of low surface energy and polarity, when mixed with an epoxy oligomer (particularly with Epidian 1, Epikote 1001 and Epidian 012 from Shell and Chemical Company Organika-Sarzynna Poland) exhibits a high level of stratification but low adhesion on steel.

D. Soucek proposed a formulation with an epoxy resin having epoxide end groups and an alkoxide oligomer (phosphate or ester end group) as the first phase, and a fluorinated vinyl-based monomer as the second phase [53,54]. The formulation includes a curing agent. Experimentally, the epoxy resin (DER 317) reacts with fatty acid (Pamolyn 380) to generate a multi-phase stratified coating wherein each individual phase (rich in a different polymeric binder) is separated from the other by a diffuse interface. Fig. 29 represents a proposed structure for the interaction between this hybrid coating and steel substrate.

Langer et al. achieved to reach a higher degree of stratification on steel with a Schiff base epoxy resin compared to commercial BPA resins, using a system containing poly(isobutyl methacrylate). The Schiff base epoxy resin indeed provides high adhesion properties on steel (3.05 MPa at pull-off test) and retains the high mechanical properties of the BPA resin. Moreover, the $-\text{CH}=\text{N}-$ group allows inhibiting corrosion and the resin has a high surface energy (52 mJ/m²), which makes it a good candidate for steel substrates [20]. This Schiff base epoxy resin was mixed with various acrylic resins and crosslinked with an amine curing agent. The highest level of stratification was obtained with the acrylic resin having the lowest surface energy value: Neocryl B700 (DSM Neoresins+). The content of epoxy resin in the bottom layer was 100% and the content of acrylic resin in the top layer was over 90%.

Finally, the thermosetting polyurethane coatings developed by Baghdachi et al. (Section 4.1.2.3) also show stratification on steel substrates [14].

4.4.3.2. Aluminum substrates. Among all the blends tested by Abbasian et al., only few mixtures of epoxy (Araldite GT 7071 from Vantico Company) and acrylic resins exhibit layering on aluminum: Degalan MB 319 with Aradur 2969 or 850 as crosslinking agent and Degalan P675 with Aradur 43BD [28].

Benjamin et al. studied mainly aluminum foil substrates, and developed successful self-layered unpigmented and pigmented systems [10]. Successful uncrosslinked (blends of epoxy resin (Epikote 1001, 1004, 1007, Shell UK Ltd.) with thermoplastic acrylic (Neocryl B700, ICI Resins), thermosetting acrylic (Crodaplast AC-500, Croda Resins Ltd.) and fluorinated polyether (Lumiflon LF 200 and LF 916, ICI Resins)), and crosslinked (Table 18) systems were developed.

In conclusion, even if the choice of the substrate is primary defined by the application, the self-layering of a system depends, as

seen previously, on the characteristics of the substrate (i.e. its surface energy, the roughness, the surface treatment if applicable...).

4.5. Processing considerations

According to Toussaint, "stratification is not influenced by the means of application as far as doctor blades, ringed bars, brushes and dipping are concerned"[8]. Moreover, it was demonstrated that the orientation of the substrate has no influence [10,14,29]. However, some paper report that spraying favors the stratification process as solvent evaporation is promoted.

Curing conditions, i.e. the processing temperature and the curing method (oven, ambient-curing, UV-curing...), are mainly dependent on the system considered and need to be in accordance with solvent evaporation and crosslinking reactions, if applicable. More precisely, the solvent used to dissolve the upper resin must not evaporate too rapidly to allow a moderate gradual increase in viscosity of the medium [8]. Temperature is a critical parameter for the process as it has also an influence on the final aspect of the coating, and more precisely on the gloss. Toussaint noticed that ambient-cured coatings have a lower gloss than coating cured at 80°C [8].

Berkau and his collaborators patented a UV-cured self-coating lacquer systems able to dry thermally, by microwave exposure or hardened by radiations (UV radiation, NIR radiation, IR radiation) [15]. These successfully self-layered lacquers were obtained by blending an alkyd resin with various polymers (selected among aminoplast resins, epoxy resins, phenolic resins, polyurethane resins, polyester resins, polyvinyl acetate, amine resins, and alkyd resins). A polymerization initiator was also added to the formulation to allow the curing. Commercial products were developed thereafter: a UV-hardenable clear lacquer UVHC 8558 (GE Bayer Silicones) based on 100% solid silicone acrylates and a water-based commercial lacquer (MB 9-744 from BASF Coatings). Another formulation requiring an X-ray spectrometer to be cured was patented in 2012: the coating, composed of waterborne organic silicon-acrylic acid, exhibited an optimal stratification after curing (Table 22) [16].

I-4-10 Conclusion

Numerous factors have to be taken into account when designing self-stratifying coatings, each factor affecting the stratification process. Even if their influence is not yet fully elucidated, some general conclusions can be drawn. Factors playing a significant role in the stratification process are:

- **Resins:** the most efficient systems include a thermoplastic and a thermoset resin, crosslinked with a hardener. The nature of the resin, as well as its combination with solvents, curing agent, pigments, substrates and additives have a non-negligible impact on the stratification level. Commercial resins are mainly used for the coating formulation, and much less frequently synthesized but in both cases, good level of stratification can be obtained.
- **Solvents:** For high surface energy resins, a solvent with a high volatility and polarity should be used. For low surface energy resins, a solvent with a low volatility and polarity is preferable. Solvents are chosen according to their respective Hansen solubility parameters and to the type of resins and are generally: xylene, a blend of MIBK: xylene or MIBK: xylene: 1-methoxy-2-propanol or xylene: butylacetate. The rate of solvent evaporation should not be too high to allow the binders to separate and to form layers before the increase in viscosity of the system.
- **Additives:** The addition of one pigment has no negative effect on the stratification process as far as its dispersion is optimal: the degree of phase separation is the same or even better than in the case of pigment-free systems. Pigments are useful for the detection of stratification, and can upgrade the properties of the coating when properly selected. Usually, titanium dioxide is blended within the thermoplastic medium and is used for its intrinsic properties (mechanical, chemical and weather resistance ...) and ease of detection by microscopic analyses. Red iron oxide, zinc phosphate and chromium oxide can also exhibit good results in self-stratifying coatings. Red iron oxide and zinc phosphate are often used for their anticorrosive properties on steel and are dispersed in the epoxy medium. The addition of a second pigment (in both phases) is difficult but can be achieved when a silane coupling agent is used. Other compatibilizers or dispersive agents have a negative effect on the coating. It has been reported that pigments stay in their

dispersion phase if there are well wetted by the respective binder in the solution in which they are dispersed. In particular systems, the migration of pigments toward the second medium can occur without affecting the stratification process.

- **Substrate:** The film-substrate interface is of primary importance for the self-layering phenomena as its characteristics will partly allow the vertical phase separation. Steel, plastics, glass and aluminum are the main substrates which have been studied up to now.
- **Curing conditions:** Curing conditions depend on the system studied. Coatings can be cured at ambient temperature or heated depending on the selected system. If a crosslinker is added, curing conditions have to be chosen with respect to the crosslinking reaction.

I-5 Conclusion and strategy

There is not a high number of publications concerning self-stratifying coatings. A large range of resins, solvents and substrates have been tested, and in many cases a blend of a thermoplastic and a thermosetting resin, including a third component, shows the highest stratification level. The use of solvent-based self-stratifying coatings is limited for general application fields because of the important use of volatile organic solvents, and since a precise control of the composition and of the application conditions is needed. When these limitations are not critical, advantages of stratification are exploited in automotive and decorative coatings, anticorrosive paints, coil-coating technology, antimicrobial coatings, wear-resistant coatings, marine paints, heavy-duty coatings, etc. Heterophase polymer-polymer structures generate the following advantages for coatings:

- Improved mechanical properties including a successful balance between hardness and flexibility.
- Elimination of internal stresses that may occur during the film formation process as well as during the coating pot life.
- Reduced permeability.
- Improvement in adhesion durability (thereby contributing to corrosion protection).
- Upgrade of chemical and light durability.

- Upgrade of weather resistance, wear resistance, surface slip, etc.¹²¹
- Selective penetration into porous substrates.

Actually, only few scenarios have been extensively studied, and the technique has not found large industrial applications yet. A wide range of conditions, as seen in this chapter, can impact the stratification of a coating and can lead to a high level of properties. The need to fire protect various materials, including polymeric substrates, has also been evidenced. No literature deals with the design of flame retardant self-stratifying coatings, whatever the substrate involved (plastic, wood, steel...). This project thus opens the door to a real challenge and a wide variety of possibilities.

The challenge of the project is thus to establish a proof-of-concept on formulating a model of self-stratifying coating showing (i) adhesive properties similar to that of a multilayered coating on polycarbonate (ii) fire retardant properties when submitted to a fire and (iii) good durability when submitted to accelerated aging tests.

The chosen model substrate in this project is polycarbonate. It is a well-known polymer for its transparency and mechanical strength, and is widely used in a variety of fields, such as electrical and electronic equipment, automotive industry and buildings. As many polymers, PC must be flame retarded to meet the strict standards in terms of fire risks. The most common flame retardants used with the bulk approach are bromine-¹³ or phosphorus-based.^{124, 125} However, their loading is usually high (10-30 wt.%) which lowers considerably the impact strength of and also results in yellowing at high-temperature or high-humidity conditions. Some additives added in low amount were successful in producing an efficient fire retardant system (for example with sodium and potassium perfluoroalkanesulfonic acids introduced at 0.05-0.5 %). However environmental issues are posed by some halogenated compounds.¹²⁶ Recent works on silicone-based components are promising, however mechanical issues still remain.^{14, 127} Finally, the use of the bulk approach to fire retard PC leads to significant drawbacks and thus, the deposit of a FR coating on the PC surface appears as an interesting alternative solution. In addition, the success of the concept consisting in applying a simple fire retardant coating has already been demonstrated.⁶ The aim is thus to develop a PC-based material possessing FR properties, i.e. preventing dripping during fire while maintaining the mechanical and optical properties of PC itself.

Concerning the choice of the resins, researchers are unanimous that an homogeneous mixture of incompatible polymers that form coatings of a polymer/polymer structure is necessary for self-stratifying phenomenon to occur.¹²⁸ Based on these considerations, a screening of various epoxy, acrylic, fluoropolymer and silicone resins will be carried out and the behavior of their mixtures will be studied depending on their intrinsic properties. In a second step, the objective will consist in managing to incorporate a specific filler (e.g. metal oxide, calcium carbonate, phosphorus based FR ...) in one of the successful systems developed in order to provide a fire retardant effect without affecting the layering process. Moreover, the influence of the presence of additives on the resistance to ageing will be evaluated. Recent works on formulating pigmented coating systems for plastic substrates led to the conclusion that pigmentation does not have a negative impact on the stratification of the resins and that the degree of phase separation is the same or even better than in the case of pigment-free systems. In order to further improve the performance of the FR systems, the better formulation in terms of stratification degree and FR performance will be studied and the flame retardant mode of action elucidated.

The strategy of the PhD thesis is depicted in Figure 14. The following chapter will be devoted to the materials as well as to the experimental techniques used in this study.

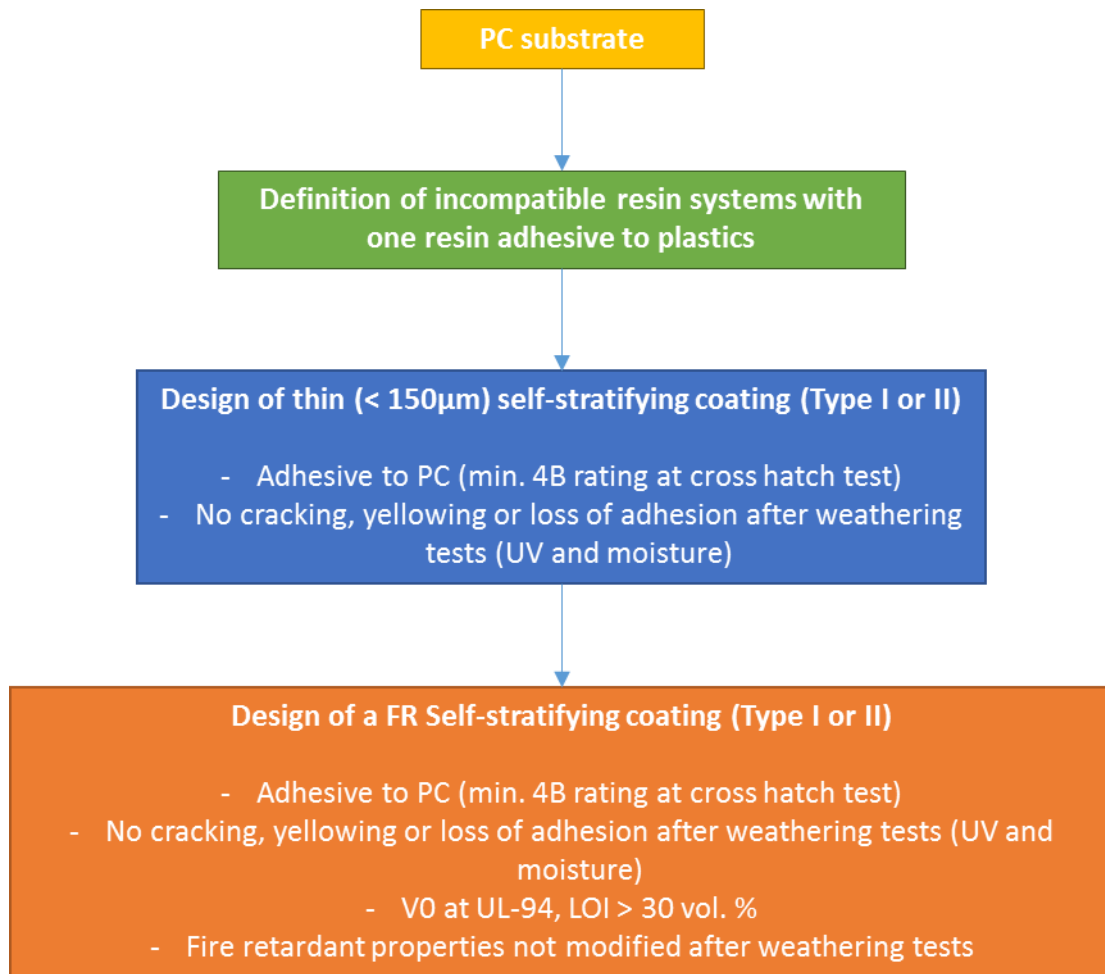


Figure 14. Strategy of the thesis

Chapter II: Materials and methods

This chapter is dedicated to the presentation of the materials (substrates, polymers, solvents and additives) and processing methods used to prepare self-stratifying fire retardant coatings. As the process of curing reaction may significantly change the thermodynamic characteristics of the systems, the optimization of the curing reactions in order to promote the layering is also carried out. Finally, test methods and experimental techniques for the characterization of both the raw materials and the coatings in terms of stratification, surface properties, thermal stability, fire performances and weathering resistance are detailed.

II-1 Raw materials

Coating systems must contain at least three components to self-stratify on a given substrate: two incompatible resins and solvent(s) (one single solvent or a solvent blend) selected according to their volatility and affinity toward the polymers. Once formulated, the coating is applied onto a substrate and cured. After film formation and stratification, a polymer/polymer bilayer system is formed and the different properties of the coating can then be evaluated.

II-1-1 Substrate

Polycarbonate is the polymeric matrix of interest in this work. Indeed, the final aim is to demonstrate that the self-stratifying approach can be used to fire retard a polymeric system. PC is a good example representative of the limits of actual bulk treatment. It is a well-known polymer for its transparency and mechanical strength, and is widely used in a variety of fields, such as electrical and electronic equipment, automotive industry and buildings. However, as many polymers, PC must be flame retarded to meet the strict standards in terms of fire risks for such applications. The deposit of a FR coating on its surface appears as an interesting alternative solution. This will be developed in detail in the chapter IV of this manuscript.

Transparent polycarbonate plates (Lexan, 10*10 cm²) were used as received from *Polydis*. Two thicknesses were considered depending on the test to be performed: 1mm-thick plates for microscopic analyses and 3 mm-thick plates to test adhesion properties, fire properties, weathering resistance, etc.

II-1-2 Resins and solvents

Resins

Different commercial resins were first selected for screening, and specific systems were then chosen according to the preliminary results. Technical data sheets of the selected systems are gathered in Appendix 2 of this manuscript.

A thermosetting system was selected to form the base layer of the film (in contact with the substrate), and a thermoplastic resin for the topcoat layer. Among them:

An epoxy resin: diglycidyl ether of bisphenol A (DGEBA) was purchased from *Sigma-Aldrich*. This epoxy resin is produced from the reaction between bisphenol A and epichlorohydrin with a basic catalyst (equivalent weight: 172-176, 100 % solids, Figure 15).

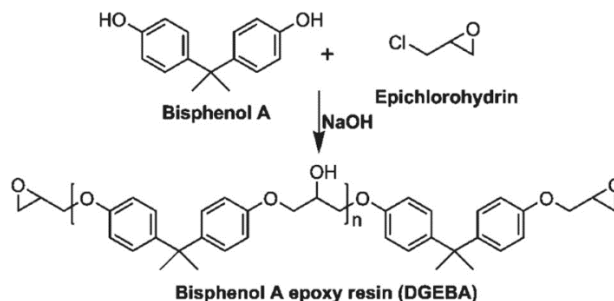


Figure 15. Synthetic route for Bisphenol A epoxy resin¹²⁹

DGEBA epoxy resin is the most spread type of epoxy used on the global market and for a wide range of applications (coatings, adhesives, composite materials, flooring, etc). It has been widely characterized, in association with various curing agents, in terms of mechanical properties, kinetics of reaction and crosslinking, addition of fillers and morphology.^{130, 131} The resin is a viscous liquid at room temperature: its Brookfield viscosity is 4000-6000 cps at 25°C which allows easy processing. In this work, the network based on the difunctional DGEBA is cured with a polyamine curing agent (Diethylenetriamine, DETA) from *Sigma Aldrich* (Figure 16).

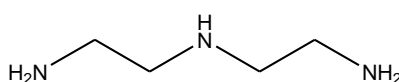


Figure 16. Chemical structure of DETA

The reaction scheme between the amine and the epoxide groups is depicted in Figure 17. The epoxy resin is a bi-functional reactant with two epoxide groups at two ends, and DETA has five reactive sites: the C-O bond in each epoxide group is broken and forms a reactive $-CH_2$ site which reacts with the amine molecule. A 100 % conversion rate is achieved if all potential covalent bonds are created, although it is rare in natural conditions (Figure 18).

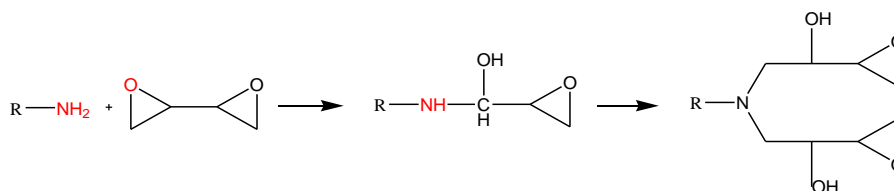


Figure 17. Reaction between an amine curing agent and an epoxide group

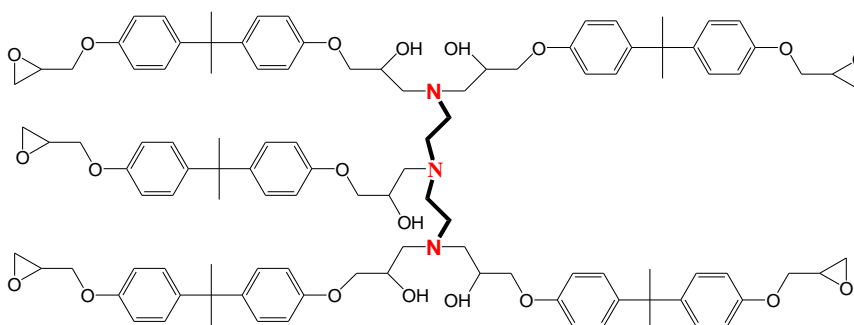


Figure 18. Molecular structure of a fully crosslinked epoxy resin with DETA

This system is intended to form the base layer of the coating, and it will be used in combination with a thermoplastic resin to form a self-stratifying composition.

A fluoropolymer resin: a fluoroethylene (FE) alkyl vinyl ether (VE) purchased from *AGC Chemicals* under the name of Lumiflon LF200 was chosen (Figure 19). This resin is a solvent soluble fluoropolymer designed for weather-resistant coatings. It has OH functionality and can be crosslinked with polyisocyanate to provide coatings with high gloss and excellent durability. Its high durability is based on its C-F bond energy, which is much higher than the energy of sunlight UV rays. This bond is able to strengthen neighbor C-C main chain bond. This system was chosen to be used as a topcoat resin. The FE part contains a 3:1 Fluorine:Chlorine ratio. The resin was supplied as 100 % solid and also solubilized at 60 wt.% in xylene.

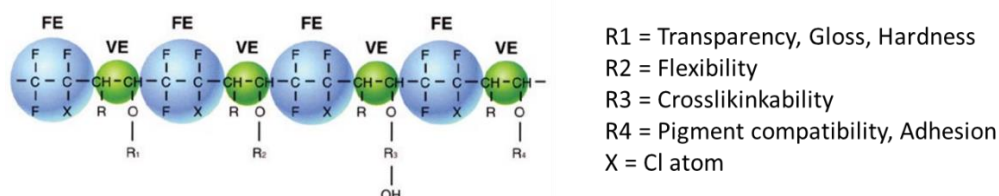


Figure 19. Chemical structure of Lumiflon LF200 resin

A silicone resin: a phenyl branched silicone oligomer containing 6 % of hydroxyl groups (RSN-217 from *Dow Corning*) was also selected to be used as a topcoat resin. This resin is usually used as a binder in both powder and liquid coatings for its excellent thermal and weathering resistance, and as a blending resin with organic resin coatings to improve their physical properties and performances.

Polydimethylsiloxane (PDMS) is well known for its high degradation temperature close to classical silicone resins.¹³² As the resin is hydroxyl terminated, it is possible to form a highly crosslinked silicone matrix by adding a particular resin modifier (7081 resin modifier provided by *Dow Corning*) to enhance the fire performance of the system. The modifier is a mixture of PDMS and silica coated with silane which usually plays the role of blowing agent in conventional intumescent coatings.³⁴ This type of resin can be used either as the base layer (in combination with the resin modifier) or as the topcoat resin (solely). Only the results when the oligomer is used as a topcoat resin are presented in this manuscript.

Solvents

A range of commercial organic solvents meeting the solubility requirements of the selected resin systems was tested: m-xylene (99 %, $T_{\text{boiling}} = 139\text{ }^{\circ}\text{C}$), butylacetate (BuAc, $\geq 99.5\%$, $T_{\text{boiling}} = 126\text{ }^{\circ}\text{C}$), methyl isobutyl ketone (MIBK, $\geq 99.5\%$, $T_{\text{boiling}} = 116\text{ }^{\circ}\text{C}$) and 1-methoxy-2-propanol ($\geq 99.5\%$, $T_{\text{boiling}} = 120\text{ }^{\circ}\text{C}$). All of them were purchased from *Sigma-Aldrich* and used as received, without any purification.

II-1-3 Fillers with specific FR properties

A set of additives has been tested in combination with binary mixtures of resins to (i) figure out their influence on the layering process in a first step, and (ii) to improve the fire

performances of the successful self-stratifying coatings developed. Table 1 gathers the set of powders and liquid fillers tested in this PhD thesis.

Table 1. List of the different fillers used

Powder fillers					
Filler type	Supplier	Color	Average particle size (μm)	Trade name	Density ($\text{g}\cdot\text{cm}^{-3}$)
Red Iron Oxide	<i>Grolman</i>	Red	0.3	Cathaycoat Red RA11A	5.0
Calcium Carbonate	<i>Solvay</i>	White	4.5	Socal 31	2.8
Zinc phosphate $\text{Zn}_3(\text{PO}_4)_2$, tetrahydrated	<i>SNCZ</i>	White	4.5	PZ20	3.3
Liquid fillers					
Filler type	Supplier	Supplied form	% Phosphorus	Trade name	Density ($\text{g}\cdot\text{cm}^{-3}$)
Bisphenol-A bis(diphenyl phosphate)	<i>ICL-Industrial Products</i>	Light yellow, viscous liquid	8.9 % of phosphorus	Fyrolflex BDP	1.254
Resorcinol bis(diphenyl phosphate)		Clear, transparent, viscous liquid	10.7 % of phosphorus	Fyrolflex RDP	1.318

The solid fillers have a twofold role: they are commonly used as pigments for industrial coatings to upgrade the coating properties (visual appearance, mechanical properties, etc.) and they can be used also for easier stratification detection. Indeed, some researchers reported that pigments well wetted in the phase in which they are dispersed remain in their original dispersion phase after the mixing of the two resins, as it was reported in the first chapter of the manuscript.¹² Some of them are also known to improve the fire performances in particular coating systems. Liquid additives were chosen mainly for their FR properties (Figure 20).

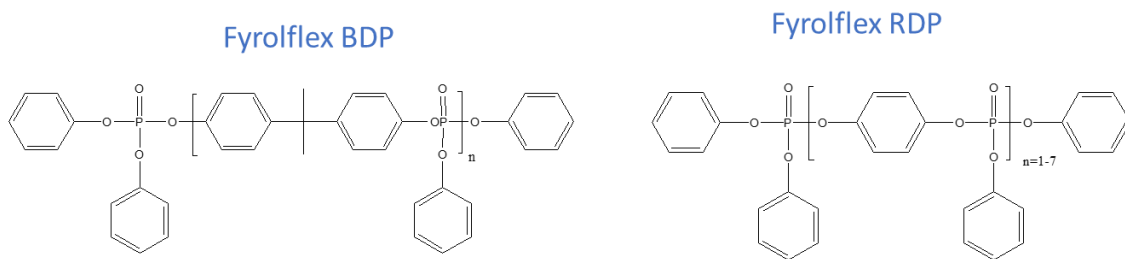


Figure 20. Chemical structure of BDP and RDP flame retardant additives

II-2 Coatings processing

II-2-1 Formulation

Processing of self-stratifying coatings is depicted in Figure 21. First of all, each resin is dissolved separately at 30 wt.% in the solvent or solvent blend chosen, by mixing it properly for 10 minutes at 300 rpm with a *Wisestir Wisd* stirrer.

When applicable, fillers are dispersed in one of the medium (depending on the system) prior to the mixing with the second resin system. In the case of a solid filler, grinding is carried out with a dissolver Dispermat (*VMA-Getzman*) until a Hegman gauge fineness value of 7 is reached. Liquid fillers are blended at 300 rpm for 10 minutes with the stirrer.

Finally, both resin systems are combined together at a 1:1 ratio and mixed for 10 minutes at 300 rpm. The curing agent is then incorporated with respect to the thermosetting system when applicable. Finally, the final formulation is mixed for 3 minutes before its application.

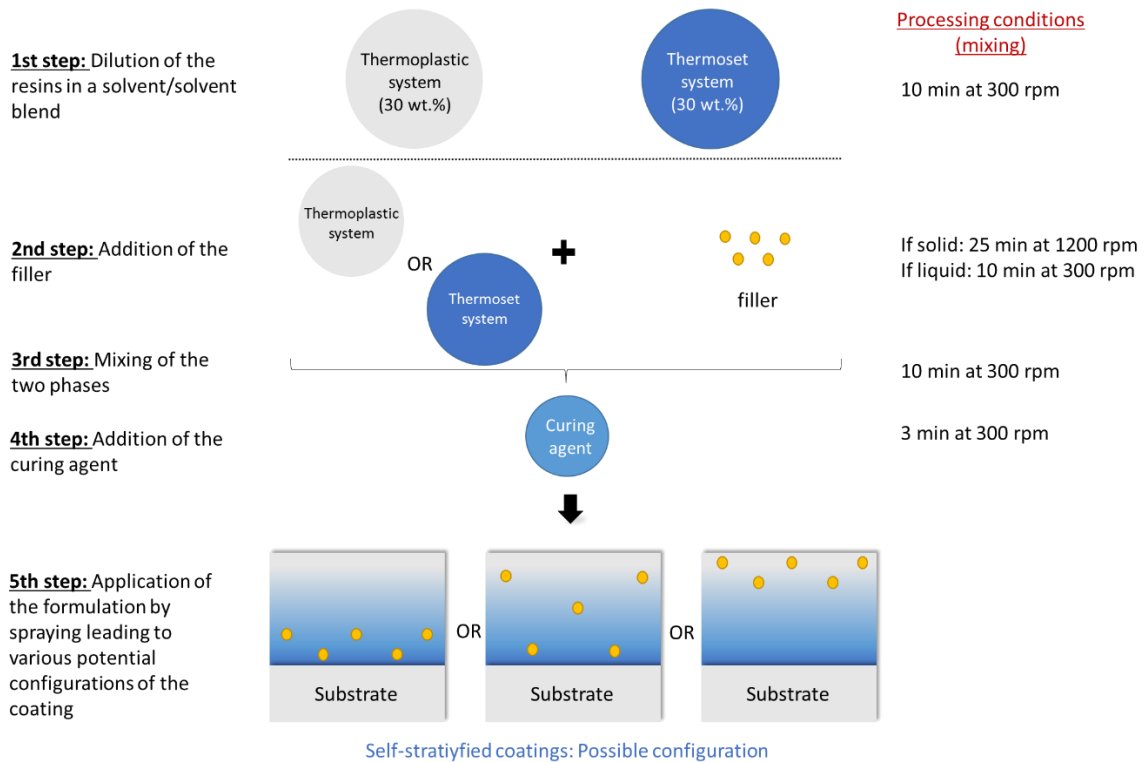


Figure 21. Processing steps for the preparation and application of self-stratifying formulations containing additives

II-2-2 Application

Coatings are then applied by spraying in a semi-industrial spraying machine (CLID apparatus) using a regular spray gun (pressurized gravity feed spray gun Devilbliss Advance HD-ADV-GP443-13 with compact buzzard and stainless steel nozzle of 1.3mm purchased from *Sinex*). An air pressure of 200 kPa was used, and the spray gun was set up so as to obtain an air flow to give a nominal wet film thickness of 200 μm after application onto the substrate.

II-2-3 Curing procedure: Optimization of the crosslinking process

It is interesting to notice that, during crosslinking reactions between the thermosetting resin and the curing agent, the system rapidly increases in molecular weight, favoring the incompatibility between the two resins.¹⁰⁹ To be optimal, the crosslinking reaction needs to precede the stratification process or the two phenomena must partially overlap. Previous

studies demonstrated that self-stratification is optimal when the crosslinking system reaches 80 % of conversion.^{133, 134}

Crosslinking reactions are exothermic. In general, the temperature of the reaction, the reaction rate and the reaction enthalpy (heat of reaction) are the main points of interest. During the reaction, the viscosity, density, and the modulus of elasticity increase due to an increase in the molar mass and crosslinking. The crosslinking process is complex because different reaction steps are involved. Basically, the growth of the polymer structure can be divided into two mechanisms of chain formation: (i) stepwise growth through elementary reactions of two functional groups, and (ii) chain growth through the attachment of monomers to the cross-linking polymer.¹³⁵ As described in the section II-1-2, curing of epoxy resins with triamine can be described as a two-step process: firstly, an epoxy group reacts with a primary amine yielding to a secondary amine, which in the second step reacts with another epoxy group yielding a tertiary amine.

Consequently, the study of the thermal behavior of the system is an effective method to study the extent of cured network structures formed with increased temperatures. The curing process is commonly determined by DSC as the ratio between the heat released by the reaction at each moment and the total heat released to determine the extent of the curing reaction. Although this procedure is useful, accuracy at high conversion is low and issues arise when monitoring fast reactions. In addition, DSC only provides overall conversion degree, which makes it impossible to independently determine epoxy and amine conversion rates. Accordingly, the curing procedure of the thermoset system has to be optimized in the first place. DSC analyses were chosen to be discussed in the following part. Other techniques were tested, such as ATR-FTIR, Raman spectroscopy and rheology measurements, however the results obtained were not as conclusive as those obtained with DSC measurements. Consequently, only the results obtained with the DSC technique will be presented in this part. ATR-FTIR and Raman spectroscopy investigations are gathered in Appendix 3.

II-2-3-1 Differential Scanning Calorimetry (DSC)

Differential Scanning Calorimetry is used to understand the behavior of a material when exposed to a temperature gradient under air or under inert conditions. It allows the

determination of many characteristic properties of a sample. Using this technique it is possible to observe melting and crystallization events as well as glass transition temperatures (T_g). DSC can also be used to study oxidation, as well as other chemical reactions.

In this study, DSC analyses have been carried out in order to determine the optimal temperature for the thermosetting system to be cured. As described previously, stratification is optimal when the crosslinking system reaches 80 % of conversion.^{133, 134}

Subsequently, analyses were performed using a DSC Q100 from *TA Instrument* under a nitrogen flow of 50 mL/min. The samples in sealed (for solid sample) or hollow open (for liquid samples) crucibles first underwent a 3 minutes isotherm at -50°C to guarantee temperature homogeneity of the specimens. Different conditions were used depending on the type of analyses performed.

Method 1: Calculation of the total heat of curing reaction

The blend thermoset resin/hardener was heated at $10^\circ\text{C}/\text{min}$ from -50°C up to 220°C for 3 minutes. The system was then cooled down to $10^\circ\text{C}/\text{min}$ and a second cycle was carried out to ensure the complete reaction of the two components (Figure 22).

Method 2: In-situ crosslinking of the epoxy/amine system

The blend thermoset resin/hardener was heated at $10^\circ\text{C}/\text{min}$ from -50°C up to the desired temperature (between 40 and 150°C depending on the temperature studied) for 2 hours. The system was then cooled down at $10^\circ\text{C}/\text{min}$ and a second cycle with an isotherm of 20 minutes was carried out to calculate the amount of polymer which has not crosslinked (Figure 22).

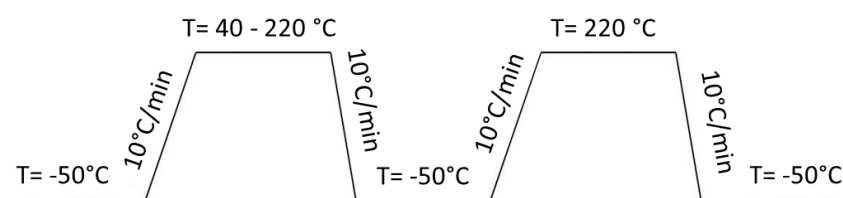


Figure 22. Schematic presentation of step wise DSC in-situ analyses

Method 3: Analyses of formerly crosslinked epoxy resin

The samples in sealed crucibles were heated up to 200 °C at 20°C/min and underwent an isotherm for 3 minutes. Then, the samples were cooled down to -50°C at 10°C/min (Figure 23). This cycle was repeated two times to ensure the complete crosslinking of the resin.

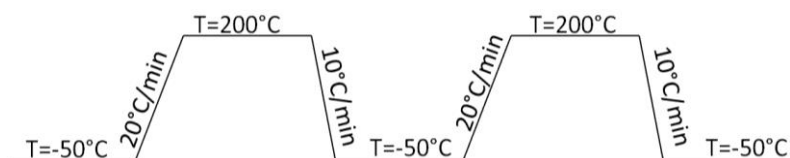


Figure 23. Schematic presentation of step wise DSC analyses after ex-situ crosslinking

Each sample was tested twice to ensure the repeatability of the results.

II-2-3-2 Investigation of the epoxy-amine conversion rate

Accordingly, DSC scans of the system before any thermal treatment was first registered following the method 1 (Figure 24).

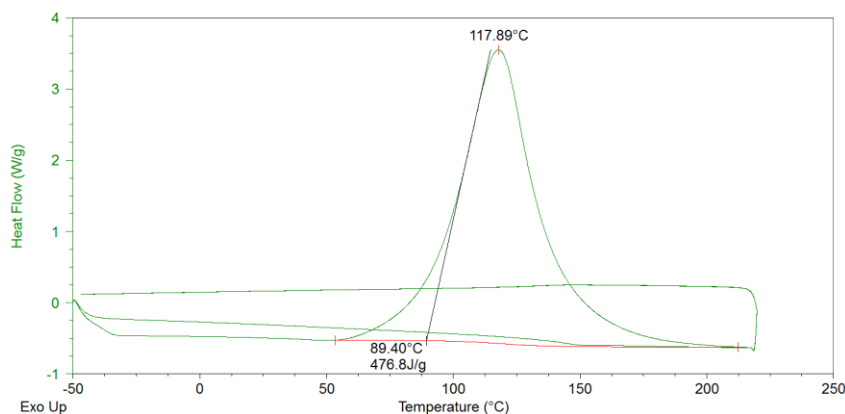


Figure 24. DSC curves of the epoxy/amine system from -50 to 220°C with a ramp of 20°C/min (2 cycles)

From the DSC curve, the total heat of reaction is determined: 476.8 J/g. Its maximum is reached at 117.4 °C, corresponding to an enthalpy of 3.55 W/g. From the total heat of reaction, the percentage of conversion can be calculated at different isothermal temperature.

To do so, the system has undergone a cure of 2 hours at different temperatures (40, 80, 110, 130 and 150 °C) and the heat release during the exothermal reaction was then calculated (Figure 25). The percentage of conversion (DH_1) was calculated according to the total heat released of the reaction (Figure 27, Table 2). Another percentage of conversion (DH_2) was calculated considering the crosslinking reactions complete at 150 °C. Indeed, no exothermal peak is discernable during the second cycle at 150 °C (Figure 26) meaning that no reaction occurred up to 200 °C. Consequently, the heat of the crosslinking reaction calculated during the isothermal at 150 °C was set for the calculation as equivalent to 100 % of conversion (Figure 27, Table 2).

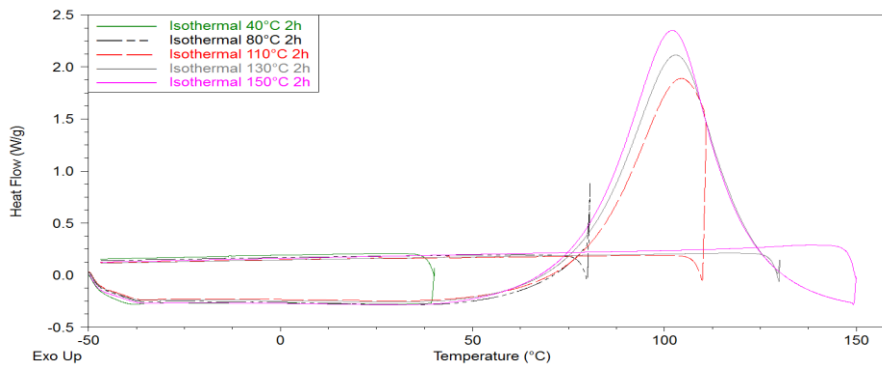


Figure 25. DSC curves of the first cycle of isotherm at 40, 80, 110, 130 and 150 °C

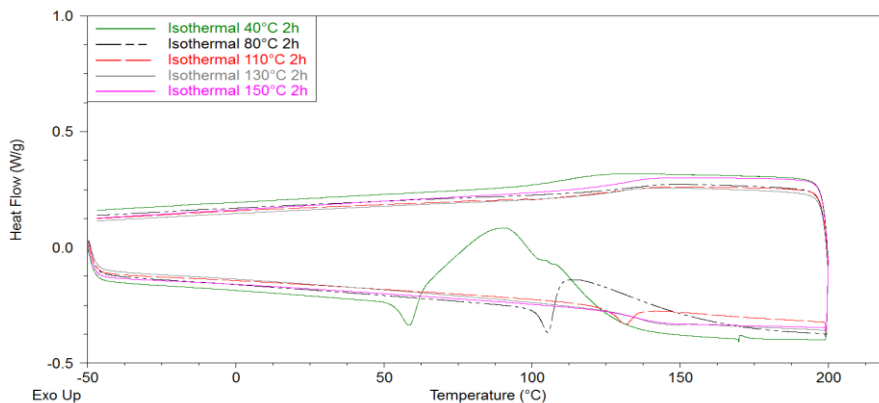
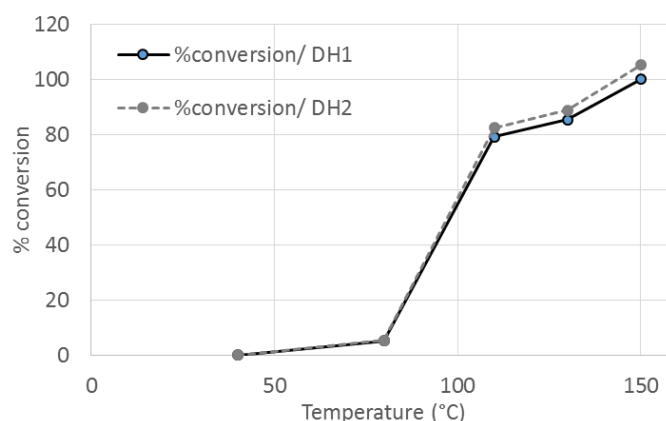


Figure 26. DSC curves of the second cycle of the in-situ crosslinking

Table 2. Heat release and percentage of conversion of the system cured at different temperature for 2 hours

Isothermal temperature (°C)	ΔH (J/g)	%Conversion (DH ₁ , %)	%Conversion (DH ₂ , %)
40	0	0	0
80	25.3	5.3	5.1
110	392.8	82.4	79.2
130	423.3	88.8	85.3
150	496.0	100.0	100.0

**Figure 27.** Epoxy group conversion in the reactive system as a function of temperature after an isothermal of 2 hours

Both percentages of conversion (DH₁ and DH₂) follow the same tendency: the slope of the curve is somehow stabilized between 40 and 80 °C and is steeper up to 150 °C. At 110 °C, 80 % of conversion is reached and 85 % at 120 °C. After that, the slope gets almost constant for higher temperature, meaning that the crosslinking reaction is almost completely achieved. From the two percentages of conversion, the 80 % of conversion are reached around 110 °C. The result is also in accordance with the maximum of heat released which occurs at 117 °C (Figure 24).

To confirm these observations, the system was then cured in the oven used for the experiments at the temperature investigated. The cured sample were then tested following the method 3, and the remaining enthalpy of reaction was calculated. From the diagram, the enthalpy of crosslinking was 85.35 J/g corresponding to a conversion rate of 17 %. Considering the experimental error used with the oven, the value obtained stays very close to the 20 % forecasted by DSC analyses.

Finally and according to the DSC measurements, the procedure was set as follows: after application on the substrate, the coating was allowed to dry at 22 °C for 24 hours in a universal heat chamber provided by *Memmert* to avoid an abrupt cure, and finally cured for 2 hours at 110 °C in a *France Etuves C3000* oven. Coatings were left at ambient temperature for at least 2 days before any experimental analysis.

Least but not the last, different isothermal duration were tested (from 30 to 120 min), but no significant difference were registered between the curves. 120 minutes was chosen to ensure a good evaporation of the solvent during the curing of the coating.

Finally, the influence of the incorporation of the second resin to the thermosetting medium was also investigated. From DSC measurements, the addition of the resin slightly shift the exothermic peak due to the crosslinking reaction toward higher temperature (the shift registered is in the range of 10 °C). This difference does not modify the conversion rate in a significant way, consequently 110 °C was kept as the optimal curing temperature.

II-3 Physico-Chemical characterizations

Physico-chemical characterizations allow identifying the optimal conditions to be used to process a self-stratifying coating, to measure the degree of stratification of the coatings and to understand the effect of a set of factors detailed in this part. Those techniques are used to optimize and characterize the layering process but also to understand the mode of action of pigments and FR fillers during the combustion of the coated materials developed.

II-3-1 Solubility measurements: Hansen's Three-Dimensional Solubility Parameters

The solubility parameters of the resins selected for this PhD thesis were determined using 54 solvents of known Hansen Solubility parameters (HSP) at a concentration of 10 % solids at (20 ± 2) °C. 100 mg of the resin was placed in a 2 ml glass vial, and 900 mg of solvent was added. The mixture was stirred at 50 rpm using an Intelli-Mixer RM-2 rotator (provided by *Elmi*) for 24 h and left to rest for extra 24 hours at (22 ± 2) °C. To obtain a more precise classification, a

second solubility test was performed by mixing 300 mg of the resin in 700 mg of each solvent (at 30 wt.% solids).

In both cases, visual observation of solubility was made 24 hours and 7 days after dissolution. A solvent is considered as a non-solvent if a two-phase system or suspended particles are observed. Results were then computed with the HSPiP software (version 4.0.05) developed by Abbott and Yamamoto to draw the solubility sphere and determine its coordinates (center and radius). The computer program uses a correlation method based on a quality-to-fit function to ensure that most of the non-solvents are located outside and most of the good solvents are located inside the Hansen sphere.¹³⁶

After the determination of the HSPs of the resins, the comparison between the solubility spheres of the two-resin system can be provided: the overlap factor V , which allows comparing the relative sizes of the common volume between the two components, can be calculated (Equation 1).

$$V = 100 \frac{C}{\frac{4}{3}\pi R_1^3} \text{ Equation 1}$$

With R_1 the volume of the smallest sphere and C the overlap volume of the spheres.

II-3-2 Surface properties

II-3-2-1 Contact Angle measurements

Contact angle measurements were used to compare the ability of both water ($\gamma = 72.8$; $\gamma^d = 21.8$; $\gamma^p = 51 \text{ mN} \cdot \text{m}^{-1}$) and diiodomethane ($\gamma = 50.8$; $\gamma^d = 50.8$; $\gamma^p = 0 \text{ mN} \cdot \text{m}^{-1}$), which have different polarities, to spread on a surface by wettability, and then to determine the surface energy. According to the Harmonic Mean method of Wu¹³⁷ and the Young's law, any surface energy can be calculated if contact angles of two reference liquids are known. For an interface between two materials, Wu expressed the interfacial surface tension by the following equation:

$$\gamma_{12} = \gamma_1 + \gamma_2 - \frac{4\gamma_1^d \gamma_2^d}{\gamma_1^d + \gamma_2^d} - \frac{4\gamma_1^p \gamma_2^p}{\gamma_1^p + \gamma_2^p} \text{ Equation 2}$$

with γ_1 and γ_2 the total energies of resins 1 and 2 respectively. This method is mostly used for the calculation of surface free energy for polymers with low surface free energy (up to 30-40 mN.m⁻¹).

Contact angles were measured with a Digidrop Contact Angle Meter GBX and a Krüss DSA-100, and the total surface tension γ , dispersive (γ^d) and polar (γ^p) components were calculated following the method of Wu (Equation 2, ASTM D 2578-67).¹³⁸

As surface tensions of the substrate and resins are critical parameters to take into account in the stratification process, they must be determined both to theoretically predict the stratification and to compare the characteristics of top and bottom layers of the resulting coatings compared to the reference resins.

When taking into account the solvent characteristics in the calculation of the surface energy, resins were primarily diluted in the selected solvent system and dried following the curing procedure of the coatings. To ensure that forecast are the most realistic, the surface tension of the crosslinked thermoset resin was measured (including the curing agent).

II-3-2-2 Adhesion measurements

The adhesion of the film on the substrates was evaluated according to the ASTM D3359-B standard using an "Elcometer 107" cross-hatch cutter.¹³⁹ The cutter chosen was a 3 mm cutter, with 6 tooth, corresponding to the measurements of thicknesses up to 250 μm . Using this procedure, the best adhesion rating is classified as 5B, and the lowest as 0B (Figure 28).

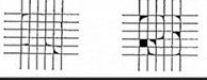
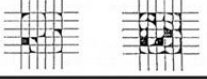
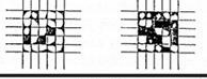
Classification	% of Area Removed	Surface of Cross-cut Area From Which Flaking has Occured for 6 Parallel Cuts & Adhesion range by %
5B	0% None	
4B	Less than 5%	
3B	5 - 15%	
2B	15 - 35%	
1B	35 - 65%	
0B	Greater than 65%	

Figure 28. Classification of the adhesion using the cross-hatch test¹⁴⁰

II-3-2-3 Color changes measurements

The effect of weathering on the visual aspect of the most successful self-stratifying coatings developed was evaluated by colorimetry. During the ageing, $L^*a^*b^*$ measurements were performed before, during and after ageing.

Color changes and reflectance were recorded using a Datacolor CHECK 3 portable spectrophotometer from *Datacolor Industry*. In the CIE (“Commission Internationale de l’Eclairage”, or International Commission on Illumination) $L^*a^*b^*$ system, L^* represents the lightness of color ($L^* = 0$ for the absolute black, $L^* = 100$ for absolute white), the a^* value indicates the color position between red and green (a^* is green at one extremity ($a^* > 0$) and red at the other ($a^* < 0$)) and the b^* value represents the color position on a yellow/blue scale ($b^* > 0$ indicate blue and $b^* < 0$ indicates yellow). a^* and b^* values are close to zero for neutral colors (white and gray) and increase in magnitude for more saturated or intense color (pure color) (Figure 29).

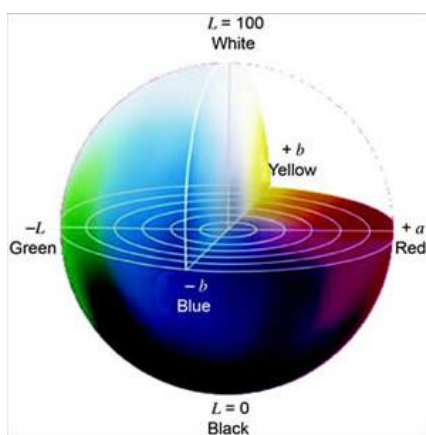


Figure 29. Color space of CIE Lab system¹⁴¹

The difference in color between two samples (ΔE) can be calculated using Equation 3, with ΔL^* representing the lightness difference, Δa^* and Δb^* the differences in a^* and b^* values respectively.

$$\Delta E = \sqrt{(\Delta L^*)^2 + (\Delta a^*)^2 + (\Delta b^*)^2} \quad \text{Equation 3}$$

II-3-3 Thermal study: Thermo-Gravimetric Analyses (TGA)

The changes in thermal degradation profile often observed in polymers in the presence of many fillers can be a significant factor influencing the action of fire retardant fillers. Thermo-gravimetric analysis (TGA) provides insights concerning the nature of filler/polymer interactions, together with their relative decomposition temperatures.

Thermogravimetric Analysis (TGA) allows monitoring changes in physical and chemical properties of a material by measuring its weight loss while it is heated according to a specific temperature ramp. Then, the derivative of the TG curve (DTG) allows determining the mass loss rate at a given temperature, and thus permit to identify the main decomposition steps of the material.

In this thesis, TG measurements were carried out using a Discovery TGA provided by *TA Instrument*. Samples were put in open vitreous alumina crucibles, and gas flow rate was set at 50 mL/min. Nitrogen or air was chosen depending on the desired conditions, respectively under pyrolysis or thermo-oxidative atmosphere. Samples underwent an isotherm at 50 °C for

120 minutes for thermal homogeneity, then a heating ramp of 20 °C/min was set to ensure that the samples did not experience significant temperature or mass gradients, making the effect of mass and heat transfers negligible. Each experiment was repeated at least twice to ensure repeatability of the results.

Samples were analyzed either without any thermal treatment, or with the same curing procedure used for the coatings (i.e. dried for 24 hours at (22 ± 2) °C and cured for 2 hours at 110 °C).

Difference weight loss curves were also calculated (Equation 4) to determine a potential increase or decrease in the thermal stability of the formulations due to the incorporation of a filler in the system. These curves represent the difference between the experimental TG curves for the mixture ($w_{exp}(T)$) and the linear combination of TG curves ($w_{theo}(T)$) for the neat components (Equation 5).

$$\Delta w(T) = w_{exp}(T) - w_{theo}(T) \text{ Equation 4}$$

$$w_{theo}(T) = X1 * w_{resin} + X2 * w_{filler} \text{ Equation 5}$$

Where w_{resin} and w_{filler} correspond to the weight determined from the experimental TG curves; X1, X2 the weight percentage of the sole resin and sole filler respectively. If $\Delta w(T) < 0$, then the experimental weight loss is higher than the theoretical one. This shows that the reactivity and/or interaction between the polymer and the filler leads to a thermal destabilization of the material. If $\Delta w(T) > 0$, then the system is thermally stabilized.

The next part of this chapter is dedicated to the description of the chemical analyses which were used to characterize the composition of solid films or residues obtained after fire tests, to some extent to evaluate the degree of stratification and finally to follow the extent of the curing reaction between the epoxy and the amine curing agent (Appendix 3).

II-3-4 Chemical analysis

II-3-4-1 Fourier Transform Infrared spectroscopy (FTIR)

Attenuated Total Reflexion (ATR) with a diamond crystal was used in conjunction with the Fourier Transform Infrared spectroscopy (FTIR) to examine the materials, the coatings and also the residues after fire testing. The analysis and comparison of spectra can provide information about the concentration of each resin at both surfaces, and can lead to the degree of stratification.¹⁰²

The total internal energy of a molecule can be determined by the sum of rotational, vibrational and electronic energy levels in a first approximation. FTIR spectroscopy studies the interactions between matter and electromagnetic fields in the infrared region: by absorbing IR radiation, a molecule can be excited to a higher vibrational state. Using this technique, light is absorbed at distinct frequencies in a liquid, solid or gas, which corresponds to the vibrational frequencies of the bonds in the sample. Electromagnetic waves belonging to the infrared domain enter the diamond ATR crystal (made of high refractive index) at an angle of typically 45° (relative to the surface of the crystal) and are totally reflected at the crystal to sample interface. The evanescent wave (fraction of light reaching the sample) extends beyond the surface of the crystal into the sample held in contact with the crystal (penetration depth: 0.5 – 3 μm). In regions where the sample absorbs energy, the wave is attenuated. The reflected radiation is then returned to the detector, which records the attenuated IR signal (the interferogram) used to generate an IR spectra.

Room temperature FTIR-ATR spectra were recorded between 400 and 4000 cm⁻¹ using a Fourier transformed infrared spectrometer (ThermoScientific) Nicolet iS50. The spectra processed by OMNIC software resulted from 64 scans using a resolution of 4 cm⁻¹.

The extent of curing of the epoxy resin and amine hardener was monitored from 40 to 190 °C using a Pike GladiATR™ (*Pike Technologies*) displayed by a Watlow SD. A ramp of 10 °C/min was applied and one spectra was recorded every 10 °C using the same processing conditions described previously. The reference peak used as an internal standard for the normalization of epoxy peak absorbance is phenylene at 830 cm⁻¹ (γ_{CH} aromatics).

II-3-4-2 Raman spectroscopy

Raman spectroscopy is used to provide a molecular fingerprint to materials. It is due to the scattering of light by the vibrating molecules, and it is commonly used in combination with FTIR spectroscopy, as a complementary technique to study the concentration of a selected polymer. Raman and FTIR spectroscopy differ in some key fundamental ways. Raman spectroscopy depends on a change in polarizability of a molecule, whereas FTIR spectroscopy depends on a change in the dipole moment. FTIR spectroscopy is sensitive to hetero-nuclear functional group vibrations and polar bonds, especially OH stretching in water. Raman, on the other hand, is sensitive to homo-nuclear molecular bonds. For example, it allows distinguishing C-C, C=C and C≡C bonds. Both methods have advantages and limitations, but when combined, these two methods become a powerful tool to characterize a large set of materials.

Raman spectroscopy measurements were performed with a LabRam HR visible infinity instrument equipped with liquid nitrogen cooled CDD detector from *Horiba Jobin Yvon*. The spectra were recorded at 473 nm with a laser power of 0.6 mW. The extent of curing of the epoxy resin and amine hardener was monitored from 25 to 100 °C, one spectra being recorded every 5 °C.

II-3-5 Microscopic analyses

In this work, microscopic analyses were used for different purpose: (i) to measure the thickness of a coating, (ii) to assess the degree of stratification by cross-section analyses, (iii) to determine the location of the fillers through the thickness of a film, (iv) to assess the quality of the junction between two layers in laminated systems and (v) to analyze the residues during and after fire tests. Depending on the nature of the samples tested, different preparation methods have been tried and optimized to allow the most accurate and efficient mappings.

II-3-5-1 Sample preparation

Coatings applied on polycarbonate

The specimens for microscopic characterizations were obtained by cryo-fracture in liquid nitrogen. The coated sample was dug in the liquid, cooled for 30 seconds, removed and broken with a hammer to allow a clean and neat finish of the cross section.

Char residues

The char residues obtained from fire tests were embedded in epoxy resin and polished.

Carbon metallization was finally carried out before any further microscopic characterization on all samples, whatever its preparation method, with a Bal-Tec SCD005 sputter coater.

II-3-5-2 Electronic microscopy

Electronic microscopy with chemical analyses is another efficient tool to provide information about the degree of self-stratification: a mapping of a characteristic chemical element can provide information about the relative concentration of each resin on either both interfaces or in the inner coating structure. The analysis of cross-sections gives information about both non-homogeneous-in-layer and heterophase polymer structures.^{142, 143}

Scanning electron microscopy with X-Ray mapping (SEM-EDX)

Scanning Electron Microscopy (SEM) uses a focused beam of high energy electrons to generate signals at the surface of the specimens. The signals that derive from electron-sample interactions reveal information about the sample including morphology, chemical composition and crystalline structure. The electron beam leads to the emission of secondary and back scattered electrons (BSE) (amongst other species) which are then collected over a selected surface area, and generate a two-dimensional image. Quantitative or semi-quantitative analyses of selected areas can also be performed (using Energy Dispersive X-ray spectroscopy or EDX) to determine chemical compositions.

SEM images were obtained at various levels of magnification on a Hitachi S4700 with field emission gun. Images were recorded at 5.0 or 7.0 kV and 20 μ A. The difference in chemical

composition between top and bottom coating surface was characterized by cross-section X-Ray mappings (EDX analysis) at 13.0 kV, 25 μ A.

Electron probe micro analysis with Wavelength-Dispersive Spectroscopy (EPMA-WDS)

Electron probe micro analysis (EPMA) is also a particle-beam technique (typical energy = 5-30 keV). It is a qualitative and quantitative method of non-destructive elemental analysis of micron-sized volume at the surface of the materials, with sensitivity in the range of the hundred ppm. The aim of an EPMA is mainly to acquire precise elemental analyses at very small spot sizes (> 1-2 μ m) primarily by Wavelength Dispersive Spectroscopy (WDS). The characteristic X-rays are detected at particular wavelengths (depending on the emitting species) and their intensity is recorded to identify the sample's composition. WDS spectrometers are based on the Bragg's law and use various moveable, shaped nanocrystals as monochromators, they allow a better detection resolution than EDX.

In this thesis, a Cameca SX100 electron probe microanalyser was used to perform elemental analysis on the cross-section of the coatings (electron interaction volume 1 μ m³) and on char residues. BSE images and X-ray mappings were carried out at 15 kV, 40 nA. On BSE pictures, the darkest parts correspond to the "lightest" elements. On mappings, red parts correspond to the highest concentration of the selected element, and black ones to zero concentration.

For every specimen, Carbon (C), Oxygen (O) and Nitrogen (N) were detected by X-ray analyses (SEM-EDX or EPMA). However, as the polymer matrices used are composed of those same elements, it was difficult to detect the interface between the substrate and the coatings. Consequently, attention was directed towards other specific elements composing the resin of interest whenever possible.

When the coating contained silicon, attention was turned to the silicium element (Si). In the fluoropolymer resin, the Fluor Ethylene part contains a 3:1 Fluorine (F)/Chlorine ratio. With this system, Chlorine (Cl) was chosen as characteristic element rather than fluorine as it is easier to detect (heavier element than fluorine). Table 3 gathers the different chemical elements constituting either the resins or fillers that have been selected for the work.

Table 3. Elements and X-ray energies used for SEM-EDX and EPMA analyses

Element	Symbol	X-ray energy (keV)
Carbon	C	0.277
Oxygen	O	0.525
Nitrogen	N	0.392
Silicium	Si	1.740
Fluorine	F	0.677
Chlorine	Cl	2.622
Iron	Fe	6.405
Calcium	Ca	3.692
Phosphorus	P	2.010
Zinc	Zn	8.637

Digital microscopy

A digital microscope is a variation of traditional optical microscopes as it does not contain eyepieces: optics and a charge-coupled device (CDD) camera act as a detector, and images are displayed on a monitor. It allows creating 3D images based on automatically captured images. A digital microscope VHX-1000 (supplied by Keyence) was used in this work to look at residues morphology and aspect after fire tests.

The last part of this chapter is dedicated to the description of the different fire tests that were used to investigate the fire performances of the systems developed.

II-3-6 Fire testing methods and characterization of the mode of action of materials during combustion

Four methods were used to evaluate the fire retardant properties of the coating/polycarbonate systems: the Limiting Oxygen Index (LOI), the UL-94 test, the Mass Loss Calorimeter and the characterization of the residues using a tubular furnace.

Specimens for LOI and UL-94 tests were prepared as follows: polymer plates were cut with a saw band to give barrels of a dimension of 100*10*3 mm³. Barrels were then placed horizontally in the spray chamber and maintained to allow the spraying on all sides until a wet film thickness of 200 µm was reached. The curing procedure was then follow as previously described.

II-3-6-1 Limiting oxygen index (LOI)

The Limiting Oxygen Index (LOI, *Equation 6*) is measured using a Fire Testing Technology (FTT) instrument on plaque of dimension $100 \times 10 \times 3 \text{ mm}^3$ according to the standard “oxygen index” test (ISO 4589-2¹⁴⁴). This test allows measuring the minimum concentration of oxygen in a nitrogen/oxygen mixture required to just support combustion of a test sample at room temperature. This test allows evaluating the relative flammability of materials, their ignitability and inflammation. The specimen is clamped vertically into a glass cylinder in a controlled atmosphere, and the top of the sample is ignited with a burner (Figure 30). Materials having a LOI value below 21 vol.% O₂ are called combustible, and those with a LOI value above 21 vol.% O₂ are flame retarded.

$$LOI = 100 * \frac{[O_2]}{[O_2] + [N_2]} \quad \text{Equation 6}$$

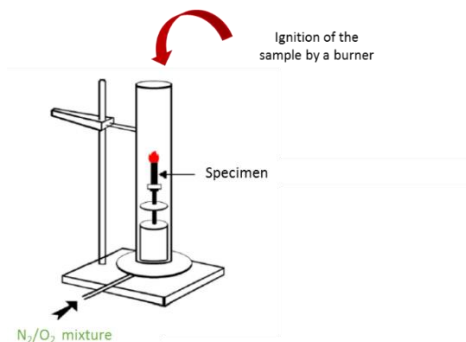


Figure 30. Experimental set of LOI test

II-3-6-2 UL-94

UL-94 test is a vertical burning qualitative test performed according to IEC 60695-11-10¹⁴⁵ on $100 \times 10 \times 3 \text{ mm}^3$ plates (Figure 31). It describes the tendency of a material to extinguish or to spread the flame after ignition of the material. Glowing and flaming combustion and the occurrence of flaming drops (with ignition of a cotton sample) are taken into account to rate the samples from V0 to non-classified (NC), where V0 is the best rating (short burning times

without ignition of cotton) and NC the worst. Table 4 depicts the criteria conditions to meet V0, V1 or V2 classifications.

In this study, a blue flame with a 20 mm high central cone was applied for 10 seconds at the bottom edge of the vertical specimen. The flame was then removed and the time of flameout was recorded. The blue flame was then applied for extra 10 seconds and removed. After the second burning, the time to extinguish and the afterglow time were registered. Dripping and ignition of a cotton placed below the specimen were also carefully followed. A set of 5 plates of diameter 3 mm was tested for each system.

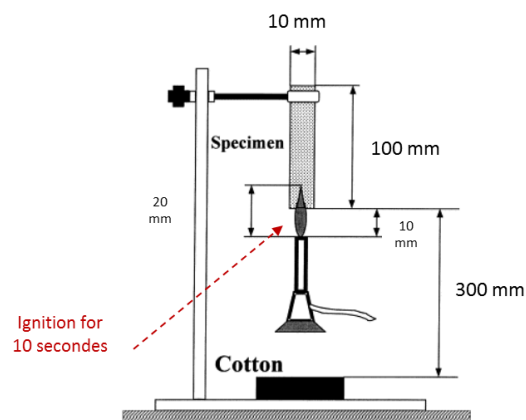


Figure 31. Scheme of UL-94 apparatus

Table 4. UL-94 classification

Criteria	V-0	V-1	V-2
Total flaming combustion for each specimen	≤ 10s	≤ 30s	≤ 30s
Flaming and glowing combustion for each specimen after second burner flame application	≤ 30s	≤ 60s	≤ 60s
Total flaming combustion for all 5 specimen	≤ 50s	≤ 250s	≤ 250s
Cotton ignited by flaming drops	NO	NO	YES
Glowing or flaming combustion of any specimen to holding clamp	NO	NO	NO

II-3-6-3 Mass loss calorimeter (MLC)

The Mass Loss Calorimeter (MLC) allows simulating the fire conditions at a small bench scale according to ISO 13927 (Figure 32).

A Fire Testing Technology (FTT) Mass Loss Calorimeter was used to perform measurements on samples following the procedure defined in ASTM E906. The equipment is identical to the one used in oxygen consumption cone calorimetry (ASTM E-1354-90), except that a thermopile in the chimney is used to obtain heat release rate (HRR) rather than employing the oxygen consumption principle. Our procedure involved exposing specimens measuring $100 \times 100 \times 3 \text{ mm}^3$ (according to ISO-13927 standard) in horizontal orientation. Samples were wrapped in aluminum foil leaving the upper surface exposed to the heater and were placed on an insulating ceramic backing board at a distance of 35 mm from cone base. External heat flux of 50 kW/m^2 was used to carry out the experiments. 50 kW/m^2 corresponds to the common heat flux for a fully-developed fire (high external flux, large length scale, ambient temperature above auto-ignition temperature, low ventilation).¹⁴⁶ Experiments were first performed at a lower flux (35 kW/m^2) corresponding to a mild fire scenario, however the coatings applied on polycarbonate did not ignite, even after 30 minutes of exposures (one example is depicted in appendix 4).

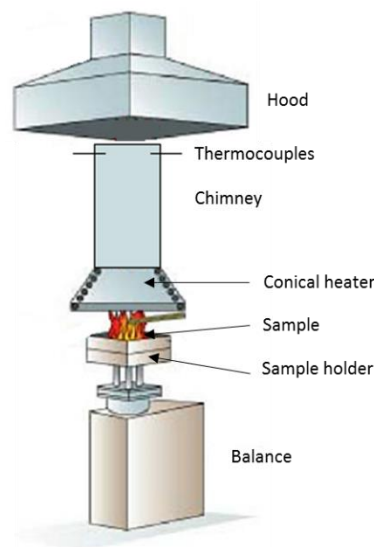


Figure 32. Schematic of the Mass Loss Calorimeter

The MLC was used to determine the main characteristic fire parameters (Figure 33): heat release rate (HRR) as a function of time, time to ignition (TTI), time to flameout (TFO), maximum HRR (peak of heat release rate, pHRR), time to peak of HRR (tpHRR), total heat release (THR), mass loss rate (MLR) and specific mass loss rate (SMLR). The specific mass loss

rate is calculated as the ratio between the MLR and the surface of the sample exposed to the MLC external irradiance level (i.e. 88.4 cm^2 - ISO 5660 standard).^{147, 148} Here, the TTI, HRR, pHRR, THR, MLR and SMLR of coated plastics were evaluated and compared to those of raw samples. Experiments were performed three times to ensure repeatability of results and the presented curves are the worst among the repetitions. The values were found to be reproducible within $\pm 10 \%$ (relative standard deviation).

Finally, to understand the mode of action of the coatings toward the plastic substrate and its behavior during combustion, the most successful self-stratified coatings were removed from the cone base after their ignition (at TTI, Figure 33) and after flame out (TOF). The remaining coating was then analyzed by means of ATR-FTIR and microscopic analyses.

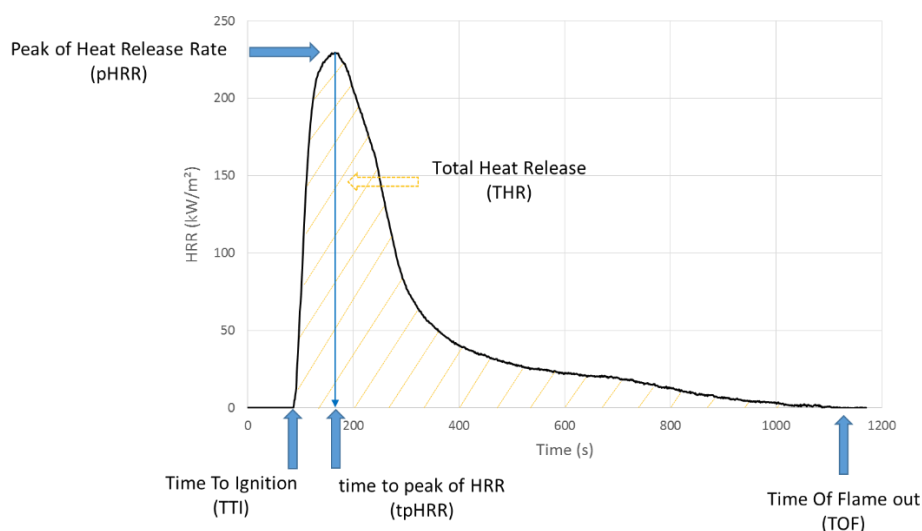


Figure 33. Schematic curve obtained after MLC test and its characteristics values

II-3-6-4 Characterization of the solid residues

The thermal treatment consists to submit a sample in a furnace at a determined temperature under controlled nitrogen gas flow to simulate the pyrolysis conditions (Figure 34). The treatment temperature are determined according to thermogravimetric analyses as they correspond to the characteristic degradation step of the systems.

Heat treatments were realized on the raw materials and on the coating systems in a tubular furnace under nitrogen flow ($75 \text{ mL}\cdot\text{min}^{-1}$). A heating of $10 \text{ }^\circ\text{C}/\text{min}$ is applied from the ambient to the treatment temperature followed by an isotherm for 3 h. The sample is then cooled to ambient temperature. The collected residues were then analyzed using the digital microscopy.

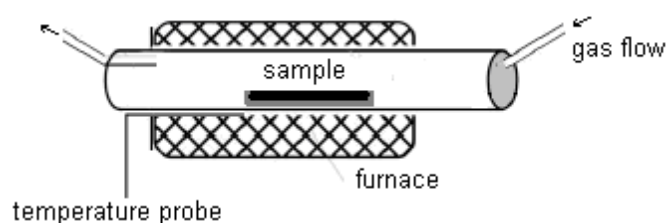


Figure 34. Schematic representation of the tubular furnace used for thermal treatment

II-3-6-5 Pyrolysis-gas chromatography- Mass spectrometry (Py-GCMS)

The Pyrolysis-gas chromatography spectrometry (Py-GCMS) device was provided by Shimadzu (Figure 35). The device consists of a micro-furnace pyrolyzer (Frontier Lab PY-2020iD) coupled with a GC/MS (Shimadzu GCMS QP2010 SE). Analyses are performed on $200 \mu\text{g}$ sample under helium atmosphere (inert conditions) through a desorption mode which consists in heating the sample at high heating rate in the pyrolyzer furnace, while heavy evolved gases condense at the beginning of the GC column and volatile fragments are detected after ionization. After the thermal treatment in the pyrolyzer furnace, condensed products are desorbed and separated in the GC column to finally be analyzed by the mass spectrometer.

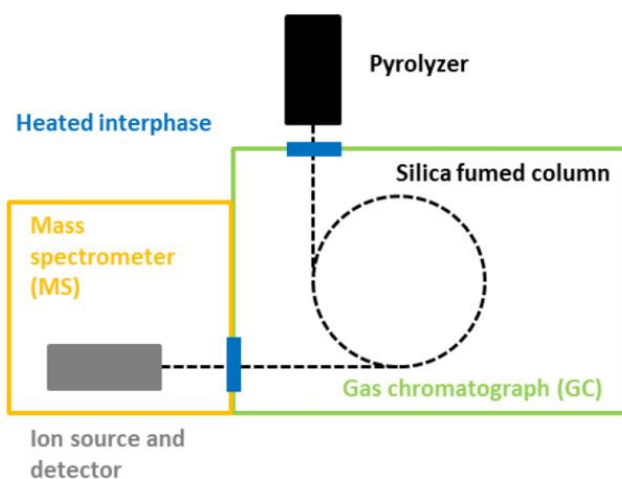


Figure 35. Schematic presentation of the Py-GCMS device

Samples (in a stainless steel cup) are heated up from 80 to 800 °C with a heating ramp of 60 °C/min. After the decomposition process, evolved gases are introduced into the GCMS system whereas a part of the gases is split by boiling point to avoid blockage in the column or saturation of the detector. Released decomposition gases are separated using a 30 m long fumed silica capillary column (30 m * 0.25 mm * 0.25 µm film thickness). The temperature of the column is set to 35 °C during the desorption process. The column is then heated up to 320 °C with a heating ramp of 10 °C/min followed by an isotherm at 320 °C for 6 min. The linear velocity of the carrier gas (helium) is set to 40 cm/s. The separated gases and fragments are then analyzed with the quadrupole mass spectrometer with an Electron-Impact (IE) ionization source. The IE spectra are recorded at 70 eV with a mass scan of 2 scans per second. The interface between the pyrolyzer and the GC is heated up to 320 °C; the interface GC/MS to 280 °C. The temperature of the ion source is set to 230 °C. Data is analyzed using the GC/MS post-run analysis from Shimadzu and F-Search from Frontier lab, whereas products are identified using NIST and F-search database.

II-3-6-6 Pyrolysis combustion flow calorimeter (PCFC)

The combustibility of the gas phase was evaluated with a pyrolysis combustion flow calorimeter (PCFC) provided by Fire Testing Technology Ltd (Figure 36). PCFC was developed by Lyon¹⁴⁹ from FAA and allows measuring the flammability of 10 mg of materials. Samples

were placed in open alumina pans and were degraded under nitrogen atmosphere at a heating rate of 1 °C/s and with a nitrogen flow of 80 cc/min. The decomposition gases were then burnt in a nitrogen/oxygen mixture with 80 cc/min and 20 cc/min flows respectively. The heat release during the combustion of the material is measured as a function of the temperature using an oxygen analyzer, according to the Huggett relation.¹⁵⁰ Using a heating ramp of 1 °C/s, pHRR value in W/g equals heat release capacity (HRC) in J/(g.K).

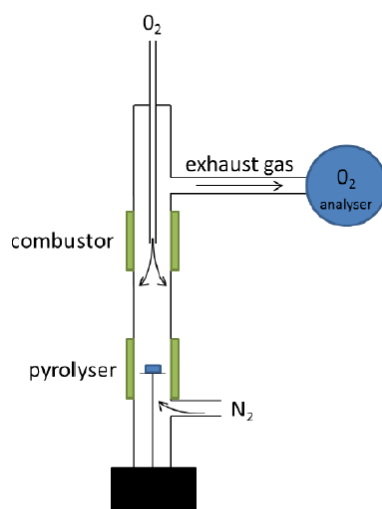


Figure 36. Schematic of Pyrolysis Combustion Flow Calorimeter

In order to obtain the most reliable results, the maximum oxygen consumption has to reach around 50 % of the total O₂ mixture. That is to say, starting from a mixture containing 20 % of O₂, the peak of consumption has to reach 10 ± 3 % of O₂. When decomposition gases are released, a certain amount of time is needed from them to reach the combustor, where the oxygen analyzed measures the oxygen depletion. Therefore, a slight shift of temperature is often observed between TG and PCFC analyses (approximately + 20 °C in PCFC).

II-4 Accelerated ageing testing

One objective of the work is to figure out the impact of ageing on the properties of the self-stratified coatings and on its fire performances. Accordingly, experiments were performed on both plates (for visual and chemical analyses, adhesion rating and cone calorimeter tests) and barrels (for LOI and UL-94 tests). Before any testing, samples were dried 24 h in a vacuum chamber at 60 °C in order to eliminate the excess of humidity and to perform all characterizations in the same controlled conditions. Total duration of the tests was 8 weeks with intermediate characterizations every two weeks. The evolution of the coating aspect and color, adhesion and fire properties of the samples were investigated by comparing the properties of aged materials to those of unaged material. MLC tests were performed only after 8 weeks of exposure.

II-4-1 Ageing under UV-rays exposure

Accelerated weathering under UV-rays was realized by exposing the samples to both temperature and UV rays. For this purpose, a weathering chamber from *Q-lab* (QUV/se: UV, condensation and control irradiance SOLAR EYE, Figure 37) was used. The device was equipped with 8 UV lamps (UVA 340) at 0.89 W/m² irradiance.

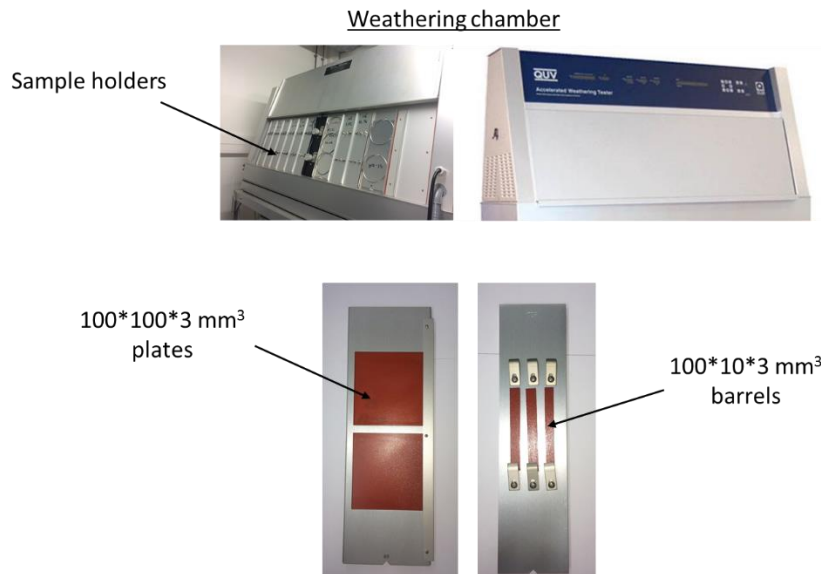


Figure 37. Q-LAB, QUV/se weathering chamber and sample holders

The weathering conditions chosen are derived from a ISO 4892-3 standard¹⁵¹: cycles of 4 hours under UV irradiation at 60 °C followed by 4 hours in the dark at 50 °C were applied. The specimens (plates and barrels, Figure 37) were attached to the test panel and exposed to these consecutive cycles without interruption for 8 weeks. Barrels of diameter 3 mm were turned on the opposite side every week to ensure a uniform exposition on each side.

II-4-2 Ageing under temperature and relative humidity conditions

Accelerated ageing tests of uncoated and coated plastics were carried out in a humidity chamber (HCP 108 supplied by *Memmert*, Figure 38). The temperature was kept constant at 60°C while the humidity was set to 75 % relative humidity (T/RH experiment).



Figure 38. Humidity chamber test HCP 108

II-5 Conclusion

In the first part of this chapter, the raw materials used for the preparation of the formulations as well as the proceeding methods were presented. Afterwards, materials and protocols used to evidence the stratification and characterize the coatings in terms of physical properties, thermal stability and fire performances were described. Finally, the procedure used to stimulate accelerated ageing of materials were presented.

The following chapter investigates theoretically and experimentally the behaviors of binary and ternary blends in order to obtain perfect self-layered coatings on polycarbonate. The influence of the most relevant factors is studied, and the most successful systems will be selected for the next part of the work.

Chapter III: *Design of self-stratifying coatings*

In this chapter, the self-stratification of binary and ternary blends on a polycarbonate substrate is investigated. The first section deals with the prediction of layering considering two theoretical models described in the literature review: the Hansen approach and the model based on surface and interfacial energies. The design of particular blends applied on polycarbonate is then investigated, and the influence of the most significant factors toward the layering process is especially discussed.

III-1 Introduction

It has been shown in the first chapter that a self-stratifying system is based on incompatible polymer blends, which can produce a two-phase mixture. This chapter will now focus on the design of a perfectly stratified film on a polycarbonate substrate, corresponding to the formation of two well distinct and homogeneous layers (type I), or a film in which the phase separation is characterized by a homogeneous concentration gradient more or less pronounced in the film thickness (type II).

Practically, binders for such coatings are usually four component systems: two incompatible resins and two solvents selected according to their volatility and their affinity with one of the polymers. According to these considerations, the following resins have been selected, among other materials, for their properties and promising results in the literature:

- ✚ One epoxy resin : DGEBA
- ✚ One silicone resin : Silicone 217
- ✚ One fluoropolymer resin: Lumiflon LF200

Epoxies are the most widely used structural resin due to their exceptional mechanical and chemical properties, and particularly since they have excellent adhesion ability to a wide variety of materials. Silicone oligomers or polymers are widely used as additives for their immediate incompatibility with conventional resins. As decompatibilizers, they are able, to some extent, to substantially accelerate the phase separation process with moderate or negligible influence on the composition of equilibrium solutions.¹⁴³ Fluoropolymer resins in particular demonstrated promising results when combined with epoxide in terms of self-stratification on both plastic and metallic substrates.^{12, 109, 111, 123, 134}

The chosen strategy to investigate the concept of layering using silicone, fluoropolymer and epoxy resins, is to study theoretically and experimentally different approaches combining solubility, compatibility and surface energy measurements. As the mechanisms driving stratification depend, amongst other factors, on raw materials, solvents, curing agent and type of fillers, their effects are deeply investigated.

Results are presented in the form of a discussion in which, part of different published articles are incorporated:

- Beaugendre, A., Degoutin, S., Bellayer, S., Pierlot, C., Duquesne, S., Casetta, M., Jimenez, M. (2017), *Self-stratifying epoxy/silicone coatings*, *Progress in Organic Coating*, 103: 101-110. [doi: 10.1016/j.porgcoat.2016.10.025]
- Beaugendre, A., Saidi, S., Degoutin, S., Bellayer, S., Pierlot, C., Duquesne, S., Casetta, M., Jimenez, M. (2017), *One pot flame retardant and weathering resistant coatings for plastics: a novel approach*, *RSC Advances*, 7, 40682 – 40694. [doi: 10.1039/c7ra08028j]

III-2 Prediction of stratification

In this section, the feasibility of producing self-stratifying coating compositions is theoretically investigated. As it was shown in chapter I, different theoretical models have been developed in order to predict whether a given system should stratify and among them: (i) the Hansen approach¹³³, based on the solubility parameters of resins, and (ii) a model based on the surface and interfacial energies^{109, 110, 123}, including thermodynamic and surface properties.

Those approaches have been applied to the sets of binary mixtures chosen for screening. Each combination contains a thermoplastic and a thermoset resin: their solubility behaviors and their compatibility are first determined using the Hansen's solubility approach, and in a second part, the surface and interfacial tensions are calculated and used to evaluate the probability of a system to stratify using the second model. Theoretical investigations including the epoxy/silicone and epoxy/fluoropolymer systems were published.^{142, 152}

III-2-1 Solubility parameters – Hansen approach

Hansen solubility parameters (HSP) are widely used for the characterization of polymers, surfaces and particular materials (pigments, fillers, fibers ...) as reported in chapter I. Since it is clear that, solubility parameters are critical parameters to take into account for the self-

stratification, they have to be determined for the materials used in the paint formula. In this PhD work, the Hansen approach is meant to be a starting point for predicting the compatibility between binary mixtures of polymers. Researchers are indeed unanimous that a homogeneous mixture of incompatible polymers that forms a coating with a polymer/polymer composite structure is necessary for self-stratifying phenomenon to occur. In addition, the solvents chosen for the formulation have to be selected in order to have in the initial stage a 3D solubility parameter which is located within the intersection volume of the solubility spheres of both resins.

The first part is dedicated to the determination of the HSP of the selected resins, and in a second part, the compatibility between particular resin combinations is investigated. Finally, those studies will allow the choice of suitable resin systems, which could theoretically results in self-stratifying coatings. The chosen systems will then be tested experimentally.

III-2-1-1 Hansen solubility spheres

After the dilution of each resin in the 54 solvents of known solubility at 10 wt.%, dispersive (δ_d), polar (δ_p), hydrogen-bonding (δ_h), the total Hansen solubility (δ_{tot}) parameters and the radius of the solubility spheres were calculated. Results are gathered in Table 5.

Table 5. Hansen Solubility Parameters of the selected resins diluted at 10 wt.%

Resins	δ_d (J.cm ⁻³) ^{1/2}	δ_p (J.cm ⁻³) ^{1/2}	δ_h (J.cm ⁻³) ^{1/2}	δ_{tot} (J.cm ⁻³) ^{1/2}	Radius (MPa ^{1/2})
Epoxy DGEBA	19.5	19.4	4.3	27.9	19.9
Silicone S217	17.7	16.1	5.6	24.7	15.6
Fluoropolymer LF200	19.4	3.4	13.6	23.9	13.5

The solubility sphere of the epoxy resin (DGEBA) has the highest radius ($R = 19.9 \text{ MPa}^{1/2}$): it has higher chances to interact with other solubility spheres compared to the fluoropolymer resin, which has a lower radius; thus less chance to overlap with other spheres in the Hansen space. Some solvents can still be identified as outliers since they are located on the wrong side of the Hansen sphere boundaries (dotted blue circles and red squares, Figure 39).

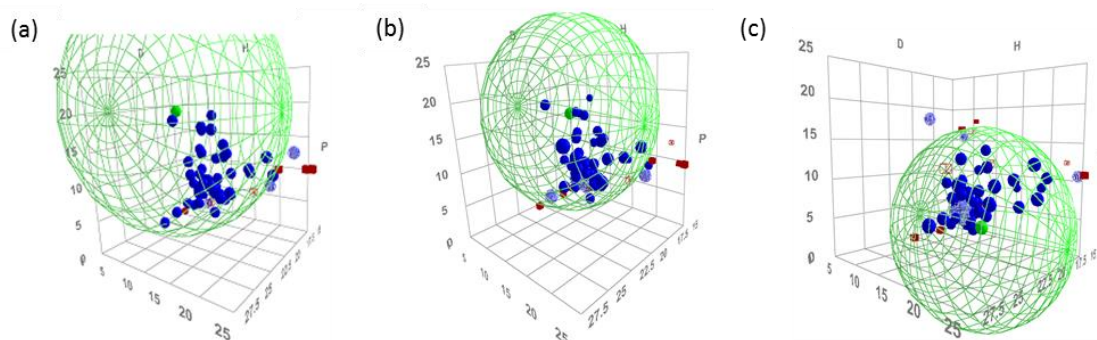


Figure 39. Hansen solubility spheres of (a) Epoxy DGEBA, (b) Silicone S217 , (c) Lumiflon LF200 resins diluted at 10 wt.%

The mathematical model used for the calculation assumes that the solubility volume is spherical, which can explain this misfit. However, spherical view is a practical tool to rapidly determine if a solvent would dissolve the resin or not for a given concentration (Table 6).¹³⁶ Experimentally, an inside solvent has a RED number (Equation 11, p. 48) <1 (blue filled circle) and an outside solvent has a RED number >1 (red filled square). A “Wrong Out” solvent is a solvent that should be inside but has a RED number >1 (red dotted square). A “Wrong In” solvent is a solvent that should be outside but has a RED number ≤ 1 (blue dotted circle). Table 6 gathers the solvents, which are located on the wrong side of the sphere, and their quantities. It allows determining the accuracy of the model.

Table 6. Accuracy of the model according to the location of the solvent in the Hansen space

Resins	Solvents				
	In	Out	Ratio In/Out	Wrong In	Wrong Out
Epoxy DGEBA	47	7	7.0	Liquid Paraffin, 1-Butanol	Dipropyl Amine, Solketal, Methanol
Silicone S217	44	10	4.4	Liquid Paraffin, 1-butanol	Methyl Oleate, Tetrahydronaphthalene, Dipropyl Amine, Solketal
Fluoropolymer LF200	43	11	4.0	Acetic Anhydride, DMSO, Glycerol Triacetate, Dimethyl Phthalate, Carbone Disulfide	Propylene Carbonate, Diethyl Ether, Methyl Oleate, 2-Nitropropane, Nitroethane, Ethylene Glycol, Dipropyl Amine

The choice of the solvent is crucial for the stratifying process to occur. The selected solvent or solvent blend has to dissolve both resins to allow the preparation of the formulation and its application onto a substrate. Moreover, it needs to meet requirements in terms of polarity and volatility. As a matter of fact, solvents which do not dissolve the chosen resins can already be set apart (Table 7). None of the resins is soluble in water and glycerol.

Table 7. List of solvents which do not dissolve the selected resins at 10 wt.%

Resins	No solubility
Epoxy DGEBA	Water , cyclohexane, paraffin liquid, propylene glycol, ethylene glycol, glycerol , 1-butanol
Silicone S217	Water , cyclohexane, carbon disulfide, paraffin liquid, β -pinene, propylene glycol, ethylene glycol, glycerol , methanol, 1-butanol
Fluoropolymer LF200	Acetic Anhydride, DMSO, γ -butyrolactone, acetonitrile, glycerol triacetate, dimethyl phthalate, water , cyclohexane, carbon disulfide, glycerol , methanol

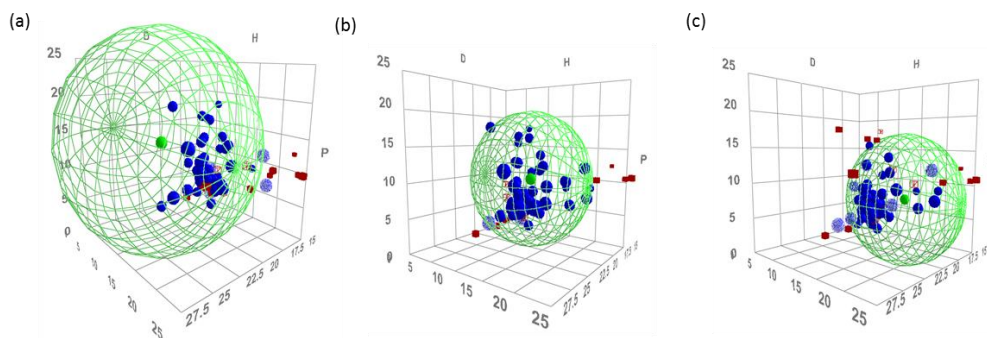
In order to obtain reasonable accuracy for the determination of a Hansen solubility sphere, a large number of solvents is required.¹⁵³ In the usual 10 wt.% conditions, the ratio between good and poor solvents is quite high (between 3.1 and 7, Table 8). Additional experiments were carried out at a concentration of 30 wt.% so that the method is more discriminating and in order to try to make a more effective classification. In these conditions, more accurate results are obtained particularly with the epoxy (ratio of 3 at 30 wt.% compared to 7 at 10 wt.%, Table 8). HSP and radii are detailed in Table 9 and the Hansen spheres are depicted in Figure 40.

Table 8. List of solvents which do not dissolve the selected resins at 30 wt.% after 7 days

Resins	Solvents				
	In	Out	Ratio In/Out	Wrong In	Wrong Out
Epoxy DGEBA	39	15	3.0	Isopropyl Laurate, Geraniol, Tetraethylene Glycol, ADMA	Diethyl ether, MIBK, Methylal, Solketal, Dipropyl Amine
Silicone S217	43	11	4.0	Liquid Paraffin, 1-chlorobutane, Pyridine	Tetrahydronaphthalene, Dipropyl Amine
Fluoropolymer LF200	37	17	2.2	Acetic Anhydride, Acetonitrile, Glycerol Triacetate, Liquid Paraffin Tetraethylene Glycol	m-xylene, Tetrahydronaphthalene, Methylal, m-Cresol, Pyridine, N-Methyl-2-Pyrrolidone

Table 9. HSP and radius of the selected resins diluted at 30 wt.%

Resins	δ_d ($\text{J}\cdot\text{cm}^{-3}$) ^{1/2}	δ_p ($\text{J}\cdot\text{cm}^{-3}$) ^{1/2}	δ_h ($\text{J}\cdot\text{cm}^{-3}$) ^{1/2}	δ_{tot} ($\text{J}\cdot\text{cm}^{-3}$) ^{1/2}	Radius ($\text{MPa}^{1/2}$)
Epoxy DGEBA	22.3	13.4	7.0	26.9	16.5
Silicone S217	17.5	9.7	9.4	22.1	11.0
Fluoropolymer LF200	12.9	5.7	8.7	16.6	12.1

**Figure 40.** Hansen solubility spheres of (a) Epoxy DGEBA, (b) Silicone S217, (c) Lumiflon LF200 resins diluted at 30 wt.%

Finally, the epoxy resin belongs to the resins having the highest radius ($16.5 \text{ MPa}^{1/2}$), followed by the fluoropolymer ($12.1 \text{ MPa}^{1/2}$) and the silicone resin ($11.0 \text{ MPa}^{1/2}$). More reasonable ratio

are obtained at this solid percentage, particularly with the epoxy and fluoropolymer resins (with respectively 8 and 6 additional solvents being outside the solubility spheres at 30 wt.% compared to the ones at 10 wt.%). Moreover, solubility was also checked after 21 days, and a particular observation was made at such solid percentage (30 wt.%): the silicone resin appears to be no longer soluble in m-xylene. Yet, it was specified by Vink that one of the solvents used for self-stratifying compositions must be a solvent for one of the resins and a non-solvent for the second resin.^{122, 134} Consequently, as the epoxy resin is soluble in this specific solvent, even after 21 days, m-xylene should represent a solvent of choice.

Once the compatibility behavior of a given polymer towards solvents is determined, it allows a comparison with other resins: if two materials have their solubility spheres located in sufficiently distinct positions ($V < 80\%$), then they are expected to be only partially compatible. If one of the values is close to 100%, it can be assumed that the two resins will be mutually compatible. If both values are below 80%, then it can be expected that the blend will form two phases after mixing. On a theoretical and experimental level, the more similar δ_d , δ_p , δ_h , the more compatible the polymers.

III-2-1-2 Prediction of the compatibility between resin binary mixtures

A blend of a crosslinkable and thermoplastic resin is chosen as a starting point. In addition to the epoxy resin, the selected silicone can form a crosslinked network when used in combination with a resin modifier. Consequently, both resins were considered in the theoretical investigations. Therefore, the “target polymer” corresponds to the crosslinkable resin (e.g. epoxy or silicone resins). The overlap factor is calculated for each target polymer in combination with a thermoplastic resin. $V_{\text{resin 1}}$ represents the percentage (by volume) of the resin 1 solubility sphere that is occupied by the sphere of the other polymer (resin 2), and $V_{\text{resin 2}}$ the percentage (by volume) of the resin 2 solubility sphere that is occupied by the resin 1 solubility sphere.

➤ *Prediction of the compatibility of epoxy based blends*

Systems are studied considering the HSP obtained at 10 and 30 wt.% and after 48 hours and 7 days (Table 10). Solubility spheres are depicted in Figure 41, and the coordinates of the spheres are gathered in Appendix 5.

Table 10. Overlap factors between the epoxy DGEBA and thermoplastic resins when diluted at 10 and 30 wt.%, and after 48 hours and 7 days at 30 wt.%

	10 wt.%		30 wt.%	
Target polymer : Epoxy resin DGEBA	$V(\text{DGEBA})^*/V(X)^{**}$	Overlap factor	$V(\text{DGEBA})^*/V(X)^{**}$	Overlap factor
Silicone S217	51 %/ 99 %	>100 %	23 %/ 77 %	>100 %
Lumiflon LF200	13 %/ 38 %	42 %	18 %/ 7 %	63 %
	30 wt.% After 48 hours		30 wt.% After 7 days	
Target polymer : Epoxy resin DGEBA	$V(\text{DGEBA})^*/V(X)^{**}$	Overlap factor	$V(\text{DGEBA})^*/V(X)^{**}$	Overlap factor
Silicone S217	41 %/ 92 %	>100 %	23 %/ 77 %	75 %
Lumiflon LF200	16 %/ 53 %	44 %	18 %/ 7 %	63 %

* $V(\text{DGEBA})$ = percentage (by volume) of the crosslinkable resin solubility sphere that is occupied by the sphere of other polymer, ** $V(X)$ = percentage (by volume) of the second polymer solubility sphere that is occupied by the crosslinkable resin solubility sphere.

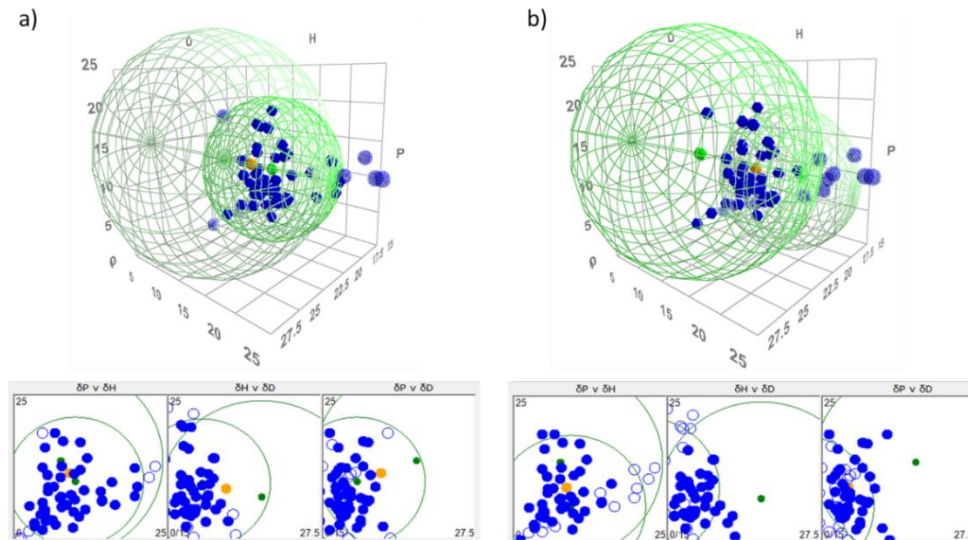


Figure 41. Solubility spheres of binary mixtures of the epoxy DGEBA resin with a) Silicone 217 and b) Lumiflon LF200 in the Hansen space and projection in $(\delta p; \delta h)$, $(\delta h; \delta d)$ and $(\delta p; \delta d)$ maps of the solubility spheres at 30 wt.% and after 7 days (green circle with a dot center).

Blend of epoxy and silicone resin¹⁴²

Based on those results, 51 % of the thermoset resin solubility sphere is occupied by the sphere of the silicone resin, whereas V_{silicone} is equal to 99 %, meaning that the silicone sphere is totally

included in the solubility sphere of the epoxy resin when resins are diluted at 10 wt.%. Then, the calculation of the overlap factor between the resins leads to a value higher than 100 %. Therefore, according to this model, the incompatibility between the epoxy and the silicone resins is theoretically not guaranteed.¹²³

At 30 wt.% and after 48 hours, an overlap superior to 100 % is still obtained, even if a less substantial portion of the spheres overlaps. However, after 7 days, an incompatibility between the two resins appears: a minor portion of the epoxy sphere is comprised in the silicone solubility sphere (23 % compared to 41 % after 48 hours) and the overlap factor is reduced: 75 %. **Consequently, the Hansen model does not predict the stratification of the system when the resins are diluted at 10 wt.%, but it does predict the incompatibility after 7 days using a 30 wt.% dilution.**

To our knowledge, as silicone resins have never been considered for self-stratifying coatings, no comparison can be drawn with such resin combination. Nevertheless, high levels of stratification were already obtained with systems having an overlap factor $V > 90$ %.¹¹¹

Blend of epoxy and fluoropolymer resins¹⁵²

At 10 wt.%, the radius of the solubility sphere of the fluoropolymer resin is lower than the one of the epoxy (13.5 compared to 19.9 MPa^{1/2}), meaning that it has the lowest probability to interact with the other solubility sphere in the Hansen space. 38 % represents the percentage by volume of the fluoropolymer resin solubility sphere that is occupied by the sphere of the epoxy resin, whereas only 13 % of the epoxy sphere is occupied by the solubility sphere of the fluoropolymer resin. The overlapping area of the two solubility spheres C is equal to 42 %, suggesting that the two polymers are theoretically incompatible. This result is in accordance with various studies based on blends of fluoropolymer (particularly Lumiflon LF200 grade) and different grades of epoxy resins (overlap factor below 80 %).¹¹¹

When diluted at 30 wt.% and if the solubility is checked after 48 hours, the probability of the system to stratify is close to the probability obtained at 10 wt.% (44 %). However, 7 days after the dilution, the probability decreases (but stays constant, at least up to 21 days): V is equal to 63 % compared to 44 % after 48 hours. Nonetheless, the model still predicts the stratification.

Finally, the HSP of the epoxy and fluoropolymer resins meet the requirement to allow the stratification of the system at 10 and 30 wt.%. The layering is nevertheless promoted by a low solid percentage and by an application shortly after the proper dilution of each resin.

➤ *Prediction of the compatibility of silicone based blends*

In this part, the silicone resin represents the target polymer (thermoset resin). The prediction of stratification is evaluated when combining the resin with the thermoplastic fluoropolymer resin (Table 11). Only the results obtained at 10 wt.% are presented in this section.

Table 11. Overlap factors considering the silicone resin as target polymer (10 wt.%)

Target polymer : Silicone S217	$V^*(S217)/V^{**}(X)$	Overlap factor
Lumiflon LF200	23 %/ 36 %	37 %

* $V(S217)$ = percentage (by volume) of the crosslinkable resin solubility sphere that is occupied by the sphere of other polymer, ** $V(X)$ = percentage (by volume) of the second polymer solubility sphere that is occupied by the crosslinkable resin solubility sphere.

The combination of the silicone resin with the fluoropolymer resin is theoretically promising: the overlap factor is even lower in the case of the silicone resin as thermosetting system ($V = 37\%$) compared to the epoxy resin. If the two systems are enough compatible to form a homogeneous solution after their mixing, the resulting coating could theoretically lead to a high degree of layering.

III-2-1-3 Conclusion

Based on the results obtained at 10 wt.%, the most promising systems would be a blend of silicone with the fluoropolymer resin ($V = 37\%$). A blend of the epoxy resin DGEBA with the fluoropolymer ($V = 42\%$) seems also theoretically favorable.

Other resins were part of the screening (see Appendix 6) and were not an attractive choice considering the overlap factor with all other thermoplastic resins ($> 100\%$). They are consequently not presented in this section.

In addition and based on these results, favorable conditions for the experiments can be postulated:

- The layering of the epoxy/silicone would be the most favorable if the paint is formulated at least 7 days after the proper dilution of the resins at 30 wt.%.
- Likewise, the combination of the epoxy DGEBA and fluoropolymer LF200 would be promoted by using a low solid percentage and a rapid utilization of the diluted resins.

III-2-2 Surface energy approach

After a large screening (not presented in this manuscript) and according to the state of the art (chapter I) and solubility considerations, four solvents and solvent combinations have been selected: m-xylene and blends of BuAc: m-xylene (1: 1), MIBK: m-xylene (1: 1) and MIBK: xylene: 1-methoxy-2-propanol (50:30:20). Considering the boiling temperature and polarity index of each solvent, the MIBK: xylene blend has the highest volatility and polarity, and the pure xylene the lowest (Table 12).

Table 12. Boiling temperature of the tested solvents

Solvent	T _{boiling} (°C)	Polarity index	Saturation vapor pressure (hPa, 20 °C)
Xylene	139	Non-polar, 2.5	8.0
BuAc	126	4.0	10.7
1-methoxy-2-propanol	120	2.2	11.5
MIBK	116	4.2	14.8

The surface tension of polycarbonate and of the binders (pure and diluted in the different solvent systems) is determined by contact angle technique following the method of Wu described in the experimental part (Table 13). The epoxy resin is crosslinked beforehand to be as close as possible to the experimental conditions.

Table 13. Values of contact angle and surface tensions following the method of Wu for the selected substrates and resins¹³⁷

		θ_{water} (°)	$\theta_{\text{diiodomethane}}$ (°)	γ (mN.m ⁻¹)	γ^p (mN.m ⁻¹)	γ^d (mN.m ⁻¹)
Substrate						
Polycarbonate (Lexan)		77 ± 3	24 ± 2	55.4	8.9	46.6
Pure resins						
Crosslinked epoxide		82 ± 6	46 ± 6	45.1	7.7	37.3
Fluoropolymer		102 ± 2	63 ± 6	31.2	2.2	29.0
Silicone		102 ± 3	53 ± 7	35.1	1.1	34.0
Diluted resins						
Xylene	Epoxide	104 ± 2	36 ± 3	37.0	-0.5	37.6
	Fluoropolymer	87 ± 1	50 ± 2	41.7	6.5	35.2
	Silicone	81 ± 6	41 ± 5	48.0	8.1	39.9
BuAc: xylene (1: 1)	Epoxide	87 ± 3	46 ± 4	43.3	6.2	37.1
	Fluoropolymer	84 ± 2	49 ± 3	43.6	7.6	36.0
	Silicone	93 ± 2	34 ± 3	45.7	2.9	42.8
MIBK: xylene (1: 1)	Epoxide	108 ± 7	36 ± 2	27.6	-1.8	29.4
	Fluoropolymer	80 ± 2	49 ± 1	45.4	9.3	36.0
	Silicone	85 ± 3	35 ± 2	48.6	6.1	42.5
MIBK: xylene: 1- meth-2- propanol (5:3:2)	Epoxide	74 ± 2	44 ± 3	49.8	11.5	38.3
	Fluoropolymer	78 ± 1	48 ± 2	46.3	9.7	36.5
	Silicone	75 ± 3	37 ± 4	51.9	10.4	41.5

From these results, the three conditions for self-stratification (Equation 26-28, section I-4-8) of the unfilled binary combinations of polymers applied on PC were calculated (Table 14).^{142,}

¹⁵² Results given in a colored background are not in accordance with the model. Values of the interfacial energies are gathered in Appendix 7.

Table 14. Prediction of stratification on PC of the combination of the epoxide resin with either the fluoropolymer or silicone resins. Results given in a color background are not in accordance with the model.

Conditions based on surface energy (mN.m ⁻¹)		$\gamma_{s1}-\gamma_{s2}-\gamma_{12}$ > 0	$\gamma_{s1}-\gamma_1-\gamma_{s2}+\gamma_2$ ≥ 0	$\gamma_s-\gamma_{s2}-\gamma_{12}-\gamma_1$ > 0
Pure resins	Epoxide/ Fluoropolymer	-10.8	7.2	12.0
	Epoxide/ Silicone	-11.5	3.5	7.3
Xylene	Epoxide/ Fluoropolymer	0.9	4.4	3.3
	Epoxide/ Silicone	0.7	-0.6	-3.2
BuAc: xylene (1:1)	Epoxide/ Fluoropolymer	-3.0	-3.8	4.9
	Epoxide/ Silicone	-1.7	-1.7	8.4
MIBK: xylene (1:1)	Epoxide/ Fluoropolymer	1.9	1.3	-8.1
	Epoxide/ Silicone	2.2	-1.9	-11.0
MIBK: xylene: 1-meth-2- propanol (5: 3: 2)	Epoxide/ Fluoropolymer	-0.4	3.4	7.0
	Epoxide/ Silicone	0.6	-1,3	2.4

Prediction of the stratification of the Epoxy/Fluoropolymer blend

According to the model, if pure resins and the resins diluted in a blend of either MIBK: xylene or MIBK: xylene: 1-methoxy-2-propanol are considered, two out of three conditions are satisfied. With a blend of BuAc: xylene, only one condition is fulfilled. Finally, the highest probability to stratify is obtained if xylene is used as solvent.

Prediction of the stratification of the Epoxy/Silicone blend

From the calculations, no system satisfies the three conditions given by the model. Considering the pure resins and a blend of MIBK: xylene: 1-methoxy-2-propanol, two out of three conditions are fulfilled. If the whole system is taken into account, the probability of layering with xylene or with the binary solvent blends is likely the same on PC: one out of three conditions is verified. Thus, the system based on epoxy/silicone resins and including a curing agent should theoretically not stratify considering the theoretical model based on surface energy.

III-2-3 Conclusion

Prediction of stratification does not lead to the same conclusions depending on the approach and on the conditions. The second model seems closer to the real system as it takes into account the influence of the curing agent, of the substrate and in some case the solvents.

Now, the design of the different systems is necessary to confirm (or not) the results of the predictive models. The different coatings were thus prepared, and cured according to the experimental procedure described in chapter 2. Stratification behavior as well as physical properties (aspect, adhesion, pigment dispersion, etc.) were experimentally investigated using different techniques (visual observations, SEM-EDX or EPMA-WDS, ATR-FTIR, contact angle and cross-hatch adhesion testing). Also, influence of selected solvent systems, crosslinking agent and pigments was deeply analyzed.

III-3 Self-stratification on polycarbonate substrate

From the theoretical and bibliographical investigations, two main systems were chosen: the epoxy/silicone and the epoxy/fluoropolymer combinations. Other binary blends were also tested (acrylic/silicon, etc.) and lead to efficient self-stratified films but results were not as promising as the results obtained with the two selected systems and won't be presented in this manuscript for more clarity. In a first instance, the layering behavior of unfilled binary blends of resins has been deeply considered. The influence of selected solvent or solvent blends, crosslinking agent and pigments is investigated. Finally, the experimental results are compared with the theoretical data.

III-3-1 Stratification of binary blends

The layering behavior of the epoxy/silicone and epoxy/fluoropolymer systems is first investigated. Then, the focus is put on the combination of the binary blends with particular

solid fillers. As the main results obtained for each system have already been published, the article is presented in a first instance. Then, a short discussion is proposed which includes the presentation of non-published additional results.

III-3-1-1 Stratification of unfilled epoxy/silicone blends¹⁴²

In this work, an innovative self-stratifying coating based on an epoxy/silicone blend has been developed and applied on polycarbonate. The self-stratification level of this system was evidenced by microscopic analyses coupled with X-ray mappings. The influence of solvents and of the curing agent on the stratification process has also been investigated, first for pigment free systems and then for pigmented systems. Results are presented in the form of a discussion in which part of the following published article are incorporated:

- Beaugendre, A., Degoutin, S., Bellayer, S., Pierlot, C., Duquesne, S., Casetta, M., Jimenez, M. (2017), *Self-stratifying epoxy/silicone coatings*, *Progress in Organic Coating*, 103: 101-110. [doi: 10.1016/j.porgcoat.2016.10.025]

First, the influence of solvent and curing agent on the stratification process was investigated in the case of pigment free systems.

Influence of solvent

Depending on the solvent used, different stratification and interlayer patterns were obtained (Table 15). The organization of layers was determined by microscopic analysis, and each layer composition was determined by X-ray mappings.

Table 15. Resulting coatings appearance, adhesion and stratification patterns of unpigmented uncrosslinked and crosslinked systems

	Solvent	Appearance of the coating	Cross hatch testing	Stratification pattern
Crosslinked	Xylene	Rough, small bubbles	5B	I
	BuAc: xylene (1: 1)	Rough, small bubbles	5B	I
	BuAc: xylene (3: 1)	Rough, small bubbles	5B	I
	MIBK: xylene (1: 1)	Smooth, glossy	5B	IV
Uncrosslinked	Xylene	Cracks, rough and opaque	5B	I
	BuAc: xylene (1: 1)	Transparent, smooth and glossy	5B	I

With xylene, a quite uniform multi-layer system is obtained through the film thickness, leading to a stratification pattern of Type I (Figure 42).

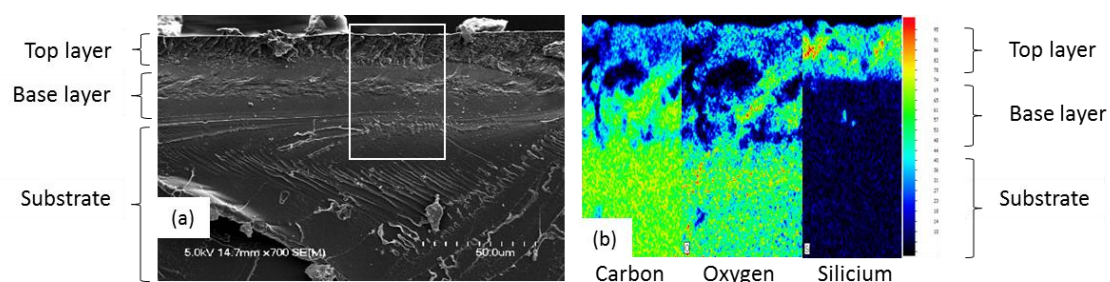


Figure 42. SEM micrograph of a cross-section of an epoxy/silicone based coating in xylene: (a) self-stratifying coating, (b) EDX mapping of Carbon, Oxygen and Silicium

EDX mapping showed that the epoxide layer is the base layer in contact with the substrate, and the silicone layer is at the interface with air. Interlayer adhesion failures appear in some areas of the film, but this phenomenon could be due to the sample preparation method (cryofracture) before microscopic observations. With a blend of MIBK: xylene, the more volatile and polar solvent system, the upper part of the coating is mainly composed of silicone but there are also inclusions of island shaped regions of silicone in the base layer, rich in epoxy resin. The degree of stratification can thus be classified as a Type IV pattern. The blends of BuAc: xylene (3: 1 and 1: 1 ratios) give rise to a perfect stratification (Type I) (Figure 43 a), quite uniform along the film and without any interlayer adhesion failure (Figure 43 b).

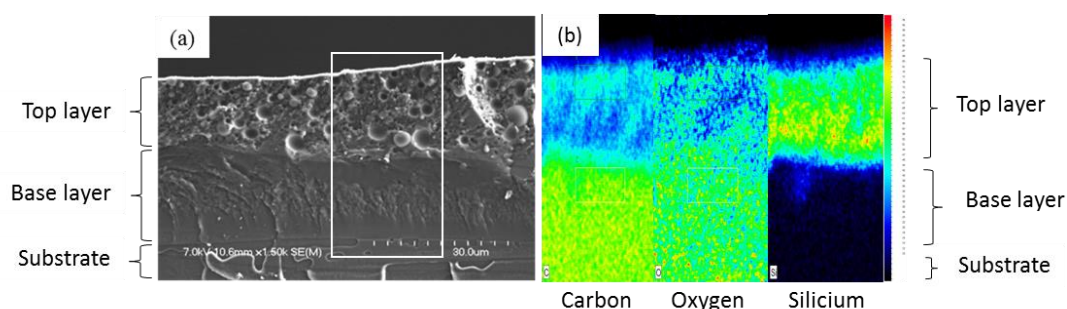


Figure 43. SEM micrograph of a cross-section of an epoxy/silicone based coating in butylacetate: xylene (1: 1): (a) self-stratified coating, and the corresponding (b) EDX mappings of Carbon, Oxygen and Silicon (from left to right)

Thus, from the microscopic analyses, it has been shown that the higher the rate of solvent evaporation, the more spontaneous the stratification. However, the rate of solvent evaporation should not be too high because the binders need sufficient time to form a heterogeneous structure before the crosslinking reaction is complete (and before the viscosity of the system becomes too high). Moreover, phase separation should occur immediately after the application of the coating, as a result of solvent evaporation. With the MIBK: xylene solvent system, evaporation occurs too rapidly, leading to the gelation of the system before the complete formation of heterophase structures and crosslinking, giving rise to a Type IV pattern.

As a result, the epoxy/silicone system dissolved in a blend of BuAc: xylene (1: 1 ratio) is considered as the most promising system. Indeed, if the ease of coating preparation is taken into account, solvent emission appears to be inferior during the spraying with a 1: 1 ratio compared to a 3: 1 ratio, allowing an easier handling and a lower amount of solvent used to reach a 200 μm wet film thickness. The SEM picture shows a Type I stratification, the epoxy and silicone layers being perfectly stratified. As proven by EDX analysis, the top layer is composed of the silicone resin (Figure 43 b).

The influence of the curing agent in the selected system was then investigated and compared to the corresponding systems containing xylene.

Influence of crosslinkage induced by the curing agent

Hardeners can influence the stratification as much as any other components of the system: they can affect both the compatibility between the resins and the gelation speed of the system, and therefore the phase separation behavior. In some cases, the presence of chemical bonding between the top and bottom layers can even be evidenced.¹¹⁴ Moreover, a too reactive catalyst can inhibit completely the occurrence of a concentration gradient or a layering because the full system gelifies and crosslinks too rapidly.¹³⁴

The effect of the curing agent is strongly dependent on the selected resins. It can crosslink a particular thermosetting resin and at the same time be incompatible with the thermoplastic resin.

To investigate the influence of the crosslinkage induced by the amine curing agent on the stratifying behavior, a comparative study was performed between crosslinked and uncrosslinked systems in xylene and BuAc: xylene (at a 1: 1 ratio). The main issue is the undried-like film obtained with uncrosslinked systems after curing in the oven, particularly with xylene, which boiling temperature (139 °C) is above the curing temperature (110 °C). Type I stratification patterns and the best adhesion rating (5B) are obtained in all cases; however, the interlayer sharpness and the film aspect are different (Table 15, Figure 44). With xylene, it was not possible to obtain a clear cut of the cross section as the film is more elastic. It creates a less defined interlayer, and a non-uniform film and top surface (rough and coarse structures). The visual appearance is also affected: an opaque film with cracks was formed when uncrosslinked, and a rough transparent film with small bubbles was obtained when crosslinked. In BuAc: xylene system, the effect of the hardener is less pronounced: the interlayer is well defined but leads in some areas of the film to a more convoluted separation between the two phases in the case of crosslinked systems.

The crosslinking reaction causes the formation of small bubbles at the surface of the coating, leading to poor adhesion in some areas.

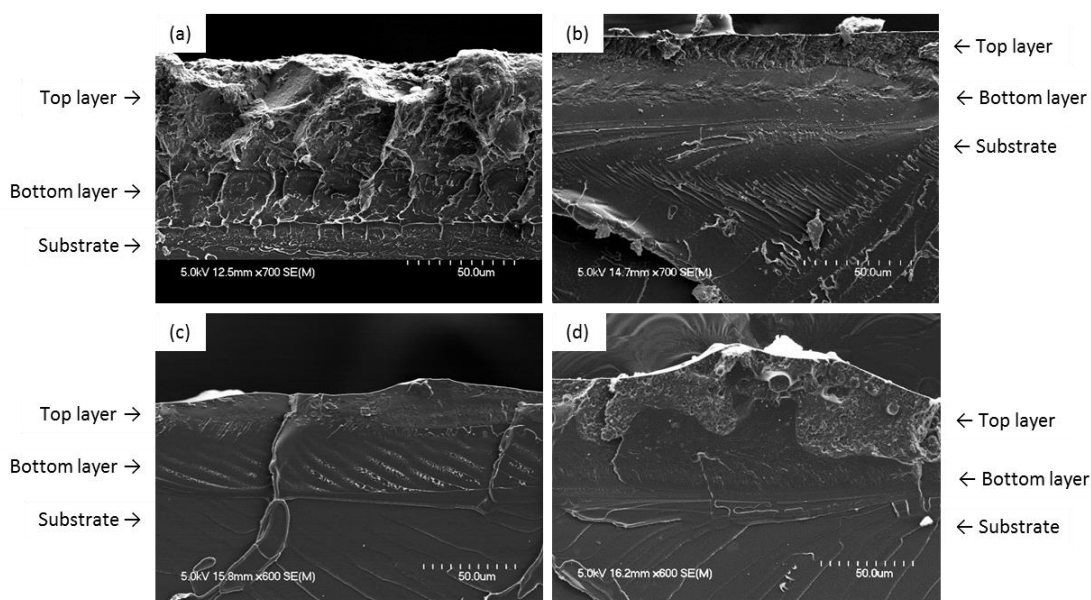


Figure 44. Comparison between uncrosslinked (a, c) and crosslinked (b, d) epoxy/silicone self-stratified coatings in xylene (a, b) and BuAc: xylene (1: 1) (c, d)

To conclude, the choice of the hardener is not trivial as it can react with the thermoplastic resin and can favor -or disfavor- the degree of incompatibility between the polymers. Therefore, the incompatibility, both between the resins and with the crosslinker, must not be too high to enable the coating preparation and to avoid the negative effect on stratification.

III-3-1-2 Stratification of unfilled epoxy/fluoropolymer blends¹⁵²

In this work, the self-layering concept has been studied using a mixture of epoxy and fluoropolymer resins. First, the ability of the unfilled system to stratify is investigated through experimental analysis.

Similarly, results are presented in the form of a discussion in which, part of the following published article are incorporated:

- Beaugendre, A., Saidi, S., Degoutin, S., Bellayer, S., Pierlot, C., Duquesne, S., Casetta, M., Jimenez, M. (2017), *One pot flame retardant and weathering resistant coatings for plastics: a novel approach*, RSC Advances, 7, 40682 – 40694. [doi: 10.1039/c7ra08028j]

Unfilled binary blends were formulated and applied on PC. Table 16 gathers the results obtained for the different coatings in terms of visual appearance, thickness, adhesion and stratification pattern (observed using SEM cross-sections).

Table 16. Resulting appearance, thickness, adhesion and stratification pattern of unfilled binary blends

Solvent	Appearance of the coating	Thickness ($\mu\text{m} \pm 5$)	Cross hatch testing	Stratification pattern
Xylene	Rough, uniform, opaque	60	5B	I
MIBK: xylene (1: 1)	Rough, uniform, opaque	35	5B	I
BuAc: xylene (1: 1)	Rough, uniform, opaque, glossy	65	5B	I
MIBK: xylene: 1-methoxy-2-propanol (50:30:20)	Uniform, glossy, opaque	85	2B	I

All unpigmented formulations lead to a type I stratification pattern (Table 16) but the visual appearance and the adhesion properties depend on the solvent used. With pure xylene and a MIBK: xylene blend, the coatings look similar (rough, uniform and opaque) and the best adhesion level is obtained (5B). On the contrary, the use of BuAc: xylene and MIBK: xylene: 1-methoxy-2-propanol solvent blends increases the gloss retention of the coating, even if adhesion properties are different: the best adhesion level is obtained with BuAc: xylene (5B), compared to a 2B rating for the MIBK: xylene: 1-methoxy-2-propanol blend.

Regarding the SEM micrographs, when a MIBK: xylene solvent blend is used, the stratification is clearly evidenced: two uniform layers are obtained, with a well-defined interlayer (Figure 45 a). Similar layering behaviors are obtained with the other solvent media. Then, to determine the composition of the two layers, EDX cross section mappings were carried out (Figure 45 b). According to those considerations, the chlorine X-ray mappings allow demonstrating that the upper layer is mostly composed of the fluoropolymer resin, and that the base layer, at the interface with the substrate, should be consequently mainly composed of the epoxy resin. The X-Ray mappings are similar whatever the solvent used.

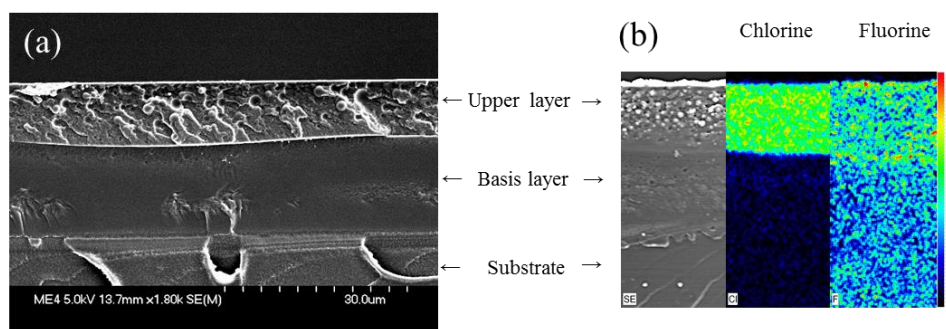


Figure 45. (a) SEM micrograph and (b) EDX X-ray mappings of Chlorine and Fluorine on a cross-section of an epoxy/fluoropolymer based coating in MIBK: xylene (1:1)

Thus, experimental characterizations revealed that, whatever the solvent used with the epoxy/fluoropolymer system, a type I stratification pattern is obtained. Visual appearance and adhesion are not really affected, except with the MIBK: xylene: 1-methoxy-2-propanol solvent blend. These results allow making comparisons between the predictions given by the two theoretical models and the experimental results.

Contact angle measurements and infrared spectra of the resins (with and without solvents) and of the upper layer of the stratified films were also recorded to support the results (Figure 46, Table 17). However, neither the preparation of free standing films nor the delamination of the coatings from the PC were possible. Consequently, no comparison with the bottom layer of the film could be done. In addition, residual solvent was still remaining (> 10 wt.%) which makes the comparison of contact angle data not reliable enough to draw precise conclusions.

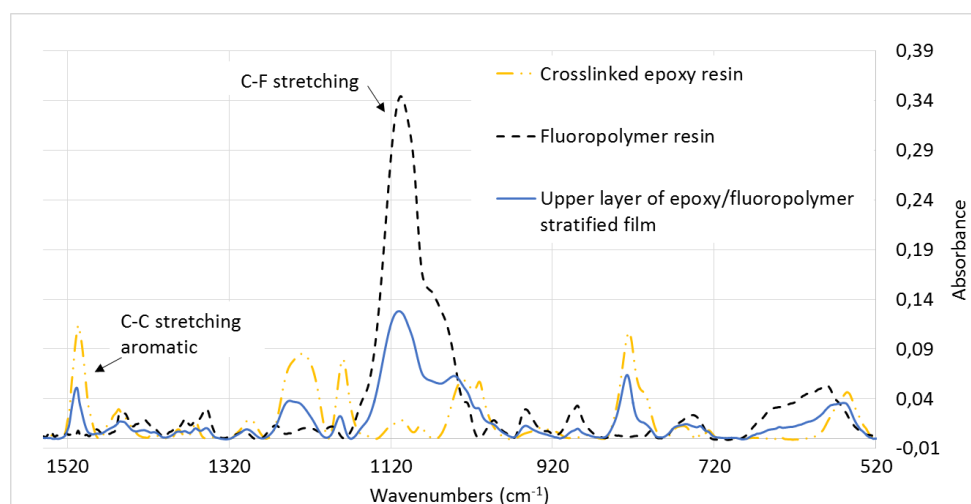


Figure 46. FTIR spectra of the crosslinked epoxy and fluoropolymer resins, and of the top layer of the epoxy/fluoropolymer stratified film

Table 17. Contact angle and surface energy data of the crosslinked epoxy and fluoropolymer resins

	$\theta_{\text{water}}(^{\circ})$	$\theta_{\text{diodomethane}}(^{\circ})$	γ ($\text{mN}\cdot\text{m}^{-1}$)	γ^{d} ($\text{mN}\cdot\text{m}^{-1}$)	γ^{p} ($\text{mN}\cdot\text{m}^{-1}$)
Fluoropolymer resin*	101 ± 2	63 ± 5	31	29	2
Fluoropolymer resin (after curing)	83 ± 2	49 ± 3	44	36	8
Crosslinked epoxy resin*	83 ± 11	96 ± 6	45	37	8
Crosslinked epoxy resin (after curing)	87 ± 3	46 ± 4	43	37	6
Upper layer of the epoxy/fluoropolymer film	85 ± 2	55 ± 1	40	33	8

*No solvent

The Hansen approach, which predicted the incompatibility between the epoxy and fluoropolymer resins, is in accordance with the experimental observations: the model based on interfacial energy and surface tension predicted stratification for systems based on pure xylene and on the MIBK: xylene blend and the designed coatings confirm this prediction. For the other solvent blends however, even if the three theoretical conditions were not satisfied, layering is observed experimentally. However, it can be noticed that the system for which two out of three conditions were not satisfied using this approach corresponds to the worst adhesion (2B) compared to the other systems (5B). Finally, for the BuAc: xylene solvent blend, the unsatisfied condition was very close to 0 and a great adhesion was obtained (5B).

The influence of the addition of particular solid filler in two systems was then evaluated.

III-3-1-3 Stratification of pigmented binary blends of thermoplastic and thermoset resins

Some researchers reported that pigments well wetted in the phase in which they are dispersed remain in their original dispersion phase after the mixing of the two resins.¹² Consequently, pigments were primarily used for stratification detection, before being carefully selected for upgrading the coating properties. Also, the absorbing properties of pigments, their particle size as well as their affinity toward a medium can influence the process.

As most of the paints used in the industry contain pigments, subsequent investigations have been carried out on pigmented systems. The pigments chosen in this study were red iron oxide (Fe_2O_3), calcium carbonate (CaCO_3) and zinc phosphate ($\text{Zn}_3(\text{PO}_4)_2$) for their inertness, relevancy for commercial applications, and also for their ease of detection by cross section X-ray analysis of Fe, Zn, P or Ca.

Different combinations have been tested, which differ in terms of pigments, solvent or solvent blend, and phase in which pigments are dispersed. The aim is to figure out the influence of (i) the pigments, (ii) the solvent and (iii) the incorporation phase in terms of stratification pattern, coatings appearance and adhesion properties (Table 18).

Table 18. Resulting coatings characteristics and stratification pattern of pigmented formulations

N°	Solvent	Pigment	Pigmented phase	Pigment location after film formation	Appearance of the coating	Cross hatch testing	Stratification pattern
1	Xylene	Fe ₂ O ₃	Epoxy	Silicone layer	Good pigments dispersion, smooth	4B	I
2	Xylene		Silicone		Bubbles, medium pigments dispersion, rough	4B	I
3	BuAc: xylene (1: 1)		Epoxy		Smooth, good pigments dispersion	5B	I
4	BuAc: xylene (1: 1)		Silicone		Smooth, medium pigments dispersion	5B	I
5	MIBK: xylene (1: 1)		Epoxy		Smooth, good pigment dispersion	5B	IV
6	Xylene	Zn ₃ (PO ₄) ₂	Epoxy	Through the whole thickness	Bubbles and cracks	3B	I
7	BuAc: xylene (1: 1)		Epoxy	Silicone layer	Rough, good pigments dispersion	5B	I
8	BuAc: xylene (1: 1)		Silicone	Silicone layer	Rough, good pigments dispersion	5B	I
9	Xylene	CaCO ₃	Epoxy	Through the whole film thickness	Large bubbles along the whole coating	1B	I
10	BuAc: xylene (1: 1)		Epoxy	Interface epoxy/silicone	Rough, good pigments dispersion	5B	I
11	BuAc: xylene (1: 1)		Silicone	Silicone layer	Bad pigments dispersion, cracks, small bubbles	4B	III

Influence of pigments on the stratification process

Each pigment was tested in combination with different solvents in the epoxy/silicone systems (Table 18).

The cross-section X-Ray mappings of the coated PC confirm the self-stratification of the epoxy/silicone system for almost all systems. Thus, the same stratification pattern is obtained for the formulations with and without (Table 16) pigments, except for calcium carbonate where a type III pattern was obtained when pigments were incorporated in the silicone phase (formulation 11, Table 18). In that case, poor pigment dispersion was also observed, leading to the appearance of cracks and bubbles along the coating.

In the case of the formulations pigmented with red iron oxide or zinc phosphate, perfect stratification (type I pattern) was obtained in all cases, with the silicone layer being the top layer, as it was demonstrated with unpigmented formulations (Table 16). Thus, it seems that Fe_2O_3 and $\text{Zn}_3(\text{PO}_4)_2$ have no negative effect on the stratification process. To confirm this statement, an additional experiment was made with the epoxy/silicone/ Fe_2O_3 formulation, but using the MIBK: xylene blend as solvent medium (Formulation 5, Table 18). In fact, it was shown that for the corresponding formulation without pigments, the stratification had not have enough time to be complete because the solvent evaporation rate was too high, leading to a type IV pattern.

An incomplete stratification is also displayed on Figure 47 when a blend of MIBK: xylene (1: 1) is used for the pigmented formulation. This pattern confirms the inertness of pigment toward stratification, as exactly the same pattern was obtained with unpigmented formulation. In order to identify more precisely the location of the pigment and the silicone resin, cross section X-ray mappings of iron (Fe) (Figure 47 b) and silicium (Si) (Figure 47 c) were carried out by EPMA. From these micrographs, it is noticeable that the upper layer is rich in silicone resin and Fe_2O_3 pigment, but large islands of same composition go from the base region to the upper layer. The silicone resin and the pigments had not enough time to completely migrate toward the air interface. However, as the pigment dispersion is relatively good with this formulation, the adhesion is not affected (5B rating).

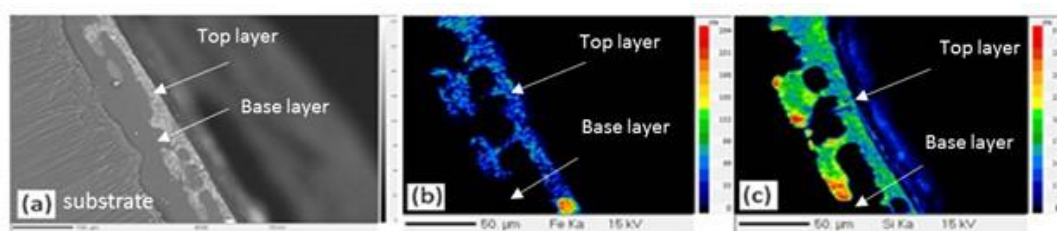


Figure 47. Back scattered image of the cross-section of the self-stratifying coating of the epoxy/silicone system in MIBK: xylene (1: 1) with Fe_2O_3 (Formulation 5, Table 18) and the corresponding EPMA X-ray mappings of (b) Iron and (c) Silicon

Consequently, it was shown that pigments have no effect on the stratification level in the epoxy/silicone system, whatever the stratification pattern for the corresponding formulations

without pigments (from type I to type IV). Now, the results of Table 18 are examined more precisely to see the influence of the solvent on the quality and the properties of the coating.

Influence of solvent on the stratification level and on the adhesion properties

As previously demonstrated with unpigmented systems, the type of solvent medium has an influence on the stratification behavior. In fact, the MIBK: xylene solvent blend led to a type IV stratification pattern whereas, using pure xylene or BuAc: xylene, a type I stratification was obtained. It was shown that this phenomenon was dependent on the evaporation rate of the solvent: if the evaporate rate is too high, perfect stratification should not have sufficient time to occur. The results of Table 18 prove that, except for formulation 11, the presence of pigments has no influence on the stratification pattern compared to the corresponding formulations without pigments.

If the coating properties are now considered, it can be seen from Table 18 that the type of solvent has a strong influence on the adhesion. More precisely, if pure xylene is used, the presence of pigments has a negative influence on the adhesion of the coating. Without pigments, the best rating (5B) was obtained whereas a 4B rating is obtained with Fe_2O_3 (formulation 1, Table 18), 3B with $\text{Zn}_3(\text{PO}_4)_2$ (formulation 6, Table 18), and 1B with CaCO_3 (formulation 9, Table 18). On the contrary, with a blend of BuAc: xylene (1:1), the coatings exhibit the same excellent adhesion properties with the three pigments (formulations 3, 7 and 10, Table 18) as with the unpigmented coatings (5B rating).

Thus, the cross-section of the epoxy/silicone/ Fe_2O_3 self-stratified coating in xylene (formulation 1, Table 18) was examined more precisely to identify the location of pigments and of the silicone resin. EPMA X-ray mappings of iron (Fe) (Figure 48 b) and silicium (Si) (Figure 48 c) were carried out. The X-ray mappings indicate that pigments are located in the silicone layer i.e. in the topcoat layer of the coating. Pigments are not uniformly dispersed in the silicone resin: they are rather close to the interface with the epoxy resin, and form aggregates. Some cracks are also noticeable along the cross-section (Figure 48 a), which are certainly responsible for the 4B adhesion rating obtained for this particular coating. On the contrary, the pigment dispersion is optimal for the epoxy/silicone/ Fe_2O_3 self-stratified coating in BuAc: xylene (formulation 3, Table 18). Thus, it can be assume that the quality of the pigment dispersion has an influence on the adhesion properties.

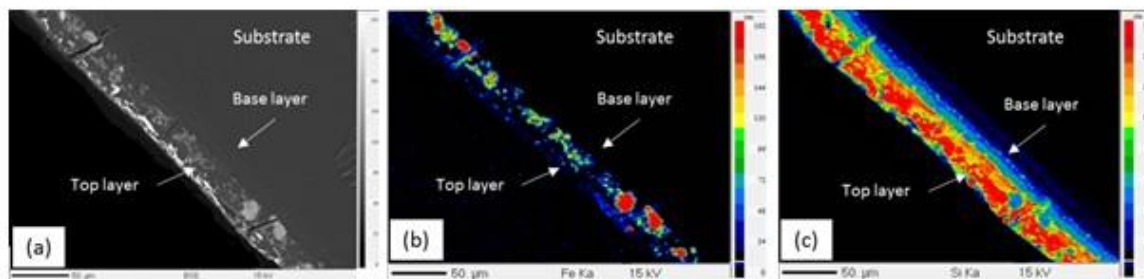


Figure 48. EPMA BSE micrographs of a cross-section of an epoxy/silicone coating in xylene with Fe_2O_3 : (a) self-stratifying coating, (b) Iron analysis, (c) Silicon analysis

With zinc phosphate, a negative effect on the adhesion properties can also be noted when xylene is considered: 3B rating was obtained compared to 5B with the unpigmented system and the systems diluted in BuAc: xylene (Formulations 7 and 8, Table 18). Also, visual appearance was affected (apparition of bubbles and cracks).

With calcium carbonate, solvent has mainly an effect on pigment dispersion, thus affecting the visual appearance and adhesion of the coating. A nice coating with well dispersed pigments was obtained with a blend of xylene: BuAc (1: 1) and a pigmented epoxy medium (Formulation 11, Table 18). However, the use of pure xylene resulted in the apparition of large bubbles along the whole coating (Formulation 9, Table 18). The effect on the adhesion of the coating was catastrophic. It caused total coating adhesive failure (cohesive failure) from the substrate and a 1B adhesion.

Influence of pigments incorporation phase

The location of pigments after stratification depends on the pigments and solvent medium used.

If red iron oxide is considered (formulations 1 to 5, Table 18), pigments always appear in the silicone phase after stratification, whatever the solvent medium and the incorporation phase. In the case of zinc phosphate, pigments can be found in the silicone phase (formulations 7 and 8, Table 18) or through the whole film thickness (formulation 6, Table 18). For this second pigment, it is likely that the solvent has an influence on the pigment location.

Thus, contrary to what it is reported in the literature with other different systems when two pigmented resins are mixed^{109, 134} pigments do not necessarily remain in the phase in which they have been dispersed (Table 18). Benjamin *et al.* demonstrated that on metallic substrate, red iron oxide and zinc phosphate remain in the epoxy phase (the more polar medium) after stratification.¹¹¹ Our results show that it is obviously not applicable for polycarbonate substrate as pigments mainly migrate to the silicone phase or are found through the whole film thickness if the solvent medium is not adapted.

For calcium carbonate, the behavior is more complex and the pigment location seems to depend on the incorporation phase. Pigments stay in their dispersion phase if they are incorporated in the silicone medium. But when calcium carbonate is blended in the epoxy medium, pigments are found either through the whole film thickness (formulation 9, Table 18) or at the interface between the two resins (formulation 10, Table 18 and Figure 49). However, the silicium X-ray mappings proves that the stratification is not impaired in this last case (Figure 49 c). Consequently, calcium carbonate has more affinity with the silicone resin than with the epoxy resin.

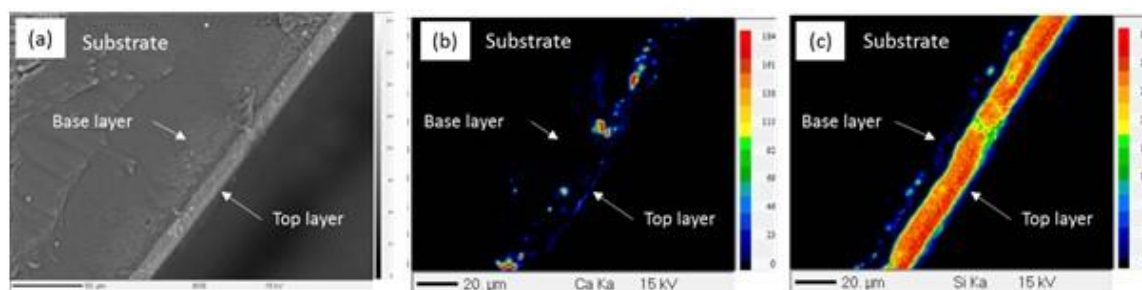


Figure 49. (a) EPMA BSE micrographs of self-stratifying coating of an epoxy/silicone system in BuAc: xylene (1: 1) with CaCO₃ (formulation 10) and the corresponding X-ray mappings of (b) Calcium and (c) Silicium

It is interesting to notice that pigments indeed do not have the same affinity with either the topcoat or the basis resin. For example, it is not necessary to disperse red iron oxide in the medium for which it has the highest affinity, since whatever the solvent used, it always migrates in the silicone phase without affecting the stratification type. It even appears that dispersing red iron oxide and calcium carbonate in the epoxy medium enhances the dispersion

and the visual aspect of the coating. In some cases when the dispersion is not optimal, it can lead to interlayer adhesion failure. Adhesion is however slightly impacted with calcium carbonate (4B instead of 5B, formulation 11, Table 18) and not impacted with Fe_2O_3 , whatever the incorporation phase (formulations 1, 2 and 3, 4, Table 18).

Conclusion: Self-stratification of the epoxy/silicone system

In the case of a three components system, the Hansen approach well predicted the stratification. However, it is noteworthy to notice that the amine curing agent is not taken into account in the model. Consequently, the model should be considered carefully. The model based on surface energy does not give consistent results according to the state of the resin (pure or diluted). This aspect will be further discussed in the section III-3-1-5 of this chapter.

To conclude, the epoxy/silicone system diluted in a BuAc: xylene (1: 1) solvent blend leads to very promising results: it gives rise to the best stratification pattern (type I) with a great adhesion (5B rating) to polycarbonate and a nice visual appearance.

In this work, it was emphasized that the solvent influences the stratification level: the higher the evaporation rate, the better the stratification. Although, the rate of evaporation should not be too high because the system reaches the gel point before the completion of phase separation. Also, pigments show no negative effect on the stratification process, only the visual appearance and the adhesion of the coating can be affected, depending mainly on their dispersion and on the wettability of the pigment. Iron oxide is the most versatile pigment amongst the filler tested: it is the less affected by the type of solvent or the incorporation phase compared to calcium carbonate, with which such modifications can completely prevent the occurrence of stratification or affect the visual appearance of the coating. Zinc phosphate is also a good candidate. It has been evidenced that pigments chosen in this work have a higher affinity with the silicone resin, and thus in most cases do not remain in their dispersing phase if they have been incorporated in the epoxy resin.

Last, but not least, stratification can be influenced by crosslinkage induced by the curing agent: a too reactive hardener can be incompatible with the materials used in the system (the thermoplastic resin, pigments ...). It can also react with the thermoplastic resin, thus

preventing, in some case, the stratification process and also impacting the adhesion and the visual appearance of the resulting coating.

From those analyses, additional queries emerged, which led to the study of two factors: (i) the amount of pigment and (ii) the percentage of solid resin in the formulation. An additional publication is at this point being written and contains the results and discussion which deal with these points (Appendix 8).

The influence of the incorporation of red iron oxide on the stratification behavior of the epoxy/fluoropolymer system was then evaluated.

III-3-1-4 Stratification of pigmented binary blends of thermoplastic and thermoset resins

According to the state of the art, fillers dispersed in an epoxy medium remain in this phase during the formation of the film.¹¹¹ The epoxy/fluoropolymer systems previously described were tested, incorporating red iron oxide in the epoxy resin. SEM micrographs and EDX mappings are given in Figure 50 and Figure 51 respectively. Filler location, visual appearance of the solid films, thicknesses, adhesion rating and the resulting stratification patterns are detailed in Table 19.

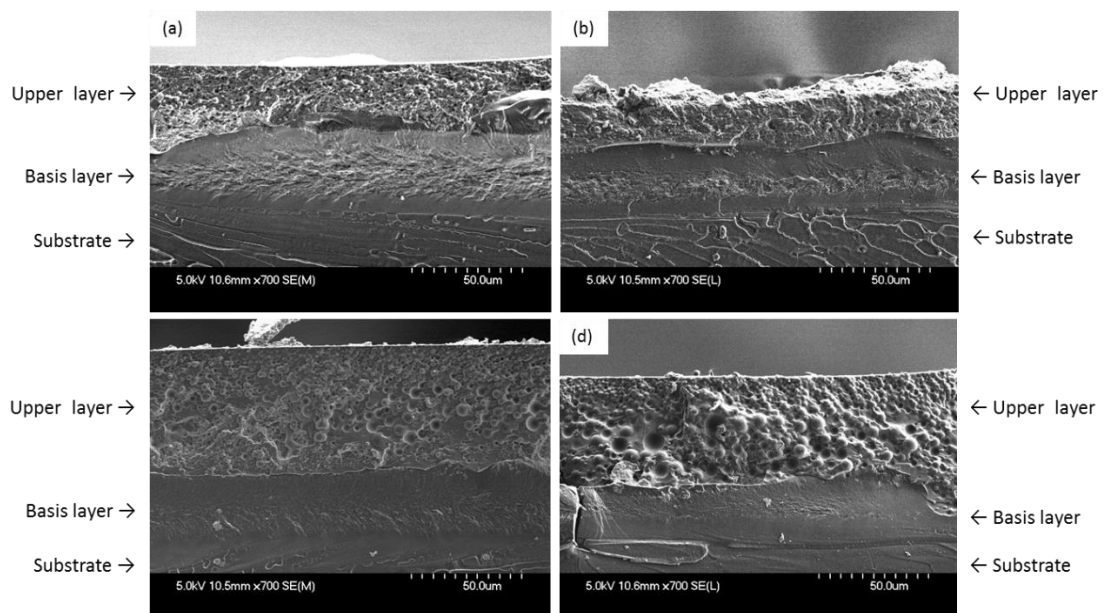


Figure 50. SEM micrographs of cross-sections of the epoxy/fluoropolymer based coating in (a) xylene, (b) BuAc: xylene (1:1), (c) MIBK: xylene (1:1), (d) MIBK: xylene: 1-methoxy-2-propanol (50:30:20)

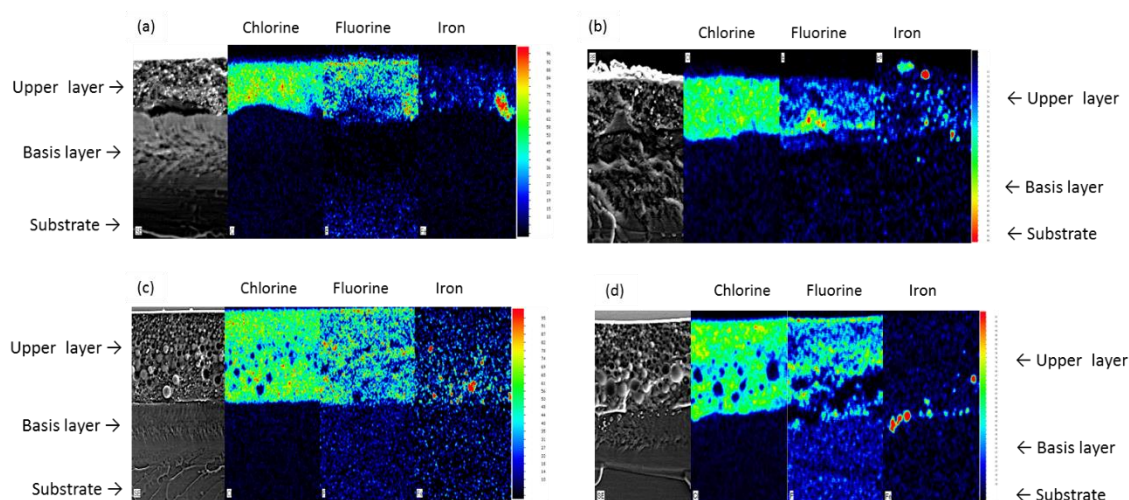


Figure 51. EDX X-ray mappings of Chlorine, Fluorine and Iron on cross-sections of epoxy/fluoropolymer based coating in (a) xylene, (b) BuAc: xylene (1:1), (c) MIBK: xylene (1:1), (d) MIBK: xylene: 1-methoxy-2-propanol (50:30:20)

Table 19. Resulting coatings appearance, adhesion and stratification pattern of Fe_2O_3 containing coatings

Solvent	Pigment location after film formation	Appearance of the coating	Thickness ($\mu\text{m} \pm 5$)	Cross hatch testing	Stratification pattern
Xylene	Fluoropolymer layer (some aggregates)	Smooth, good pigment dispersion	70	4B	I
MIBK: xylene (1:1)	Fluoropolymer layer	Rough, medium pigment dispersion, small bubbles	85	4B	I
BuAc: xylene (1:1)	Fluoropolymer layer	A little rough, good pigment dispersion	60	4B	I
MIBK: xylene: 1-methoxy-2-propanol (50:30:20)	Interphase epoxy/fluoropolymer layers	Rough, bad pigment dispersion	75	1B	I

The SEM micrographs and the cross-section X-Ray mappings confirm the self-stratification of the epoxy/fluoropolymer systems whatever the solvent or solvent blend used: for all

formulations, a type I stratification is obtained (Figure 51 a, b, c, d) and the fluoropolymer layer still appears to be the top layer, as it was already the case for unfilled formulations. Thus, experiments confirm that iron oxide has no significant influence on the self-layering process. While it is clear that it does not impact the layering process, its affinity toward the resins and the dispersion quality however differ according to the selected solvent or solvent blend. When xylene, blends of BuAc: xylene or MIBK: xylene are used, iron oxide is located in the fluoropolymer layer (Figure 51 a, b, c), even if it was initially dispersed in the epoxy medium. This means that, contrary to what is mentioned in the state of the art, iron oxide does not remain in its primary dispersion phase, but migrates in the phase for which it has the highest affinity (here the fluoropolymer).

Considering the ternary blend of MIBK: xylene: 1-methoxy-2-propanol (Figure 50 d and Figure 51 d), the migration of the filler is stopped at the interface between the two resins, pigments dispersion is not optimal and aggregates are noticeable: red iron oxide migrates toward the fluoropolymer phase during the film formation but has not enough time to reach that phase due to the fast evaporation rate of this solvent blend. In fact, according to the boiling temperature of the pure solvents, the MIBK: xylene: 1-methoxy-2-propanol blend (respectively 116, 139 and 120 °C) has the lowest boiling temperature among the different solvents used. These microscopic observations directly reflect the visual appearance of the coating: the film is composed of an opaque phase (the resins) in which red aggregates are dispersed. It leads to poor adhesion: 2B is obtained compared to 4B for the other formulations.

Considering the MIBK: xylene blend, which has the second lowest boiling temperature, even if iron oxide has migrated toward the fluoropolymer phase, the distribution is not homogeneous and aggregates are still observed in the lower part of the fluoropolymer phase. However, the dispersion of iron oxide is one of the best (Figure 51 c). It means that the evaporation rate of the MIBK: xylene blend was not too high to prevent the migration of iron oxide in the fluoropolymer phase but was nonetheless too high to allow a good distribution in the whole layer. All these results prove that the solvent choice is of primary importance: stratification is based on demixing, for which time and mobility are needed. Very high evaporation rates result in frustrated mixed coating and affect the quality of the resulting

coating. A good compromise has to be found when selecting the solvent as it affects the formation of the film, the pigment dispersion and the adhesion properties.

To conclude about systems filled with red iron oxide, it was shown that this filler does not influence the layering behavior of the epoxy/fluoropolymer system, whatever the solvent used. However, adhesion properties and visual appearance of the film are affected by the filler's dispersion which mainly depends on the evaporation rate of the solvent or solvent blend. The coating designed with a blend of BuAc: xylene seems to combine the best adhesion and visual appearance.

Conclusion: Self-stratification of the epoxy/fluoropolymer system

It was shown that the system diluted in a blend of butylacetate: xylene (1: 1 ratio) exhibits a perfect stratification and excellent adhesion onto polycarbonate when a 200 µm wet thick coating was applied. The top layer of the one pot coating was found to be composed of the fluoropolymer resin, and the base layer of the crosslinked epoxy resin. The solvents have proven to hugely affect the quality of the resulting film, and have to be chosen very carefully. Indeed, they can impact both adhesion properties and pigment dispersion – and thus visual appearance of the coating - in a negative manner.

Incorporation of red iron oxide in the epoxy phase has no negative effect on the layering behavior. Moreover, we have shown that the filler has a higher affinity with the fluoropolymer resin, and thus does not remain in the phase where it was initially dispersed (i.e. the epoxy resin). It was also shown that the evaporation rate of solvents influences the migration of fillers toward the fluoropolymer medium. When a blend of MIBK: xylene: 1-methoxy-2-propanol (50:30:20) is used, fillers have not enough time to migrate toward the topcoat layer and are thus trapped at the interface between the two resins. This poor pigment dispersion is detrimental to the film aspect and to the adhesion properties.

III-3-1-5 Comparison between experimental and theoretical models

Type I epoxy/silicone and epoxy/fluoropolymer self-stratified films were obtained with blends of BuAc: xylene and pure xylene. In the case of the other solvent blends, perfect stratification was exhibited only in the case of fluoropolymer-based coatings.

Based on those blends, the Hansen model well predicted the self-stratification for both systems ($V = 44\%$ for the epoxy/fluoropolymer blend and $V = 75\%$ for the epoxy/silicone blend). However, the model based on surface and interfacial tensions shows some discrepancies according to the state of the resin (pure polymer or diluted). If the BuAc: xylene blend is considered, one out of three conditions were validated for both systems whereas stratification was obtained in both cases. If the blends of solvents are examined, no consistency between the results is exhibited: with the epoxy/silicone blend, the stratification quality decreases with increasing solvent evaporation rate whereas the prediction of the model does not follow this guideline. The divergence between the theoretical predictions and the experimental results could be explained in a twofold manner. On the first hand, the calculation made to predict the direction in which the layering will proceed considered the surface energy of the final components or the pure polymer (100% solid). But the composition of the phases varies continuously until the complete formation of the solid film, and the evaporation of the solvents (which is not always complete according to the curing temperature). Moreover, it was shown in a paper that the surface tension of a polymer solution above 50 wt.% is extremely dependent on resin concentration. On the other hand, the addition of the amine curing agent to the system influences both the stratification process (due to the crosslinking reaction) and the surface energies and the influence of the curing agent is not taken into account in the model.

III-3-1-6 General conclusion on binary blends

By investigating the influence of different factors on the self-layering process, the feasibility of producing unfilled and filled self-stratified epoxy/silicone and epoxy/fluoropolymer systems on polycarbonate substrates was evidenced.

It was shown that the BuAc: xylene (at a 1: 1 ratio) solvent blend leads to very promising results on the epoxy/silicone unfilled system: it gives rise to the best stratification pattern (type I) with a great adhesion (5B rating) to polycarbonate and a nice visual appearance. With the epoxy/fluoropolymer system, the most promising results were obtained with the BuAc: xylene solvent blend. Xylene and a blend of MIBK: xylene (1: 1) are also good candidates however some disparities in the pigment dispersion and migration are noticeable in the solid film. A 4B adhesion rating on PC was obtained in all case combined with a nice visual appearance.

Finally, the choice of the solvent is of primary importance: stratification is based on demixing, for which time and mobility are needed. Very high evaporation rates will result in frustrated mixed coating and will affect the quality of the resulting coating. A good compromise has to be found when selecting the solvent: the higher the evaporation rate, the more spontaneous the film formation and thus the stratification. Moreover, its choice can also impact the quality of the resulting film by modifying the quality of fillers dispersion, and consequently the adhesion properties.

Two successful epoxy-based self-stratifying coatings have thus been developed based on those results, and meet the requirements needed for our specifications (type I or II self-layered coating, good adhesion and filler dispersion and nice visual appearance). Finally, introduction of two fillers have also been tested in combination with the epoxy and silicone resins but were not successful in producing a self-layered coating: no stratification was observed, whatever the combination investigated.

At this point, the study of binary blends of resins in which pigment or solid fillers were added have been a central focus. Their effect on the stratification process and the properties of the resulted solid film have been studied in two different resin system. The idea was then to study the influence of liquid additives, i.e. ternary blends, on the layering process, the properties of the resulting film and also to analyze the migration of the filler through the film thickness.

III-3-2 Stratification of ternary blends

The addition of particular fillers influence the formation of heterophase polymer structure and their resulting properties. Most of the additives have a rather negative effect on the phase separation in self-stratifying compositions, and do not allow reaching sufficiently interesting properties compared to the usual multilayered systems. Literature results have proved that liquid fillers (for example wetting, levelling, anti-flotting, surface active or dispersing agents) generally impair the stratification process.^{102, 109, 134, 143} As an exception, some silicone or fluorine-containing oligomers added in minor amount (1 wt.%) were proven to substantially accelerate the phase separation process with a moderate or negligible influence on the solutions equilibrium.¹⁴³ To our knowledge, no paper relates to the study of the addition of a substantial amount of a functional liquid additive in a self-stratifying composition. In this work, the goal is to design a self-stratifying coating on a polycarbonate substrate, incorporating a liquid additive. To do so, film forming compositions based on a curable epoxy and a silicone resin (to produce coatings with a heterophase polymer matrix structure) in combination with liquid fillers [(bisphenol-A- bis(diphenyl phosphate) - BDP and resorcinol bis(diphenyl phosphate) - RDP)] will be considered.¹⁴² As the final aim of this work is to obtain flame retardant coatings, BDP and RDP were selected as potential flame retardant additives in the formulation. In the present part, only the self-stratification in presence of two liquid resins, a liquid filler and a hardener will be investigated. Only the results obtained with the BuAc: xylene (1: 1) solvent blend are presented as it led to the best compromises.

III-3-2-1 Stratification study

RDP and BDP were introduced at 2.5 and 5 wt.% into the formulation, and all selected parts, being mixed, produced homophase solutions before application. The formation of separated in-layers coating structure was then checked (Table 20).

Table 20. Fillers location, appearance of the coating, adhesion rating and stratification pattern for the epoxy/silicone coatings filled with RDP and BDP at 2.5 and 5 wt.%

Filler	wt. %	Fillers location after film formation	Appearance of the coating	Thickness (μm)	Cross hatch testing	Stratification pattern
No filler	0	-	Slightly rough, glossy	55	5B	I
RDP	2.5	Mainly silicone layer, a slight concentration gradient near the silicone-epoxy interface	Less rough than without additive, higher gloss	45	5B	II-III
	5			60	5B	I
BDP	2.5	High concentration in the silicone layer, concentration gradient in the epoxy phase decreasing from top to bottom	Less rough than without additive, higher gloss	68	4B	II-III
	5			30	4B	I

The reference system (epoxy/silicone/BuAc: xylene), previously presented in Chapter III of this manuscript, containing no liquid FR filler shows perfect stratification (type I pattern) and the best adhesion rating (5B). In presence of liquid filler, nice coatings free of bubbles or defaults were obtained in all cases. They even show slight improvement in terms of surface aspect (less rough and glossier) than the reference coating. The 5B adhesion rating is maintained after the incorporation of RDP in the system, for both amounts tested. The addition of BDP slightly impacts the adhesion of the coating: 4B rating is obtained compared to 5B with the unfilled system.

Unlike literature results, it appears that neither RDP nor BDP affect the layering process when incorporated at 5 wt.% in the formulation: a type I pattern is obtained in all cases with two layers sharply separated, as it was observed with the unfilled system. Both additives migrate towards the upper layer of the film, in the silicone medium: RDP and BDP have a higher affinity with the silicone compared to that of the epoxy (Figure 52). The migration is rather a positive phenomenon in this case as it allows concentrating the additive's properties (i.e. flame retardant properties) in the upper part of the coating, where it is the most needed in the case of a fire. With RDP, some inhomogeneities are noticeable along the film near the interface

between the two resins: some islands shaped regions rich in silicone have not totally migrated towards the upper layer of the film. A concentration gradient of phosphorus is also visible through the film thickness, although the major part of RDP has migrated towards the upper layer. With BDP, the same findings can be noticed: the silicone resin and the filler are mainly concentrated in the upper part of the coating. However, the concentration gradient of phosphorus is more pronounced through the thickness than with RDP. The difference could be explained by a higher affinity of RDP with the silicone resin, which could ease the migration of the additive to the air interface. However, the concentration gradient is much more pronounced with phosphorus than with silicone: this means that the affinity between the silicone resin and the filler is not strong enough to allow its complete migration toward the top layer. A difference of viscosity could also explain the difference in the concentration gradient between BDP and RDB containing formulations. Indeed, BDP is much more viscous than RDP (17 000 CPS¹⁵⁴ compared to 12 450 CPS with RDP¹⁵⁵). As its viscosity is higher, its migration to the upper layer may be slowed down. It is noteworthy to notice that even if the additive has not enough time to completely migrate to the upper layer of the film, it does not impair the stratification process: the layering of the silicone to the top of the coating remains perfect.

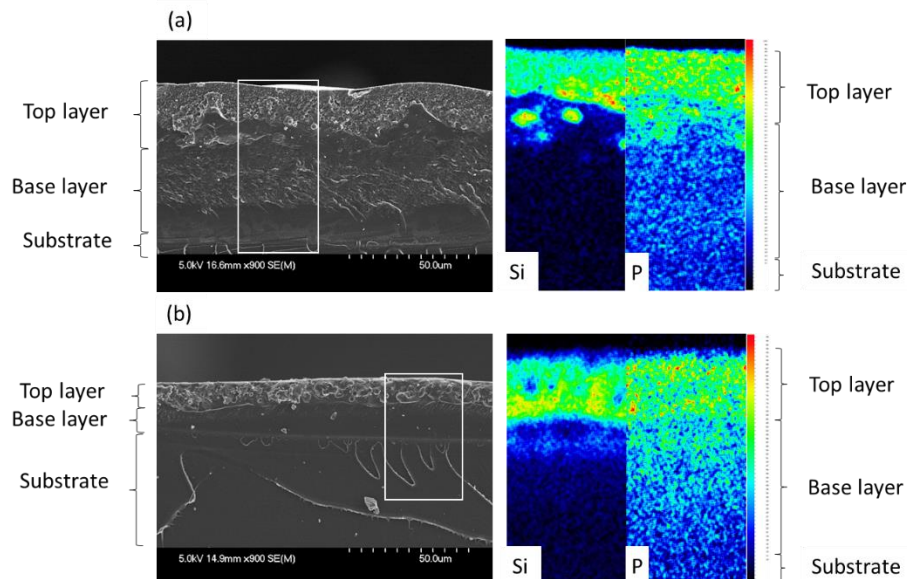


Figure 52. EDX X-ray mappings of Silicium and Phosphorus on a cross-section of an epoxy/silicone coating filled with 5 wt.% of (a) RDP and (b) BDP fillers

When a lower amount of fillers is introduced into the homogeneous composition, the layering process is affected: phase separation is evidenced (Figure 53), and also a concentration gradient of silicone through the thickness, but not uniformly formed along the film. Nevertheless, the phosphorus element is mainly found in the silicone medium. Such kind of solventborne paint, based on initially homophase solutions of incompatible polymer blends convertible into a heterophase state, can self-layer following a mechanism driven by surface tension gradient. The additive destabilizes the interface between the two phases and, in that case, influences the preferential orientation of the phases in the course of film forming process. 5 wt.% of additive appears to be a better balance as the preferential orientation of the phases is not influenced. In addition, although some incoherence in the matrix were found along the film with 2.5 wt.% (formation of isolated spherical particles composed of epoxy resin dispersed in the continuous silicon matrix, Figure 53), the incomplete phase separation did not damage the adhesion of the coating.

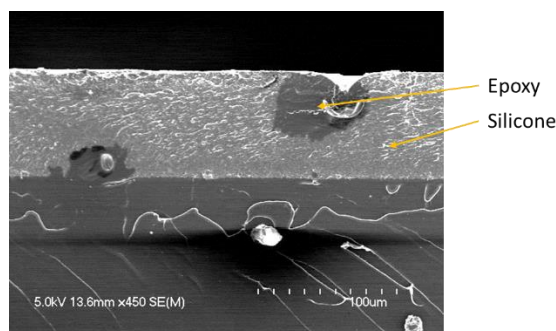


Figure 53. SEM pictures of the cross-section of the ternary system filled with 2.5 wt.% of BDP

In conclusion, when a low amount of additive is added (2.5 %), it slightly compromises self-layering in some area of the film compared to a higher amount (5 %). Some disparities in the concentration gradient, which may be due to a difference in viscosity between the two phases, is also noticed with 5 %. Finally, the filler destabilizes the equilibrium between the two solutions, but not enough in the case of 2.5 % to lead to a homogeneous formation of oriented heterophase structures, as it is observed with 5 %.

The phosphorus based fillers tested do not affect the formation of oriented heterophase structures when they are introduced at 5 %: they mostly migrate, with a concentration gradient more or less pronounced, towards the air interface with the silicone resin. Finally, coating's composition provided nice visual appearance and a high adhesion onto the polycarbonate substrate. It was proven that it is possible to add a substantial amount (5 %) of liquid functional filler in a self-layering formulation without affecting the self-stratification process, the coating aspect and the adhesion. In these formulations, the phosphorus FR additives migrate into the upper silicone layer, which can potentially lead to an effective FR effect of the coating when exposed to fire.

III-3-2-2 Conclusion

A properly selected partially incompatible polymer blend composed of silicone, of a curable epoxy resin and of a liquid functional filler successfully formed a double-layered coating, showing excellent adhesion to the underlying polycarbonate substrate. The binders, dissolved in solvents to produce a two-phase liquid medium during film formation, led to structures with sharply defined layers. The topcoat layer was found to be composed of the silicone resin, and the base layer of the curable epoxy resin. Microscopic analyses have demonstrated that phosphorus based liquid fillers do not impact the stratification process when incorporated at 5 wt.%. However, their migration to the upper layer of the coating (silicone phase) was not always complete: a concentration gradient of the additives through the film thickness is obtained, with a higher concentration toward the top of the coating. When fillers were incorporated at a lower amount (2.5 wt.%), incomplete phase separation was observed in some area of the film, although a high adhesion rating (5B and 4B respectively with RDP and BDP fillers) and nice visual appearance remained.

III-4 Conclusion

Chapter III was dedicated to the theoretical and experimental investigation of the self-stratification of binary and ternary blends on polycarbonate substrate. The influence of

different specific factors (solvent, solid and liquid fillers, the occurrence of crosslinking reactions, pigment location) was deeply studied. Two different approaches were studied, the first theoretical approach (the Hansen approach) consisted in evaluating the overlapping area of a couple of polymers to predict their probability to stratify. From these results, preferential solubility requirements and solvents were outlined. In particular, formulating the epoxy/silicone paint at least 7 days after the dilution of the resins would be the most favorable. On the contrary, the probability of the epoxy/fluoropolymer blend to stratify would be promoted by using the resins rapidly after their proper dilution. In the second theoretical approach, based on surface and interfacial energy, it has been shown that only one combination was predicted to stratify (a blend of epoxy/fluoropolymer resin diluted in xylene) although a few other combinations are close to meet the requirements depending on the solvent system chosen. It was stated that the second model seemed closer to the real system as it takes into account the influence of the curing agent and of the substrate, contrary to the Hansen approach. However, the two theoretical methods are actually complementary as the first one allows the selection of suitable solvent systems and processing conditions, and the second approach the selection of substrates and materials with promising characteristics (surface and interfacial tension) to favor the self-stratification.

Based on these two approaches, binary blends were successfully designed on polycarbonate substrate, an epoxy with either a silicone or a fluoropolymer resin. In both cases, nice aesthetics and adhesion properties were combined with a perfect layering.

Ternary blends based on epoxy, silicone and phosphorus liquid based additives were also successful in producing formulation, which self-stratify after deposition on polycarbonate. They had excellent adhesive properties and a nice visual appearance.

Further studies of these different blends allow us to show that depending on the system studied, the choice of the solvent is of primary importance as well the rate of solvent evaporation. The rate of solvent evaporation should not be too low to allow the phase to separate before the complete formation of the film.

Finally, this study demonstrates that the incorporation of solid fillers (iron oxide, calcium carbonate, zinc phosphate) in the blends can produce controversial results compared to what has been published in the literature: generally, the fillers migrate to the top layer of the

coating even if they were primarily dispersed in the epoxy phase, the base layer in contact with the substrate. Moreover, it has been shown that the selected solvent system has an influence on the dispersion state of the pigments and that fillers do not influence the layering process.

In this chapter, some successful self-stratifying coatings were developed, thus, in the next chapter, their functional properties, more particularly the fire performance and the ageing properties will be studied.

Chapter IV: Fire performances and ageing resistance of epoxy/silicone and epoxy/fluoropolymer self-layered coatings

In this chapter, the self-stratifying coatings previously developed are intended to be used as potential flame retardant (FR) surface treatments for polycarbonate.

These coatings are based on epoxy, silicone and/ or fluoropolymer resins. This choice of resins is not a trivial matter. Indeed, epoxies are extensively used due to their exceptional mechanical and chemical properties. However, their flammability is a major drawback. Traditionally, halogenated compounds are widely used as co-monomer or additive to fire retard epoxy resins, as well as boron, phosphorus¹⁵⁶⁻¹⁵⁹ or silicone-based compounds¹⁶⁰ as well as layer double hydroxide¹⁶¹, melamine¹⁶² and montmorillonite.¹⁶³ Particularly, silicon-containing components have been explored and it was shown that their addition in a relatively small amount can significantly enhance the fireproofing properties of a material.¹⁹ They can exhibit very low thermal conductivity, low heat of combustion and rate of heat release, and the release of toxic gases during their degradation is reduced compared to classical organic compounds.^{164, 165} Finally, fluoropolymers are also known for their inherent flame retardancy.¹⁶⁶

In order to enhance the fire retardant effect of a resin or a coating, FR additives are usually added. In the third chapter, it has been demonstrated that several fillers (iron oxide, calcium carbonate and two phosphorus-based additives) can be used without impacting the self-layering process, while combining excellent visual and adhesion properties. Those fillers are

also well known for their FR effect when combined with suitable resin or FR systems.^{159, 167, 168} In the frame of this study, the fire performances of the coatings previously developed were evaluated. However, only the results obtained with the system containing the most efficient additive (i.e. iron oxide, IO) is presented in this thesis.

After a short literature survey about flame retardancy and the use of iron oxide as filler or FR synergist, the FR properties of the selected coatings applied on PC are studied in detail according to LOI, UL-94 and MLC tests. Based on the thermal decomposition of the materials composing the system, and on the observations made during the fire tests, the mode of action of iron oxide both in the condensed and gas phase is investigated. Furthermore, the ability of the coating to fire retard the polymeric matrix is discussed. The last section of this chapter is dedicated to the study of the influence of ageing on the developed systems (filled and unfilled). The evaluation of the fire performances before and after weathering will also be deeply commented.

IV-1 Introduction: State of the art on flame retardancy

IV-1-1 What about a fire?

A fire can basically be split into three phases: (i) the initiating fire, (ii) the fully developed fire and (iii) the decreasing fire. The fire starts with an ignition source which set fire to the combustible material. It spreads, heats up the surroundings and once the materials have formed enough flammable gases and are sufficiently hot, flashover takes place. At this step, a whole room can be inflame in a few minutes and the temperature can reach up to 1200 °C. Later on, the fire decreases as the available fire load is consumed or can die because of oxygen deficiency. The fundamental parameters governing a fire are the combustibility, the ignitability, the spread of the flame and the heat release. Most of the flammable materials can be appropriately treated with specific FR (and eventually with the addition of a synergist) that provides effective fire proofing properties. Flame retardants act to break the combustion cycle leading to extinguish the flame or to reduce the burning rate in a number of possible ways:¹⁶⁹

- * By modifying the pyrolysis process to reduce the amount of evolving volatiles. It increases the formation of less flammable gases or of char which also acts as a barrier between the polymer and the flame.
- * By cooling of the condensed phase by endothermal decomposition of FR additives.
- * By isolating the flame from the oxygen/air supply.
- * By introducing into the plastic formulations flame inhibitors or diluting agents.
- * By reducing the heat flow back to the polymer to prevent further pyrolysis. This can be achieved by producing a protective barrier, e.g. ceramic char layer or intumescent coating, formed when the polymer is exposed to fire conditions.

IV-1-2 Thermal degradation of polymers

The combustion process of polymeric matrices can be divided in four major steps: (i) heating, (ii) decomposition, (iii) ignition and (iv) flame spread. The most significant chemical reactions interfering with the combustion process take place in the condensed and/or in the gas phases. When submitted to a heat source, the material softens, or melts in the case of a thermoplastic matrix, and when the energy given to the material is higher than that of its degradation, decomposition products (fuels) are released in the gas phase from the degradation zone. The flammable gases are mixed with the oxygen from the air and when the system reaches a critical concentration, ignition occurs. A flame is formed by the highly exothermic reactions occurring between the radicals formed from the thermal decomposition of the polymer and oxygen (Figure 54).

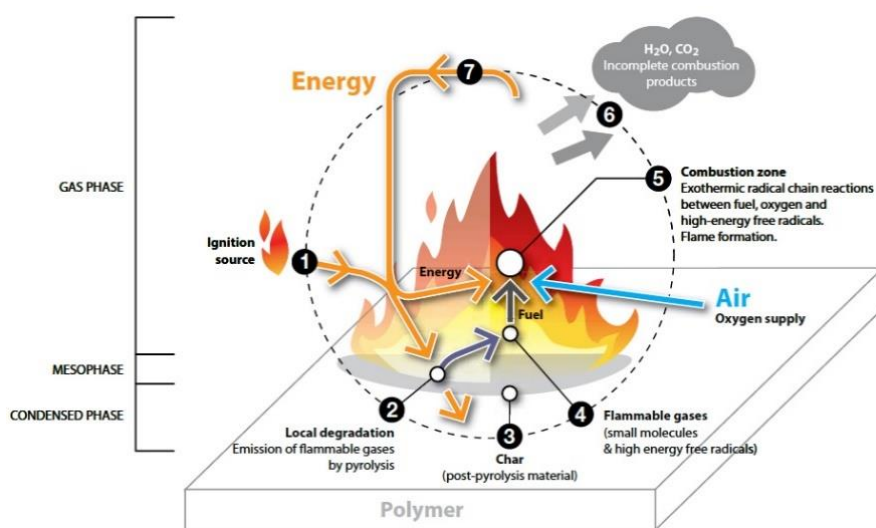


Figure 54. How materials burn?¹⁷⁰

Part of the energy of the flame is given back to the material, so that the combustion process continues without external energy. As long as degradation products evolves and oxygen

remains in sufficient amount, there is an auto-fed flame which can propagate to its surroundings.

Upon thermal decomposition, various phenomena occur in the condensed phase: melting, hydrolysis, crosslinking, charring, dripping, diffusion of volatile products and superficial accumulation of materials. The non-oxidizing thermal degradation consisting in heterolytic or homolytic chain scissions of the macromolecules can be one of the thermal degradation mechanisms, or the oxidizing thermal decomposition wherein the polymer and its degradation products react with the oxygen of the air.

IV-1-3 Mode of action of FR additives

The earliest FR for synthetic polymers were halogenated based, based on the discovery of halogenated hydrocarbons and waxes. New chemistries followed shortly thereafter, but each of these chemistries was created in response to a particular need.

IV-1-3-1 Overview of the FR's mode of action

Fireproofing additives can have a physical and/or a chemical mode of action in the gas and/or in the condensed phase depending on their nature.¹⁶⁶ They interfere with combustion during a particular stage of the process, e.g. during heating, decomposition, ignition or flame spread.

In the gas phase, the inhibition of the radical mechanism takes place due to the FR additives or/and by their decomposition products (e.g. radical scavengers). Hence, the exothermic processes are stopped, the system cools down and the supply of flammable gases may be reduced or suppressed. **In the condensed phase**, the formation of a carbon layer or ceramic protective layer on the polymer surface limits the volatilization of the fuel, oxygen diffusion and insulates the polymer underneath from the external heat. The addition of FR, such as metal hydroxide, that decomposed with an endotherm leading to a “cooling effect” is another mode of action occurring in the condensed phase. The acceleration of the polymer

decomposition is another possibility: it causes a pronounced flow of the polymer and consequently a withdrawal from the sphere of influence of the flame that breaks away.

Physical actions take place through the formation of a protective layer, by cooling and/or by dilution. Less effective physical actions can occur by cooling: the additive cools the underlying substance by endothermal decomposition, usually dehydration, to a temperature that is unable to sustain the burning process. The protection by dilution takes place through the addition of compounds (e.g. fillers such as carbonate or metal hydroxide) releasing inert gases (e.g; carbon dioxide or water) upon decomposition. These additives dilute the flammable gas in the condensed and in the gaseous phases and thus lower the concentration of combustible gases in the surrounding atmosphere. By the formation of a protective layer (intumescence phenomenon), the substance is shielded with highly porous structure, protecting the underlying material against the heat and oxygen required for combustion to take place. Heat and mass transfers between the external heat source and the material are thus reduced, and the degradation rate of the polymer is decreased, as well as the 'fuel flow' which is able to feed the flame (Figure 55).

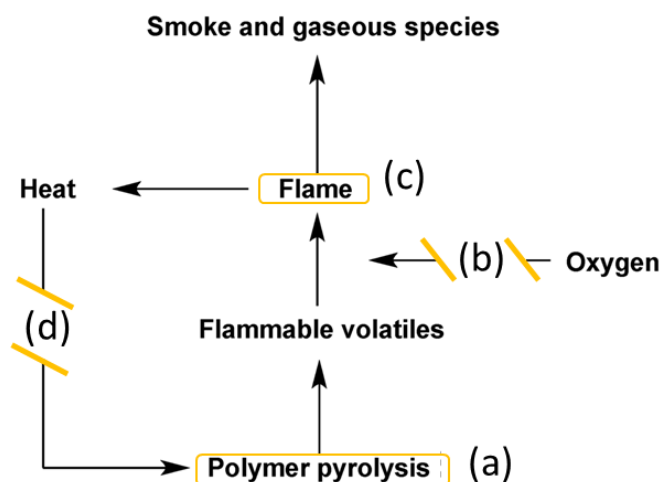


Figure 55. Schematic representation of potential mode of action of FRs (a to d) in the combustion cycle¹⁷¹

The selection of a FR for a specific polymer is governed by the chemical and physical properties of the polymer itself, its degradation characteristics and the chemical and physical properties of the FR system. An overview of the study dealing with iron oxide in flame retarded system is proposed in the following part of this chapter.

IV-1-3-2 Flame retardant characteristics of iron oxide

Nowadays, metal oxides represent more than 50 % of the fillers sold globally, mainly due to their low cost, low toxicity and minimal corrosivity.¹⁷² A high number of scientific papers appear every year dealing with iron, iron compounds or iron chemistry. However, very few of them deal with the use of iron compounds as flame retarding/smoke suppressing additives for polymers. The recent chemistry of iron has been reviewed by Silver¹⁷³ but again there are few comments on the potential uses of iron compounds in polymers.¹⁷⁴ The economic importance of iron is unsurpassed by any other element in the periodic table.

The first reports of iron compounds being used as smoke suppressants in plasticized and rigid polyvinyl chloride formulations began to appear in the 1970s and early 1980s.¹⁷⁴ Later on, the use of iron containing compounds, especially iron (III) oxide (Fe_2O_3), was investigated as powerful combustion inhibitors, smoke suppressants, thermal stabilizers and radical recombination catalysts in such formulations.¹⁷⁵⁻¹⁷⁷ It is recognized that red iron oxide ($\alpha\text{-Fe}_2\text{O}_3$) is relatively heat-stable up to 1000°C , while both yellow ($\alpha\text{-FeOOH}$) and black (Fe_3O_4) iron oxides have a limited thermal stability.¹⁷⁸

Iron oxide is particularly mentioned in the open literature as a synergistic agent (in combination with red phosphorus in PA-6 for example).¹⁷⁹⁻¹⁸¹ Indeed, it is able to promote the formation of a crosslinked network which prevents the release of small volatiles.¹⁸² Nonetheless, depending on the polymeric matrix and on the FR system used, contradictory results have been obtained in terms of fire performance. Its effectiveness has been evidenced in halogen-containing polymers (like in poly(vinyl chloride))¹⁸³⁻¹⁸⁶ and in combination with different fire retardant systems (for example in a mixture of polyphenylene oxide and zinc borate in PA-4.6¹⁸¹ or with chlorinated FR in nylon 6.6 and epoxies).^{183,175, 187} However, some disagreements lay upon the question of their effect and particularly their effectiveness in non-

halogenated systems.^{181, 188, 189} Nangrani *et al.* reported that iron oxide decreases the flammability of polycarbonate.¹⁸⁹ On the contrary, Hirschler *et al.* commented on its ineffectiveness as FR in the absence of halogen in ABS.¹⁸⁸ Recently, Laachachi *et al.* [7] have shown that Fe₂O₃ particles could also increase the thermal stability of PMMA by reducing the chain mobility as proved by the evolution of Tg.¹⁸⁷ In polypropylene, the combination with Fe-Montmorillonite is helpful to suppress smoke and leads to an improvement of the FR properties.¹⁹⁰

Last but not least, it was demonstrated that Fe₂O₃ nanoparticles play an important role in the thermal stability improvement of a silicone/Fe₂O₃ nanocomposite.^{191, 192} Thermal conduction inside the material was limited, and at the same time the kinetics of degradation of the resin decreased, as well as the gas emissions due to the increase in viscosity of the melt.

On the other hand, in the open literature, it is widely accepted that iron oxide, and particularly its hematite form, is able to absorb UVA. Its limited catalytic action compared to titanium dioxide and zinc oxide, and the absence of evident toxicity make them good candidates for various applications (e.g. cosmetics, wastewater treatment ...).^{193, 194}

Consequently, red iron oxide constitutes an interesting choice both for fire retardant and ageing purposes. The evaluation of the fire performances of the unfilled epoxy/silicone and epoxy/fluoropolymer systems is investigated and detailed hereinafter in a first part. Then, the influence of the incorporation of a low amount (from 2.5 to 10% pigment volume concentration - PVC) of ferric oxide on the fire properties of the binary systems is discussed. As the epoxy/silicone coating represents the most innovative and promising combination, its mode of action will be particularly considered in the fourth part of this chapter. The investigation of the mode of action the epoxy/fluoropolymer/IO coating are presented not presented in this manuscript. Nevertheless results are partly gathered in the published article: “*One pot flame retardant and weathering resistant coatings for plastics: a novel approach*”, RSC Advances, 7, 40682 – 40694. [doi: 10.1039/c7ra08028j]”).

IV-2 Fire performances of the self-stratifying coatings applied on PC

The following section presents the investigation of the fire performances of the epoxy/silicone and epoxy/fluoropolymer self-layering systems when combined or not with iron oxide particles (Fe_2O_3) and applied on polycarbonate. The first part gathers the results and a comparison of the fire properties obtained with both systems. It opens the discussion to the study of the thermal stability of the materials, and to the comprehension of the mechanisms of action of iron oxide particle in the most promising combination (epoxy/silicone) and of the protective role of the coating to bring fireproofing properties to the polycarbonate matrix.

IV-2-1 Development and evaluation of the FR properties of the epoxy/silicone and epoxy/fluoropolymer coatings applied on PC

The fire performances of the uncoated polycarbonate and polycarbonate coated with the unfilled and filled binary systems were evaluated using LOI, UL-94 and MLC tests. Based on those results, their thermal stability has been investigated using TG analyses in both pyrolytic and thermo-oxidative conditions. Then, microcalorimetry (PCFC) and Py-GCMS experiments were carried out to study the combustibility of the gas phase during combustion. The comprehension of the mode of action in the condensed phase has been performed by microscopic analyses of the residues which underwent different heat treatments in a tubular furnace, or of residues collected during MLC tests. ATR-FTIR spectroscopy measurements will complete those analyses.

IV-2-1-1 Fire retardancy of the PC coated with unfilled epoxy/silicone or epoxy/fluoropolymer coatings

MLC, LOI and UL-94 fire tests were performed in order to evaluate the flame retardant properties of the polycarbonate covered with unfilled coatings. HRR curves and characteristic MLC parameters are depicted in Figure 56 and Table 21. It is noteworthy to remind that no

ignition of the coated sample occurred at 35 kW/m², whereas the raw PC ignites after 319 s. and releases a total heat of 35 MJ/m² (Appendix 4).

Table 21. MLC (50 kW/m², 35 mm), LOI and UL-94 values of the uncoated and coated PC with the epoxy/silicone and epoxy/fluoropolymer mixture

		Virgin PC	Epoxy/Silicone coated PC	Epoxy/Fluoropolymer coated PC
MLC	TTI (s)	92 ± 6	148 ± 7	26 ± 2
	pHRR (kW/m ²)	231 ± 6	176 ± 4 (-24 %) ¹	250 ± 2 (+8%)
	THR (MJ/m ²)	52 ± 1	41 ± 3 (-21 %)	46 ± 3 (-12%)
	TFO (s)	1077 ± 47	903 ± 6	735 ± 30
LOI (vol.% O ₂) ¹		27	28	25
UL-94 ¹		NC	NC	NC

¹3mm thick samples

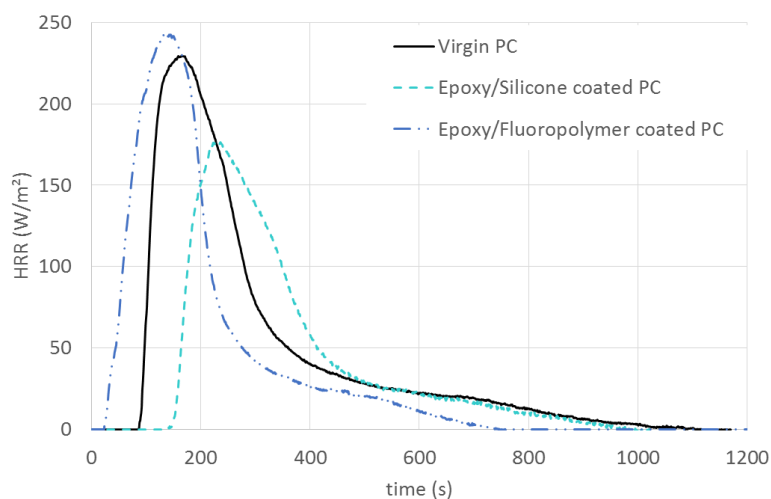


Figure 56. MLC curves of the uncoated and coated PC with the epoxy/silicone and epoxy/fluoropolymer mixtures

PC is a char forming polymer. After ignition, it melts and forms a char which swells until it reaches a height of about eight centimeters (Figure 57). The char then degrades and only ashes remain at the end of the test. The behavior of PC is different after the application of the silicone-based coating at its surface. The film forms a barrier (protective in the case of the silicone-based coating) between the heat source and the substrate: the PC swells under the coating which progressively delaminates from the edges of the plate due to the uprising of the PC char. Then, ignition occurs and the PC forms a char which rapidly goes up as it was observed with the uncoated PC. The char is then consumed and collapses before flame out takes place.

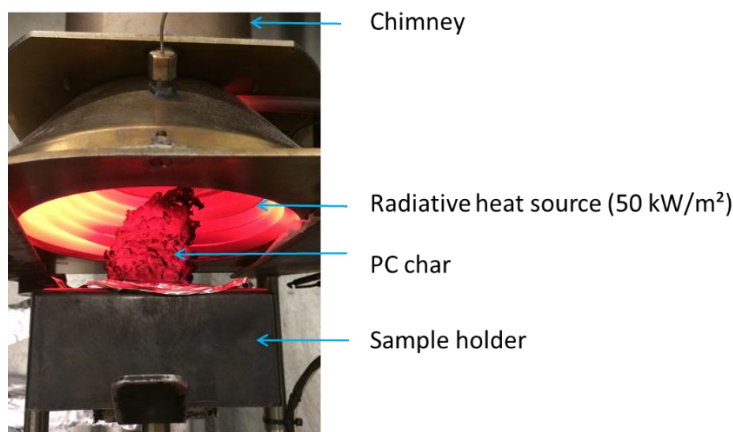


Figure 57. Picture of the polycarbonate char formed during MLC experiment before it collapses ($t = 600$ s., 50 kW/m^2 , 35 mm)

Those results evidence an improvement of the fire performances when the epoxy/silicone coating is applied: both the pHRR and THR are reduced, respectively by 24 and 21 % compared to raw PC. In addition, the coating allows delaying the ignition by more than 50 s. This results is in good agreement with the literature since thin silicone-based coatings were already proven to improve fireproofing properties of PC substrate via the formation of an expanded coating upon flaming, similarly to intumescence.²³

The application of the fluoropolymer-based self-stratified coating on PC causes a slight increase of the pHRR (+8 %). However, it remains in the margin of error. Nonetheless, the TTI is shortened (- 66 s) compared to pure PC (Table 21). One hypothesis is that the coating would be less thermally stable than the PC under radiative heat flux. Indeed, it was already reported

that shorter TTI can be related to a reduction in the thermal stability: since ignition is controlled by the supply of fuel gases, less thermally stable specimens tend to ignite earlier. In our case, the epoxy/fluoropolymer protective layer would thus be less thermally stable than the PC substrate. It could also explain the earlier mass loss with the coated PC sample compared to that of PC, leading to a broader MLR signal (Appendix 9).

The experimental conditions during UL-94 and LOI testing differ from those of MLC test in terms of fire scenario: MLC is a radiative heat flux test whereas during LOI or UL-94, a flame is applied on a specimen. Different phenomena are therefore occurring during combustion, and so the properties measured can induce different and complementary conclusions compared to those of MLC. PC is a combustible self-charring polymer and thus reaches a quite high intrinsic LOI value (27 vol.% at 3mm) compared to other common thermoplastics.¹⁹⁵ Up to 28 vol.%, the extinction of the virgin PC occurs mainly because of flaming drops or consumption of the material.

The intrinsic flame retardant properties of the coated PCs are not improved in the case of vertical burning tests: similar LOI values (27 vol.% for the raw PC compared to 28 and 25 vol.% respectively with the PC coated with the silicone- and fluoropolymer- based coatings) and a non-classified (NC) rating is obtained with the three samples.

The epoxy/silicone coating however allows reducing the flame spread of the material (visual observation) and retains somehow the flaming drops from falling down. Virgin PC is NC at 3 mm, however close to meet the requirements of V2 classification (short combustion time – 30/40 seconds - and dripping occurs with no ignition of the cotton). Even if the coated polycarbonate is still NC, the system behaves differently compared to pure PC: the combustion time is nearly null after the first ignition, but is longer after the second ignition. Also, the tendency for dripping is less pronounced.

For PC coated with the fluoropolymer based formulation, LOI value is slightly decreased compared to pure PC (25 vol.% versus 27 vol.% respectively). In that case, the dripping is more pronounced compared to the raw PC, as both the coating and the PC burn. Although the charring behavior is much more important when the coating is present, it does not prevent

the flaming and dripping. In addition, the ignition of the coated sample is quicker. The coating probably ignites earlier than the PC as already observed in MLC experiments.

In order to improve the fire retardancy of the PC by the application of a self-stratifying coating on its surface, the influence of the incorporation of a specific filler, i.e. iron oxide, in the coating formulation was investigated. Iron oxide was used as a filler in order to improve the FR properties of the system and incorporated at 10 wt.% (2.5 %PVC) in the coating formulations. The systems were then applied on polycarbonate and tested. 5 and 10 %PVC were also tested in combination with the epoxy/silicone system and are presented simultaneously.

IV-2-1-2 Fire retardancy of the PC coated with iron oxide-filled epoxy/silicone or epoxy/fluoropolymer coatings

The FR performances of the polycarbonate coated with the iron oxide filled systems were evaluated by LOI, UL-94 and MLC. LOI and UL-94 data and pictures of the resulting specimens after testing are depicted in Table 22 and Table 23.

Table 22. LOI and UL-94 ranking of coated PC with epoxy/silicone coatings filled or not with iron oxide

	Epoxy/Silicone/Fe ₂ O ₃ coated PC			
%PVC ¹	0	2.5	5	10
LOI (vol.% O ₂)	28	33	34	37
				
UL-94	NC	V0 No dripping	V0 No dripping	V0 No dripping
				

¹ PVC = Pigment Volume Concentration

Table 23. LOI and UL-94 ranking of coated PC with epoxy/fluoropolymer coatings filled or not with iron oxide

Epoxy/fluoropolymer coated PC	0 %PVC ¹	2.5 %PVC
LOI (vol.% O ₂) ²	25	32
		
UL-94 rating ¹	NC Dripping	V0 No dripping
		

¹ PVC= Pigment Volume Concentration, ² 3mm thick samples

The incorporation of iron oxide in the coated formulations allows exhibiting outstanding flame retardant performances compared to the unfilled coated PC and also to the virgin PC (Table 22, Table 23), whatever the amount of filler incorporated. With 2.5 %PVC of Fe₂O₃ added to the systems, an increase by respectively 6 and 5 vol.%O₂ of the LOI value of PC with the silicone and fluoropolymer based coating is achieved, and the best rating (V0) at UL-94 is obtained. An addition of a higher amount increases the FR properties of the epoxy/silicone system up to 37 vol.% at LOI testing are reached with 10 %PVC whereas the best rating at UL-94 is maintained.

A change in the fire behavior of coated PC is also noticeable visually due to the addition of fillers: no dripping is observed during both tests, ignition of the samples is considerably delayed and the combustion time is shortened compared to that of the unfilled systems. At UL-94 test, self-extinguishment occurs less than 6 seconds after ignition, and the resulting char is mainly formed at the beginning of the flame application. During these vertical flame tests, charring is more pronounced for the filled systems (increasingly by raising the amount of iron oxide) and occurs quicker after the ignition than for the unfilled ones. Presence of fillers also prevents dripping to occur and flame spread is much slower than for raw PC and unfilled coated PC samples.

Mass loss cone calorimetry (MLC) is another effective tool to evaluate the flammability of materials under a radiative heat flux. The filled samples were also tested at MLC in both conditions: 35 kW/m² and 50 kW/m². Likewise the unfilled coated PC, no ignition occurs at 35

kW/m² (Appendix 4). Heat release rate curves of both uncoated and coated PCs are presented in Figure 58 and Figure 59. Characteristic parameters obtained from those curves (i.e. TTI, pHRR, THR, TFO) are reported in Table 24.

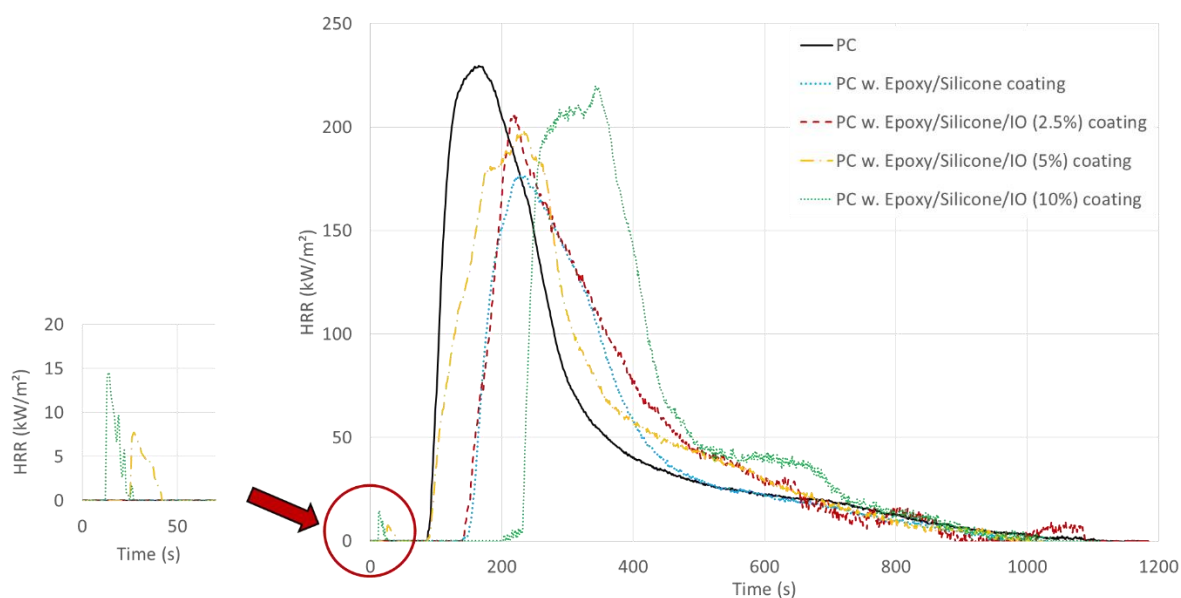


Figure 58. MLC curves of uncoated and coated PC with the epoxy/silicone/Fe₂O₃ system (50 kW/m², 35 mm)

Table 24. MLC values of unfilled and filled coated PC with the epoxy/silicone/Fe₂O₃ systems (50 kW/m², 35 mm)

%PVC ¹	Epoxy/Silicone/Fe ₂ O ₃ coated PCs				Epoxy/Fluoropolymer/Fe ₂ O ₃ coated PCs	
	0	2.5	5	10	0	2.5
TTI (s)	148 ± 7	141 ± 20	26-87 ± 2-5	13-237 ± 5-100	26 ± 2	20 ± 3
pHRR (kW/m²)	176 ± 4 (-24 %) ²	205 ± 20 (-11 %)	197 ± 1 (-15 %)	218 ± 22 (-6 %)	250 ± 2 (+8 %)	191 ± 23 (-17 %)
THR (MJ/m²)	41 ± 3 (-21 %)	47 ± 2 (-10 %)	51 ± 1 (-2 %)	49 ± 7 (-6 %)	46 ± 3 (-12 %)	29 ± 4 (-44 %)
TFO (s)	903 ± 6	1003 ± 33	889 ± 4	990 ± 100	735 ± 30	735 ± 67

¹ PVC= Pigment Volume Concentration, ² Percentage are calculated according the difference with the virgin PC

When ferric oxide is incorporated in the epoxy/silicone self-stratified system, it influences mainly the TTI. With 2.5 % of IO, the TTI is comparable to that of the unfilled coated PC. When 5 and 10 % of Fe_2O_3 are incorporated into the formulation, two TTI are registered (26 s and 87 s for 5 % of IO; 13 s and 237 s for 10 %). Flame out occurs very quickly after the first ignition, reflecting the difficulty of the coating to inflame. This effect is particularly evident for the system containing 10 % of IO as it takes a long time (237 s) for the sample to ignite again. The presence of remaining solvent in the coated film is probably responsible for this shoulder: BuAc and xylene evaporate as soon as they undergo the radiative heat flux due to their low boiling temperature. Once the system re-ignites, the enhancements in terms of heat release rate are negligible and even lowered by the incorporation of the fillers compared to the unfilled coated system. No significant improvement is obtained in terms of pHRR and THR during the combustion compared the unfilled coated PC and to the raw PC.

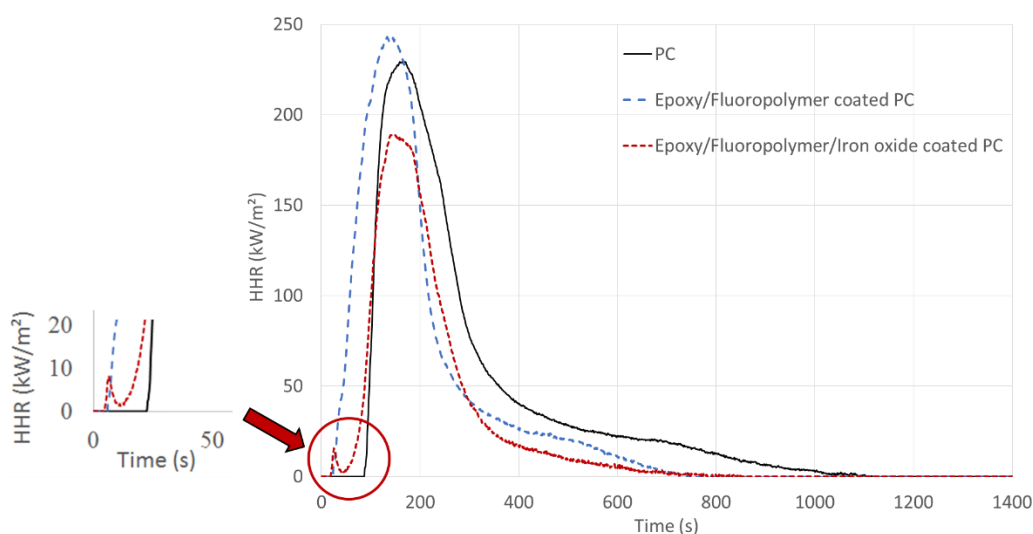


Figure 59. HRR curves obtained for PC and coated PCs with unfilled and filled epoxy/fluoropolymer formulations

On the contrary, when IO is incorporated in the epoxy/fluoropolymer coating, an improvement in the fire behavior is noticeable: a decrease of both pHRR (-17 %) and THR (-44 %) compared to pure PC is observed. The ignition of the samples occurs in the edges, i.e. in the area where the coating has delaminated, whereas ignition usually occurs in the center of the sample for specimens without fillers. In addition, the effect of IO is well noticeable by the

shoulder which appears after the ignition of the coating (between 20 and 50 sec., Figure 59), probably due to the presence of remaining solvent in the coated film, similarly to the epoxy/silicone/IO coating. The flame have difficulties in persisting compared to the unfilled epoxy/fluoropolymer coating with which the HRR raises directly after the ignition. This again suggests that the coating that includes Fe_2O_3 is a good fire barrier, confirming the observations made during UL-94 and LOI testing.

Conclusion

The FR performances of the substrate, the resins and the FR systems used to fire protect the PC were evaluated using three different fire tests which induced different fire scenarios: UL-94, LOI and MLC. MLC is exposing the sample to a radiative heat flux, while UL-94 and LOI involve physical contact with a flame.

The application of the unfilled epoxy/silicone coating onto the polycarbonate matrix allowed improving FR properties of the PC by shifting the time to ignition (+56 s) and decreasing the pHRR and HRR by respectively 24 and 21 % at MLC test. No particular enhancement was noticed with the vertical tests. The application of the unfilled fluoropolymer based coating does not allow to improve the intrinsic FR properties of the PC. On the contrary, the results are even worse: dripping and flame propagation are more pronounced during the combustion and the time before the ignition (both in the presence of a flame and a radiative heat source) is shortened.

The incorporation of iron oxide particles allows reaching further enhancements: the formation of the residue is improved, dripping is totally inhibited and a lower combustion time and flame spread is observed. The filler appears to play an important role mainly in the presence of a flame in the case of the epoxy/silicone system. Indeed, the highest improvements under a radiative heat source come from the epoxy/silicone system itself, with no iron oxide particles.

In contrast, the incorporation of IO particles allows increasing considerably the fire performances of the fluoropolymer based systems under both a flame and a radiative heat flux. Indeed, the LOI is increased by 5 vol.% O_2 and the best rating (V0) is achieved at UL-94. At MLC, a reduction of the THR by 44 % is registered.

Finally, IO particles bring additional properties to the coatings as dripping is avoided and also flame propagation. From the most relevant papers, it is established that metal oxide particles promote the formation of a crosslinked network in the solid phase, particularly when combined with phosphorus compounds that may prevent the release of small molecules such as volatiles (thermal barrier effect).¹⁹⁶ In particular, iron containing compounds may have a catalytic action, acting as synergists and smoke suppressants in some thermoplastic polymer formulations.^{182, 197} In order to investigate this aspect, the comprehension of the mode of action was achieved using different experimental techniques commented in the next section.

To conclude, these results show that the FR performances are induced by complex mode of action of IO in the epoxy/silicone and epoxy/fluoropolymer systems, and of the epoxy/silicone system by itself, in condensed phase and maybe in the gas phase too. The next section is devoted to the investigation of how the silicone-based coatings act to reduce the flammability of the PC. To achieve this, different tests were performed to understand their mode of action both in the condensed and in the gas phase.

IV-2-1-3 Comprehension of the mode of action

In order to understand the results obtained during the fire tests, and how iron oxide acts as a flame retardant, the modes of action of the epoxy/silicone and epoxy/silicone/iron oxide systems were investigated using different techniques.

At this point of the study, it seems that the epoxy/silicone coating allows forming a protective barrier at the surface of the PC, which allows to delay its ignition and to reduce, to some extent, the heat release and total heat release during the combustion. When iron oxide is added to the system, additional improvements are brought: the residue seems to be improved, the occurrence of dripping inhibited and the flame spread somehow reduced. The aim is consequently to explain the inhibition of the flame, the formation of the residue (organic or inorganic) and if an action in the gas phase occurs during the combustion.

To do so, the thermal stability of the different materials used in the system was studied under both thermo-oxidative and pyrolysis conditions. Indeed, during the combustion of a polymeric

material, it is assumed that when the flame is intense enough, most of the oxygen present is consumed: the material is thus considered to degrade in pyrolytic conditions¹⁴⁹ whereas before the ignition, the material degrades in thermo-oxidative conditions. Furthermore, when the combustion is decreasing, localized flames are observed and the oxygen may reach the material and induce oxidation. Therefore, it is there noteworthy to study how the materials behaves under both conditions.

To begin with, the thermal stability of the PC and of the materials used to formulate the coatings was studied using TG analysis.

Investigation of the thermal stability of raw materials

Pyrolysis of PC, silicone and epoxy resins

The thermal stabilities of the polycarbonate, the epoxy resin which has been crosslinked beforehand (without solvent) in respect to the curing conditions and the pure silicone resin were investigated in pyrolytic conditions (Figure 60 and Table 25).

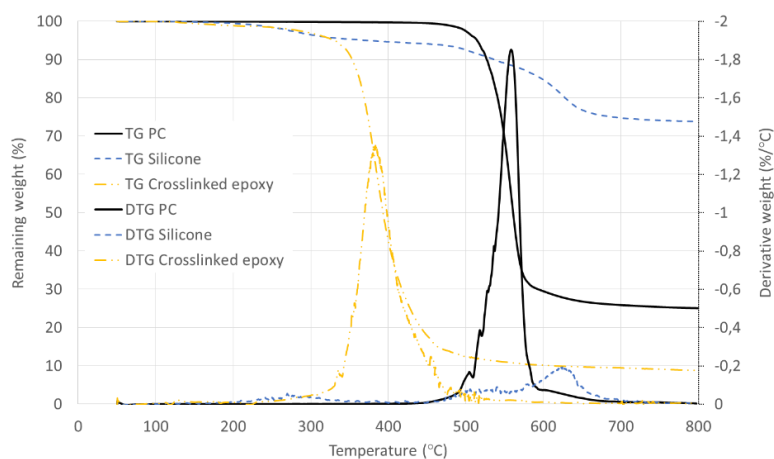


Figure 60. Pyrolytic degradation of PC, silicone and crosslinked epoxy resins (N₂, 20 °C/min)

Table 25. TG data of PC, crosslinked epoxy and silicone resins (N₂, 20 °C/min)

Pyrolytic conditions			
System	PC	Crosslinked epoxy	Silicone
T _{onset} (°C)	494	205	245
T _{max} (°C)	558	384	270
Resid. (wt.%) at T _{end}	25	8	97
DTG _{max} (%/°C)	1.83	1.33	> 0.10
T _{onset} (°C)			401
T _{max} (°C)			627
Resid. (wt.%) at T _{end}			73
DTG _{max} (%/°C)			0.20

An apparent one step decomposition process is observed for both the polycarbonate and the crosslinked epoxy resin. The epoxy decomposes almost entirely such that a residual mass of 8 wt.% is left at 800 °C, with a maximum degradation rate at 384 °C. PC is thermally more stable as it degrades at a higher temperature (558 °C) but faster (1.83 %/°C compared to 1.33 %/°C for the epoxy resin). PC is a char forming polymer and undergoes branching and eventual crosslinking to form an insoluble gel during its decomposition.¹⁹⁸ It releases carbon dioxide and bisphenol-A with lesser amounts of carbon monoxide, methane, phenol diphenyl carbonate, and 2(4-hydroxyphenyl)-2-phenyl propane during its degradation.¹⁹⁹ The epoxy resin also releases bisphenol A during its decomposition, as well as other phenolic products.

The decomposition of the silicone resin involves a three-step process and shows an excellent thermal stability (residual mass of 73 wt.% at 800 °C). The first degradation step corresponds to the release of silicone oligomers (3 wt.%) and the second and third steps (overlapped) correlate to the release of aromatic compounds (such as benzene and bisphenyl, 24 wt.%).²⁰⁰ The silicone resin is thermally more stable at high temperature (above 540 °C) compared to the polycarbonate, and also to the epoxy resin when this last is crosslinked. Under pyrolytic conditions, its main degradation step occurs at much higher temperature and with a lower degradation rate (0.2 %/°C compared to 1.8 and 1.3 %/°C respectively with the PC and the epoxy resin). Finally, its remaining mass at 800 °C is equivalent to three times the amount of residue for PC. The silicone resin is thus the material which is the most thermally stable at high temperature compared to the substrate and to the epoxy resin which composes the layer in

between the two materials. During a fire scenario, the silicone will be the resin in contact with the open flame or exposed to the heat source as it is located in the upper layer of the film. Consequently, a reasonable assumption is that the silicone resin brings the fire performances to the coated system in accordance with the thermal stability of the materials, in pyrolytic conditions. The silicone coating may soften upon heating, and then expand to some extent to protect the underlying epoxy resin and substrate. The thermal stability of the materials was then studied under thermo-oxidative conditions.

Thermo-oxidation of PC, epoxy and silicone resins

The thermal stabilities of the substrate and of the pure resins (the epoxy resin was crosslinked beforehand, without any solvent) were then investigated in thermo-oxidative conditions (Figure 61 and Table 26). An additional step is observed for each sample: both the PC and the crosslinked epoxy resin degrade in a two-step process whereas the silicone resin decomposes according to a three-step process.

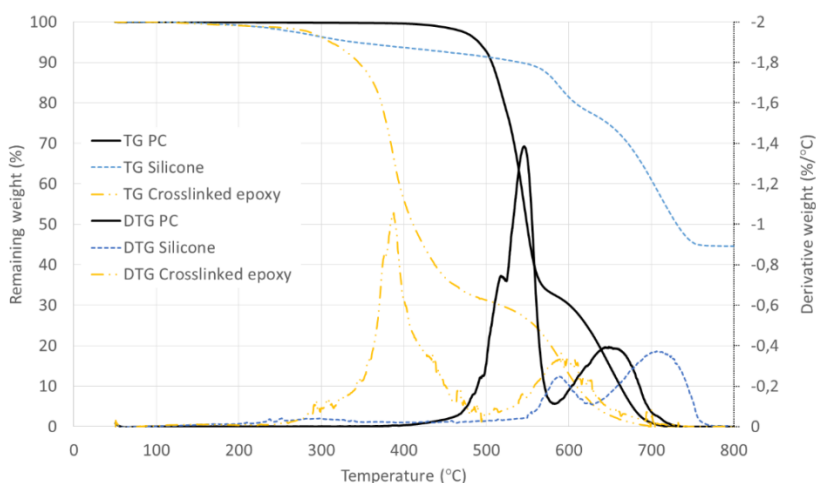


Figure 61. Thermo-oxidative degradation of PC, silicone and crosslinked epoxy resins (Air, 20 °C/min)

Table 26. TG data of PC, crosslinked epoxy and silicone resin (Air, 20 °C/min)

Thermo-oxidative conditions			
System	PC	Crosslinked epoxy	Silicone
T_{onset} (°C)	462	224	238
T_{max} (°C)	546	387	296
Resid. (wt.%) at T_{end}	32	31	90
DTG_{max} (%/°C)	1.36	1.00	> 0.10
T_{onset} (°C)	584	496	524
T_{max} (°C)	647	592	589
Resid. (wt.%) at T_{end}	0	0	77
DTG_{max} (%/°C)	0.4	0.33	0.24
T_{onset} (°C)			631
T_{max} (°C)			710
Resid. (wt.%) at T_{end}			44
DTG_{max} (%/°C)			0.36

The first decomposition step of PC and of the epoxy resin is similar to the degradation observed under pyrolytic condition (comparable maxima of temperature, respectively 546 and 387 °C versus 558 and 384 °C) but the decomposition rates are lower (1.36 and 1.00 %/°C respectively compared to 1.83 and 1.33 %/°C under N₂ atmosphere). The first degradation step leads to the formation of a transient residue that oxidized at a higher temperature. They are both completely degraded after their second degradation step. Furthermore, PC is also more thermally stable than the epoxy resin.

On the contrary, the silicone resin does not decompose entirely and maintains a high residual weight at 800 °C (44 wt.%). Three maxima of degradation are observed at 296, 589 and 710 °C: the second and third steps of degradation are more dissociated compared to what was observed under pyrolytic conditions. Moreover, the maximum temperature slightly shift toward higher temperatures. According to those results, it is possible to conclude that the silicone resin is a highly thermally stable resin compared to both the PC and the epoxy resin.

In order to figure out the influence of the addition of a filler in the system, the thermal stability of the silicone/iron oxide system needs to be studied. Indeed, the iron oxide particles are located in the silicone medium after the formation of the solid film and will most probably interact with the silicone resin in a first place. Last but not least, it was demonstrated that the silicone is probably responsible for the promising fireproofing properties obtained when

applying the coating onto the polycarbonate. In addition, it is the layer which is exposed to the flame/heat source during fire tests (Figure 43, chapter III). Consequently, the focus was placed on the thermal behavior of the silicone/iron oxide system for the next part of the study.

Investigation of the thermal stability of the silicone/iron oxide system

The thermal stability of the filled silicone system with Fe_2O_3 particles was investigated under both pyrolytic and thermo-oxidative conditions.

From the previous experiments, it was observed that the presence of iron oxide limits the flame propagation along the sample and prevents the dripping, thus enhancing the fire retardant properties of PC. The amount of residue seems also to be increased (visual observation). From the most compiled papers, it is established that metal oxide particles promote the formation of a crosslinked network that may prevent the release of small molecules such as volatiles (barrier effect). In particular, iron containing compounds may have a catalytic action, acting as synergists and smoke suppressants in some thermoplastic polymer formulations.^{182, 197} To try to evidence such effect, TG analyses were performed on the dried silicone resin (beforehand diluted at 30 wt.% and cured following the coatings curing procedure) with and without iron oxide (at 10 wt.% i.e. 2.5 %PVC, Figure 62 a) and difference weight loss curves were calculated. This amount was chosen as it offers the most promising results in terms of fire retardant enhancements, visual appearance and adhesion. Data are gathered in Table 27.

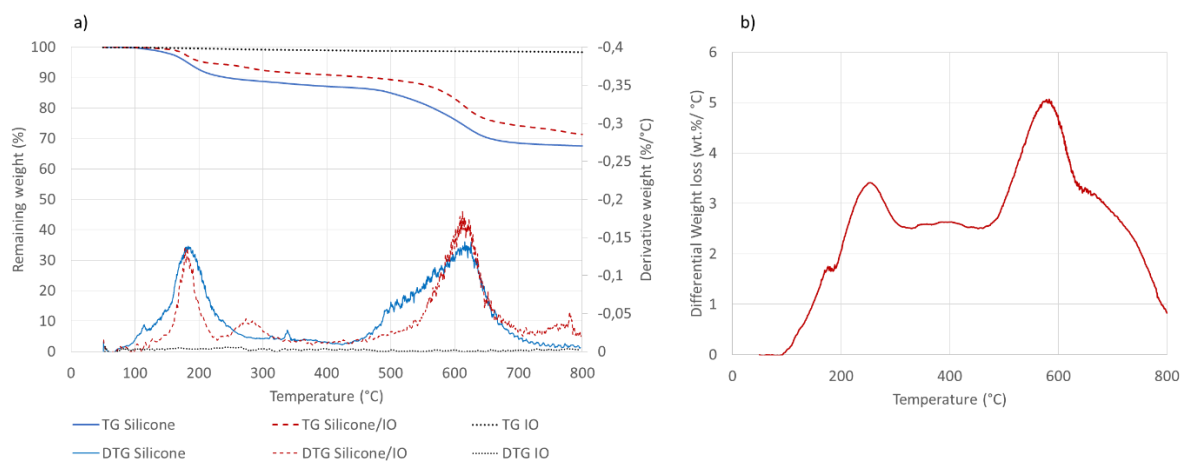


Figure 62. a) Comparison of TG and DTG curves of the silicone systems with and without iron oxide and b) Differential TGA of silicone/iron oxide system (N₂, 20 °C/min)

Table 27. TG data of silicone film, iron oxide and silicone/iron oxide systems (N₂, 20 °C/min)

Pyrolytic conditions			
System	Silicone film	Iron Oxide	Silicone + Iron Oxide
T_{onset} (°C)	96	100	114
T_{max} (°C)	177	800	181
Resid. (wt.%) at T_{end}	89	99	95
DTG_{max} (%/°C)	0.13	0.00	0.13
T_{onset} (°C)	400		232
T_{max} (°C)	628		275
Resid. (wt.%) at T_{end}	68		91
DTG_{max} (%/°C)	0.13		> 0.1
T_{onset} (°C)			409
T_{max} (°C)			613
Resid. (wt.%) at T_{end}			72
DTG_{max} (%/°C)			0.18

The silicone film degrades in two steps while exhibiting an excellent thermal stability (residual weight of 68 wt.% at 800 °C). The first degradation step may be coupled with the release of the remaining solvents from the resin’s preparation and the release of silicone oligomers (11 wt.%).²⁰⁰ The incorporation of iron oxide does not favor the formation of additional residue: with an initial loading of 10 wt.%, the residue left is 72 %, approximately what was expected from the original inorganic composition. Indeed, as the residue left by the silicone resin is equal to 68 %, 61 % of the remaining mass of the silicone/IO system is attributed to the resin

and 10 % to the IO particles, as there is almost no degradation of IO before 800 °C. Theoretically, the residual mass of the system should thus be 71 % if the original organic compositions are taken into account, which is not far from the 72 % obtained. In addition, the maxima temperatures of degradation are roughly the same (177 and 628 °C compared to 181 and 613 °C respectively during the first and last degradation steps after the incorporation of the IO), as well as the degradation rates associated.

The difference weight loss curve (see Chapter II, section II-3-3) allows highlighting the presence of specific interactions between the polymer and the additive depending on the temperature. It appears that the addition of iron oxide induces some thermal stabilization of the silicone resin in the range of temperature experimented (up to 5 wt.%/°C at 580 °C, Figure 62 b). The stabilization occurring suggests that iron oxide somehow interacts with the silicone matrix, nevertheless not in a significant way according to the results.

Under thermo-oxidative conditions, the incorporation of iron oxide does not modify the decomposition process of the resin: similar curves and remaining masses are obtained at 800 °C (Figure 63, Table 28).

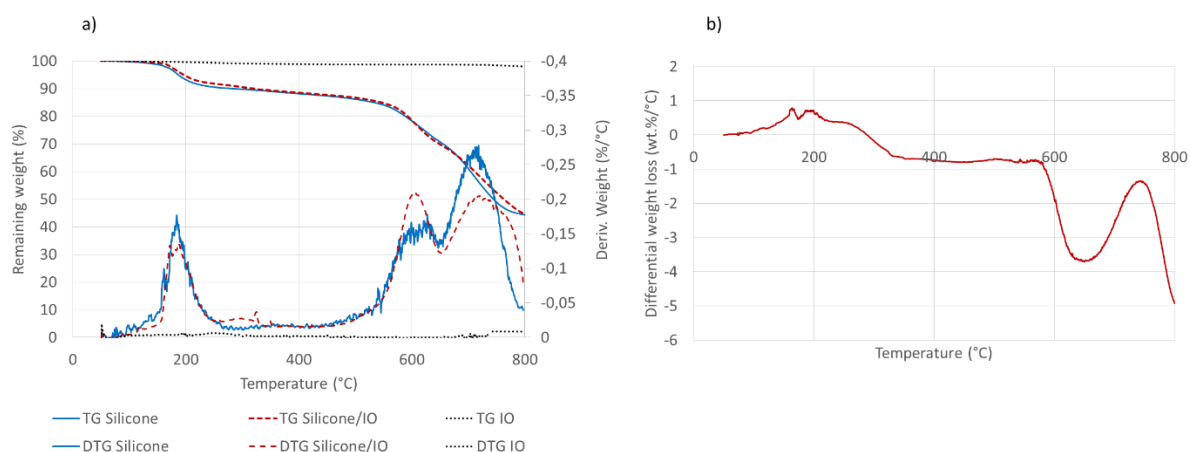


Figure 63. a) Comparison of TG and DTG curves of the silicone resin, iron oxide and the silicone/iron oxide system and b) Differential TGA of silicone/Iron oxide system (Air, 20 °C/min)

Table 28. TGA data of silicone film, iron oxide and silicone film containing iron oxide (Air, 20 °C/min)

Thermo-oxidative conditions			
System	Silicone film	Iron Oxide	Silicone + Iron Oxide
T_{onset} (°C)	92	100	105
T_{max} (°C)	184	800	187
Resid. (wt.%) at T_{end}	87	99	88
DTG_{max} (%/°C)	0.16	0.00	0.13
T_{onset} (°C)	401		401
T_{max} (°C)	624		606
Resid. (wt.%) at T_{end}	70		69
DTG_{max} (%/°C)	0.16		0.21
T_{onset} (°C)	648		652
T_{max} (°C)	711		721
Resid. (wt.%) at T_{end}	44		45
DTG_{max} (%/°C)	0.27		0.20

The decomposition rate of the second step of degradation of the silicone resin is slightly increased due to the presence of iron oxide particles (0.21 %/°C compared to 0.16 %/°C without iron oxide). On the contrary, iron oxide decreases the rate of the last decomposition step: 0.2 %/°C is logged versus 0.4 %/°C without the particles. As under pyrolytic conditions, the filler is thermally stable up to 800 °C: only a loss of 1 % is obtained. The thermal depolymerisation and thermal oxidative degradation are not restrained due to the addition of Fe₂O₃ particles. In addition, the difference weight loss curve allows highlighting specific interactions between the silicone and ferric oxide: up to 600 °C, no difference are observed whereas at higher temperature, a slight destabilization is noticed. Finally, iron oxide does not favor the formation of an additional carbonaceous char under thermos-oxidative conditions, as the residual masses are similar with the unfilled and filled systems.

Conclusion about thermal stability

In conclusion, it has been shown that the silicone resin is more thermally stable than the epoxy system and the polycarbonate at elevated temperature (above 540 °C), under both inert and air atmosphere. As it is the component which is at the interface with the air in the self-stratifying coating composition, it will consequently be the first in contact with either the heat source or the flame during the fire tests. According to these results, the silicone resin provides some thermal stability to the system, which may explain the higher time to ignition obtained during MLC experiments. Under elevated temperature, the silicone coating protects the

underlying substrate (and the epoxy resin) from decomposition and creates a barrier between the heat source and the substrate.

The influence of the incorporation of iron oxide particles on the thermal stability of the silicone resin has been investigated. It appears that specific interactions exist between the two components, but they do not stabilize or promote the formation of additional residue during the decomposition process in a significant way. Finally, it was shown that under thermo-oxidative conditions, the particles tend to destabilize the system at high temperature.

The higher thermal stability of both the silicone and the silicone/iron oxide systems compared to the substrate is in good agreement with the shift of the TTI observed during MLC test: indeed, the silicone system is directly exposed to the radiative heat source (at 50 kW/m²) during the test and tends to protect the underlying epoxy and PC. As a consequence, a reasonable assumption would be that silicone allows bringing higher thermal stability to the system and thus creates a barrier to degradation gases between the heat source and the underlying substrate. This would also be in accordance with the behavior of the coated system when exposed to a flame: the ignitability and combustibility of the material is slightly reduced thanks to the application of the film. In addition, the incorporation of iron oxide does not promote the formation of additional residue. Nevertheless, it highly reduces the combustibility and ignitability of the silicone when submitted to a flame. This effect is also noticeable under a radiative heat source as the TTI is shifted (particularly when 10 wt.% of IO are added to the system).

In the next sections, gas and condensed phases of the systems are further investigated in order to identify the nature of the interactions taking place between the silicone and the IO particles, and also to elucidate the mode of action of the expected protective barrier when the coating is exposed to a heat source or to a flame.

Gas phase analysis

In order to assess if changes in the gas phase occurs in presence of IO, the effective heat of combustion of the gases releases when the IO/silicone degrades was studied with PCFC whereas Py-GC/MS analyses were used to determine the composition of the gas phase. On

the other hand, TGA were also carried out at 60 °C/min to correlate information about the thermal degradation of the system at similar heating rate (data from PCFC and TG analysis were interpolated).

The pure silicone resin (100 % solid) and the crosslinked epoxy resin (without solvent) were first tested separately. The unfilled and filled films were tested thereafter. HRR curves and data are gathered in Figure 64 and Table 29.

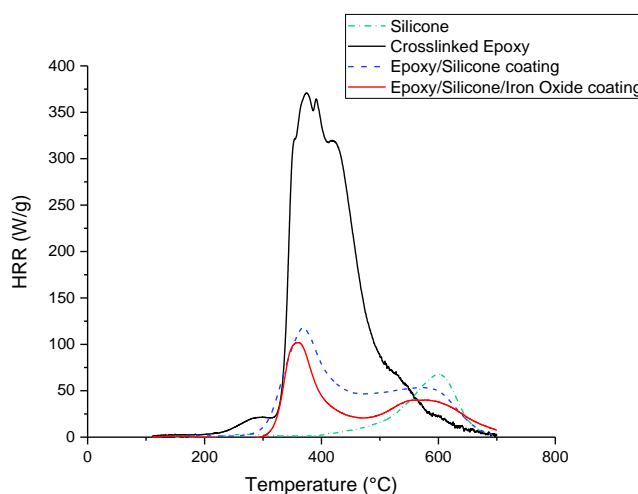


Figure 64. Heat release rates (W/g) in PCFC of silicone, crosslinked epoxy, epoxy/silicone and epoxy/silicone/IO coatings

Table 29. PCFC data of silicone, crosslinked epoxy, epoxy/silicone and epoxy/silicone/IO coatings

System	PCFC analyses					TGA (60 °C/min)	
	T _{onset} (°C)	T _{max} (°C)	pHRR (W/g)	THR (kJ/g)	Res. (%)	T _{max} (°C)	Res. (%)
Silicone	222-387	602	67.7	7.9	76	638	74
Cross. Epoxy	203	374	370.5	51.1	6	388	8
Epoxy/Silicone	275	370	117.2	20.6	39	408	40
Epoxy/Silicone /IO	302	360	101.6	14.2	48	380	52

The epoxy resin has a much higher pHRR (370.5 W/g) and THR (51.1 kJ/g) compared to the silicone resin. Its peak of heat release is centered at 374 °C and almost no residue is left (6 %),

which is in accordance with TG data. The silicone exhibits two peaks, the first one (almost negligible) starting at 222 °C, and the second one starting at 387 °C and centered at 602 °C. Its pHRR reaches 67.7 W/g and the THR 7.9 kJ/g which, once again, emphasizes its very low combustibility properties particularly compared to the epoxy resin. Blends of epoxy/silicone and epoxy/silicone/IO considerably reduce the heat release compared to the epoxy resin considered separately. Two peaks are observed, corresponding to the gases released by the epoxy (370 °C) and the silicone resins solely (602 °C). The incorporation of IO in the epoxy/silicone system reduces the Total Heat Release (by 31 % compared to the unfilled system) and slightly shifts the temperature at which the gases start to be released (+27 °C).

As the ferric oxide particles are located in the silicone layer after the formation of the solid film, it is assumed that it will interact with the silicone resin in a first place. Accordingly, the influence of the incorporation of particles in the silicone medium solely was investigated (Figure 65, Table 30).

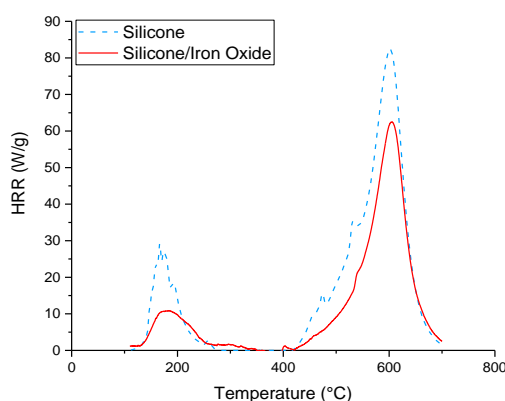


Figure 65. Heat release rate in PCFC of silicone and silicone/iron oxide systems

Table 30. PCFC data of silicone compared to the silicone/IO system

System	PCFC analyses					TGA (60 °C/min)	
	T _{onset} (°C)	T _{max} (°C)	pHRR (W/g)	THR (kJ/g)	Res. (%)	T _{max} °C	Res. (%)
Silicone	122-387	602	82.2	9.4	72	638	70
Silicone/IO	142-389	609	53.1 (-35 %)	6.0 (-36 %)	79 (+10 %)	640	77 (+10 %)

The HRR onset temperature is characterized by the release of the remaining solvent in the coatings. When incorporated in the silicone system, iron oxide decreases both the THR and the pHRR compared to the silicone resin solely by respectively 35 and 36 %. The residual mass obtained is in accordance with the TG data for both formulations and consequently supports the previous analyses which showed that the formation of a carbonaceous char is not promoted by the addition of the iron oxide particles.

The silicone resin releases gases when it degrades. Therefore, it is assumed that it will contribute to feed the flame during its decomposition. It is observed that for the silicone/IO composition, HRR and pHRR are both reduced. In addition, considering the mass introduced for the experiments, no mass transfer is expected. One reasonable assumption would be that interactions exist between some combustible decomposition products of the resins with iron oxide particles in the condensed phase, which therefore do not evolve in the gas phase. It is necessary at this step to investigate the nature of the gases evolved in the gas phase during combustion to draw reasonable conclusions and to complete the characterization.

Subsequently, Py-GC/MS experiments were carried out at 800 °C in order to identify the gases released during the combustion.

Py-GC/MS

Py-GC/MS is an efficient technique usually used in polymers science to identify the nature of polymers or of their degradation products.²⁰¹ It allows the separation of the decomposition products of the gas phase and thus the determination of their molecular structures. The aim is to identify the nature of the evolved products during the degradation of the neat silicone resin and the influence of the incorporation of ferric oxide. The chromatograms obtained are presented in Figure 66. Each numerated peak was analyzed in mass spectroscopy and peak attributions are presented in Table 31. Pyrogram obtained for neat silicone is first commented.

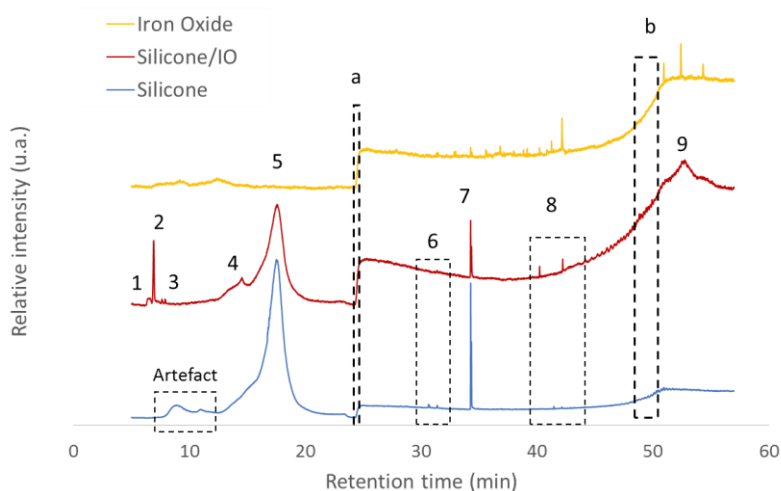


Figure 66. Comparison of silicone and silicone/IO film pyrograms obtained at 800 °C

Table 31. Identification of the decomposition products of silicone and silicone/IO systems at 800°C

	Retention time (min)	Mw (g/mol)	Silicone	Mw (g/mol)	Silicone + IO
1	6.5	-		106 116	m-xylene BuAc
2	6.9				
3	7.6				
4	14.5	78	Benzene		
5	17.5	78 106 39-91	Benzene Ethylbenzene Silicone oligomers		
6	30.6	91 128	Toluene Naphtalene		
7	34.2	154	Biphenyl		
8	40.2 51.8 52.7	43 - 277	Acetic acid, butyl ether, silicone oligomers, aromatic compounds and dihydroxy-terminated aromatic compounds		
9	51.8	98 279	Aromatic compounds		
a-b	24.5 50	18	Artefacts		

At 800 °C, the degradation products of the silicone resin are composed of low molecular weight compounds (mainly benzene, toluene and silicone oligomers), and higher molecular weight structures (bisphenyl, cyclic siloxanes and aromatic compounds). Cyclic siloxanes and hydroxy-terminated aromatic structures were characterized as the major silicone compounds in the degraded samples.

The first difference between the resin and the film containing iron oxide is due to the presence of remaining solvents (m-xylene and BuAc, peak 1 and 2) in the coating. This observation allows confirming the release of the remaining solvents observed at the beginning of MLC and TG experiments. Furthermore, changes in area ratio of the peak 6, 8 and 9 occurred in presence of the metal oxide. Py-GC/MS is only semi-quantitative, the approach is only to point out differences (increase or decrease). The structure related to the peak 6 corresponds to the release of aromatic compounds from the degradation of the silicone matrix. Lower amount of these aromatics compounds are released in the presence of ferric oxide. In addition, the two peaks exhibited in the silicone/IO chromatogram in the area 8 refer mainly to the release of linear fragments of carbonaceous chains; whereas mainly aromatic compounds are released in the case of the neat silicone at this particular elution time. Notably, hydroxy-terminated aromatic compounds are released. It is interesting to point out a study which demonstrated that the minor products of degradation of silicone compounds showed a wide array of silicon species²⁰², such as α,ω -dihydroxy polydimethylsiloxanes, (methylhydroxy) cyclic siloxanes, bis(cyclosiloxanyl)siloxane, dimethoxy polysiloxanes, di(ethoxymethyl) cyclic siloxanes and (methylpropyl) cyclic siloxanes, although additional studies would be needed to further investigate the complete molecular structure of the degradation products (for example by using hyphenated techniques as GC separation coupled to various MS detectors with the complementary use of Fourier-transform ion cyclotron resonance -FT-ICR/MS-). Last, but not the least, the peak 9, particularly intense in the presence of ferric oxide, refers to the release of aromatic compounds of high molecular weight. The formation of tridimensional network (Q-structure), as well as crosslinking network may be modify by the presence of ferric oxide, but not promoted as the residual mass belongs unchanged after decomposition.

It is interesting to notice a study performed by Gardelle et al. on the silicone 217 resin which showed similar results and established that for $T < 250$ °C, the oligomers of silicone released

are composed of T^2 and T^3 sites, and for $T > 250$ °C, the formation of tridimensional network composed of Q^3 and Q^4 structures are observed, corresponding to the released of the organic part of the silicone i.e. some aromatic compounds (Figure 67).²⁰³

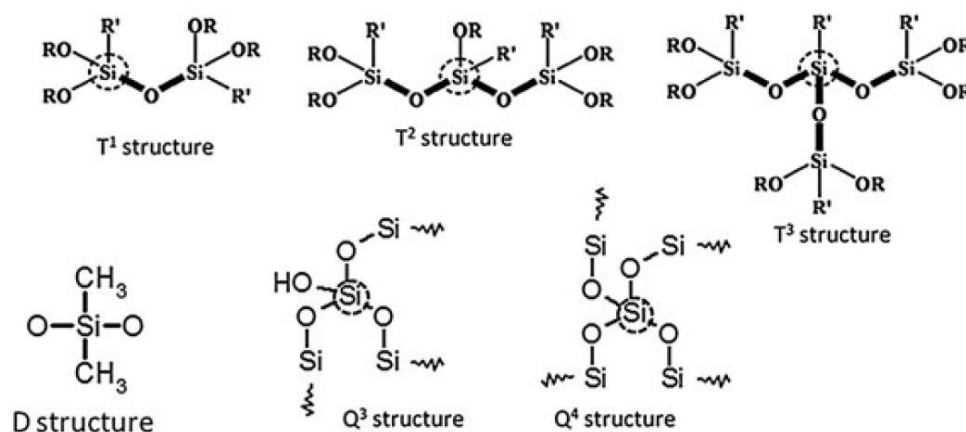


Figure 67. Schematics presentation of D, T^i and Q^i silicone structures²⁰³

Finally, the silicone matrix (which has hydroxy-terminals groups and a phenyl branched group) releases primarily cyclic aromatic compounds oligomers and minor amounts of linear products during its degradation. Similarly to hydroxyl-terminated PDMS, it may depolymerize through its chain-ends as well as by random decomposition, making the latter less stable against thermal degradation. The relative contribution of each process depends on the temperature (random scission predominates at high temperature) but also on pyrolysis conditions.²⁰⁴ These results confirmed previous studies published in the literature which have clearly demonstrated that cyclic siloxanes were the major silicon compounds formed during the PDMS thermal degradation under inter gas.^{202, 205} In addition, the degradation pathway of dimethyl siloxane polymers containing phenyl group is well established (Figure 68): benzene and complex mixtures of cyclic oligomers are released, which is in accordance with the experimental results.^{206, 207}

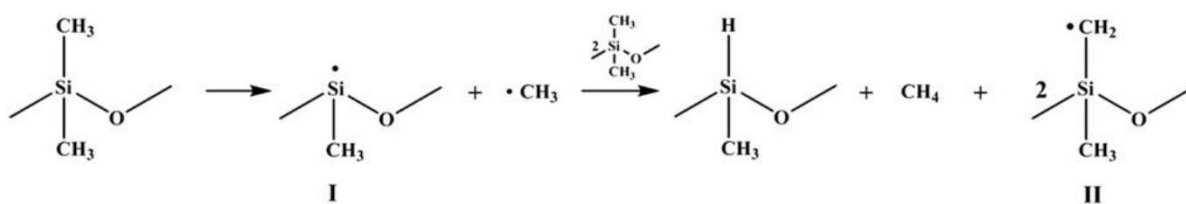


Figure 68. Proposed radical mechanism in silicone thermal degradation by Hamdani et al.²⁰⁴

Polysiloxanes which contain ionic, polar additives, as ferric oxide, even in small amounts are known to degrade by externally catalyzed mechanism. In contrast to unzipping and random scission, this mechanism involves hydrolytic cleavage of the Si–O backbone bonds, which initiate the degradation process. Like random scission, the extent of the externally catalyzed reaction depends on the nature of polymer end-groups.

Combining the TG analyses, cyclic siloxanes and aromatic compounds are characterized as the major silicone degradation compounds, representing 15 wt.% of the weight loss under inert conditions. Under thermo-oxidative conditions, an additional weight loss of 29 wt.% is observed: this can be explained by assuming that oxygen catalyzes the depolymerization of the silicone to volatile oligomers¹³², leading to a lower amount of residue compared to the results obtained in inert atmosphere. Interaction of oxygen with the degrading condensed phase depends on a complex competition between oxygen diffusion and solubility, on one hand, and degradation reaction and product evaporation on the other hand. Additional characterization such as TGA-FTIR under air would be needed to confirm those statements.

Finally, it appears that the presence of a low amount of ferric oxide (10 wt.%) modify the nature of the gas released during the decomposition of the system. Several assumptions emerged, such as a decreases of the viscosity of the melt during the degradation which could be responsible for the inhibition of dripping, and thus could explain the higher LOI value and UL-94 rating. However, rheology measurement (not presented in this manuscript) did not confirm this hypothesis. Since it was previously shown that the charring is not promoted by the addition of IO, one reasonable assumptions could be that modifications occur in the silica network formed rather than in the carbonaceous structure formed during the degradation of the silicone. The decrease of the flammability and combustibility of the silicone resin

evidenced with PCFC analyses in presence of IO and also during the fire tests may be related to the formation a more efficient barrier between the heat source or the flame and the substrate. In order to either confirm or deny these assumptions, the condensed phase is investigated in the following section.

Condensed phase analysis

Heat treatments and characterization of residues

TG experiments enable to define characteristic temperatures of degradation. Accordingly, heat treatments were performed at 300 °C in a tubular furnace and under a nitrogen flow on the silicone and the silicone/iron oxide systems (Figure 69).

From the numerical pictures, the formation of an expanded foamed structure exhibiting small cells is evidenced with the pure silicone resin. A recent paper established that the increase in expansion of a coating results in an insulative barrier in the case of this particular silicone resin, with low thermal conductivity (0.18 W/m.K) at 300 °C compared to the conductivity of the PC (0.24 W/m.K).^{208, 209}

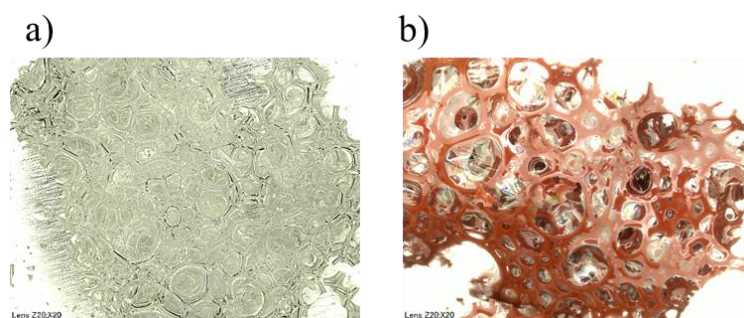


Figure 69. Numerical picture of a) Silicone, b) Silicone/IO (10 wt.%) residues after 3h at 300°C in a tubular furnace (N₂ atmosphere, Z20*20)

The incorporation of iron oxide allows the formation of more widely spaced cells compared to the pure silicone resin (Figure 69). In addition, the presence of open cells is evidenced compared to that of the neat resin. Although the formation of more widely spaced cells could be beneficial in the formation of a more efficient barrier, on the contrary, the presence of open cells could lead to the opposite effect. In addition, the thermal conductivity of iron oxide

is quite high compared to that of the silicone resin and the PC (0.58 W/m.K compared to 0.20 and 0.35 W/m.K for respectively the PC and the silicone resin at 25 °C). Accordingly, the hypotheses of the formation of a more insulative barrier can't be evidenced according to those data. Thermal conductivity measurements would be needed at this step to confirm the assumption. Finally, at 300 °C, no agglomeration of particles is detectable, nevertheless some areas appear lighter on the numerical pictures. The dispersion seems still uniform although the silicone has started to degrade.

In order to go deeper in the investigation of the mode of action in the condensed phase, residues obtained after ignition and after flame out at MLC tests were analyzed. X-ray analyses and FTIR characterizations were used in combination with the MLC shutter experiments for the investigation.

Analysis of residues obtained after ignition and combustion

The characterization of the condensed phase was performed on residues obtained when materials are exposed at 50 kW/m² with MLC. MLC shutter experiments were undertaken as soon as the coating ignites (at TTI, Figure 70), and on residues collected at the end of the experiments (Figure 72). The aim is to study residues representative of the coated PC at different steps of degradation. The final residues were collected after the flame out.

From the beginning of the experiments to the ignition, it can be observed that the substrate releases gases under the coating, which try to go through the film and are responsible for the delamination of the coating in some area (mainly around the edge of the plate). The apparition of small holes from which gases escape were noted in some case, also, bubbling is observed. Indeed, the polymer melts, and the viscosity remains apparently relatively high. This bubbling effect was noticed for both coated samples (unfilled and filled), and also for the uncoated PC.

On top of the PC, the coating darkens and retracts toward the middle of the plate. With the filled system, iron oxide is particularly noticeable in the "higher part" of the sample. Indeed, the melted PC starts to swell mainly in the middle of the plate, which causes the formation of hills where the coating remains. Finally, the ignition of the PC occurs in the areas free of coating (mainly around the edges of the plates).

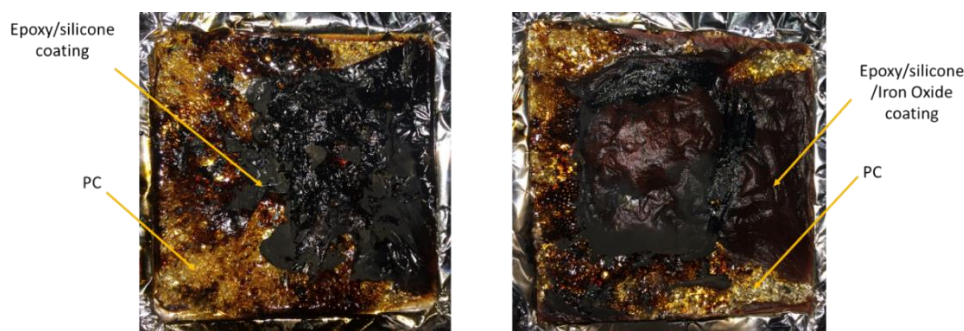


Figure 70. Pictures of the residues generated at TTI during MLC shutter experiments

During this experiment, sampling of the coating was performed in order to assess the integrity of the stratification at this step. From the chemical analyses (Figure 71 a), it is noticeable that the stratified structure of the unfilled system is undamaged at that time, with the silicone resin located at the top of the coating, and the epoxy resin at the bottom. The interlayer area seems also not impaired.

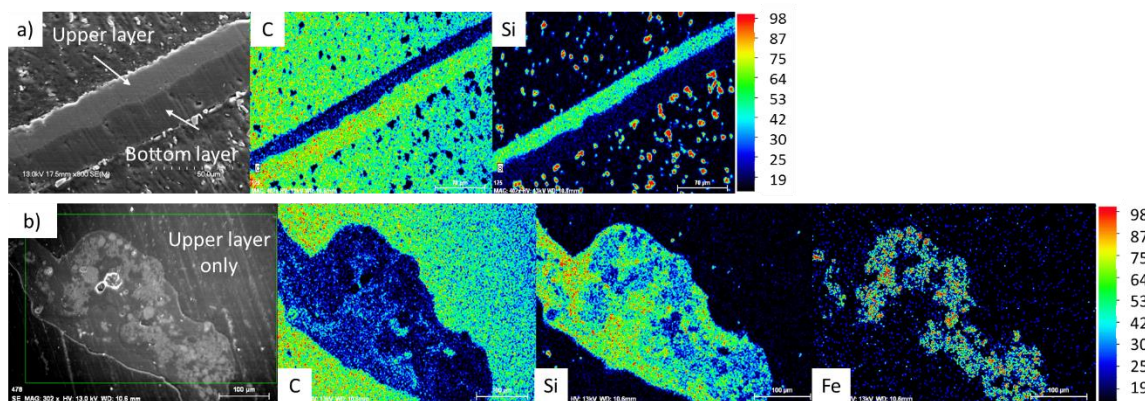


Figure 71. EPMA BSE micrographs of a cross-section of the a) epoxy/silicone and b) epoxy/silicone/iron oxide coating's residues during MLC shutter experiments, after TTI, with Carbon, Silicium and Iron X-ray detection

Contrary to the unfilled system, the boundary between the two resins in the IO containing system is affected at that stage of the experiment. On Figure 71 b, silicium and iron oxide are well noticeable however the carbon detection is very poor. The presence of the epoxy layer is not evidenced on the pictures: it is no longer cohesive with the silicone layer in this sampling.

In addition, the organic part of the silicone/IO medium has already begun to degrade at that time: bubbles coming from the release of gases are probably trapped inside the structure, and iron oxide particles aggregate at the surface of the silicone layer (Figure 69 b), which is exposed to the heat source.

After time of flameout, pictures of final residues show that almost no residual mass is left (Figure 72). Ashes from the PC remain, and also white and red residues. ATR-FTIR analyses were performed to identify the chemical composition of those residues: the white part corresponds to silica (1038 and 810 cm^{-1}) and silanol groups (3380 cm^{-1}), and a low amount of carbonaceous residues ($\text{C}=\text{C}$ stretching at 1640 cm^{-1} , which could refer to either the silicone, the epoxy or the substrate). Lastly, the red part refers mainly to a blend of silicone and iron oxide (Figure 73).

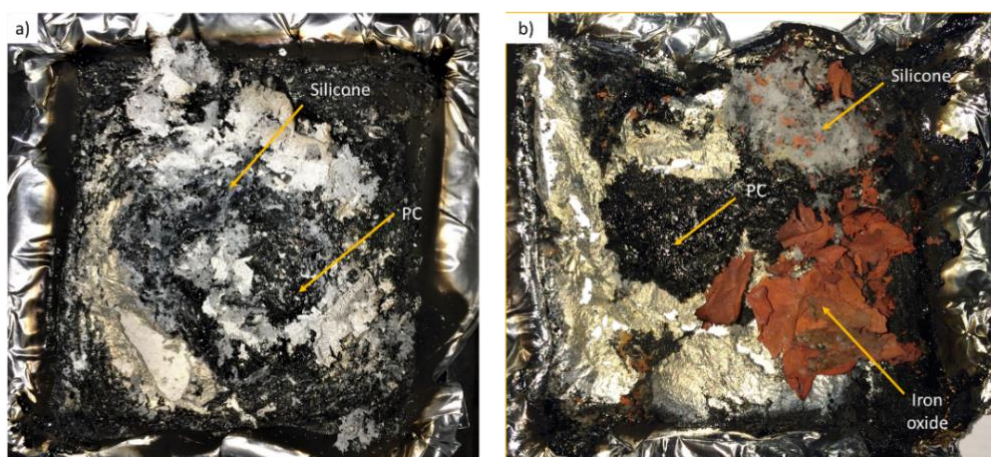


Figure 72. Pictures of the residues of epoxy/silicone and epoxy/silicone/iron oxide coatings applied on PC after MLC test

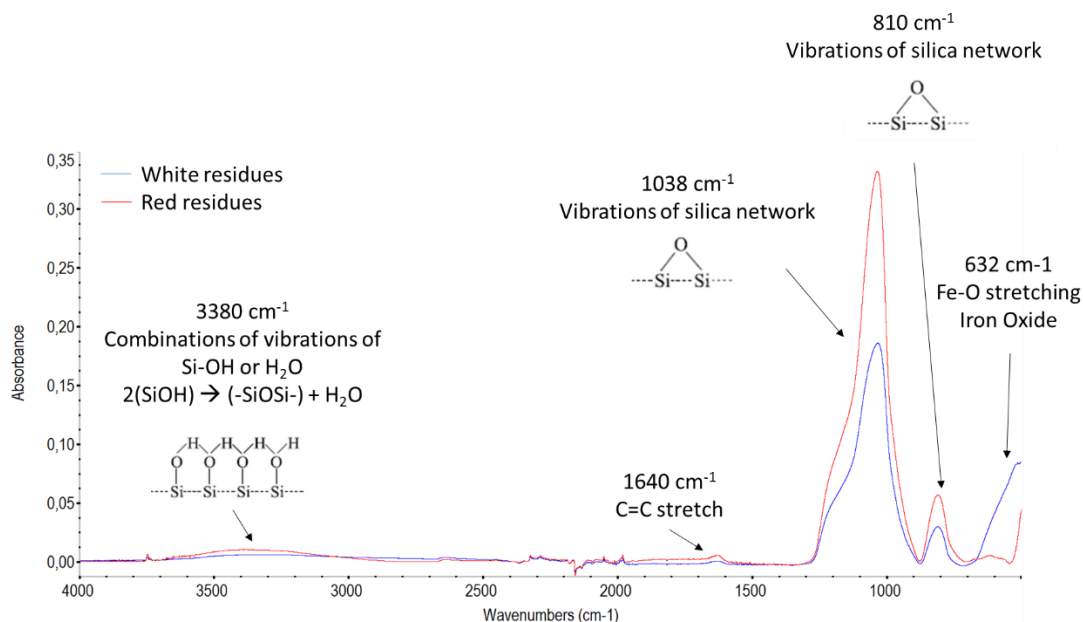


Figure 73. ATR-FTIR spectra of the white and red residues after MLC tests

From the results, it can be concluded that before the ignition, both the unfilled and filled coatings protect the PC from the heat source limiting the diffusion of flammable products from the degradation of PC. A delay of the time to ignition resulted: + 56 s and + 49 s respectively after the application of the unfilled and filled film. At that time, the unfilled coating is undamaged: the self-stratifying structure is still detectable by microscopic analyses and the interlayer adhesion remains perfectly homogeneous. When iron oxide is incorporated in the formulation, the adhesion quality between the two layers is impacted and they are no longer cohesive. At that time, the degradation of the systems has probably begun since the structure of the silicone layer is no longer homogeneous. Despite this, the same behaviors are noticeable between the two coated PCs in terms of fire properties. At TTI, and due to the high heat flux (50 kW/m^2), the PC melts under the coating and the formation of bubbles causes its delamination from the substrate. Once the gaseous products from the underlying substrate managed to escape, it causes the ignition of the sample in an area free of coating: the flame persists and propagates through the sample. The combustion becomes intense and the systems are progressively consumed. The silicone resin form a silica protective layer at the surface of the substrate, although this barrier is too thin to prevents from the combustion of

the PC. This resulted to a slightly reduced pHRR and THR, however the enhancement is not considerable. Nevertheless, the ignition is considerably delayed.

At this point, the formation of a thin protective barrier layer due to the presence of the silicone coating between the heat source and the substrate is evidenced. During MLC tests, the unfilled coating allows shifting the ignition time by 56 s and reducing both the pHRR and the THR by respectively 24 and 21 %. In the presence of IO particles, the formation of the silica network is also evidenced, and the barrier effect is maintained. Nevertheless, the application of the coating do not prevent from the degradation of the PC: it is only delayed. Also, it is noteworthy to notice that the interlayer bonding between the epoxy and the silicone layer is not as strong as in the unfilled system: the epoxy layer is dissociated from the silicone layer at the TTI. This observation rather corroborates the hypothesis made at the beginning of this chapter postulating that the IO particles interact mostly in the silicone phase (and do not influence the decomposition pathway of the epoxy resin), at least at the beginning of the decomposition process.

Finally, the formation of the barrier layer which is formed at the surface of the polycarbonate can be related to the inhibition of dripping and flame spread which is observed when the system is submitted to a flame. Accordingly, the formation of the carbonaceous layer which was evidenced during LOI and UL-94 tests would be related to the charring of the underlying epoxy and PC (which are both charring polymers): the silicone layers covers the underlying materials by forming a stable mineral structure which prevents from the dripping and flame spread.

Conclusion condensed phase analysis

The behavior of the condensed phase during combustion of the silicone and silicone/IO systems was investigated in order to characterize the formation of the protective barrier when the material burns and to study the interactions occurring between the degraded components. The condensed phase was simulated using MLC shutter experiments: residues generated at two steps of degradation (after ignition and flame out) were analyzed to observe the changes occurring when the material burns.

The application of the coating onto the polycarbonate substrate allows covering its entire surface and creating a protective barrier when submitted to a radiative heat flux or a flame. The analysis of the condensed phase shows that the ignition mainly takes place in the area where the coating has delaminated from the substrate at MLC test, due to the release of flammable gaseous products. The materials used to prepare the coating are thermally more stable than the PC itself, which makes the system more efficient in terms of fire properties resulting in a delay in the ignition time. Finally, the coating allows limiting the gas transfers from the PC to the heat source by forming a protective layer at the beginning of its degradation. The formation of such layer is promoted by the incorporation of ferric oxide. Nevertheless, the barrier formed is not thick enough to prevent the degradation of the PC and if the gases from the degradation of PC can diffuse, their concentration increase leading to the ignition of the sample. Last, but not the least, the interlayer boundary between the two phases is more cohesive without fillers and remains undamaged at TTI. On the contrary, the epoxy layer is dissociated from the topcoat layer at that time. Nevertheless, it did not influence the fire efficiency of the barrier layer formed.

The influence of iron oxide is particularly evidenced when the coated PC is submitted to a flame: V0 rating is achieved and no dripping was observed on the contrary to the raw PC and to the unfilled coated system. Self-extinguishment occurred as soon as the flame was removed from the sample. On the contrary to the assumptions made previously, the particles do not promote the formation of additional carbonaceous char. The carbonaceous structure evidenced during LOI and UL-94 fire tests is most likely to be related to the charring of the underlying epoxy and PC.

IV-2-1-4 Conclusion

In this section, the efficiency of applying a silicone based coating to fire retard polycarbonate and the modification of the behaviors of the system by the addition of iron oxide has been investigated.

On the one hand, the efficiency of the coatings to fire protect the PC matrix has been tested under two fire scenarios, i.e. under a radiative heat source or a flame, using MLC, UL-94 and LOI fire tests. From those results, the best improvements in terms of LOI are obtained with the system containing the highest amount of fillers (10 %PVC). However, adhesion of the coating is slightly impacted (4B compared to 5B with the unfilled system and with the film containing a lower amount of fillers). 2.5 and 5 %PVC thus represent the best compromise: good fire performances are obtained at LOI and UL-94 tests meanwhile the best adhesion rating is maintained. Vertical burning test shows significant enhancement in terms of fire performances compared to the unfilled system (no dripping, short combustion time and flame spread) whereas mass loss results are similar (or even slightly worse) compared with the unfilled system at 50 kW/m².

In order to assess the understanding of the mode of action of both the coating and the IO particles, the condensed and the gas phase of the materials during combustion and degradation have been analyzed. Preliminary thermogravimetric analyses demonstrated that the silicone resin, which is directly in contact with the heat source or with the flame, is thermally more stable than the substrate and the epoxy base-coat layer, under both thermo-oxidative and inert conditions. In addition, the epoxy/silicone coating exhibits a significantly reduced rate of heat release compared to the epoxy resin considered separately. Accordingly, the formation of a barrier layer when the epoxy/silicone coating is applied on PC is noted, particularly at MLC test during which a delay of the ignition (+56 s) was evidenced.

The addition of ferric oxide does not influence the thermal stability of the silicone polymer in a significant way, both under inert and thermo-oxidative conditions. Contrary to our expectations, the difference due to the addition of the iron oxide in the formulation when the coating is exposed to a radiative heat flux (MLC) is not significant: the behaviors of the epoxy/silicone/Fe₂O₃ film are rather the same compared to the unfilled system, except the TTI slightly which slightly increases in presence of Fe₂O₃. At the opposite, in the presence of a flame, the enhancements are considerable: dripping is avoided; lower combustion time and flame spread are noted. A condensed phase mechanisms may be relied as contributing to the action of ferric particles, although some changes in the gas was also noted. In particular, differences in ratio of aromatic / silicone based monomer is observed in presence of Fe₂O₃. It

could thus be expected that the presence of IO modified the silicone network resulting in a modification of the ratio of the competitive reaction occurring when the silicone degrades (evolution of silicone fragment vs. crosslinking). This result is confirmed if we consider PCFC measurement since the heat evolved when the silicone resin degrades is lower in presence of Fe_2O_3 (decrease of around 30%). Finally, it can also be proposed that the presence of iron oxide improves the protective properties of the barrier layer between the heat source or the flame and the underlying materials (the base layer and the substrate). Two hypothesis can be drawn: either the mechanical properties of this layer, mostly mineral, are reinforced by the presence of the particles or the presence of Fe_2O_3 modify the structure of the silicon network. Nonetheless further investigation are needed at this step to confirm the assumption.

IV-2-3 Proposed mode of action of the epoxy/silicone coating

In order to sum up the results obtained, a schematic representation of the mode of action of the coated PCs compared to the raw PC when submitted to a radiative heat source, i.e. MLC test, under a flux of 50 kW/m^2 ($794 \text{ }^\circ\text{C}$) is proposed (Figure 74).

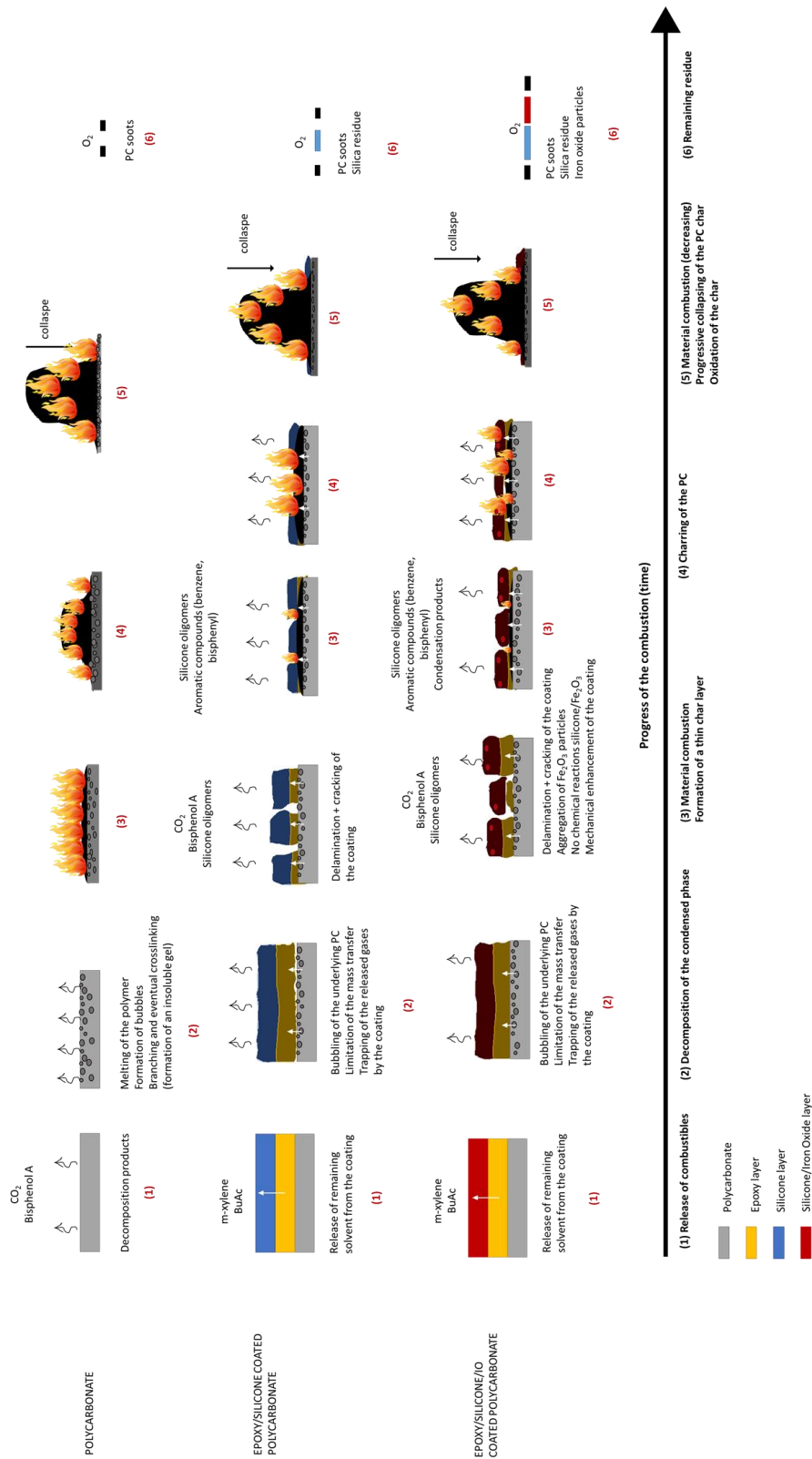


Figure 74. Schematic representation of the mode of action of the PC coated with the epoxy/silicone and epoxy/silicone/iron oxide systems

IV-3 Impact of ageing on film properties and fire performances of self-stratifying coatings applied on PC

One objective of this study was to figure out the impact of ageing on the properties of the self-stratified coatings by submitting them to accelerated ageing tests under various constraints. The effects of the temperature, relative humidity and ultra-violet (UV) light were investigated. Samples were submitted for 8 weeks to two different kinds of ageing: (i) temperature and relative humidity (T/RH), (ii) temperature and UV (T/UV). The FR properties of the systems after ageing were evaluated every two weeks using UL-94 and LOI tests, and MLC experiments were carried out after 8 weeks of ageing. Results were then compared to the non-aged specimens.

The investigation of the weather durability of the polycarbonate substrate is investigated in a first part. Then, the ageing of the unfilled silicone-based system is discussed in a second part. Similarly, the study of the systems containing ferric oxide is carried out. The ageing of the substrate is taken from the published article entitled: *One pot flame retardant and weathering resistant coatings for plastics: a novel approach*, *RSC Advance*, 2017, 7, 40682. This paper also gathers the influence of the ageing on the epoxy/fluoropolymer system (not presented in this manuscript).

IV-3-1 Ageing of polycarbonate

Ageing of polycarbonate has been widely studied during the past three decades as the yellowing and the decrease in physical properties that appears upon natural weathering limits its use. It was shown that the degradation mechanism depends on the irradiation wavelengths.^{210, 211} For wavelengths below 300 nm, the discoloration was attributed to the photo-Fries rearrangement, and for irradiation with longer wavelengths (310-350 nm), impurities and defects in the polymer chain are responsible for the yellowing.^{212, 213} Since solar radiations are longer than 300 nm, the photo-Fries pathway is insignificant for outdoor

exposures. It was also demonstrated that photoproducts which absorb the UV-visible light are formed at the surface of the polymer. Such species decrease the penetration of long wavelengths ($\lambda \geq 310$ nm) in irradiated films.²¹⁴

As expected, according to the literature and to the UV lamps wavelength chosen for the test (340 nm), PC plates yellow even after 2 weeks of exposure. Under T/RH conditions, no change in the visual appearance is noticeable, even after 8 weeks of ageing (Figure 75, Table 32).

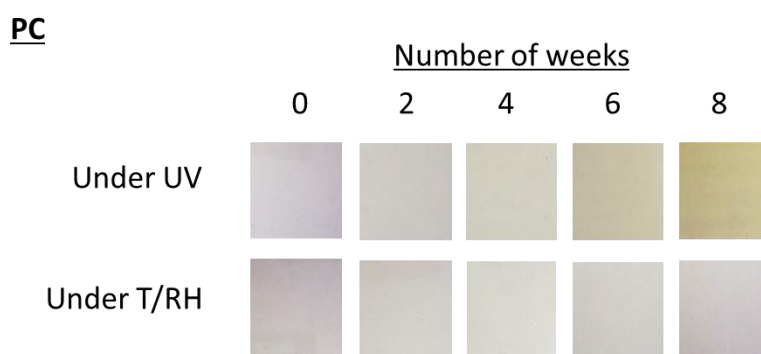


Figure 75. Visual appearance of the PC plates after UV and T/RH exposure

Table 32. L*a*b*, adhesion, UL-94 rating and LOI values obtained after weathering tests of PC under UV and T/RH conditions

Polycarbonate					
Under UV					
Time (week)	0	2	4	6	8
L*	87.5	87.4	87.7	85.0	87.8
a*	-0.8	-0.7	-1.4	-2.2	-2.7
b*	-2.8	-1.3	2.2	8.1	11.9
ΔE^*	-	1.6	5.1	11.3	15.1
UL-94	NC				
LOI (vol.%)	28	28	27	26	25
Under T/RH					
Time (week)	0	2	4	6	8
L*	87.5	87.3	87.8	87.6	87.8
a*	-0.8	-0.0	-0.1	-0.1	-0.1
b*	-2.8	-3.8	-4.0	-3.8	-3.9
ΔE^*	-	1.3	1.4	1.2	1.4
UL-94	NC				
LOI (vol.%)	28	28	27	26	26

Fire performances remain constant after 2 weeks of exposure to both weathering conditions at UL-94 and LOI. However, they start to decrease after 4 weeks of exposure: a loss of 1 vol.% in the LOI value is obtained every two weeks. Considering the UL-94 test, PC remains NC. However, a difference for the flaming time of around 10 seconds is observed between UV and R/TH aged samples (UV aged samples being the worst). The difference of burning time between the non-aged and T/RH aged samples belongs inferior to 10 s for all ageing duration, and inferior to 20 seconds with the non-aged samples. The higher degradation rate of PC considering UV ageing is also observed with the LOI values: 25 vol.% is registered after 8 weeks of exposure under UV conditions versus 26 vol.% under T/RH. Virgin PC is thus more affected by UV ageing compared to the T/RH conditions. Finally, a slight reduction of the pHRR is observed for the aged samples at MLC (Figure 76, Table 33). Nevertheless the values remain close to the range of the experimental error of the apparatus (respectively -15 and -13 % after UV and T/RH ageing).

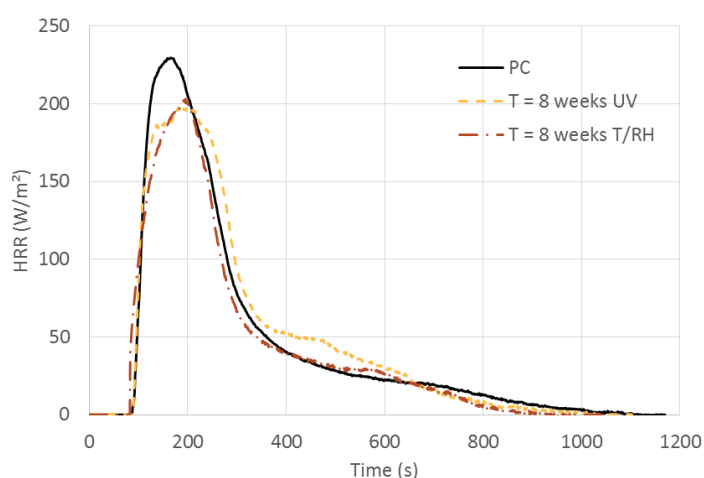


Figure 76. MLC curves of the polycarbonate before ageing, and after 8 weeks of ageing under UV and T/RH conditions

Table 33. MLC data of the polycarbonate before ageing, and after 8 weeks of ageing under UV and T/RH conditions

Polycarbonate			
Ageing (8 weeks)	No ageing	UV	T/RH
TTI (s)	92	90	83
TFO (s)	1077	915	936
pHRR (kW/m²)	231	197 (-15 %)	202 (-13 %)
THR (MJ/m²)	52	53 (+2 %)	46 (-12 %)

On the first hand, the ageing of the PC coated with the unfilled epoxy/silicone based coating was evaluated. The influence of the incorporation of iron oxide particles in the systems is studied in a second part.

IV-3-2 Ageing of polycarbonate coated with unfilled epoxy-based self-stratifying system

Under UV

Results show an evolution in color of the plates coated with the epoxy/silicone blend during ageing under UV (Table 34, Figure 77). Indeed, ΔE^* between the unaged and aged sample reaches 25.9 after 8 weeks of exposure. L^* is constant and a^* varies from -0.4 to -2.7. This change means that there is a slight color change which tends toward green after ageing. Finally, the major change is registered with the b^* value. It increases from -3.9 to 21.8 after 8 weeks of ageing: the color of the coated samples tends to yellow over ageing, which proves that the coating does not prevent the yellowing of the samples.

Table 34. L*a*b*, adhesion, UL-94 and LOI value of the aged epoxy/silicone self-stratifying system applied on PC under UV and T/RH conditions

Coated PC with epoxy/silicone system					
Under UV					
Time (week)	0	2	4	6	8
L*	85.6	85.9	85.8	86.3	84.4
a*	-0.4	-2.0	-2.4	-2.4	-2.7
b*	-3.9	13.5	14.7	14.4	21.8
ΔE*	-	17.5	18.7	18.4	25.9
Adhesion	5B				
UL-94	V0				
LOI (vol.%)	28				
Under T/RH					
Time (week)	0	2	4	6	8
L*	85.6	89.2	88.3	88.6	88.4
a*	-0.4	-0.1	-0.0	-0.2	-0.1
b*	-3.9	-4.5	-3.7	-3.5	-3.4
ΔE*	-	3.6	2.7	3.0	2.8
Adhesion	5B				
UL-94	V0				
LOI (vol.%)	28				

Epoxy/Silicone coated PC

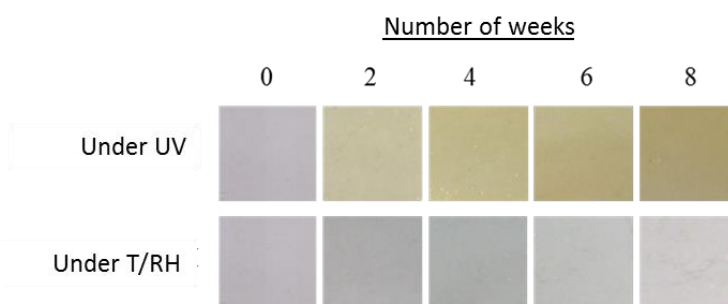


Figure 77. Visual appearance of the PC and coated PC with the epoxy/silicone mixture after UV and T/RH exposure

The comparison with the data of raw PC shows that yellowing appears faster (from the first two weeks of ageing) and is even more pronounced when a coating is applied. This yellowing

could be reasonably attributed to the epoxy resin which is well known for having poor resistance to UV.²¹⁵ Indeed, few hours under UV exposure lead to the chalking and yellowing of the epoxy resin due to photo-degradation (similar to that of PC). Moreover, neither blistering nor removal of paint are noticed during the test: the best rating (5B) is still obtained after 8 weeks of weathering. No change in the fire retardant properties at LOI and UL-94 tests compared to the non-aged samples is observed whatever the weathering conditions.

Moreover, no particular modification in the fire behavior of the materials was registered during the three fire tests. A slight shift of the TTI toward lower values is observed at MLC test: the change of the properties of the epoxy may be responsible for this shift and affects somehow the silicone resin as is it well known that silicones are highly stable under UV rays in the regions 300-400 nm.²¹⁶

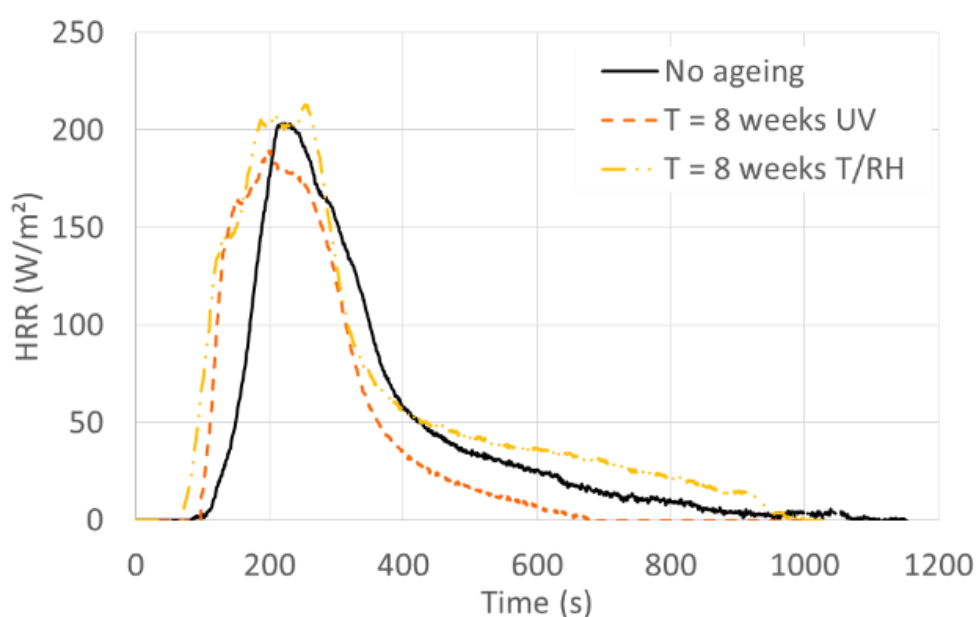


Figure 78. MLC curves of the coated PC with the epoxy/silicone system before ageing, and after 8 weeks of ageing under UV and T/RH conditions

Table 35. MLC data of the coated PC with the epoxy/silicone system before ageing, and after 8 weeks of ageing under UV and T/RH conditions

Coated PC with Epoxy/Silicone system			
Ageing (8 weeks)	No ageing	UV	T/RH
TTI (s)	148 ± 7	98	72
TFO (s)	903 ± 6	689	852
pHRR (kW/m ²)	176 ± 4	189 (+7 %)	212 (+20 %)
THR (MJ/m ²)	41 ± 3	41 (+0 %)	61 (+50 %)

Under T/RH

PC samples coated with the unfilled self-stratified systems lead to very promising results after 8 weeks of exposure under T/RH conditions: color changes are negligible ($\Delta E^* < 3.6$), no change neither in the visual appearance (blistering, cracks...) nor in the adhesion or the fire retardant performances (LOI, UL-94) occurs (Table 34, Figure 77). However, it seems that the ignition of the epoxy/silicone coated PC after 8 weeks of ageing is favored compared to the non-aged sample at the MLC test (Table 35, Figure 80). In addition, both THR and pHRR are increased. Ageing of silicone resins under humidity conditions have already demonstrated some changes in the properties, mainly resulting from the decomposition of the chemical bonding between polysiloxane backbones and methyl groups. This hydrolysis leads to the formation of polar siloxanols, which can also condense to rigid crosslinked structures.^{217, 218} In addition, it turned out that water molecules from humidified gases can accelerate ageing, leading to a loss of properties.²¹⁹

Similarly, the influence of the incorporation of ferric oxide in the silicone-based coated PCs was investigated.

IV-3-3 Ageing of polycarbonate coated with the epoxy-based self-stratified FR system after incorporation of iron oxide particles

Both under UV and T/RH conditions, no change in the visual appearance ($\Delta E^* < 3.7$) nor in the adhesion (5B rating remains constant for all samples) are noticeable (Table 36, Figure 79): the coating even stops the UV rays from reaching the substrate (Table 37). Indeed, by comparing the b^* value of the front (where the coating is applied) and back side of the plate (free of coating), no yellowing is registered. Additionally, microscopic observations of the polished cross-section of the plate confirmed the postulate. Lastly, no modification of the fire behavior in terms of UL-94 and LOI tests (Table 38) is observed: the excellent fire properties are influenced neither by UV rays, nor by the temperature and the humidity.

Table 36. $L^*a^*b^*$, adhesion, UL-94 and LOI logged during weathering test of PC under UV and T/RH conditions

Coated PC with epoxy/silicone/ Fe_2O_3 system					
Under UV					
Time (week)	0	2	4	6	8
L^*	36.5	38.3	36.3	32.8	35.2
a^*	19.1	17.5	19.0	19.3	17.1
b^*	11.7	11.5	12.2	12.3	12.1
ΔE^*	-	2.4	0.5	3.7	2.3
Adhesion	5B				
UL-94	V0				
LOI (vol.%)	33				
Under T/RH					
Time (week)	0	2	4	6	8
L^*	36.5	36.1	35.8	35.7	36.1
a^*	19.1	18.5	18.8	19.9	19.0
b^*	11.7	11.7	11.5	12.2	11.6
ΔE^*	-	0.7	0.8	1.2	0.4
Adhesion	5B				
UL-94	V0				
LOI (vol.%)	33				

Epoxy/Silicone/Iron Oxide coated PC

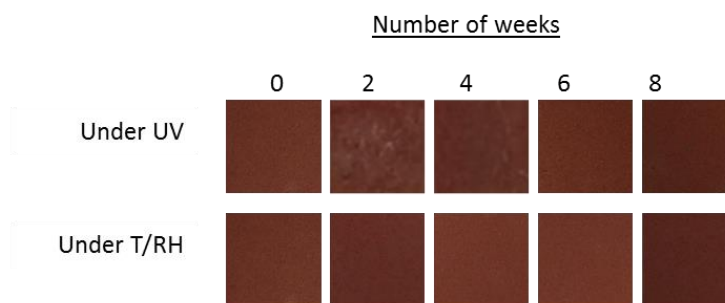


Figure 79. Visual appearance of the epoxy/silicone/Fe₂O₃ coated plates after UV and T/RH exposure

Table 37. L*a*b* values logged of the PC, and of the front and back side of the PC plate after 8 weeks of ageing under UV conditions

Coated PC with Epoxy/Silicone/Iron Oxide system			
	PC	Coating side	Back side
L*	37.9	39.5	38.2
a*	28.1	29.8	29.1
b*	19.3	23.4	22.3

During MLC experiments, the TTI for the epoxy/silicone/IO coated PC is slightly shortened after ageing, nevertheless, it does not impact neither the pHRR nor the THR in a significant way (the results are in the range of experimental error). The addition of iron oxide particles allows somehow stabilizing the silicone resin, in addition to prevent from the yellowing of the coating. Particularly, it permits to prevent from reducing the FR properties of the system under T/RH conditions. One assumption could be the formation of chemical bonding with the inorganic material which would protect from the oxidative demethylation. Although further investigation are required to confirm the postulate.

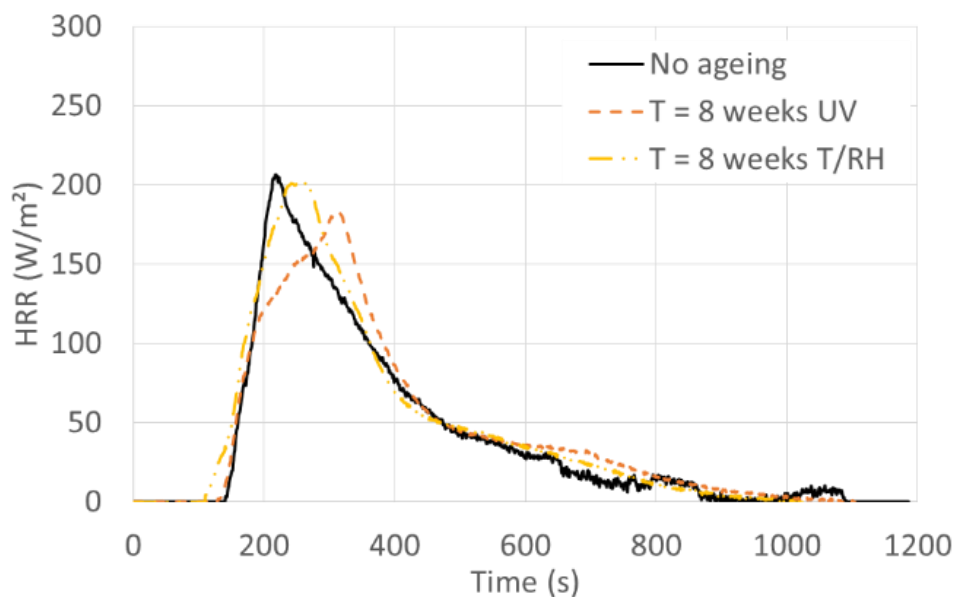


Figure 80. MLC curves of the coated PC with the epoxy/silicone/IO system before ageing, and after 8 weeks of ageing under UV and T/RH conditions

Table 38. MLC data of the coated PC with the epoxy/silicone/IO system before ageing, and after 8 weeks of ageing under UV and T/RH conditions

Coated PC with Epoxy/Silicone/Iron Oxide system			
Ageing (8 weeks)	No ageing	UV	T/RH
TTI (s)	141 ± 20	127	110
TFO (s)	1003 ± 33	1034	934
pHRR (kW/m²)	205 ± 20	181 (-12 %)	200 (-2 %)
THR (MJ/m²)	47 ± 2	50 (+6 %)	51 (+9 %)

IV-3-4 Conclusion

To conclude, T/RH weathering tests are very conclusive: minor effects on the adhesion and on the aesthetic aspect of the films are registered after 8 weeks of exposure. Both the unfilled and filled silicone-based coatings prevent from the decrease of the fireproofing performances registered in the presence of a flame after the ageing of the raw PC. The only issues encountered were noted during MLC measurements: in presence of the epoxy/silicone

coating, the TTI is shortened and the THR is raised indicating some reduction of the FR properties of the coating. Although, the incorporation of ferric particles solves those losses of performances.

Under UV, the properties of the systems (adhesion and FR performances after UL-94 and LOI tests) are also maintained. However, the unfilled coatings do not prevent from the infiltration of the UV rays: the yellowing is even more pronounced when the PC is coated with the epoxy-based paint. This phenomenon is due to the presence of the epoxy resin which also yellowed under UV. The topcoat layer (silicone-based) consequently does not prevent from the UV infiltration to the underlying materials. Nevertheless, the incorporation of ferric oxide allows to solve this issue: no yellowing of the system is registered after 8 weeks of exposure.

IV-4 Conclusion

In this chapter, the fire behaviors and ageing resistance of surface treated polycarbonate by self-stratifying compositions were investigated. From the results obtained in the third chapter, one coating composition was carefully selected: a silicone-based coating diluted in a blend of BuAc: xylene. In this chapter, the emphasis was placed on the influence of the addition of a particular metal oxide, i.e. red iron oxide, on both the FR and ageing properties.

It was first shown that incorporation of iron oxide in silicone-based coating significantly improves the fire performances of the coated PC by forming a protective layer at the surface of the substrate which inhibits completely the occurrence of dripping, decreases the flame spread and the combustibility of the material in the presence of a flame. Under radiative heat flux, the enhancement of the fire performances were not as significant as in the first fire scenario investigated, nevertheless some modifications of the behaviors were registered during combustion.

In the case of the silicone-based coating, the thermal stability of the PC coated system is significantly enhanced thanks to the silicone resin which is greatly stable, even at high

temperature, releases low heat of combustion and contributes to the formation of a barrier layer which protects the substrate from the heat source or the flame. The incorporation of iron oxide particle does not influence significantly the thermal stability of the film both under pyrolytic and thermo-oxidative conditions, although it permits to decrease the heat release during combustion: the most probable assumptions would be that the particles modify the structure of the silica network formed which allow enhancing the barrier effect of the silicone-based layer. It is noteworthy to notice that the formation of additional carbonaceous char is not promoted by the addition of ferric oxide, although it is very likely that additional mechanical properties are brought to the system which consequently strengthened the barrier layer formed. It therefore results a delay in the ignition, the inhibition of the flame spread and a drastic reduction of the combustibility of the coating when submitted to a flame. Under a radiative heat flux (50 kW/m^2), it was found that the thermoplastic film was responsible for the enhancement of the FR properties obtained after the application of the film by delaying the ignition and reducing the heat released combustion. The incorporation of ferric oxide did not bring additional enhancements in this fire scenario.

Last, but not least, a great stability over ageing under T/RH is obtained when both the unfilled and filled coatings are applied on PC and submitted to vertical fire tests: the VO rating is maintained as well as the LOI value of each system, on the contrary to the PC with which FR performances decrease after 4 weeks ageing, both under UV and T/RH conditions. Under UV, the yellowing of the non-filled coated PCs is however accelerated compared to that of raw PC. Nevertheless, this issue is solved by the addition of ferric oxide particles which are well known for they high stability under UVA exposure.

To conclude, the use of metal oxide as only and sufficient flame retardant is a very specific exception. As well, these systems can only be used where the color of the product is not of importance. Results suggests that even with thermally stable fillers, other factors have a role in influencing fire retardancy, such as particle geometry, surface chemistry and possible thermal conductivity which would need a particular attention.

This novel approach represents a proof of concept to flame retard durably polycarbonate in a low-cost and fast manner, simultaneously maintaining the mechanical properties of PC. Efforts

have now to be put on the development of more transparent self-stratifying coatings with similar flame retardant as well as weathering resistant properties. Finally, it is noteworthy that the incorporation of iron oxide leads to much better FR performances with only 10 wt.% incorporated in the coating's formulation compared to an unfilled system.

This chapter provided a better understanding and analysis of the behaviors of surface-treated PCs by self-stratifying coatings when the systems were submitted to different fire tests. It is a solid basis to keep developing fire retardant self-stratifying coatings not only for polycarbonate substrates. Nonetheless, some part of the understanding of the mechanism of action remain unclear or were indirectly demonstrated. In addition, some assumptions need to be confirmed. In this context, outlook will be proposed at the end of this work.

General conclusion

This work aimed at demonstrating the feasibility to design self-stratifying coatings on polycarbonate substrate for fire retardant purpose. Literature review showed that the self-layering concept can generate many advantages for polymer coatings including costs reduction (mainly by decreasing the amount of solvent used and processing time), enhancement of coating's properties, i.e. (i) mechanical properties, partly by including a successful balance between hardness and flexibility and by eliminating internal stresses, (ii) adhesion and adhesion durability, thereby contributing to corrosion protection, (ii) chemical resistance and durability, etc. Finally, this concept promotes the eco-development of products by limiting the release of VOCs during the processing. It was shown that this approach can be used for the development of new original coatings due to its versatility depending on the nature of the materials chosen. In this context, a screening of commercially available resins and solvents was primarily performed to select the best candidates in order to produce self-layered compositions designable for fire retardant matter.

On the one hand, the goal was to prove the applicability of the concept on polycarbonate, by developing effective layered films with excellent adhesion and weather durability. The screening generated promising results mainly with two resin combinations diluted in a blend of BuAc: xylene (1: 1): epoxy/silicone and epoxy/fluoropolymer. Moreover, the study revealed that the theoretical model used to predict the stratification behaviors of a binary system needs to be carefully considered as a high number of parameters are not taken into account in the calculations. Also, the processing conditions are dependent on the choice of the resins and have to be properly set up. Adhesion and fillers dispersion were the main parameters influenced by the choice of fillers and solvent. Finally, such separation is most likely to proceed via a spinodal mechanism, as a fast change of the parameters of state occurs (due to evaporation of highly volatile solvents). The systems developed have a unique composition and structure resulting from spontaneous phase separation, which promotes the effect of the thermoplastic resin compared to the brittle epoxy matrix.

On the other hand, the aim was to find particular additives which allow improving the fireproof properties of polycarbonate by the application of a coating without influencing, or not significantly, the self-stratification of the binary blends during the formation of the solid film. In this context, iron oxide particles were found to be the best candidate (among calcium carbonate and two phosphorus based liquid fillers) when incorporated at 10 wt.% in the

thermosetting medium. Primarily, the influence of the additive on the thermal degradation of the films was investigated and elucidated. Although ferric oxide does not influence the thermal stability of the coating, it was found that the particles allow inhibiting completely the occurrence of dripping and flame spread by reducing the combustibility and the ignitability of the systems when submitted to a flame. A more efficient barrier layer is formed compared to the unfilled coatings. Under a radiative heat flux, the silicone resin (and not the ferric particles) brings the additional FR performances noted with the coated PCs compared to that of raw PC. Finally, very high durability of the heterogeneous structures has been proven.

The formation of an efficient barrier layer in presence of the particles was found to be the main mode of action of the iron oxide filler: mass transfers were especially decreased, thus limiting the feeding of the flame. The detailed mode of action has not been ascertained and a number of hypotheses may be considered, a beneficial effect on the silica residue morphology being our most likely explanation.

This work is the first study highlighting the potential of self-stratifying compositions to produce fire retardant coatings. The potential of such coating is very wide and can be applied for a variety of coatings composition. In summary, this work confirms that self-stratifying fire retardant coatings may be valorized as flame retardant surface treatments for polymeric substrates and offers the possibility of developing more sustainable and efficient coatings (Figure 81). As a conclusion, this work can be used as basis for further work, aiming at the valorization of self-stratifying coatings for the development of new original flame retardant systems.

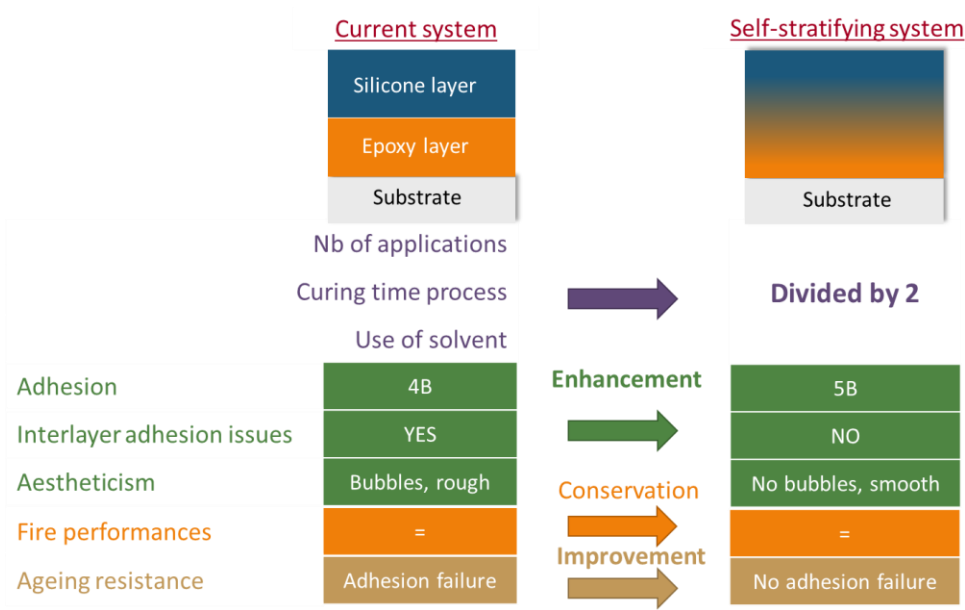


Figure 81. Comparison between the current system and the self-stratifying system to fire retard PC by surface treatment

Outlooks

Considering the multidisciplinary nature of this PhD work, many outlooks emerge.

Although physical properties measurements were not within the scope of our project, further evaluation could be helpful regarding the applications of the developed coatings. In fact, knowing the impact of fillers on both the layering process and the physico-chemical properties of the coating, and on the mechanism of degradation when submitted to a flame or a heat source, interesting outlooks would be to work on the impact of the morphology, the size, the surface properties and the dispersion state of the filler. The first step would be related to the elucidation of the complete mode of action of the iron oxide grade used for the study, as some aspects need to be studied further. To do so, it would be interesting to test the coatings developed on a non-charring polymeric substrate (polypropylene for example) to ensure the formation of the carbonaceous structure observed during LOI and UL-94 tests is related to the charring of the substrate and the epoxy layer. Then, different additional grades of iron oxide could be of interest to compare the results obtained: nano-sized and surface treated particles for example.²²⁰ Moreover, a variety of iron compounds were found to be effective in the absence of halogen and in the presence of a char forming resin, and also a variety of salts including ferric borate, ferric phosphate, ferric aluminosilicate, micaceous hematite, iron-rich clay, etc. which could lead to very promising results.¹⁸¹ It is worth mentioning that ferric phosphates and silicates are rather light in color, atypical for ferric compounds but could be a very encouraging alternative to obtain light coated PC, as commercial exploitation of iron compounds has been severely restricted due to their color. In the temperature range normally encountered in paint and coatings application, it was already proven that the color of iron oxide particles remains practically unchanged on the contrary to yellow or black iron oxide which can be converted to Fe₂O₃ (hematite) at elevated temperatures (by dehydration or oxygenation respectively).

Furthermore, one additional fire test which could lead to a better understanding of the mechanism of action of iron oxide is the smoke box test. Indeed, the smoke suppressing effect of these particles was emphasized by burning PVC and PVC/ABS blends and led to the conclusion that the Lewis-acid activity of some iron (III) compounds formed in situ may play a part in the smoke suppressing effect.^{184, 185} In addition, polymer structure is important: polymers with aromatic groups in the side chain (or generating aromatic groups during

combustion) give high smoke densities. The ability of iron compounds to suppress smoke production has been rationalized in terms of the Lewis acid properties of iron (III) chloride in relation to its catalytic function by invoking the fact that iron promotes an ionic decomposition mechanism.¹⁷⁵ In this respect, complementary analyses on the two systems developed in this PhD work could lead to further understanding of the mechanism of action attributed to iron oxide.

The third major outlook concerns the broadening of the self-stratifying approach for fire resistant purpose. The proof of concept to flame retard polymers by self-stratifying coatings was validated and thus opens the door to a variety of possibilities to set up novel original coatings for this matter. In a previous research made by Gardelle et al.²⁰³, it was demonstrated that the silicone 217 resin has intrinsic insulating properties. In particular, it exhibits a low heat conductivity which makes it a good candidate to fire protect steel structures. In the light of that fact, the development of a thick silicone-based self-stratified coating on steel could be a very promising and innovative alternative solution. The challenge is however more complex compared to plastics as, on one hand, steel is not a convenient substrate to be prepared for SEM characterization (its cutting for cross section analyses is very sensitive). On the other hand, the coatings applied on PC did not exceed 130 μm , which could be too thin, depending on the application, to obtain efficient and durable fire protection for steel. Such thickness could meet the requirement for indoor applications if the fireproofing effect is effective enough to meet the required specifications. For outdoor applications, the required thickness can reach up to 6 mm (for offshore platforms for example). Accordingly, the main challenge for outdoor applications will be to increase the thickness of the coating without impacting the layering process nor the quality of the coated film, and to incorporate intumescent additives into the formulation. The main and obvious solution would be to increase the viscosity of the paint solution by raising the percentage solid of resins in the formulation. The incorporation of a thickener would be trickier as it was already demonstrated that the degree of layering was impacted, although some FR additives could fit. Finally, it was noticed that the interfacial tension between the substrates and the silicone resin was lower with steel ($\gamma_{s2} = 5.51 \text{ mN/m}$) than with PC ($\gamma_{s2} = 7.88 \text{ mN/m}$). In self-stratifying coating compositions, the resin having the highest surface free energy usually migrates towards the interface with the substrate, and interfacial tension between the resin in contact with the substrate and the substrate (γ_{s1})

should be very low (here, $\gamma_{s1, \text{steel}} < \gamma_{s1, \text{PC}}$). A lower interfacial energy between the substrate and the resin that migrates to the interface with the air could possibly interfere with the phase separation in the homogeneous blend, if the process is driven by surface tensions. In this context, adequate surface treatments of steel may be in favor of the layering. In that respect, other polymeric substrates could also be investigated. As a starting point, preliminary studies have proven the potential of the epoxy/silicone coating for layering on steel (type II pattern, Figure 82), but to a lesser extent compared to PC. Such results were validated for a range of thicknesses going from 20 to 130 μm . To prepare the sample for SEM characterization, ionic-polishing was found to be the best compromise. However, 10 hours of polishing are required for each sample. In this regard, the technique needs some improvement. Lastly, we proved that up to 50 wt.% solid, layering of the two phases was compromised on PC. An experimental design would be necessary here to investigate the influence of the thickness of the coating and of the percentage solid in the formulation. An alternative solution would be the modification of the solvent blend or solvent ratio.

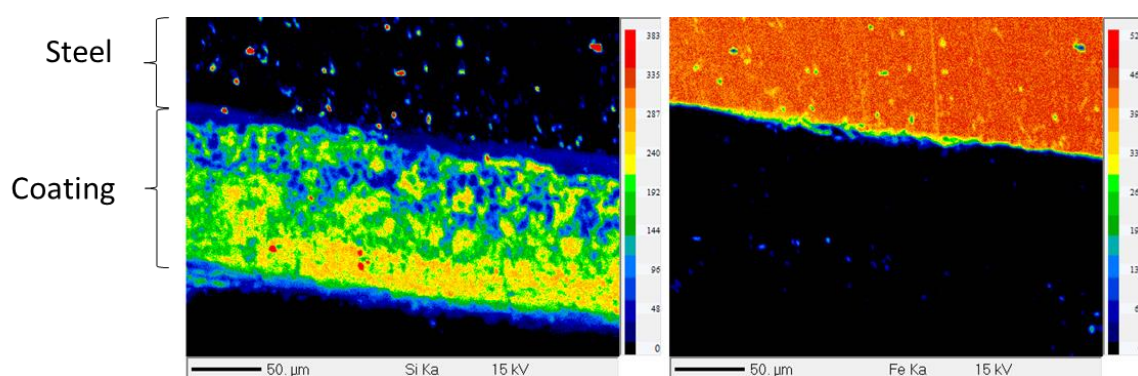


Figure 82. SEM X-Ray analyses of Si and Fe of an epoxy/silicone system applied on stainless steel (dry film thickness = 130 μm)

Additionally, in order to increase the FR properties of the system, the addition of specific FR fillers or intumescent FR could be experimented. Some systems were already tested on steel using additives dispersed in the epoxy phase (iron oxide, calcium carbonate and RDP). However, the results were less conclusive than those obtained on PC (Figure 83). The degree of phase separation was altered and particles were found in the epoxy medium whereas they

migrated towards the silicone phase when applied on PC. Thus, the behavior of the systems differs depending on the substrate: further investigations are needed to deeply understand the predominant parameters.

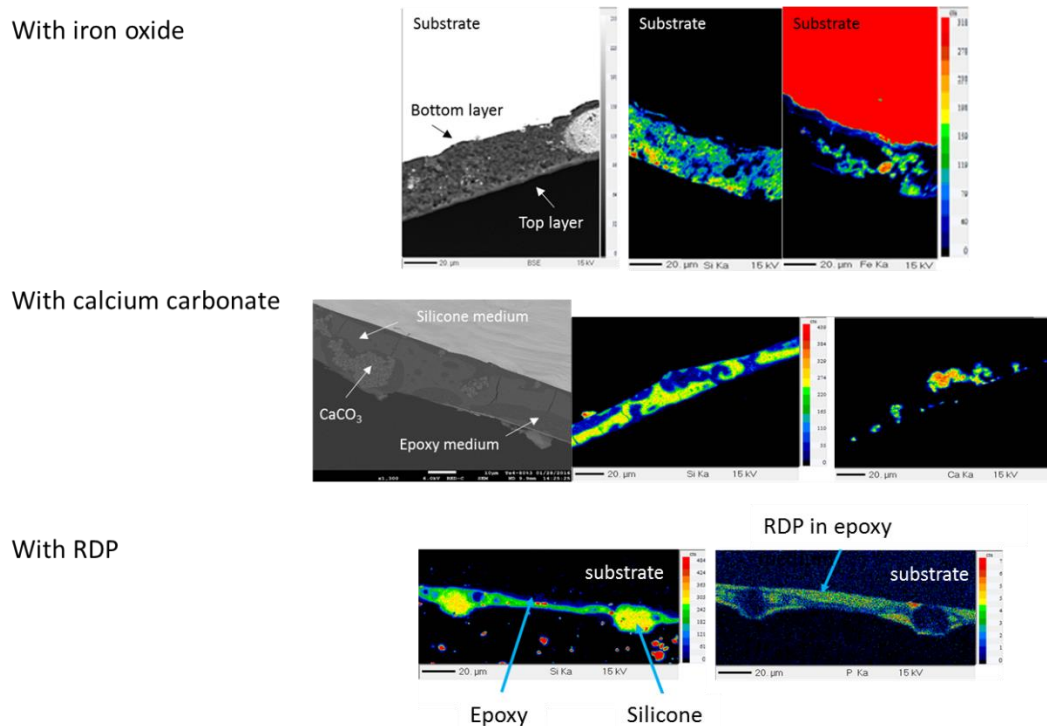


Figure 83. EDX X-ray mappings of Silicon and Iron, calcium or phosphorus on a cross-section of an epoxy/silicone coating filled Fe_2O_3 , calcium carbonate or RDP and applied on steel

Last, but not the least, the self-stratifying concept favors an industrial eco-efficient development of products, taking into account the reduction of solvents and labor cost. Looking at the finishing industry in general, the main driving force for technical changes is the lowering of volatile organic compounds (VOC) emissions and the adjustment (shortening) of the time of film formation. In this regard, an emerging problem is the recyclability, the environmental impact of the FR polymers and the toxicity of the solvents used. The use of xylene in the formulation is the first major drawback here, as well as of non-biodegradable polymers. The first solution would be to replace the solvent, or at least to reduce its amount in the BuAc: xylene blend, as BuAc is a greener solvent. However a compromise will have to

be found between the toxicity and the solubility requirements of the system. A solvent which has a low solubility parameter with one of the resins would be the best choice.

An additional outlook would be the investigation of the durability of the flame retardant coating developed. To that end, additional tests could be carried out like salt spray chamber ageing, water immersion and dirt pick up resistance depending upon the targeted application scenario. The migration of the fillers in the coating during ageing could also be considered in the case of a loss of FR performances. Lastly, analysis of the coating's life cycle (LCA studies) could definitely lead to an interesting measurement of the environmental impact of the system.

The combination of continued technical innovation with improved cost efficiency represents the central challenge of the coatings industry. Self-stratifying coatings remain outside conventional coating technology (based on the use of compatible polymers and oligomers), but some of them are able to provide coatings with valuable properties. Their stratification to the top or bottom interfaces could bring improved adhesion, or instead, anti-adhesion properties, as well as wear, block and chemical resistance, better weather stability and reduced price. This technology may be transferred to other areas using solvent- or water-borne liquid systems or organosolv types to find new applications in particular for coil-coatings, adhesives, baking/storing enamels, gloss paint with high pigment volume concentration in the base layer, pigments-free opaque polymer coatings and bio-based sustainable coatings. Similarly, printing inks could be a good candidate since different interfaces are required to have different characteristics at the top and bottom surface.¹¹¹

This PhD work (STIC project - ANR-14-CE27-0010) has been funding by the ANR (Agence Nationale de la Recherche), and supported by the MATIKEM competitiveness cluster.

List of Figures, Tables and Equations

List of figures

Figure 1. 2013 World production of plastic materials (thermoplastics and polyurethanes) ² and Growth in Global Plastic Production 1950-2014 ³	18
Figure 2. The different approaches to fire retard a polymeric matrix.....	19
Figure 3. Global flame retardant chemicals market between 2014 and 2020 ⁴	19
Figure 4. Flame retardant self-stratifying coatings concept (STIC Project).....	21
Figure 5. Number of publications from 1992 to 2016 including "self-stratifying", "self-stratification" or "self-layering" terms (Scopus April 2017)	21
Figure 6. Bulk treatment approach to fire retard a polymeric matrix	27
Figure 7. Reactive approach to fire retard a polymeric matrix	28
Figure 8. Schematic representation of Layer-By-Layer assembly: the different steps are repeated until the desired number of bilayers is obtained	31
Figure 9. Self-stratifying approach.....	36
Figure 10. Film formation process for solventborne paint	38
Figure 11. Steps of self-stratifying concept compared to common process ¹¹⁸	39
Figure 12. Film forming process with self-stratifying coatings ¹²⁰	40
Figure 13. Type I to IV patterns defining the degree of stratification of a coating ¹⁰⁹	40
Figure 14. Strategy of the thesis	72
Figure 15. Synthetic route for Bisphenol A epoxy resin ¹²⁹	75
Figure 16. Chemical structure of DETA	75
Figure 17. Reaction between an amine curing agent and an epoxide group	76
Figure 18. Molecular structure of a fully crosslinked epoxy resin with DETA	76
Figure 19. Chemical structure of Lumiflon LF200 resin	77
Figure 20. Chemical structure of BDP and RDP flame retardant additives	79
Figure 21. Processing steps for the preparation and application of self-stratifying formulations containing additives.....	80
Figure 22. Schematic presentation of step wise DSC in-situ analyses.....	82
Figure 23. Schematic presentation of step wise DSC analyses after ex-situ crosslinking.....	83
Figure 24. DSC curves of the epoxy/amine system from -50 to 220°C with a ramp of 20°C/min (2 cycles).....	83
Figure 25. DSC curves of the first cycle of isotherm at 40, 80, 110, 130 and 150 °C	84
Figure 26. DSC curves of the second cycle of the in-situ crosslinking.....	84
Figure 27. Epoxy group conversion in the reactive system as a function of temperature after an isothermal of 2 hours	85
Figure 28. Classification of the adhesion using the cross-hatch test ¹⁴⁰	89
Figure 29. Color space of CIE Lab system ¹⁴¹	90
Figure 30. Experimental set of LOI test.....	97
Figure 31. Scheme of UL-94 apparatus.....	98
Figure 32. Schematic of the Mass Loss Calorimeter	99
Figure 33. Schematic curve obtained after MLC test and its characteristics values	100
Figure 34. Schematic representation of the tubular furnace used for thermal treatment	101
Figure 35. Schematic presentation of the Py-GCMS device	102
Figure 36. Schematic of Pyrolysis Combustion Flow Calorimeter	103
Figure 37. Q-LAB, QUV/se weathering chamber and sample holders	105
Figure 38. Humidity chamber test HCP 108	106
Figure 39. Hansen solubility spheres of (a) Epoxy DGEBA, (b) Silicone S217, (c) Lumiflon LF200 resins diluted at 10 wt.%	111
Figure 40. Hansen solubility spheres of (a) Epoxy DGEBA, (b) Silicone S217, (c) Lumiflon LF200 resins diluted at 30 wt.%	113
Figure 41. Solubility spheres of binary mixtures of the epoxy DGEBA resin with a) Silicone 217 and b) Lumiflon LF200 in the Hansen space and projection in (δ_p ; δ_h), (δ_h ; δ_d) and (δ_p ; δ_d) maps of the solubility spheres at 30 wt.% and after 7 days (green circle with a dot center).	115

Figure 42. SEM micrograph of a cross-section of an epoxy/silicone based coating in xylene: (a) self-stratifying coating, (b) EDX mapping of Carbon, Oxygen and Silicium.....	123
Figure 43. SEM micrograph of a cross-section of an epoxy/silicone based coating in butylacetate: xylene (1: 1): (a) self-stratified coating, and the corresponding (b) EDX mappings of Carbon, Oxygen and Silicium (from left to right)	124
Figure 44. Comparison between uncrosslinked (a, c) and crosslinked (b, d) epoxy/silicone self-stratified coatings in xylene (a, b) and BuAc: xylene (1: 1) (c, d).....	126
Figure 45. (a) SEM micrograph and (b) EDX X-ray mappings of Chlorine and Fluorine on a cross-section of an epoxy/fluoropolymer based coating in MIBK: xylene (1:1)	128
Figure 46. FTIR spectra of the crosslinked epoxy and fluoropolymer resins, and of the top layer of the epoxy/fluoropolymer stratified film	129
Figure 47. Back scattered image of the cross-section of the self-stratifying coating of the epoxy/silicone system in MIBK: xylene (1: 1) with Fe ₂ O ₃ (Formulation 5, Table 18) and the corresponding EPMA X-ray mappings of (b) Iron and (c) Silicium	132
Figure 48. EPMA BSE micrographs of a cross-section of an epoxy/silicone coating in xylene with Fe ₂ O ₃ : (a) self-stratifying coating, (b) Iron analysis, (c) Silicium analysis.....	134
Figure 49. (a) EPMA BSE micrographs of self-stratifying coating of an epoxy/silicone system in BuAc: xylene (1: 1) with CaCO ₃ (formulation 10) and the corresponding X-ray mappings of (b) Calcium and (c) Silicium.....	135
Figure 50. SEM micrographs of cross-sections of the epoxy/fluoropolymer based coating in (a) xylene, (b) BuAc: xylene (1:1), (c) MIBK: xylene (1:1), (d) MIBK: xylene: 1-methoxy-2-propanol (50:30:20)	137
Figure 51. EDX X-ray mappings of Chlorine, Fluorine and Iron on cross-sections of epoxy/fluoropolymer based coating in (a) xylene, (b) BuAc: xylene (1:1), (c) MIBK: xylene (1:1), (d) MIBK: xylene: 1-methoxy-2-propanol (50:30:20).....	138
Figure 52. EDX X-ray mappings of Silicium and Phosphorus on a cross-section of an epoxy/silicone coating filled with 5 wt.% of (a) RDP and (b) BDP fillers.....	145
Figure 53. SEM pictures of the cross-section of the ternary system filled with 2.5 wt.% of BDP	146
Figure 54. How materials burn? ¹⁷⁰	154
Figure 55. Schematic representation of potential mode of action of FRs (a to d) in the combustion cycle ¹⁷¹	156
Figure 56. MLC curves of the uncoated and coated PC with the epoxy/silicone and epoxy/fluoropolymer mixtures	160
Figure 57. Picture of the polycarbonate char formed during MLC experiment before it collapses (t = 600 s., 50 kW/m ² , 35 mm).....	161
Figure 58. MLC curves of uncoated and coated PC with the epoxy/silicone/Fe ₂ O ₃ system (50 kW/m ² , 35 mm)	165
Figure 59. HRR curves obtained for PC and coated PCs with unfilled and filled epoxy/fluoropolymer formulations	166
Figure 60. Pyrolytic degradation of PC, silicone and crosslinked epoxy resins (N ₂ , 20 °C/min)	169
Figure 61. Thermo-oxidative degradation of PC, silicone and crosslinked epoxy resins (Air, 20 °C/min)	171
Figure 62. a) Comparison of TG and DTG curves of the silicone systems with and without iron oxide and b) Differential TGA of silicone/Iron oxide system (N ₂ , 20 °C/min)	174
Figure 63. a) Comparison of TG and DTG curves of the silicone resin, iron oxide and the silicone/iron oxide system and b) Differential TGA of silicone/Iron oxide system (Air, 20 °C/min)	175
Figure 64. Heat release rates (W/g) in PCFC of silicone, crosslinked epoxy, epoxy/silicone and epoxy/silicone/IO coatings.....	178
Figure 65. Heat release rate in PCFC of silicone and silicone/iron oxide systems	179
Figure 66. Comparison of silicone and silicone/IO film pyrograms obtained at 800 °C	181
Figure 67. Schematics presentation of D, T ⁱ and Q ⁱ silicone structures ²⁰³	183
Figure 68. Proposed radical mechanism in silicone thermal degradation by Hamdani et al. ²⁰⁴	184
Figure 69. Numerical picture of a) Silicone, b) Silicone/IO (10 wt.%) residues after 3h at 300°C in a tubular furnace (N ₂ atmosphere, Z20*20).....	185
Figure 70. Pictures of the residues generated at TTI during MLC shutter experiments	187
Figure 71. EPMA BSE micrographs of a cross-section of the a) epoxy/silicone and b) epoxy/silicone/iron oxide coating's residues during MLC shutter experiments, after TTI, with Carbon, Silicium and Iron X-ray detection	187

Figure 72. Pictures of the residues of epoxy/silicone and epoxy/silicone/iron oxide coatings applied on PC after MLC test	188
Figure 73. ATR-FTIR spectra of the white and red residues after MLC tests	189
Figure 74. Schematic representation of the mode of action of the PC coated with the epoxy/silicone and epoxy/silicone/iron oxide systems	194
Figure 75. Visual appearance of the PC plates after UV and T/RH exposure.....	196
Figure 76. MLC curves of the polycarbonate before ageing, and after 8 weeks of ageing under UV and T/RH conditions.....	197
Figure 77. Visual appearance of the PC and coated PC with the epoxy/silicone mixture after UV and T/RH exposure.....	199
Figure 78. MLC curves of the coated PC with the epoxy/silicone system before ageing, and after 8 weeks of ageing under UV and T/RH conditions.....	200
Figure 79. Visual appearance of the epoxy/silicone/Fe ₂ O ₃ coated plates after UV and T/RH exposure	203
Figure 80. MLC curves of the coated PC with the epoxy/silicone/IO system before ageing, and after 8 weeks of ageing under UV and T/RH conditions.....	204
Figure 81. Comparison between the current system and the self-stratifying system to fire retard PC by surface treatment.....	212
Figure 82. SEM X-Ray analyses of Si and Fe of an epoxy/silicone system applied on stainless steel (dry film thickness = 130 μm)	216
Figure 83. EDX X-ray mappings of Silicium and Iron, calcium or phosphorus on a cross-section of an epoxy/silicone coating filled Fe ₂ O ₃ , calcium carbonate or RDP and applied on steel	217
Figure 84. Raman spectra of the epoxy/amine system from 30 to 100 °C at 473 nm	254
Figure 85. ATR-FTIR spectra of the system epoxy/amine from 80 to 190°C. The direction of the arrow indicates the evolution of the band with increasing temperature	255
Figure 86. MLC curves of polycarbonate and coated PCs with the epoxy/silicone and epoxy/silicone/iron oxide system (35 kW/m ² , 35 mm)	256
Figure 87. Hansen solubility spheres of (a) acrylic BR106, (b) Silicone 3055 and (c) Acrylic B875 diluted at 10 wt.%	258
Figure 88. EDX X-ray mappings of a) Silicium and iron and b) Silicium and Calcium on cross-sections of an epoxy/silicone coating filled with 10 %PVC of a) iron oxide and b) calcium carbonate	262
Figure 89. SEM images of epoxy/silicone self-layered system at a) 40 wt.% and b) 50 wt.% of resins sprayed on PC	263
Figure 90. MLR curves of PC, and coated PC with and without IO particles	264

List of Tables

Table 1. List of the different fillers used	78
Table 2. Heat release and percentage of conversion of the system cured at different temperature for 2 hours .	85
Table 3. Elements and X-ray energies used for SEM-EDX and EPMA analyses	96
Table 4. UL-94 classification	98
Table 5. Hansen Solubility Parameters of the selected resins diluted at 10 wt.%.....	110
Table 6. Accuracy of the model according to the location of the solvent in the Hansen space	111
Table 7. List of solvents which do not dissolve the selected resins at 10 wt.%	112
Table 8. List of solvents which do not dissolve the selected resins at 30 wt.% after 7 days	113
Table 9. HSP and radius of the selected resins diluted at 30 wt.%.....	113
Table 10. Overlap factors between the epoxy DGEBA and thermoplastic resins when diluted at 10 and 30 wt.%, and after 48 hours and 7 days at 30 wt.%	115
Table 11. Overlap factors considering the silicone resin as target polymer (10 wt.%)	117
Table 12. Boiling temperature of the tested solvents	118

Table 13. Values of contact angle and surface tensions following the method of Wu for the selected substrates and resins ¹³⁷	119
Table 14. Prediction of stratification on PC of the combination of the epoxide resin with either the fluoropolymer or silicone resins. Results given in a color background are not in accordance with the model.....	120
Table 15. Resulting coatings appearance, adhesion and stratification patterns of unpigmented uncrosslinked and crosslinked systems	123
Table 16. Resulting appearance, thickness, adhesion and stratification pattern of unfilled binary blends.....	127
Table 17. Contact angle and surface energy data of the crosslinked epoxy and fluoropolymer resins	129
Table 18. Resulting coatings characteristics and stratification pattern of pigmented formulations.....	131
Table 19. Resulting coatings appearance, adhesion and stratification pattern of Fe ₂ O ₃ containing coatings...	138
Table 20. Fillers location, appearance of the coating, adhesion rating and stratification pattern for the epoxy/silicone coatings filled with RDP and BDP at 2.5 and 5 wt.%	144
Table 21. MLC (50 kW/m ² , 35 mm), LOI and UL-94 values of the uncoated and coated PC with the epoxy/silicone and epoxy/fluoropolymer mixture	160
Table 22. LOI and UL-94 ranking of coated PC with epoxy/silicone coatings filled or not with iron oxide	163
Table 23. LOI and UL-94 ranking of coated PC with epoxy/fluoropolymer coatings filled or not with iron oxide	164
Table 24. MLC values of unfilled and filled coated PC with the epoxy/silicone/Fe ₂ O ₃ systems (50 kW/m ² , 35 mm)	165
Table 25. TG data of PC, crosslinked epoxy and silicone resins (N ₂ , 20 °C/min)	170
Table 26. TG data of PC, crosslinked epoxy and silicone resin (Air, 20 °C/min)	172
Table 27. TG data of silicone film, iron oxide and silicone/iron oxide systems (N ₂ , 20 °C/min).....	174
Table 28. TGA data of silicone film, iron oxide and silicone film containing iron oxide (Air, 20 °C/min)	176
Table 29. PCFC data of silicone, crosslinked epoxy, epoxy/silicone and epoxy/silicone/IO coatings	178
Table 30. PCFC data of silicone compared to the silicone/IO system.....	179
Table 31. Identification of the decomposition products of silicone and silicone/IO systems at 800°C	181
Table 32. L*a*b*, adhesion, UL-94 rating and LOI values obtained after weathering tests of PC under UV and T/RH conditions.....	196
Table 33. MLC data of the polycarbonate before ageing, and after 8 weeks of ageing under UV and T/RH conditions.....	198
Table 34. L*a*b*, adhesion, UL-94 and LOI value of the aged epoxy/silicone self-stratifying system applied on PC under UV and T/RH conditions.....	199
Table 35. MLC data of the coated PC with the epoxy/silicone system before ageing, and after 8 weeks of ageing under UV and T/RH conditions.....	201
Table 36. L*a*b*, adhesion, UL-94 and LOI logged during weathering test of PC under UV and T/RH conditions	202
Table 37. L*a*b* values logged of the PC, and of the front and back side of the PC plate after 8 weeks of ageing under UV conditions.....	203
Table 38. MLC data of the coated PC with the epoxy/silicone/IO system before ageing, and after 8 weeks of ageing under UV and T/RH conditions	204
Table 39. Technical data of Silicone RSN-0217	252
Table 40. Technical data of Lumiflon LF200.....	252
Table 41. MLC values of virgin PC, epoxy/silicone and epoxy/silicone/iron oxide coated PC (35 kW/m ² , 35 mm)	256
Table 42. Coordinates of the junction between the Hansen sphere of the epoxy resin and the silicone and fluoropolymer spheres, their C and overlap factor when diluted at 10 wt.%.....	257
Table 43. Coordinates of the junction between the Hansen sphere of the epoxy resin and the silicone and fluoropolymer, their C and overlap factor when diluted at 30 wt.% after 7 days	257
Table 44. Coordinates of the junction between the Hansen sphere of the silicone resin and the fluoropolymer spheres, their C and overlap factor when diluted at 10 wt.%	257
Table 45. Hansen Solubility Parameters of the selected resins diluted at 10 wt.%.....	258
Table 46. Overlap factors between the epoxy DGEBA, Silicone 3055 and 217 and various thermoplastic resins when diluted at 10 wt.%, after 7 days	259

Table 47. Interfacial energy between the epoxy, silicone or fluoropolymer resin on PC 260

Table 48. Pigments location, appearance of the coating, adhesion rating and stratification pattern resulted from the epoxy/silicone coatings filled with Fe₂O₃ and CaCO₃ at 2.5, 5 and 10 %PVC 261

Table 49. MLC data obtained for PC, and coated PC with unfilled and filled formulations 264

List of Equations

Equation 1. Overlap factor V.....87

Equation 2. Interfacial surface tension.....87

Equation 3. Difference in color between two samples.....90

Equation 4. Difference weight loss curves.....91

Equation 5. Linear combination of TG curves (theoretical weight loss)91

Equation 6. Limiting Oxygen Index (LOI)97

References

1. International Association of Fire and Recue Services (CTIF), Report n°21: World Fire Statistics, in G. National committees CTIF of Russia, USA , Center of Fire Statistics of CTIF 2016, 2016.
2. PlasticsEurope, Plastics - the Facts 2014, Analysis of European plastics production & demand by PlasticsEurope, <http://www.plastics.gl/market/plastics-the-facts-2014/>. [Accessed Jun 7, 2017]
3. R. Opsomer and J. Pennington, What are the drawbacks of today's plastics economy?, 2016, <https://www.weforum.org/agenda/2016/03/what-are-the-drawbacks-of-todays-plastics-economy/>. [Accessed April 11, 2017]
4. M.R. Store, Global Flame Retardant Chemicals Market Set for Rapid Growth, To Reach Around USD 10.0 Billion by 2020, <http://www.marketresearchstore.com>. [Accessed April 11, 2017].
5. S. Duquesne, M. Jimenez and S. Bourbigot, Fire Retardancy of Polymers: New Strategies and Mechanisms, presented at the 11th (FRPM '07), Bolton, UK, 4-6 July, 2009.
6. M. Jimenez, S. Duquesne and S. Bourbigot, Fire protection of polypropylene and polycarbonate by intumescent coatings, *Polymer Advanced Technologies*, 2012, **23**, 130-135.
7. H. Gallou, M. Jimenez, S. Duquesne, C. Jama, R. Delobel, S. Bourbigot and X. Couillens, Fire retardant polyamide cast item including an intumescent coating, Rhodia Operations, WO2011045426, 2011.
8. C. Pagella and R. Epifani, Intumescent coatings for polymer substrates, *Polymer Paint Colou Journal*, 2013, **203**, 38-41.
9. V.V. Verkholtantsev, Nonhomogeneous-in-layer coatings, *Progress in Organic Coatings*, 1985, **13**.
10. R. Berkau, M. Gailberger, T. Gruber, K. Holdik, G. Meichsner, F. Mezger, Coating composition for forming self-layering or self-coating lacquer systems, US Patent 7186772 B2, 2007.
11. V.V. Verkholtantsev, Exploiting self-stratification, *European Coating Journal*, 2005, 20.
12. E. Langer, H. Kuczyńska, E. Kamińska-Tarnawska and J. Łukaszczyk, Self-stratifying coatings containing barrier and active anticorrosive pigments, *Progress in Organic Coatings*, 2011, **71**, 162-166.
13. T. Ishikawa, I. Maki, T. Koshizuka and K. Takeda, Thermal degradation and flame retardancy of polycarbonate as a flame retardant polymer, *Zairyo/Journal of the Society of Materials Science, Japan*, 2004, **53**, 1301-1308.
14. J. Wang and Z. Xin, Flame retardancy, thermal, rheological, and mechanical properties of polycarbonate/polysilsesquioxane system, *Journal of Applied Polymer Science*, 2010, **115**, 330-337.
15. M. Le Bras, G. Camino, S. Bourbigot, R. Delobel and L. N. Gordon, Fire Retardancy of Polymers - The Use of Intumescence, *Fire Retardancy of Polymers - The Use of Intumescence*, The Royal Society of Chemistry, Cambridge, UK, 1998.
16. Y.P. Khanna, E.M. Pearce, Flame retardant Polymeric Materials, 1978, 2-10.

17. R.E. Lyon, Solid state thermochemistry of flaming combustion, *Fire Retardancy of Polymeric Materials*, 2000, 191-447.
18. P. Joseph and J. R. Ebdon, Phosphorus-Based Flame Retardants, in *Fire Retardancy of Polymeric Materials*, C.A. Wilkie and A.B. Morgan, ed. CRC Press, Boca Raton, FL, USA, 2nd ed., 2010, pp. 107-127.
19. W.H. Awad, Recent Developments in Silicon-Based Flame Retardants, in *Fire Retardancy of Polymeric Materials*, C.A. Wilkie and A.B. Morgan, ed. CRC Press, Boca Raton, FL, USA, 2nd ed., 2010 pp. 187-206.
20. T. Kashiwagi, T.G. Cleary, G.C. Davis and J.H. Lupinski, A non-halogenated, flame retarded polycarbonate, Presented at the International Conference for the Promotion of Advanced fire-resistant Aircraft Interior Materials, Atlantic City, NJ, 9-11 Feb, 1993, pp. 175-187.
21. P.G. Pape and D.J. Romenesko, The role of silicone powders in reducing the heat release rate and evolution of smoke in flame retardant thermoplastics, *Journal of Vinyl and Additive Technology*, 1997, **3**, 225-232.
22. Z. Han, A. Fina and G. Camino, Organosilicon Compounds as Polymer Fire Retardants , in *Polymer Green Flame Retardants*, ed. Elsevier, 2014, pp. 389-418.
23. S. Bourbigot, B. Gardelle, M. Jimenez, S. Duquesne and V. Rerat, Silicone-based coatings for reaction and resistance to fire of polymeric materials, Presented at the 22nd Annual Conference on Recent Advances in Flame Retardancy of Polymeric Materials, Stamford, CT, 23-25 May, 2011, pp. 243-251.
24. R. Buch, J. Shields, T. Kashiwagi, T. Cleary and K. Steckler, The influence of surface silica on the pyrolysis of silicones, Presented at the NISTIR annual conference on fire research, 2-5 Nov, Gaithersburg, MD, 1998.
25. S.Y. Lu and I. Hamerton, Recent developments in the chemistry of halogen-free flame retardant polymers, *Progress in Polymer Science*, 2002, **27**, 1661-1712.
26. J.W. Gu, G.C. Zhang, S.I. Dong, Q.Y. Zhang and J. Kong, Study on preparation and fire-retardant mechanism analysis of intumescent flame-retardant coatings, *Surface and Coatings Technology*, 2007.
27. S. Duquesne, S. Magnet, C. Jama and R. Delobel, Intumescent paints: fire protective coatings for metallic substrates, *Surface and Coatings Technology*, 2004, **180-181**, 302-307.
28. A.R. Horrocks, P.J. Davies, B.K. Kandola and A. Alderson, The potential for volatile phosphorus-containing flame retardants in textile back-coatings, *Journal of Fire Sciences*, 2007, **25**, 523-540.
29. C. Jama, A. Quedé, P. Goudmand, O. Dessaux, M. Le Bras, R. Delobel, S. Bourbigot, J.W. Gilman and T. Kashiwagi, Fire and Polymers: Materials and Solutions for Hazard Prevention, G.L. Nelson and C.A. Wilkie, ACS Symposium Series 797, American Chemical Society Publication, Washington, DC, 2001, pp. 200.
30. R.A. Lopez, Fire retardant compositions and methods for preserving wood products, US Patent 6620349 B1, 2003.

31. A.R. Horrocks, M.Y. Wang, M.E. Hall, F. Summonu and J.S. Pearson, Flame retardant textile back coatings, Part E. Effectiveness of phosphorus-containing flame retardants in textile back-coating formulations, *Polymer International*, 2000, **49**, 1049-1091.
32. P. Sorensen, Application of the Acid/Base Concept Describing the Interaction between Pigments, Binders and Solvents, *Journal of Paint Technology* 1975, **47**, 31.
33. L.J. Gay Lussac, Note sur la propriété qu'ont les matières salines de rendre les tissus incombustibles, *Annales de Chimie et de Physique*, 1821, **18**, 211-218.
34. B. Gardelle [online], Development and resistance to fire of intumescent silicone based coating - Fire protection of steel in simulated fire, Université des sciences et technologies de Lille, 2013.
35. S. Duquesne, Jimenez, M. and Bourbigot, S., Aging of the Flame-Retardant Properties of Polycarbonate and Polypropylene Protected by an Intumescent Coating, *Journal of Applied Polymer Science*, 2014, **131**, 39566.
36. R.K. Iler, Multilayers of colloidal particles, *Journal of Colloid and Interface Science*, 1966, **21**, 569-594.
37. G. Decher and J. D. Hong, Buildup of ultrathin multilayer films by a self-assembly process, 1 consecutive adsorption of anionic and cationic bipolar amphiphiles on charged surfaces, *Makromolekulare Chemie. Macromol Symposia*, 1991, **46**, 321-327.
38. H.L. Tan, M.J. McMurdo, G. Pan and P.G. Van Patten, Temperature Dependence of Polyelectrolyte Multilayer Assembly, *Langmuir*, 2003, **19**, 9311-9314.
39. Z. Sui, D. Salloum and J. B. Schlenoff, Effect of Molecular Weight on the Construction of Polyelectrolyte Multilayers: Stripping versus Sticking, *Langmuir*, 2003, **19**, 2491.
40. S.S. Shiratori and M.F. Rubner, pH-Dependent Thickness Behavior of Sequentially Adsorbed Layers of Weak Polyelectrolytes, *Macromolecules*, 2000, **33**, 4213-4219.
41. R.A. McAloney, M. Sinyor, V. Dudnik and M. C. Goh, Atomic Force Microscopy Studies of Salt Effects on Polyelectrolyte Multilayer Film Morphology, *Langmuir*, 2001, **17**, 6655-6663.
42. K. Apaydin, A. Laachachi, J. Bour, V. Toniazzo, D. Ruch and B. Vincent, Polyelectrolyte multilayer films made from polyallylamine and short polyphosphates: Influence of the surface treatment, ionic strength and nature of the electrolyte solution, *Colloids and Surfaces A: Physicochemical and Engineering Aspects*, 2012, **415**, 274-280.
43. E.M. Sauer, R.M. Flessner, S.P. Sullivan, M.R. Prausnitz and D.M. Lynn, Layer-by-layer assembly of DNA- and protein-containing films on microneedles for drug delivery to the skin, *Biomacromolecules*, 2010, **11**, 3136-3143.
44. O. S. Sakr, O. Jordan and G. Borchard, Novel Layer-by-Layer Deposition Technique for the Preparation of Double-Chambered Nanoparticle Formulations, *Journal of Pharmaceutical Sciences*, 2015, **104**, 2637-2640.
45. H. Shimomura, Z. Gemici, R. E. Cohen and M. F. Rubner, Layer-by-Layer-Assembled High-Performance Broadband Antireflection Coatings, *ACS Applied Materials & Interfaces*, 2010, **2**, 813-820.

46. D.J. Schmidt, E.M. Pridgen, P.T. Hammond and J.C. Love, Layer-by-Layer Assembly of a pH-Responsive and Electrochromic Thin Film, *Journal of Chemical Education*, 2010, **87**, 208-211.
47. R. Montazami, V. Jain and J. Heflin, High contrast asymmetric solid state electrochromic devices based on layer-by-layer deposition of polyaniline and poly(aniline sulfonic acid), *Electrochimica Acta*, 2010, **56**, 990-994.
48. W.S. Jang, I. Rawson and J.C. Grunlan, Layer-by-layer assembly of thin film oxygen barrier, *Thin Solid Films*, 2008, **516**, 4819-4825.
49. M.A. Priolo, D. Gamboa, K.M. Holder and J.C. Grunlan, Super Gas Barrier of Transparent Polymer–Clay Multilayer Ultrathin Films, *Nano Letters*, 2010, **10**, 4970-4974.
50. Y.S. Kim, R. Davis, A.A. Cain and J.C. Grunlan, Development of layer-by-layer assembled carbon nanofiber-filled coatings to reduce polyurethane foam flammability, *Polymer*, 2011, **52**, 2847-2855.
51. A.J. Mateos, A.A. Cain and J.C. Grunlan, Large-Scale Continuous Immersion System for Layer-by-Layer Deposition of Flame Retardant and Conductive Nanocoatings on Fabric, *Industrial & Engineering Chemistry Research*, 2014, **53**, 6409-6416.
52. Y.S. Kim and R. Davis, Multi-walled carbon nanotube layer-by-layer coatings with a trilayer structure to reduce foam flammability, *Thin Solid Films*, 2014, **550**, 184-189.
53. A. Laachachi, V. Ball, K. Apaydin, V. Toniazzo and D. Ruch, Diffusion of Polyphosphates into (Poly(allylamine)-montmorillonite) Multilayer Films: Flame Retardant-Intumescent Films with Improved Oxygen Barrier, *Langmuir*, 2011, **27**, 13879-13887.
54. A.A. Cain, C.R. Nolen, Y.C. Li, R. Davis and J.C. Grunlan, Phosphorous-filled nanobrick wall multilayer thin film eliminates polyurethane melt dripping and reduces heat release associated with fire, *Polymer Degradation and Stability*, 2013, **98**, 2645-2652.
55. Y.C. Li, J. Schulz and J.C. Grunlan, Polyelectrolyte/Nanosilicate Thin-Film Assemblies: Influence of pH on Growth, Mechanical Behavior, and Flammability, *ACS Applied Materials & Interfaces*, 2009, **1**, 2338-2347.
56. K. Apaydin, A. Laachachi, T. Fouquet, M. Jimenez, S. Bourbigot and D. Ruch, Mechanistic investigation of a flame retardant coating made by layer-by-layer assembly, *RSC Advances*, 2014, **4**, 43326-43334.
57. S. Bourbigot, E. Devaux and X. Flambard, Flammability of Polyamide-6/Clay Hybrid Nanocomposite Textiles, *Polymer Degradation and Stability*, 2002, **75**, 397-402.
58. Y.S. Kim, Y.C. Li, W.M. Pitts, M. Werrel and R.D. Davis, Rapid Growing Clay Coatings to Reduce the Fire Threat of Furniture, *ACS Applied Materials & Interfaces*, 2014, **6**, 2146.
59. S. Laik [online], Investigation of polyhedral oligomeric silsesquioxanes for improved fire retardancy of hybrid epoxy-based polymer systems, Institut National des Sciences Appliquées (INSA) de Lyon, Ecole Doctoral Matériaux de Lyon, 2014.
60. F. Carosio, J. Alongi and G. Malucelli, α -Zirconium phosphate-based nanoarchitectures on polyester fabrics through layer-by-layer assembly, *Journal of Materials Chemistry*, 2011, **21**, 10370-10376.

61. J. Alongi, F. Carosio and G. Malucelli, Layer by layer complex architectures based on ammonium polyphosphate, chitosan and silica on polyester-cotton blends: flammability and combustion behaviour, *Cellulose*, 2012, **19**, 1041-1050.
62. G. Laufer, F. Carosio, R. Martinez, G. Camino and J. Grunlan, Growth and fire resistance of colloidal silica-polyelectrolyte thin film assemblies, 2011.
63. T. Zhang, H.Q. Yan, M. Peng, L. Wang, H. Ding and Z. Fang, Construction of flame retardant nanocoating on ramie fabric via layer-by-layer assembly of carbon nanotube and ammonium polyphosphate, *Journal of Colloid and Interface Science*, 2013, 356, 69.
64. K. Apaydin [online], Development, characterization and fire retardant mechanism of layer-by-layer and plasma coatings, Université des sciences et technologies de Lille, 2014.
65. F. Carosio, A. Di Blasio, J. Alongi and G. Malucelli, Green DNA-based flame retardant coatings assembled through Layer by Layer, *Polymer*, 2013, **54**, 5148-5153.
66. G. Huang, J. Yang, J. Gao and X. Wang, Thin Films of Intumescent Flame Retardant-Polyacrylamide and Exfoliated Graphene Oxide Fabricated via Layer-by-Layer Assembly for Improving Flame Retardant Properties of Cotton Fabric, *Industrial & Engineering Chemistry Research*, 2012, 51, 12355-12366.
67. F. Carosio, C. Negrell-Guirao, A. Di Blasio, J. Alongi, G. David and G. Camino, Tunable thermal and flame response of phosphonated oligoallylamines layer by layer assemblies on cotton, *Carbohydrate Polymers*, 2015, **115**, 752-759.
68. F. Carosio and J. Alongi, Influence of layer by layer coatings containing octapropylammonium polyhedral oligomeric silsesquioxane and ammonium polyphosphate on the thermal stability and flammability of acrylic fabrics, *Journal of Analytical and Applied Pyrolysis*, 2016, **119**, 114-123.
69. F. Carosio, A. Di Blasio, J. Alongi and G. Malucelli, Layer by layer nanoarchitectures for the surface protection of polycarbonate, *European Polymer Journal*, 2013, **49**, 397-404.
70. J. Alongi, A. Di Blasio, F. Carosio and G. Malucelli, UV-cured hybrid organic-inorganic Layer by Layer assemblies: Effect on the flame retardancy of polycarbonate films, *Polymer Degradation and Stability*, 2014, **107**, 74-81.
71. J. Alongi, F. Carosio, A. Frache and G. Malucelli, Layer by Layer coatings assembled through dipping, vertical or horizontal spray for cotton flame retardancy, *Carbohydrate Polymers*, 2013, **92**, 114-119.
72. J. Alongi, F. Carosio and G. Malucelli, Current emerging techniques to impart flame retardancy to fabrics: An overview, *Polymer Degradation and Stability*, 2014, **106**, 138-149.
73. S. Attia, J. Wang, G.M. Wu, J. Shen and J.H. Ma, Review on sol-gel derived coatings: Process, techniques and optical applications, *Journal of Materials Science and Technology*, 2002, **18**, 211-218.
74. Y. Shi, Y. Wang, X. Feng, G. Yue and W. Yang, Fabrication of superhydrophobicity on cotton fabric by sol-gel, Applied Surface Science, *Applied Surface Science*, 2012, **258**, 8134-8138.

75. R. Taurino, E. Fabbri, D. Pospiech, A. Synytska and M. Messori, Preparation of scratch resistant superhydrophobic hybrid coatings by sol–gel process, *Progress in Organic Coatings*, 2014, **77**, 1635-1641.
76. M. Akhlouch, A. Calleja, X. Granados, S. Ricart, V. Boffa, F. Ricci, T. Puig and X. Obradors, Hybrid sol–gel layers containing CeO₂ nanoparticles as UV-protection of plastic lenses for concentrated photovoltaics, *Solar Energy Materials and Solar Cells*, 2014, **120**, 175-182.
77. G. Ramos, F. del Monte, B. Zurro, K. J. McCarthy, A. Baciero and D. Levy, Luminescent Properties of Sodium Salicylate Films Prepared by the Sol–Gel Method, *Langmuir*, 2002, **18**, 984-986.
78. B. Mahltig, D. Fiedler and H. Böttcher, Antimicrobial Sol–Gel Coatings, *Journal of Sol-Gel Science and Technology*, 2004, **32**, 219-222.
79. B. Mahltig, T. Grethe and H. Haase, Antimicrobial Coatings Obtained by Sol–Gel Method, in *Handbook of Sol-Gel Science and Technology*, ed. L. Klein, M. Aparicio and A. Jitianu, Springer International Publishing, Cham, 2016, pp. 1-27.
80. J. Alongi, M. Ciobanu and G. Malucelli, Novel flame retardant finishing systems for cotton fabrics based on phosphorus-containing compounds and silica derived from sol-gel processes, *Carbohydrate Polymers*, 2011, **85**, 599-608.
81. J. Alongi, M. Ciobanu and G. Malucelli, Thermal stability, flame retardancy and mechanical properties of cotton fabrics treated with inorganic coatings synthesized through sol–gel processes, *Carbohydrate Polymers*, 2012, **87**, 2093-2099.
82. C.L. Chiang and C.C.M. Ma, Synthesis, characterization and thermal properties of novel epoxy containing silicon and phosphorus nanocomposites by sol–gel method, *European Polymer Journal*, 2002, **38**, 2219-2224.
83. C. Mai and H. Militz, Modification of wood with silicon compounds. inorganic silicon compounds and sol-gel systems: a review, *Wood Science and Technology*, 2004, **37**, 339-348.
84. D. Shang, X. Sun, J. Hang, L. Jin and L. Shi, Flame resistance, physical and mechanical properties of UV-cured hybrid coatings containing low-hydroxyl-content sols via an anhydrous sol-gel process, *Progress in Organic Coatings*, 2017, **105**, 267-276.
85. D. Shang, X. Sun, J. Hang, L. Jin and L. Shi, Preparation and stability of silica sol/TPGDA dispersions and its application in the UV-curable hybrid coatings for fire protection, *Journal of Sol-Gel Science and Technology*, 2013, **67**, 39-49.
86. D. Vangeneugden, S. Paulussen, O. Goossens, R. Rego and K. Rose, Aerosol-Assisted Plasma Deposition of Barrier Coatings using Organic-Inorganic Sol-Gel Precursor Systems, *Chemical Vapor Deposition*, 2005, **11**, 491-496.
87. F. Xu, X. Sun, J. Hang, D. Shang, L. Shi, W. Sun and L. Wang, Synthesis, characterization and flame retardant of UV-curable hybrid coatings containing SiO₂–P₂O₅–B₂O₃ via sol–gel method, *Journal of Sol-Gel Science and Technology*, 2012, **63**, 382-388.
88. I. Errifai, C. Jama, R. Delobel, R. Jaeger and A. Mazzah, Elaboration and Grafting of Cold Plasma Organo-Phosphorus Copolymers on Polyamide 6: New Approach to Flame Retardancy, *Molecular Crystals and Liquid Crystals*, 2010, **486**, 316-324.

89. S. Bourbigot, C. Jama, M. Le Bras, R. Delobel, O. Dessaux and P. Goudmand, New approach to flame retardancy using plasma assisted surface polymerisation techniques, *Polymer Degradation and Stability*, 1999, **66**, 153-155.
90. B. ScharTEL, G. Kühn, R. Mix and J. Friedrich, Surface Controlled Fire Retardancy of Polymers Using Plasma Polymerisation, *Macromolecular Materials and Engineering*, 2002, **287**, 579-582.
91. M.J. Tsafack and J. Levalois-Grützmacher, Towards multifunctional surfaces using the plasma-induced graft-polymerization (PIGP) process: Flame and waterproof cotton textiles, *Surface and Coatings Technology*, 2007, **201**, 5789-5795.
92. B. Edwards, A. El-Shafei, P. Hauser and P. Malshe, Towards flame retardant cotton fabrics by atmospheric pressure plasma-induced graft polymerization: Synthesis and application of novel phosphoramidate monomers, *Surface and Coatings Technology*, 2012, **209**, 73-79.
93. B. Paosawatyanong, P. Jermsutjarit and W. Bhanthumnavin, Graft copolymerization coating of methacryloyloxyethyl diphenyl phosphate flame retardant onto silk surface, *Progress in Organic Coatings*, 2014, **77**, 1585-1590.
94. K. Kamlangkla, S. K. Hodak and J. Levalois-Grützmacher, Multifunctional silk fabrics by means of the plasma induced graft polymerization (PIGP) process, *Surface and Coatings Technology*, 2011, **205**, 3755-3762.
95. M. J. Tsafack and J. Levalois-Grützmacher, Plasma-induced graft-polymerization of flame retardant monomers onto PAN fabrics, *Surface and Coatings Technology*, 2006, **200**, 3503-3510.
96. C. Chaiwong, S. Tunma, W. Sangprasert, P. Nimmanpipug and D. Boonyawan, Graft polymerization of flame-retardant compound onto silk via plasma jet, *Surface and Coatings Technology*, 2010, **204**, 2991-2995.
97. J. Bardon, K. Apaydin, A. Laachachi, M. Jimenez, T. Fouquet, F. Hilt, S. Bourbigot and D. Ruch, Characterization of a plasma polymer coating from an organophosphorus silane deposited at atmospheric pressure for fire-retardant purposes, *Progress in Organic Coatings*, 2015, **88**, 39-47.
98. M. Jimenez, S. Bellayer, B. Revel, S. Duquesne and S. Bourbigot, High-Throughput Fire Testing for Intumescent Coatings, *Industrial and Engineering Chemistry Research*, 2013, **52**, 729-743.
99. S. Duquesne, M. Jimenez and S. Bourbigot, Aging of the Flame-Retardant Properties of Polycarbonate and Polypropylene Protected by an Intumescent Coating, *Journal of Applied Polymer Science*, 2014, **131**, 39561-39569.
100. S. Farris, S. Pozzoli, P. Biagioni, L. Duó, S. Mancinelli and L. Piergiovanni, The fundamentals of flame treatment for the surface activation of polyolefin polymers – A review, *Polymer*, 2010, **51**, 3591-3605.
101. Enercon Industry, Corona, Plasma and Flame Treating for Plastics, <http://www.enerconind.com/corona-pretreatment-machine.aspx>. [Accessed June 6, 2017]

102. V.V. Verkholtantsev and M. Flavian, Epoxy thermoplastic heterophase and self-stratifying coatings, *Modern paint and coatings*, 1995, **85**, 100-106.
103. W. Funke, Preparation and Properties of Paint Films with Special Morphological Structure, *Journal of Oil Colour Chem Association*, 1976, **59**, 398-403.
104. C. Carr, S. Benjamin and D. J. Walbridge, Fluorinated resin in self-stratifying coatings, *European Coatings Journal*, 1995, **4**, 262-266.
105. H. Murase and W. Funke, *XVth FATIPEC Congress, Congress Book 2*, Netherlands Association of coatings Tehcnologists, Amsterdam, 1980, pp. 387-409.
106. Kansai Paint Co. Ltd, Powder Coating Method For Forming Multilayer Coatings, GB Patent 1 570 540 A, 1980.
107. C. Carr, Multilayered paint films from single coat systems, *Journal of the Oil and Colour Chemists' Association*, 1990, **10**, 403-404.
108. V.V. Verkholtantsev, Coatings Based on Polymer/Polymer Composites, *Journal of Coatings Technology*, 1992, **64**, 51-59.
109. A. Toussaint, Self-stratifying coatings for plastic substrates (BRITE EURAM PROJECT RI 1B 0246 C(H)), *Progress in Organic Coatings*, 1996, **28**, 183-195.
110. D.J. Walbridge, Self-stratifying coatings — an overview of a European Community Research Project, *Progress in Organic Coatings*, 1996, **28**, 155-159.
111. S. Benjamin, C. Carr and D.J. Walbridge, Self-stratifying coatings for metallic substrates, *Progress in Organic Coatings*, 1996, **28**, 197-207.
112. H. Warson, *XXI FATIPEC Congress Book, Journal & Coating Technology*, 1992, **II**, pp. 7-10.
113. I. Nikiforow, J. Adams, A.M. König, A. Langhoff, K. Pohl, A. Turshatov and D. Johannsmann, Self-Stratification During Film Formation from Latex Blends Driven by Differences in Collective Diffusivity, *Langmuir*, 2010, **26**, 13162-13167.
114. J. Baghdachi, H. Perez, P. Talapatcharoenkit and B. Wang, Design and development of self-stratifying systems as sustainable coatings, *Progress in Organic Coatings*, 2015, **78**, 464-473.
115. W. Fang, Waterborne organic silicon-acrylic acid self-stratifying coating, CN Patent 101724326 B, 2012.
116. L. Wu and J. Baghdachi, Self-stratifying Polymers and Coatings, in *Functional Polymer Coatings: Principles, Methods, and Applications*, John Wiley & Sons, Vol. 12, 2015, pp. 197-214.
117. J. Baghdachi, Coatings go to work, *European Coatings Journal*, 2016, 24-28.
118. V.V. Verkholtantsev, Self-stratifying coatings for industrial applications, *Pigment and Resin Technology*, 2003, **32**, 300-306.
119. E. Langer, S. Waśkiewicz, H. Kuczyńska and G. Kamińska-Bach, Self-stratifying coatings based on Schiff base epoxy resins, *Journal of Coatings Technology and Research*, 2014, **11**, 865-872.

120. M. D. Soucek, Self-stratifying Corrosion Resistant Coatings, <https://www.uakron.edu/dotAsset/539e26ee-b1be-4073-8772-f3106b507c53.pdf>. [Accessed Dec 22, 2016]
121. V. V. Verkholtantsev, Heterophase and self-stratifying polymer coatings, *Progress in Organic Coatings*, 1995, **26**, 31-52.
122. A. Beaugendre, S. Degoutin, S. Bellayer, C. Pierlot, S. Duquesne, M. Casetta and M. Jimenez, Self-stratifying coatings: A review, *Progress in Organic Coatings*, 2017, **110**, 210-241.
123. C. Carr and E. Wallstöm, Theoretical aspects of self-stratification, *Progress in Organic Coatings*, 1996, **28**, 161-171.
124. E.A. Murashko, G.F. Levchik, S.V. Levchik, D.A. Bright and S. Dashevsky, Fire-retardant action of resorcinol bis(diphenyl phosphate) in PC-ABS blend. II. Reactions in the condensed phase, *Journal of Applied Polymer Science*, 1999, **71**, 1863-1872.
125. K. Huang and Q. Yao, Rigid and steric hindering bisphosphate flame retardants for polycarbonate, *Polymer Degradation and Stability*, 2015, **113**, 86-94.
126. Ishikawa T, Maki I, Koshizuka T, Ohkawa T and T. K, Effect of Perfluoroalkane Sulfonic Acid on the Flame Retardancy of Polycarbonate, *Journal of Macromolecular Science. Pure and Applied Chemistry*, 2004, **41 A**, 523-535.
127. M. Iji and S. Serizawa, New flame-retarding polycarbonate resin with silicone derivative for electronics products, *Nec Research & Development*, 1998, **39**, 82-87.
128. W. Funke, Preparation and properties of paint films with special morphological structure, *Journal of the Oil and Colour Chemists' Association*, 1976, **59**, 398-403.
129. S. Ma, T. Li, X. Liu and J. Zhu, Research Progress on Bio-based Thermosetting Resins, *Polymer International*, 2015, **65**, 164-173.
130. B. Ellis, Introduction to the Chemistry, Synthesis, Manufacture, and Characterization of Epoxy Resins, Blackie Academic & Professional, an imprint of Chapman & Hall, London, UK, 1993.
131. S.V. Levchik and E.D. Weil, Thermal decomposition, combustion and flame-retardancy of epoxy resins: a review of the recent literature, *Polymer International*, 2004, **53**, 1901-1929.
132. G. Camino, S.M. Lomakin and M. Lazzari, Polydimethylsiloxane thermal degradation Part 1. Kinetic aspects, *Polymer*, 2001, **42**, 2395-2402.
133. C.M. Hansen, *The 3D solubility parameter and solvent diffusion coefficient*, Aarhus Stiftsbogtrykkerie A/S, Copenhagen, 1967.
134. P. Vink and T. L. Bots, Formulation parameters influencing self-stratification of coatings, *Progress in Organic Coatings*, 1996, **28**, 173-181.
135. S. Sauerbrunn and R. Riesen, Thermosets: how to Avoid Incomplete Curing, <http://www.americanlaboratory.com/913-Technical-Articles/482-Thermosets-How-to-Avoid-Incomplete-Curing/>. [Accessed Aug 17, 2017]

136. A. Benazzouz, L. Moity, C. Pierlot, V. Molinier and J.M. Aubry, Hansen approach versus COSMO-RS for predicting the solubility of an organic UV filter in cosmetic solvents, *Colloids and Surfaces A: Physicochemical and Engineering Aspects*, 2014, **458**, 101-109.
137. S. Wu, Polar and nonpolar interactions in adhesion, *Journal of Adhesion*, 1973, **5**, 39.
138. Determination of wetting tension of polyethylene and polypropylene films and coatings (Modified viscking analytical technique), ASTM Standards D2578-67, Part 36, 1982.
139. Standard Test Methods for Rating Adhesion by Tape Test, ASTM Standards D3359-17, 2017.
140. Elcometer, Elcometer 107 Cross Hatch Cutter, <http://www.elcometer.com/en/coating-inspection/adhesion-testers/cross-hatch-adhesion-testers/elcometer-107-cross-hatch-cutter.html>. [Accessed Jun 6, 2017]
141. ColorCodeHex, Color Space Color Model, <https://www.colorcodehex.com/color-model.html>. [Accessed Jun 6, 2017]
142. A. Beaugendre, S. Degoutin, S. Bellayer, C. Pierlot, S. Duquesne, M. Casetta and M. Jimenez, Self-stratifying epoxy/silicone coatings, *Progress in Organic Coatings*, 2017, **103**, 101-110.
143. V.V. Verkholtantsev and M. Flavian, Polymer structure and properties of heterophase and self-stratifying coatings, *Progress in Organic Coatings*, 1996, **29**, 239-246.
144. ISO 4589-2, Determination of burning behaviour by oxygen index, 2017.
145. NF EN 60695-11-10, Essais relatifs aux risques du feu - Partie 11-10 : flammes d'essai - Méthodes d'essai horizontale et verticale à la flamme de 50 W, 2013.
146. B. ScharTEL and T.R. Hull, Development of fire-retarded materials—Interpretation of cone calorimeter data, *Fire and materials*, 2007, **31**, 327-354.
147. J. Luche, T. Rogaume, F. Richard and E. Guillaume, Characterization of thermal properties and analysis of combustion behavior of PMMA in a cone calorimeter, *Fire Safety Journal*, 2011, **46**, 451-461.
148. ISO 5 660, Reaction to fire tests—heat release, smoke production and mass loss rate - Part 1 Heat release rate (cone calorimeter method), 2002.
149. R.E. Lyon and R.N. Walters, Pyrolysis combustion flow calorimetry, *Journal of Analytical and Applied Pyrolysis*, 2004, **71**, 27-46.
150. C. Huggett, Estimation of rate of heat release by means of oxygen consumption measurements, *Fire and materials*, 1980, **4**, 61-65.
151. ISO-4892-3, Methods of exposure to laboratory sources - Part 3: Fluorescent UV lamps, 2013.
152. A. Beaugendre, S. Saidi, S. Degoutin, S. Bellayer, C. Pierlot, S. Duquesne, M. Casetta and M., Jimenez, One pot flame retardant and weathering resistant coatings for plastics: a novel approach, *RSC Advance*, 2017, **7**, 40682 - 40694.
153. M. Levin and P. Redelius, Determination of Three-Dimensional Solubility Parameters and Solubility Spheres for Naphthenic Mineral Oils, *Energy & Fuels*, 2008, **22**, 3395-3401.

154. ICL Industrial Product, Fyrolflex® BDP, Typical properties, http://icl-ip.com/wp-content/uploads/2012/05/090625_Fyrolflex_BDP.pdf. [Accessed Aug 29, 2017]
155. ICL Industrial Product, Fyrolflex RDP, Typical properties, <http://icl-ip.com/products/fyrol-rdp/>. [Accessed Aug 29, 2017]
156. Z. Wang, E. Han and W. Ke, Effect of nanoparticles on the improvement in fire-resistant and anti-ageing properties of flame-retardant coating, *Surface and Coatings Technology*, 2006, **200**, 5706-5716.
157. C.S. Wu, Y.L. Liu and Y.S. Chiu, Epoxy resins possessing flame retardant elements from silicon incorporated epoxy compounds cured with phosphorus or nitrogen containing curing agents, *Polymer*, 2002, **43**, 4277-4284.
158. X. Li, Y. Ou and Y. Shi, Combustion behavior and thermal degradation properties of epoxy resins with a curing agent containing a caged bicyclic phosphate, *Polymer Degradation and Stability*, 2002, **77**, 383-390.
159. C. Xie, B. Zeng, H. Gao, Y. Xu, W. Luo, X. Liu and L. Dai, Improving thermal and flame-retardant properties of epoxy resins by a novel reactive phosphorous-containing curing agent, *Polymer Engineering & Science*, 2014, **54**, 1192-1200.
160. L. A. Mercado, M. Galià and J. A. Reina, Silicon-containing flame retardant epoxy resins: Synthesis, characterization and properties, *Polymer Degradation and Stability*, 2006, **91**, 2588-2594.
161. C.H. Tseng, H.B. Hsueh and C.Y. Chen, Effect of reactive layered double hydroxides on the thermal and mechanical properties of LDHs/epoxy nanocomposites, *Composites Science and Technology*, 2007, **67**, 2350-2362.
162. A. Toldy, N. Tóth, P. Anna and G. Marosi, *Polymer Degradation and Stability*, 2006, **91**, 585-592.
163. B. Guo, D. Jia and C. Cai, Effects of organo-montmorillonite dispersion on thermal stability of epoxy resin nanocomposites, *European Polymer Journal*, 2004, **40**, 1743-1748.
164. F.Y. Hshieh and R.R. Buch, Controlled-atmosphere cone calorimeter studies of silicones, *Fire and Materials*, 1997, **21**, 265-270.
165. R. Buch, Rate of heat release and related fire parameters for silicones, *Fire Safety Journal*, 1991, **17**, 1-12.
166. C. A. Wilkie and A. B. Morgan, *Fire retardancy of polymeric materials*, Group T. & F., ed. CRC press, Boca Raton, FL, USA, 2009.
167. X.L. Chen, C.M. Jiao and Y. Wang, Synergistic effects of iron powder on intumescent flame retardant polypropylene system, *Express Polymer Letters*, 2009, **3**, 359-365.
168. F. Laoutid, M. Lorgouilloux, D. Lesueur, L. Bonnaud and P. Dubois, Calcium-based hydrated minerals: Promising halogen-free flame retardant and fire resistant additives for polyethylene and ethylene vinyl acetate copolymers, *Polymer Degradation and Stability*, 2013, **98**, 1617-1625.
169. D. Price, G. Anthony and P. Carty, Introduction: polymer combustion, condensed phase pyrolysis and smoke formation, in *Fire Retardant Materials*, ed. CRC press, 2001.

170. EFRA, How do they work?, *How materials burn?*, 2016, <http://www.cefic-efra.com/index.php/en/how-do-they-work-sp-2254-en-gb>. [accessed Mar 3, 2007]
171. D. Price, K. Pyrah, T.R. Hull, G.J. Milnes, J.R. Ebdon, B. J. Hunt and P. Joseph, Flame retardance of poly(methyl methacrylate) modified with phosphorus-containing compounds, *Polymer Degradation and Stability*, 2002, **77**, 227-233.
172. P. Hornsby, Fire-Retardant Fillers, in *Fire Retardancy of Polymeric Materials*, ed. CRC press, Boca Raton, FL, USA, 2010, pp. 163-185.
173. J. Silver, Introduction to Fe chemistry, in *The chemistry of iron*, Glasgow, UK, Blackie Academic and Professional, 1993.
174. P. Carty, Flame retardants: iron compounds, their effect on fire and smoke in halogenated polymers, in *Plastics Additives: An A-Z reference*, ed. G. Pritchard, Springer Netherlands, Dordrecht, 1998, pp. 307-314.
175. P. Carty, E. Metcalfe and S. White, A review of the role of iron containing compounds in char forming/smoke suppressing reactions during the thermal decomposition of semi-rigid poly(vinyl chloride) formulations, *Polymer*, 1992, **33**, 2704-2708.
176. G. A. Olah, Freidel Crafts and Related Reactions. Volume I: General Aspects, *Inorganic Chemistry*, 1964, **3**, 1205-1206.
177. H. Marsh, D. Crawford and D.W. Taylor, Catalytic graphitization by iron of isotropic carbon from polyfurfuryl alcohol, 725–1090 K. A high resolution electron microscope study, *Carbon*, 1983, **21**, 81-87.
178. S. Krishnan, R.L. Price and R.J. White, Iron oxide pigmented, polycarbonate compositions, US Patent 4650823 A, Mobay Corporation, 1987.
179. G.F. Levchik, S.A. Vorobyova, V.V. Gorbarenko, S.V. Levchik and E.D. Weil, Some Mechanistic Aspects of the Fire Retardant Action of Red Phosphorus in Aliphatic Nylons, *Journal of Fire Sciences*, 2000, **18**, 172-182.
180. F. Laoutid, L. Ferry, J. M. Lopez-Cuesta and A. Crespy, Flame-retardant action of red phosphorus/magnesium oxide and red phosphorus/iron oxide compositions in recycled PET, *Fire and materials*, 2006, **30**, 343-358.
181. E.D. Weil and N.G. Patel, Iron compounds in non-halogen flame-retardant polyamide systems, *Polymer Degradation and Stability*, 2003, **82**, 291-296.
182. E. Gallo, U. Braun, B. Scharrel, P. Russo and D. Acierno, Halogen-free flame retarded poly(butylene terephthalate) (PBT) using metal oxides/PBT nanocomposites in combination with aluminium phosphinate, *Polymer Degradation and Stability*, 2009, **94**, 1245-1253.
183. R.L. Markezich, Flame retardants: synergisms involving halogens, in *Plastics Additives: An A-Z reference*, ed. G. Pritchard, Springer Netherlands, Dordrecht, The Netherlands, 1998, pp. 327-338.
184. P. Carty and B.M. Adger, Iron-containing organometallic compounds as flame-retarding/smoke-suppressing additives for semi-rigid poly(vinyl chloride), *Applied Organometallic Chemistry*, 1990, **4**, 127-131.

185. P. Carty, E. Metcalfe and T.J. Saben, Thermal analysis of plasticized PVC containing flame retardant/smoke suppressant inorganic and organometallic iron compounds, *Fire Safety Journal*, 1991, **17**, 45-56.
186. W.P. Whelan, Synergistic flame-retardant activity of iron compounds in halogen-containing nitrile polymer compositions, *Journal of Fire Retardant Chemistry*, 1979, **6**, 206-219.
187. A. Laachachi, M. Cochez, M. Ferriol, J.M. Lopez-Cuesta and E. Leroy, Use of oxide nanoparticles and organoclays to improve thermal stability and fire retardancy of poly(methyl methacrylate), *Materials Letters*, 2005, **59**, 36-39.
188. M.M. Hirschler, Reduction of smoke formation from and flammability of thermoplastic polymers by metal oxides, *Polymer*, 1984, **25**, 405-411.
189. K.J. Nangrani, R. Wenger and P.G. Daugherty, Effect of pigments on the flammability of reinforced thermoplastics, *Plastics compounding*, 1988, **11**, 27-31.
190. H. Liu, Q. Zhong, Q. Kong, X. Zhang, Y. Li and J. Zhang, Synergistic effect of organophilic Fe-montmorillonite on flammability in polypropylene/intumescent flame retardant system, *Journal of Thermal Analysis and Calorimetry*, 2014, **117**, 693-699.
191. A. Laachachi, E. Leroy, M. Cochez, M. Ferriol and J. M. Lopez Cuesta, Influence of TiO₂ and Fe₂O₃ fillers on the thermal properties of poly(methyl methacrylate) (PMMA), *Polymer Degradation and Stability*, 2005, **89**, 344-352.
192. T. Kashiwagi, J.W. Gilman, K.M. Butler, R.H. Harris, J.R. Shields and A. Asano, Flame retardant mechanism of silica gel/silica, *Fire and materials*, 2000, **24**, 277-289.
193. L. Truffault [online], Synthèse et caractérisation de nanoparticules à base d'oxydes de cérium et de fer pour la filtration des UV dans les produits solaires, Université d'Orléans, 2010.
194. P. Xu, G.M. Zeng, D.L. Huang, C.L. Feng, S. Hu, M.H. Zhao, C. Lai, Z. Wei, C. Huang, G.X. Xie and Z.F. Liu, Use of iron oxide nanomaterials in wastewater treatment: A review, *Science of The Total Environment*, 2012, **424**, 1-10.
195. S. SA, Fire Resistance (LOI), <http://omnexus.specialchem.com/polymer-properties/properties/fire-resistance-loi>. [Accessed Mar 3, 2007]
196. E. Gallo, B. Schartel, D. Acierno and P. Russo, Flame retardant biocomposites: Synergism between phosphinate and nanometric metal oxides, *European Polymer Journal*, 2011, **47**, 1390-1401.
197. P. Carty and S. White, The Importance of Char Forming Reactions in Thermoplastic Polymers, *Fire and Materials*, 1994, **18**, 151-166.
198. J.E. Robertson, Thermal Degradation Studies of Polycarbonate, Virginia Polytechnic Institute, Blackburg, Virginia, 2001.
199. H. Yan, C.X. Lu, D.Q. Jing and X.I. Hou, Chemical degradation of amine-cured DGEBA epoxy resin in supercritical 1-propanol for recycling carbon fiber from composites, *Chinese Journal of Polymer Science*, 2014, **32**, 1550-1563.
200. B. Gardelle, S. Duquesne, C. Vu and S. Bourbigot, Thermal degradation and fire performance of polysilazane-based coatings, *Thermochimica Acta*, 2011, **519**, 28-37.

201. P. Kusch, Application of Pyrolysis-Gas Chromatography/Mass Spectrometry (Py-GC/MS), in *Comprehensive Analytical Chemistry*, ed. T.A.P. Rocha-Santos and A.C. Duarte, ed. Elsevier, 2017, vol. 75, pp. 169-207.
202. F. Chainet, L.L. Meur, C.P. Lienemann, J. Ponthus, M. Courtiade and O.F.X. Donard, Characterization of silicon species issued from PDMS degradation under thermal cracking of hydrocarbons: Part 2 – Liquid samples analysis by a multi-technical approach based on gas chromatography and mass spectrometry, *Fuel*, 2014, **116**, 478.
203. B. Gardelle, S. Duquesne, V. Rerat and S. Bourbigot, Thermal degradation and fire performance of intumescent silicone-based coatings, *Polymer Advanced technologies*, 2012, **24**, 62-69.
204. S. Hamdani, C. Longuet, D. Perrin, J.M. Lopez-cuesta and F. Ganachaud, Flame retardancy of silicone-based materials, *Polymer Degradation and Stability*, 2009, **94**, 465-495.
205. F. Chainet, C.P. Lienemann, M. Courtiade, J. Ponthus and O.F.X. Donard, Silicon speciation by hyphenated techniques for environmental, biological and industrial issues: A review, *Journal of Analytical Atomic Spectrometry*, 2011, **26**, 30-51.
206. G. Deshpande and M.E. Rezac, Kinetic aspects of the thermal degradation of poly(dimethyl siloxane) and poly(dimethyl diphenyl siloxane), *Polymer Degradation and Stability*, 2002, **76**, 17-24.
207. N. Grassie, K.F. Francey, I.G. Macfarlane, The thermal degradation of PDMS. Part 4: poly(dimethyl/diphenyl siloxane), *Polymer Degradation and Stability*, 1980, **2**, 67-83.
208. Netzsch, Polycarbonate - Conductivité thermique, <https://www.netzsch-thermal-analysis.com/fr/materiaux-applications/polymeres/polycarbonate-conductivite-thermique/>. [Accessed Sep 3, 2007]
209. J.E.J. Staggs, Thermal conductivity estimates of intumescent chars by direct numerical simulation, *Fire Safety Journal*, 2010, **45**, 228-237.
210. C.E. Hoyle, H. Sha and G.L. Nelson, Photochemistry of bisphenol-A based polycarbonate: the effect of the matrix and early detection of photoFries product formation, *Journal of Polymer Science Part A: Polymer Chemistry*, 1992, **30**, 1525-1533.
211. N. Nagai, H. Okumura, T. Imai, I. Nishiyama, Depth profile analysis of the photochemical degradation of polycarbonate by infrared spectroscopy, *Polymer Degradation and Stability*, 2003, **81**, 491-496.
212. A.L. Andradý, N.D. Searle, L.F.E. Crewdson, Wavelength sensitivity of unstabilized and UV stabilized polycarbonate to solar simulated radiation, *Polymer Degradation and Stability*, 1992, **35**, 237-247.
213. M. Diepens and P. Gijsman, Influence of light intensity on the photodegradation of bisphenol A polycarbonate, *Polymer Degradation and Stability*, 2009, **94**, 34-38.
214. A. Rivaton, Recent advances in bisphenol-A polycarbonate photodegradation, *Polymer Degradation and Stability*, 1995, **49**, 163-179.
215. N. Rajagopalan and A. S. Khanna, Effect of nano-ZnO in lowering yellowing of aliphatic amine-cured DGEBA-based epoxy coatings on UV exposure, *International Journal of Scientific and Research Publications*, 2013, **3**, 1-11.

216. C. Madeleine-Perdrillat [online], Approche expérimentale et théorique de la dégradation des polydiméthylsiloxanes, Université Blaise Pascal, Clermont-Ferrand II, 2011.
217. G. Ducom, B. Laubie, A. Ohannessian, C. Chottier, P. Germain and V. Chatain, Hydrolysis of polydimethylsiloxane fluids in controlled aqueous solutions, *Water Science and Technology*, 2013, **68**, 813-820.
218. E.P. Plueddemann, *Silane Couplings Agents*, 2nde Ed., Springer Science+Business Media, LLC, Midland, MI, USA, 1991.
219. H. Chang, Z. Wan, X. Chen, J. Wan, L. Luo, H. Zhang, S. Shu and Z. Tu, Temperature and humidity effect on aging of silicone rubbers as sealing materials for proton exchange membrane fuel cell applications, *Applied Thermal Engineering*, 2016, **104**, 472-478.
220. Z. Wang, E. Han and W. Ke, Effect of nanoparticles on the improvement in fire-resistant and anti-ageing properties of flame-retardant coating, *Surface and Coatings Technology*, 2006, **200**, 5706-5716.
221. G. Socrates, *Infrared and Raman characteristic group frequencies: tables and charts*, John Wiley & Sons, 3rd Ed, 2004.
222. R.E. Lyon, K.E. Chike and S.M. Angel, In-situ cure monitoring of epoxy resins using fibreoptic Raman spectroscopy, *Journal of Applied Polymer Science*, 1994, **53**.
223. H.H. Dannenberg, W.R., Determination of cure and analysis of cured epoxy resins, in *Analytical Chemistry*, 1956, vol. 28, pp 81-90.
224. MG. González, J.C. Cabanelas and J. Baselga, Applications of FTIR on Epoxy Resins - Identification, Monitoring the Curing Process, Phase Separation and Water Uptake, *Infrared Spectroscopy - Materials Science, Engineering and Technology*, Prof. Theophanides Theophile (Ed.), InTech, 2012.

Appendix

Appendix 1: Self-stratifying coatings: A review

Progress in Organic Coatings 110 (2017) 210–241



Contents lists available at ScienceDirect

Progress in Organic Coatings

journal homepage: www.elsevier.com/locate/porgcoat

Review

Self-stratifying coatings: A review

A. Beaugendre^a, S. Degoutin^a, S. Bellayer^a, C. Pierlot^b, S. Duquesne^a, M. Casetta^a,
M. Jimenez^{a,*}^a Univ. Lille, CNRS, UMR 8207, UMET, Unité Matériaux et Transformations, ENSCL, F 59 000 Lille, France^b Univ. Lille, CNRS, UMR 8181, EA CMF-4478/Unité de Catalyse et de Chimie du Solide, F 59 000 Lille, France

ARTICLE INFO

Article history:

Received 18 January 2017
Received in revised form 7 March 2017
Accepted 9 March 2017
Available online 23 March 2017

Keywords:

Self-stratifying coatings
Self-layering
Surface tension
Solubility parameters
Incompatible polymer blend
Heterophase

ABSTRACT

Self-stratifying coatings are promising coating systems based on incompatible polymer blends which can produce polymer/polymer laminate. A complex multi-layer or gradient coating structure is formed from one single coat, providing an undercoat and finishing coating. The preferential distribution of concentration through the film thickness greatly eliminates the interfacial adhesion failure without compromising the advantages of a multi-layer system, and thus favors an industrial eco-efficient process. Powder, water-borne and solventborne coating systems are able to stratify: the most well-known and effective systems are described in this review. Finally, this concept constitutes a great possible versatile process for a broad range of applications and could thus favor the development of new products, taking into account the reduction of solvent and labor cost

© 2017 Elsevier B.V. All rights reserved.

Contents

1. Introduction	211
1.1. Historical background	211
1.2. The concept	211
1.3. Degree of stratification	212
1.4. Evaluation of stratification	213
1.4.1. Characterization methods	213
1.4.2. Coatings properties	214
2. Factors affecting self-stratification	216
2.1. Theoretical aspect of self-Stratification	216
2.1.1. Kinetic and thermodynamic conditions for stratification	216
2.1.2. Mechanisms of self-stratification	216
2.2. Experimental aspect of self-Stratification	220
2.2.1. The formulation of the coating	220
2.2.2. Hansen's solubility parameters	222
2.2.3. The substrate	225
2.2.4. The processing	225
3. Models to build self-stratifying systems	226
3.1. UNIFAC model	226
3.1.1. Theory	226
3.1.2. Experimental approaches to check the validity of the model	227
3.2. Model based on surface energy	228
3.2.1. Theory	228
3.2.2. Experimental approaches to check the validity of the model	229

* Corresponding author.

E-mail address: maude.jimenez@univ-lille1.fr (M. Jimenez).

3.3.	Model based on Hansen solubility parameters	230
3.4.	Model based on phase state diagram	231
4.	Promising self-stratifying coatings	232
4.1.	Resins	232
4.1.1.	Binary blends of thermoplastic and non-crosslinked thermoset resins	232
4.1.2.	Blend of thermoplastic and thermoset resins involving a curing agent	233
4.2.	Solvents	235
4.3.	Additives	236
4.3.1.	Addition of one pigment	236
4.3.2.	Addition of more than one pigment	236
4.3.3.	Addition of an adhesion promoter	237
4.4.	Substrate	237
4.4.1.	Plastics substrates	237
4.4.2.	Glass substrates	237
4.4.3.	Metallic substrates	237
4.5.	Processing considerations	238
4.6.	Conclusion	238
5.	Challenges and future applications	239
5.1.	Self-Stratifying coatings for industrial applications	240
5.2.	Future potential applications for developing self-stratifying coatings	240
6.	Conclusion	240
	Acknowledgements	240
	References	240

1. Introduction

Conventionally, coating systems are composed of several layers, each layer providing a specific function. A common three layer coating system consists of a primer and a topcoat with an intermediate coating whose composition depends on the desired properties (Fig. 1). The primer brings corrosion resistance and enhances adhesion of the coating to the substrate, while the topcoat provides the aesthetics aspect, the durability, scratch and chemical resistance.

This multilayer system requires complex formulation for each layer, long time application and curing procedures which are not always adapted to industrial constraints, contributing also to environmental waste generation, pollution and to the use of excessive amount of energy. To overcome these drawbacks, a new effective and economical concept has been developed which aims at reducing the number of layers while providing a coating with equivalent or better performance than a multilayered system. This approach allows a one-step formation of complex multi-layer or gradient coating structures which, after application on a substrate, spontaneously form two distinct layers, thus providing an undercoat and finishing coating in one step (Fig. 2).

During the film formation process, the coating separates spontaneously into two continuous adherent functional layers to form a thermodynamically stable layered coating. The preferential distribution of concentration through the film thickness greatly eliminates the interfacial adhesion failure without compromising the advantages of a multi-layer system [1–3].

This concept constitutes an eco-efficient process for various application fields and industrial applications (automotive, self-healing . . .), and several patents have already been published.

The purpose of this review is to present the theoretical and experimental aspects of the self-layering concept. The different models reported in the literature to predict the stratification will be considered, and the most promising systems, with their experimental and theoretical approach, will be presented.

1.1. Historical background

About two decades ago, Funke and his collaborators published some work on self-stratifying coatings and introduced the concept of blending incompatible polymers to allow a one-step formation

of complex multi-layer or gradient coating structures. They used a mixture of two powdered polymers applied on a metallic substrate and tried to minimize the free interfacial energy by heating both polymers above their melting temperature (T_m). From these results, they defined the characteristics necessary for a coating to spontaneously layer in terms of solubility parameters and by capillary rise test (combination of surface tension and viscosity measurements) [4]. From those results, specific formulations for stratified powder coatings were patented [5].

Later on, the concept was applied to liquid solvent-based [6–10] and waterborne [11,12] paints, with the use of selective coagulation, electrodeposition, substrate wetting or penetration processes to create specific driving forces for self-stratification. V. Verkholantsev tested formulations based on liquid coatings from two polymers diluted in a common solvent. He succeeded to extend the theory that phase separation can occur as the solvent evaporates with subsequent layer formation, thus resulting in a film which has better overall performances than when the components are applied separately [7,13].

Self-stratifying coatings are promising coating systems, and provide major advantages including economic benefit, decreased time of processing (application of only one layer), no contamination between layers, improved interlayer bonding; thus, less chance of inter-layer adhesion failure is expected. It combines optimized surface and adhesion properties in one coating composition. The enhancement of adhesive properties to a substrate contributes to protection against corrosion (for metallic substrates), and to the upgrading of surface properties like the enhancement of chemical durability, ultraviolet (UV) and weather resistance. As a sustainable process, it helps reducing emissions and energy consumption [14].

Up to now, these coatings have been developed for automotive applications [15], self-healing coatings, weather-resistant or corrosion resistant solvent based coatings [13], waterborne coatings [16] and research works are still in progress to improve the process [14,17].

1.2. The concept

A coating system is formulated with a mixture of several chemical substances which are categorized as binder, volatile

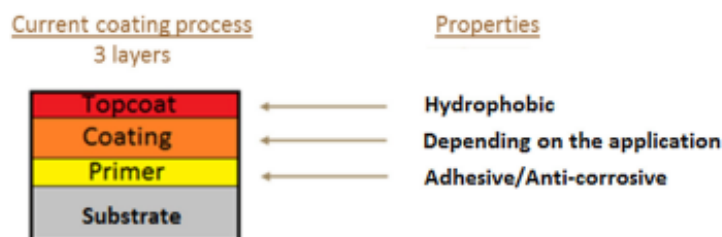


Fig. 1. Common coating system.



Fig. 2. Self-stratifying approach.

components, pigments and additives. The binder constitutes the continuous film that allows the adhesion to the substrate whereas volatile components are liquid substances used to adjust the coating system to a suitable viscosity for application, allowing the film formation to occur. Pigments are insoluble solid particles which bring, among others, the color to the coating; additives such as catalysts, stabilizers, flow modifiers, etc. are added to the formulation to adjust the coating properties.

During film formation, physical and chemical changes occur and the volatile components evaporate, therefore enabling the drying of the liquid coating mixture into a solid state film. During the evaporation process, entanglement of the polymer chains occurs, forming a tight-knit matrix. After film formation, further reactions like oxidation or crosslinking (e.g., two-component epoxies and urethanes) are required to generate a cross-linked film of higher molecular weight. The film formation process for a solventborne coating is depicted in Fig. 3. For powdered coating systems, the powder melts upon heating, leading to the formation of a solid state film. The self-stratification occurs at this stage of the process.

Under certain conditions, the development of film-forming formulations based on an homogeneous mixture of incompatible polymers can lead to the formation of a polymer/polymer laminated structure. When phase separation takes place, it results in a fine heterophase polymer structure and liquid polymer blend compositions form non-homogeneous in-layer (self-stratified) coatings (Fig. 4) [18].

Experimentally, to produce an homogeneous solution, two incompatible resins are dissolved in a common solvent or in a mixture of several solvents, and the coating is applied in a single step. The mixing of the incompatible resins must take place just before the application on a substrate since chemical and physical changes occur directly after the mixing. The separation thus occurs, followed by stratification forming a two-layer coating system. If the system is crosslinkable (blend of thermoplastic and crosslinkable resins), the molecular weight rapidly increases due to crosslinking reactions until the gel point is reached. A 3D network is then built which separates from the solution because of its increasing insolubility and decreasing swellability. The solution is expelled from the nets, and meanwhile it becomes poorer in crosslinkable species and richer in thermoplastic resin [8].

The self-stratification can be induced by physical and/or chemical changes occurring at one or more of the different stages of the

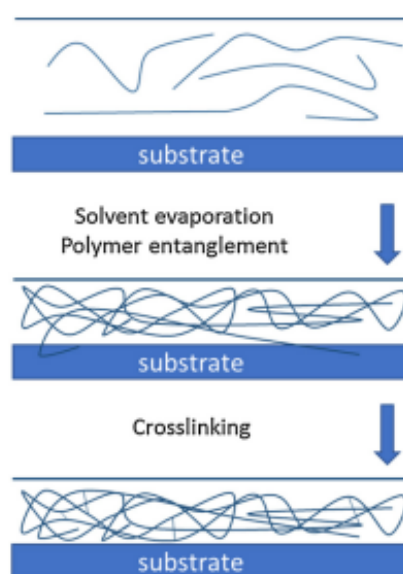


Fig. 3. Film formation process for solventborne paint.

process: (a) during solvent evaporation, (b) during heat and/or mass exchange, (c) during chemical reaction [13]. The simplified process is illustrated in Fig. 5.

Finally, each layer performs a specific function: the lower layer promotes adhesion and protects the substrate while the upper layer brings an aesthetic aspect and provides protection against atmospheric conditions [20]. The lower layer is also referred to as the basis resin, and the upper layer as the stratifying resin.

1.3. Degree of stratification

Mixtures of incompatible polymer blends can lead to different degrees of stratification after the formation of the film, which can

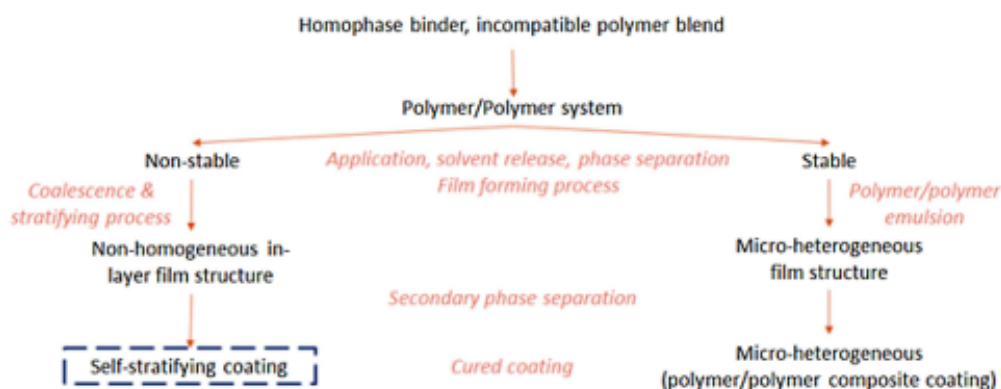


Fig. 4. Steps of self-stratifying concept compared to common process [18].

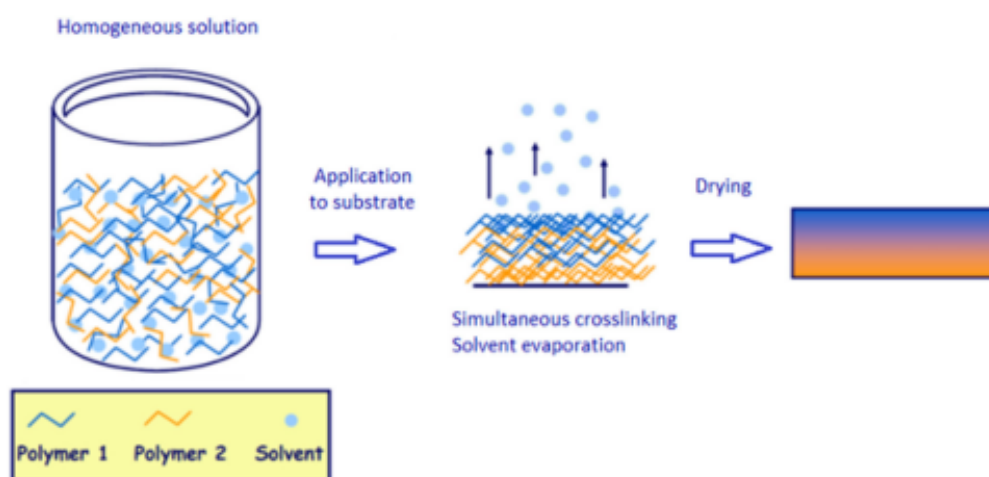


Fig. 5. Film forming process with self-stratifying coatings [19].

be rated from I to IV (Fig. 6). Film surface and cross-section analyses allow determining such classification [8].

The type I pattern is related to a perfect stratification. The mixture of incompatible polymers gives rise to two well distinct and homogeneous layers. The phase separation corresponding to a type II pattern leads to a stratification characterized by a homogeneous concentration gradient more or less pronounced through the film thickness. In the type III pattern, there is formation of isolated spherical particles of various diameters composed of only one resin, or of mostly one resin, dispersed in the continuous matrix of the other polymer. A concentration gradient of the spherical particles can appear throughout the film thickness. Finally, the type IV pattern is composed of large islands or isthmus shaped regions very rich in one of the components or constituted of only that component. The coalescence of spherical particles can be responsible for the formation of the islands, which can exhibit, like in the previous pattern, a concentration gradient.

However, it is important to notice that a 100% degree of stratification can lead to a significant reduction of interlayer adhesion and thus to poor properties [20].

1.4. Evaluation of stratification

Self-stratification in coatings can be expressed in terms of [21]:

- Concentration: concentration difference in one resin between the base and top layers of the coating, or determination of the concentration in one selected polymer through the coating thickness.
- Thickness: determination of the thickness of layers having distinct polymer structure or composition.
- Properties: properties of both coating interfaces can be analyzed (hardness, chemical resistance, glass transition temperature ...).

1.4.1. Characterization methods

Analysis of the stratification can be carried out with unpigmented and pigmented systems. Various analytical methods are used to characterize both the surface of dried coatings and the cross sections of films. Most evaluations can be performed by visual or microscopic examinations. The visual appearance of unpigmented films can reveal the layering: translucent or cloudy films generally indicate respectively compatibility or incompatibility, whereas color difference can be used with pigmented systems. Also, the occurrence of fine, medium or coarse structures refer to some extent to the degree of incompatibility. Irradiation of the sample with UV light might be an alternative for an easier analysis as it can lead to the discoloration of some binders.

Attenuated Total Reflectance—Fourier Transformed Infrared spectroscopy (ATR-FTIR) is used to analyze the top and bottom surfaces of coated film after its delamination from the substrate.

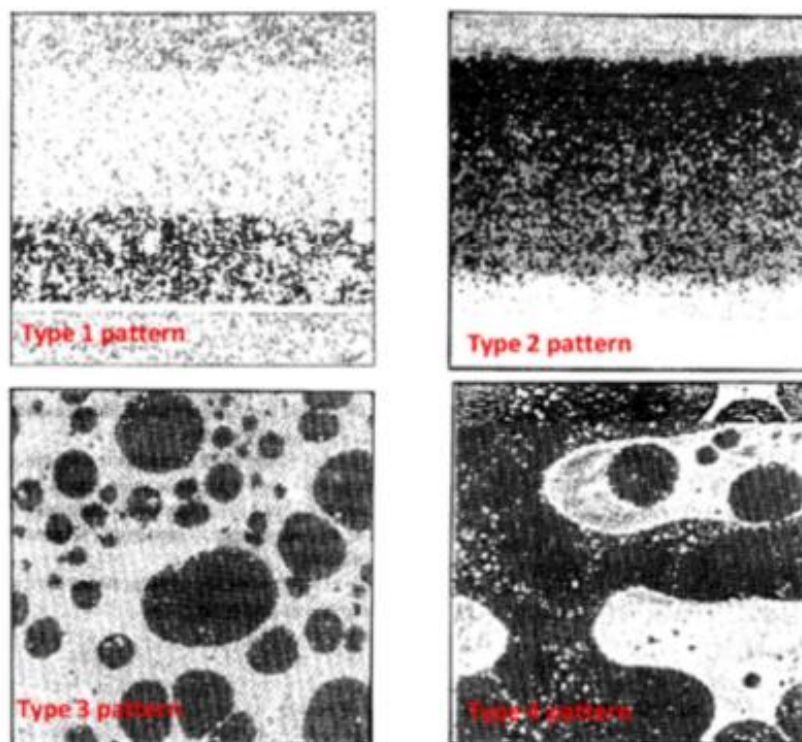


Fig. 6. Type I to IV patterns defining the degree of stratification of a coating [8].

The analysis and comparison of spectra can provide information about the concentration of each polymer at both surfaces, and lead to the degree of stratification. Fig. 7 gives an example of ATR-FTIR film surface analysis of an epoxy/vinyl self-stratified coating (75/25 wt.%, 120 μm Dry Film Thickness (DFT)) applied by spray on aluminum foil and delaminated. The absorption bands of vinyl resin at 1100 cm^{-1} are twice as intense on the top interface than on the base layer [21].

Raman spectroscopy may be used as a complementary technique to study the concentration of a selected polymer, on both sides of the removed coating or through the film thickness by mapping.

Scanning Electron Microscopy with X-ray analysis (SEM-EDX) is another efficient tool to provide information about the degree of self-stratification: a mapping of a characteristic chemical element can provide information about the concentration of each polymer on either both interfaces or in the inner coating structure (Fig. 8). The analysis of cross-sections (mainly obtained by fragile cut) gives information about both non-homogeneous-in-layer and heterophase polymer structures, especially when combined with microprobe analysis [22,23].

The pigmentation of the systems allows to use other analytical tools to determine the degree of pigment distribution, and thus stratification: reflectance spectrophotometry, color difference and optical polarizational-interdifferential microscope biolar [24].

Atomic Force Microscopy (AFM) allows working on cross-sections of films (particularly for multiphase latexes or organic coatings whose composition is not homogeneous). This technique has been used by Asawarala to make pictures of a self-stratified acrylic/styrene acrylic blend prepared by cryogenic microtoming (Fig. 9). The blend containing Low Surface Energy components

(LSE drivers) shows a layering effect through the thickness. Therefore, the AFM technique allowed demonstrating that, in addition to migrating to the surface, the LSE drivers could favor stratification throughout the film [25].

1.4.2. Coatings properties

Common coating tests can be used to characterize self-stratified coatings (adhesion tests – pull-off, cross hatch cutter, bench test –, gloss and color retention, resistance to weathering, chemicals ...), and to compare them to a coating obtained after the application of successive layers.

Tests with a climatic chamber (salt spray chamber) can be performed to evaluate changes in terms of blistering size, density and width of the corrosion around the scratch (overall coating measurement). For example, QUV A weathering tests were carried by Asawarala and his collaborators to compare the gloss retention and color difference in a tinted light blue paint with three systems: a paint formula containing 25% of a self-stratifying acrylic latex replacing a styrene acrylic latex in the formulation, a styrene acrylic paint and a two coat system containing a styrene acrylic and an acrylic clear coat used as the standard [25]. Table 1 reports results obtained after 2500 h exposure in QUV A climatic chamber.

Results show higher gloss retention with the self-stratifying paint compared to classical styrene acrylic paint. Moreover, the self-stratifying paint has a gloss retention relatively close to the clear coated standard paint. Additionally, quite comparable color difference is obtained between the control and the self-stratifying coating after 2500 h of QUV A exposure (respectively 5 versus 6.5% in the change of color) whereas the non stratifying styrene acrylic paint shows a significant drop in its color change after exposure (26% difference). In that case, self-stratifying coatings can thus be

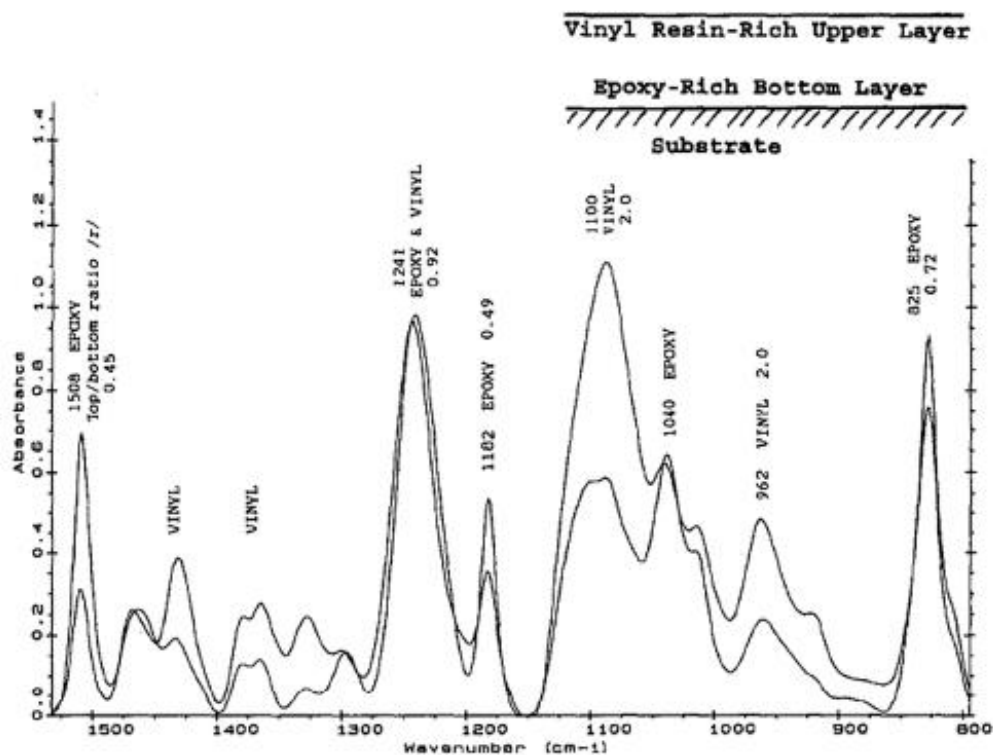


Fig. 7. ATR-FTIR spectra of a self-stratified epoxy/vinyl coating [21].

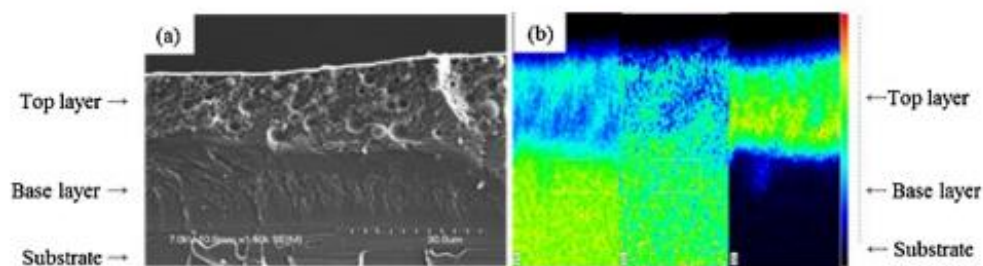


Fig. 8. SEM micrograph of a cross-section of an epoxy/silicone based coating in butylacetate: xylene (1:1): (a) self-stratified coating, and the corresponding (b) EDS mappings of Carbon, Oxygen and Silicon [23].

Table 1
QUV A results after 2500 h.

	Gloss retention (%)			Color difference ΔE (NBS units)
	60 °C at 0 h	60 °C at 2500 h	% retention	
Self-stratifying acrylic/styrene acrylic	84	59	70	6.5
Styrene acrylic	84	14	16	26
Clear coat/styrene acrylic	87	71	81	5

compared to the two-coat paint system in terms of gloss and color retention.

Finally, the self-stratifying coating approach can be used for a broad range of applications, and depending on the nature of the

coating, stratification can be evidenced by various characterization methods. In addition to be economically attractive, improved properties can be obtained if all the factors affecting the stratification can be controlled and adjusted.

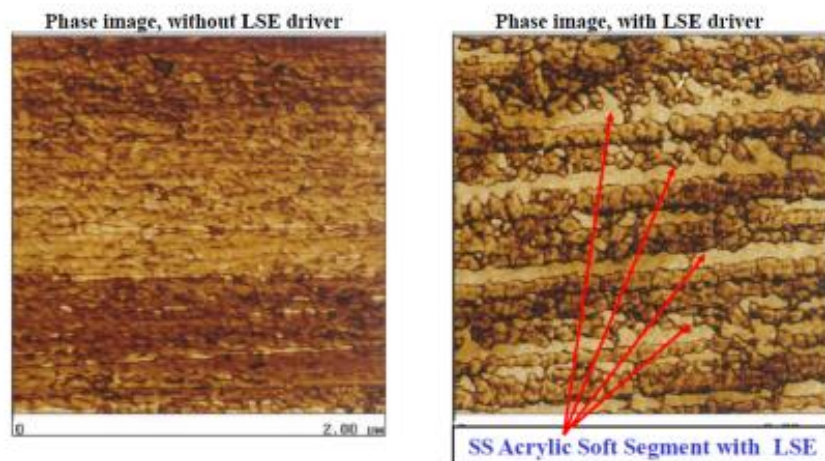


Fig. 9. Cross-sectional AFM: 25% self-stratifying acrylic in a styrene acrylic medium.

The section 2 to 4.5 are presented in the chapter I of this manuscript.

4.6. Conclusion

In this part of the paper, it was shown that numerous factors have to be taken into account when designing self-stratifying coatings, each factor affecting the stratification process. Even if their influence is not yet fully elucidated, some general conclusions can be drawn.

Factors playing a significant role in the stratification process are:

- **Resins:** the most efficient systems include a thermoplastic and a thermoset resin, crosslinked with a hardener. The nature of the resin, as well as its combination with solvents, curing agent, pigments, substrates and additives have a non-negligible impact on the stratification level. Commercial resins are mainly used for the

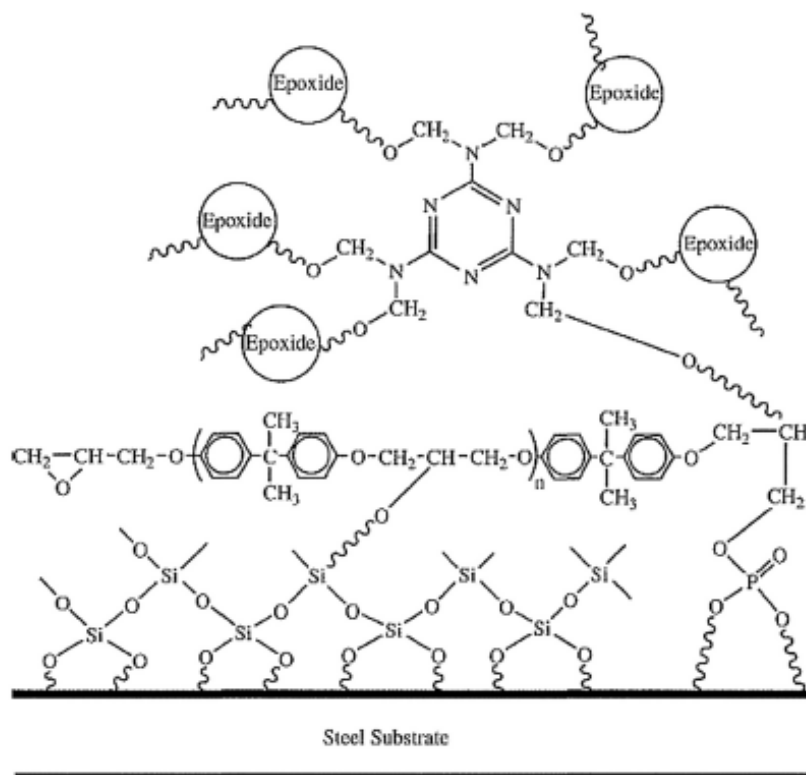


Fig. 29. Proposed mechanism for the interaction between hybrid coatings and a steel substrate [53].

coating formulation, and much less frequently synthesized but in both cases, good level of stratification can be obtained.

- **Solvents:** For high surface energy resins, a solvent with a high volatility and polarity should be used. For low surface energy resins, a solvent with a low volatility and polarity is preferable. Solvents are chosen according to their respective Hansen solubility parameters and to the type of resins and are generally: xylene, a blend of MIBK: xylene or MIBK: xylene: 1-methoxy-2-propanol or xylene: butylacetate. The rate of solvent evaporation should not be too high to allow the binders to separate and to form layers before the increase in viscosity of the system.
- **Additives:** The addition of one pigment has no negative effect on the stratification process as far as its dispersion is optimal: the degree of phase separation is the same or even better than in the case of pigment-free systems. Pigments are useful for the detection of stratification, and can upgrade the properties of the coating when properly selected. Usually, titanium dioxide is blended within the thermoplastic medium and is used for its intrinsic properties (mechanical, chemical and weather resistance...) and ease of detection by microscopic analyses. Red iron oxide, zinc phosphate and chromium oxide can also exhibit good results in self-stratifying coatings. Red iron oxide and zinc phosphate are often used for their anticorrosive properties on steel and are dispersed in the epoxy medium. The addition of a second pigment (in both phases) is difficult but can be achieved when a silane coupling agent is used. Other compatibilizers or dispersive agents have a negative effect on the coating. It has been reported that pigments stay in their dispersion phase if there are well wetted by the respective binder in the solution in which they are dis-

persed. In particular systems, the migration of pigment toward the second medium can occur without affecting the stratification process.

- **Substrate:** The film-substrate interface is of primary importance for the self-layering phenomena as its characteristics will partly allow the vertical phase separation. Steel, plastics, glass and aluminum are the main substrates which have been studied up to now.
- **Curing conditions:** Curing conditions depend on the system studied. Coatings can be cured at ambient temperature or heated depending on the selected system. If a crosslinker is added, curing conditions have to be chosen in respect with the crosslinking reaction.

5. Challenges and future applications

The self-stratifying concept generates many advantages for polymer coatings. In terms of cost, it allows producing multilayer film structures by one-coat application, increasing the pot life of the coating, and reducing production costs and processing time. In terms of coating properties, it allows considerable enhancement of: (i) mechanical properties, partly by including a successful balance between hardness and flexibility and by eliminating internal stresses, (ii) permeability reduction, (iii) adhesion and adhesion durability enhancement, thereby contributing to corrosion protection, (iv) chemical resistance and durability, weather and wear resistance, etc.

The reduction of diffusion mobility of low molecular species is also lowered by heterophase structures which can provide addi-

tional insulating properties to the coatings [62]. In particular, very high durability of epoxy/thermoplastic heterogeneous structures has been proven. This system has a unique composition and structure resulting from spontaneous phase separation, which promotes the effect of the thermoplastic resin compared to the brittle epoxy matrix. Due to these interesting properties, self-stratifying coatings have been developed and suggested for various applications, which are described in the next paragraph.

5.1. Self-Stratifying coatings for industrial applications

The ability to form and control heterophase coating structures allow developing some new commercial resins mixtures that are incompatible or partially compatible presenting with regular film forming process.

Various self-stratifying formulations have already been developed, such as for example:

- Smart coatings: adhesion properties can be improved particularly in the case of complex substrates such as silicones and polyolefins [1,63].
- Anti-fouling coatings: the heterophase approach allows creating porous permeable structures used for antifouling applications [1].
- Insulating coatings: dense “self-healing” polymer/polymer heterophase structures can be formed.
- Sustainable coatings: Baghdachi developed thermosetting polyurethane coating formulations for automotive applications [14].
- Cavitation-resistant/damping coatings for marine uses [19,64].
- Anti-corrosion and maintenance coatings [13,63,65].
- Heavy-duty anti-corrosion coatings for rusty substrates [1].
- Cationic electro-deposition processes [66].
- UV-cured wood finishes [67].
- Combined processes of metal pre-treatment and priming by chemideposition [68].
- Self-cleaning coatings [69].
- Self-lubricating and self-healing coatings.
- Adhesives technology.
- Waterborne coating [16].
- Wear-resistant coatings [70].
- Surface rich antimicrobial coating, highly effective hydrophobic/oleophobic coatings [14].

The self-stratifying coatings can generally be used in coil coating, printing inks, lining, laminates, wall-papers, polymeric films and membranes. They remain outside conventional coating technology (based on the use of compatible polymers and oligomers), but some of them are able to provide coatings with valuable properties. Their stratification to the top or bottom coating interfaces could bring improved adhesion, or instead, anti-adhesion properties, as well as wear, block and chemical resistance, better weather stability and reduced price, especially when one-coat application coatings are used instead of multicoated systems.

5.2. Future potential applications for developing self-stratifying coatings

Further studies on self-stratifying coatings could find new applications in particular for:

- Coil-coatings (solvent-based, water-based and organosolv types),
- High-solid or solvent-free coating.
- Surface-functional direct-to-metal coatings (release, anti-mar ...).
- Baking/Storing enamels,

- Automotive base coat/clear coat combinations [18].
- Gloss paint with high pigment volume concentration in the base layer,
- Pigments-free opaque polymer coatings,
- Fire retardant and intumescent coatings,
- Bio-based sustainable coatings.

This technology may be transferred to other areas using solvent-borne liquid systems, like adhesives where two dissimilar materials are to be bonded together. Similarly, printing inks could be a good candidate since different interfaces are required to have different characteristics at the top and bottom surface [10].

6. Conclusion

There is not a significant number of publications concerning self-stratifying coatings.

A large range of resins, solvents and substrates have been tested, and in many cases a blend of a thermoplastic and a thermosetting resin, including a third component, shows the highest stratification level. The use of solvent-based self-stratifying coatings is limited for general application fields because of the important use of volatile organic solvents, and since a precise control of the composition and of the application conditions is needed. When these limitations are not critical, advantages of stratification are exploited in automotive and decorative coatings, anticorrosive paints, coil-coating technology, antimicrobial coatings, wear-resistant coatings, marine paints, heavy-duty coatings, etc.

Heterophase polymer-polymer structures generate the following advantages for coatings:

- Improved mechanical properties including a successful balance between hardness and flexibility.
- Elimination of internal stresses that may occur during the film formation process as well as during the coating pot life.
- Reduced permeability.
- Improvement in adhesion durability (thereby contributing to corrosion protection).
- Upgrading of chemical and light durability.
- Upgrading of weather resistance, wear resistance, surface slip, etc [21].
- Selective penetration into porous substrates.

Actually, only a few scenarios have been extensively studied. A wide range of conditions, as seen in this review, can impact the stratification of a coating and can lead to a high level of properties.

Acknowledgements

The authors gratefully acknowledge the support of the french ANR (Agence Nationale de Recherche) for funding this work (ANR-14-CE27-0010) and the competitiveness cluster MATIKEM to support the project.

References

- [1] V.V. Verkholtantsev, M. Flavian, Epoxy thermoplastic heterophase and self-stratifying coatings. *Mod. Paint Coat.* 85 (1995) 100–106.
- [2] W. Funke, Preparation and properties of paint films with special morphological structure. *J. Oil Colour Chem. Assoc.* 59 (1976) 398–403.
- [3] C. Carr, S. Benjamin, D.J. Walbridge, Fluorinated resin in self-stratifying coatings. *Eur. Coat. J.* 4 (1995) 262–266.
- [4] H. Murase, W. Funke, XVth FATIPEC Congress, Netherland Association of Coatings Technologists, Congress Book 2, Amsterdam, 1980, pp. 387–409.
- [5] Kansal Paint Co., Ltd., UK Patent 1 570 540 (1980).
- [6] C. Carr, Multilayered paint films from single coat systems. *J. Oil Colour Chem. Assoc.* 10 (1990) 403–404.

- [7] V.V. Verkholtantsev, Coatings based on polymer/polymer composites, *J. Coat. Technol.* 64 (1992) 51–59.
- [8] A. Toussaint, Self-stratifying coatings for plastic substrates (Brite euram project RI 1B 0246 C(H)), *Prog. Org. Coat.* 28 (1996) 183–195.
- [9] D.J. Walbridge, Self-stratifying coatings—an overview of a European Community Research Project, *Prog. Org. Coat.* 28 (1996) 155–159.
- [10] S. Benjamin, C. Carr, D.J. Walbridge, Self-stratifying coatings for metallic substrates, *Prog. Org. Coat.* 28 (1996) 197–207.
- [11] H. Warson, XXI FATIPEC congress, *Pigm. Resin Technol.* 21 (1992) 7–10.
- [12] I. Nikiforow, J. Adams, A.M. König, A. Langhoff, K. Pohl, A. Turshatov, D. Johannsmann, Self-stratification during film formation from latex blends driven by differences in collective diffusivity, *Langmuir* 26 (2010) 13162–13167.
- [13] V.V. Verkholtantsev, Nonhomogeneous-in-layer coatings, *Prog. Org. Coat.* 13 (1985).
- [14] J. Baghdachi, H. Perez, P. Talapatcharenkit, B. Wang, Design and development of self-stratifying systems as sustainable coatings, *Prog. Org. Coat.* 78 (2015) 464–473.
- [15] R. Berkau, M. Gailberger, T. Gruber, K. Holdik, G. Meichsner, F. Mezger, Coating composition for forming self-layering or self-coating lacquer systems, US Patent 7186772 B2 (2007).
- [16] Waterborne organic silicon-acrylic acid self-stratifying coating, CN Patent 101724326B (2012).
- [17] L. Wu, J. Baghdachi, Self-stratifying polymers and coatings, in: L. Wu, J. Baghdachi (Eds.), *Functional Polymer Coatings—Principle, Methods and Applications*, John Wiley & Sons, Inc., Hoboken, New Jersey, USA, 2015, pp. 197–217.
- [18] V.V. Verkholtantsev, Self-stratifying coatings for industrial applications, *Pigm. Resin Technol.* 32 (2003) 300–306.
- [19] M.D. Soucek, Self-stratifying Corrosion Resistant Coatings, The University of Akron <https://www.uakron.edu/dotAsset/539e526ee-b531be-4073-8772-f3106b4507c4053.pdf>, [Accessed 22 December 2016].
- [20] E. Langer, S. Waškiewicz, H. Kuczyńska, G. Kamińska-Bach, Self-stratifying coatings based on Schiff base epoxy resins, *J. Coat. Technol. Res.* 11 (2014) 865–872.
- [21] V.V. Verkholtantsev, Heterophase and self stratifying polymer coating, *Prog. Org. Coat.* 26 (1995) 31–52.
- [22] V.V. Verkholtantsev, M. Flavian, Polymer structure and properties of heterophase and self-stratifying coatings, *Prog. Org. Coat.* 29 (1996) 239–246.
- [23] A. Beaugendre, S. Degoutin, S. Bellayer, C. Pierlot, S. Duquesne, M. Casetta, M. Jimenez, Self-stratifying epoxy/silicone coatings, *Prog. Org. Coat.* 103 (2017) 101–110.
- [24] E. Langer, H. Kuczyńska, E. Kamińska-Tarnawska, J. Łukaszczyk, Self-stratifying coatings containing barrier and active anticorrosive pigments, *Prog. Org. Coat.* 71 (2011) 162–166.
- [25] A. Asarawala, P. Mackulin, R. Krafcik, D. Klimovich, Self-stratifying Coating—The Next Generation of Performance, SSPC: The Society for Protective Coatings, 2011, pp. 1–9.
- [26] W.D. Harkins, A. Feldman, Films. The spreading of liquids and the spreading coefficient, *J. Am. Chem. Soc.* 44 (1922) 2665–2685.
- [27] E. Alyamac, H. Gu, M.D. Soucek, Interface-driven phase-separated coatings, *J. Coat. Technol. Res.* 11 (2014) 665–683.
- [28] A. Abbasian, S.R. Ghaffarian, N. Mohammadi, Investigation of factors affecting stratification phenomenon in epoxy acrylic coatings, *Iran. Polym. J.* 13 (2004) 61–68.
- [29] P. Vink, T.L. Bots, Formulation parameters influencing self-stratification of coatings, *Prog. Org. Coat.* 28 (1996) 173–181.
- [30] I. Hopkinson, M. Myatt, Phase separation in ternary polymer solutions induced by solvent loss, *Macromolecules* 35 (2002) 5153–5160.
- [31] E. Langer, H. Kuczyńska, E. Kamińska-Tarnawska, J. Łukaszczyk, G. Kamińska-Bach, Changes of solubility parameters during evaporation of solvents as a factor influencing the self-stratification of epoxy/acrylic systems, *Prog. Org. Coat.* 66 (2009) 228–234.
- [32] P. Mokarian-Tabari, M. Geoghegan, J.R. Howse, S.Y. Heriot, R.L. Thompson, R.A.L. Jones, Quantitative evaluation of evaporation rate during spin-coating of polymer blend films: control of film structure through defined-atmosphere solvent-casting, *Eur. Phys. J. E* 33 (2010) 283–289.
- [33] J. Baghdachi, Functional coatings: coatings go to work, *Eur. Coat. J.* (2016) 24–28.
- [34] J. Hildebrand, R.L. Scott, *Regular Solutions*, Prentice-Hall Inc., Englewood Cliffs, NJ, USA, 1962.
- [35] J. Hildebrand, R.L. Scott, *The Solubility of Nonelectrolytes*, 3rd ed., Reinhold, New York, USA, 1950.
- [36] J. Burke, *Solubility Parameters: Theory and Application*, vol. 3, The Book and Paper Group ANNUAL, Austin, Texas, 1984.
- [37] C.M. Hansen, *Hansen Solubility Parameters, A User's Handbook*, 2nd ed., CRC Press, 2007, pp. 1–26.
- [38] C.M. Hansen, *The Three Dimensional Solubility Parameter and Solvent Diffusion Coefficient*, Danish Technical Press, Copenhagen, 1967.
- [39] C.M. Hansen, *Solubility in the coatings industry*, Skand. Tidsskr. Faerg. Lack 17 (1971).
- [40] I. Prigogine, *The Molecular Theory of Solutions*, North-Holland Publishing Co., Amsterdam, 1957.
- [41] C. Carr, E. Wallstöm, Theoretical aspects of self-stratification, *Prog. Org. Coat.* 28 (1996) 161–171.
- [42] H. Kuczyńska, E. Langer, E. Kamińska-Tarnawska, D. Kulikov, E. Indekin, Study of self-stratifying compositions, *J. Coat. Technol. Res.* 6 (2009) 345–352.
- [43] S. Liang, N.M. Neisius, S. Gaan, Recent developments in flame retardant polymeric coatings, *Prog. Org. Coat.* 76 (2013) 1642–1665.
- [44] S. Wu, Polar and nonpolar interactions in adhesion, *J. Adhes.* 5 (1973) 39–55.
- [45] O. Olabisi, L.M. Robeson, M.T. Shaw, *Polymer-polymer Miscibility*, Academic Press, London, 1979.
- [46] V.V. Verkholtantsev, Self-stratifying coatings, *Eur. Coat. J.* (2000) 24.
- [47] N.F. Bunkin, A.V. Lobeyev, Light-induced phase transitions in stratifying liquid mixtures, *Coll. Surf. A: Physicochem. Eng. Asp.* 129–130 (1997) 33–43.
- [48] V.V. Verkholtantsev, Exploiting self-stratification, *Eur. Coat. J.* (2005) 20.
- [49] P. Murias, H. Maciejewski, H. Galina, Epoxy resins modified with reactive low molecular weight siloxanes, *Eur. Polym. J.* 48 (2012) 769–773.
- [50] M. Rakotomalala, S. Wagner, M. Döring, Recent developments in halogen free flame retardants for epoxy resins for electrical and electronic applications, *Materials* 3 (2010) 4300–4327.
- [51] A. Toldy, P. Anna, I. Csontos, A. Szabó, G. Marosi, Intrinsically flame retardant epoxy resin—Fire performance and background—Part I, *Polym. Degrad. Stab.* 92 (2007) 2223–2230.
- [52] E. Alyamac [online], Self-stratifying coatings, The Graduate Faculty of The University of Akron, In Partial Fulfillment of the Requirements of the Degree Master of Science (2009), pp. 1–267.
- [53] M.D. Soucek, Multi-phase self-stratifying coating exhibiting gradient behavior, US Patent 8691342 B2 (2014).
- [54] M.D. Soucek, C.G. Templeman, M. Ishii, Self-stratifying coating, Toyota Motor Engineering & Manufacturing North America, Inc., Toyota Motor Corporation, University of Akron, North America, US Patent 8492001 B2 (2013).
- [55] J. Baghdachi, H.R.P. Hernandez, C.G. Templeman, Self-stratifying automotive topcoat compositions and processes, Toyota Motor Engineering & Manufacturing North America, Inc., US Patent 7863375 B2 (2011).
- [56] J. Baghdachi, H.R.P. Hernandez, C.G. Templeman, H. He, Methods and compositions for pigmented self-stratifying coatings, Toyota Motor Engineering & Manufacturing North America, Inc., Eastern Michigan University, US Patent 8044140B2 (2011).
- [57] M.B. Yagci, S. Bolca, J.P.A. Heuts, W. Ming, G. de With, Antimicrobial polyurethane coatings based on ionic liquid quaternary ammonium compounds, *Prog. Org. Coat.* 72 (2011) 343–347.
- [58] M.W. Urban, Why organic coatings stratify, *Eur. Coat. J.* 1–2 (2003) 36–38.
- [59] P.J. Mackulin, R.B. Krafcik, Hybrid latex particles for self-stratifying coatings, The Sherwin-Williams Company, US Patent 20140303281 A1 (2014).
- [60] BRITE Project RI 1B 0246 C(H) Technical Review of Research, TNO, Rep. TNO, Delft, Netherlands (1989), pp. 12.
- [61] V.V. Verkholtantsev, Coatings based on polymer/polymer composites, *Prog. Org. Coat.* 18 (1990) 43–77.
- [62] V. Verlag, Self-stratifying coatings, *Eur. Coat. J.* (2000) 24.
- [63] R. Bongiovanni, A. Vitale, Smart multiphase polymer coatings for the protection of materials, *Smart Composite Coatings and Membranes*, M.F. Montemor (Ed.), Woodhead Publishing series in Composites Science and Engineering, 2015, pp. 215–469.
- [64] Y.B. Shleomenzon, I.I. Morozova, V.P. Pavlova, S.B. Gordeeva, V.V. Verkholtantsev, *Lakokrasochnye Materiali Ikh Primen* 2 (1979) 8.
- [65] V.V. Krylova, I.I. Kainova, V.V. Verkholtantsev, *Lakokrasochnye Materiali Ikh Primen* 4 (1984) 32.
- [66] R.D. Khanolkar, Latest trends in electrodeposition paints, *Paint Ink Int.* (1995) 4–6.
- [67] R. Bongiovanni, F. Montefusco, A. Priola, N. Macchioni, S. Lazzeri, L. Sozzi, B. Ameduri, High performance UV-cured coatings for wood protection, *Prog. Org. Coat. Polym. Mater.* 45 (2002) 359–363.
- [68] V.V. Verkholtantsev, Coatings for active substrates: Part 2: chemically and energy-activated substrates, *Eur. Coat. J.* 9 (2002) 44–49.
- [69] R. Bongiovanni, V. Lombardi, A. Priola, C. Tonelli, A. Di Meo, Surface properties of acrylic coatings containing perfluoropolyether chains, *Surf. Coat. Int. B: Coat. Trans.* 86 (2003) 53–57.
- [70] L.S. Strelkatchinskaya and V.V. Verkholtantsev, Preparation and Properties of Coatings, NIITEIM, Moscow, 1982, pp. 29–31.

Appendix 2: Technical data sheets of the polymers of interest used in the thesis

Silicone RSN-0217 (Dow Corning)

Table 39. Technical data of Silicone RSN-0217

Property	Range	Unit	CTM ¹
Appearance	Flake resin, white		
Solids Content	99	%	0208
Tg	64 (147)	°C (°F)	0936
Hydroxyl content	6.0	%	0598
Melt Viscosity at 107°C (225 °F)	92,000	cP	0874
Melt Viscosity at 150°C (302 °F)	1410	cP	0874
Flash Point closed cup	138 (280)	°C (°F)	0090
Theoretical Residual Silicon Dioxide	47	%	
Degree of Substitution	1.0		
Solubility	Ketones, esters, chlorinated solvents, alcohols, aromatic hydrocarbons and solvent blends with a Kauri-butanol value > 50		

¹CTM: Corporate Test Method correspond to ASTM (American Society for Testing and Materials) standard tests in most instances

Lumiflon LF200 (60% in xylene, AGC Chemicals)

Table 40. Technical data of Lumiflon LF200

Property	Range	Unit
Appearance	Transparent	
Tg	35	°C
Hydroxyl value	52	mgKOH/g-polymer
Acid value	0	mgKOH/g-polymer
Solid content	60	%
Solvent	Xylene	
Specific gravity (at 25°C)	1.12	
Viscosity	20.10-4	m ² /s

Appendix 3: Investigation of the epoxy-amine reaction by spectroscopy

As described in the experimental part (chapter II), curing of epoxy resins with triamine can be described as a two-step process: firstly, an epoxy group reacts with a primary amine yielding to a secondary amine, which in the second step reacts with another epoxy group yielding a tertiary amine. Considering these chemical reactions, the process can be monitored through the evolution of concentration of epoxy groups and tertiary amines. The concentration of species is quantitatively related to the area of the absorption band only in the linear region, where Lambert Beer's law is satisfied. Taking this into account, changes in concentration of epoxy groups may be determined by measuring the area of the absorption bands at 3050 cm^{-1} , 1252 (Raman spectroscopy) or at 915 cm^{-1} (FTIR spectroscopy). Nevertheless, following curing by IR is not always easy, because the epoxy band at high wavenumbers shows low sensitivity to changes in concentration as a consequence of its intrinsic low intensity. This may induce some uncertainty at the final stages of reaction when the concentration of epoxy groups is small. For in-situ monitoring processes such as curing, the interpretation of FTIR and Raman spectra, and the assignment of bands have been widely used for characterization of organic compounds. Both qualitative and quantitative information can be obtained by this technique, although its use in epoxy systems is quite restricted because of the location and intensity of the oxirane ring absorptions.

Band attribution

Raman spectroscopy. Raman bands corresponding to epoxy vibration are in the range of 1230 and 1280 cm^{-1} (breathing of the epoxide ring).^{221, 222} The band at 915 cm^{-1} assigned to the epoxide ring deformation is much weaker. **FTIR spectroscopy.** Two characteristic absorptions of the oxirane ring are observed in the range between 4000 and 400 cm^{-1} . The first one at 915 cm^{-1} is attributed to the C-O deformation of the oxirane group, although some works done by Dannenberg²²³ showed that this band does not correspond exclusively to this deformation but also to some other unknown process. The second band is located at 3050 cm^{-1} and is attributed to the C-H tension of the methylene group of the epoxy ring. This band is not very useful since its intensity is low and it is also very close to the strong O-H absorptions; but in low polymerization degree of epoxy monomers it can be used as a qualitative indicative of the

presence of epoxy groups. The broad band at 3500 cm^{-1} is assigned to O-H stretching of hydroxyl groups, revealing the presence of dimers or high molecular weight species.²²⁴ The hydroxyl bands are sometimes useful for characterization although its quantitative use is very limited. Its position in the spectra also limit its use: the N-H stretching is very close to the strong absorption band, while the deformation band is located in the region where many signals corresponding to organic bonds appear, including the bonds of the solvent used for the dilution (m-xylene).

Raman spectroscopy

Raman spectra were collected from 30 to $100\text{ }^{\circ}\text{C}$ (temperature limit for the use of the spectrometer) every $10\text{ }^{\circ}\text{C}$. When observing the bands at 1252 cm^{-1} and 1230 cm^{-1} (Figure 84 a), they are decreasing while the temperature increases. The intensity of the band at 1230 cm^{-1} decreases mainly between 70 and $80\text{ }^{\circ}\text{C}$, between which a gap is noticeable. The intensity of a peak is proportional to the concentration of the substance in the sample analyzed, what can be interpreted as the consuming of the free epoxide groups during the vitrification of epoxy resin curing process. On the other hand, an apparent reducing of the Raman peak at 915 cm^{-1} is logged (Figure 84 b). Once again, a gap between 70 and $80\text{ }^{\circ}\text{C}$ is well noticeable. At lower temperature (below $80\text{ }^{\circ}\text{C}$), the band is discernable but its intensity does not follow any trend.

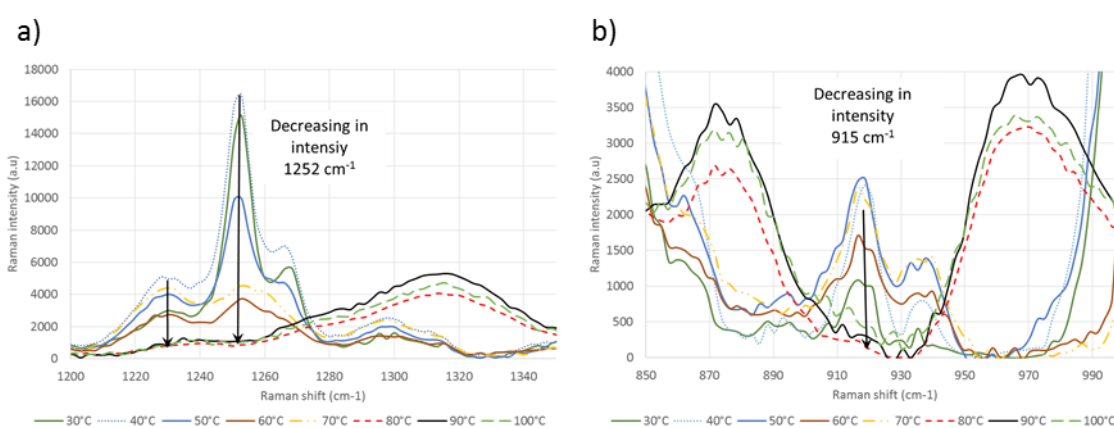


Figure 84. Raman spectra of the epoxy/amine system from 30 to $100\text{ }^{\circ}\text{C}$ at 473 nm

ATR-FTIR spectroscopy

Spectra were recorded using a heated plate every $10\text{ }^{\circ}\text{C}$ between 80 and $190\text{ }^{\circ}\text{C}$. The reference peak used as an internal standard for the normalization of epoxy peak absorbance is

phenylene at 830 cm^{-1} (γ_{CH} aromatics, Figure 85). The band characteristic of the epoxy function is well defined at 915 cm^{-1} . As the intensity from the spectra recorded between 30 and $80\text{ }^{\circ}\text{C}$ were similar, there are not presented in the figure for more clarity. The same phenomena were noted on the Raman spectra, which could significates that the curing reaction is not ongoing at such temperatures: crosslinking process would start around $80\text{ }^{\circ}\text{C}$.

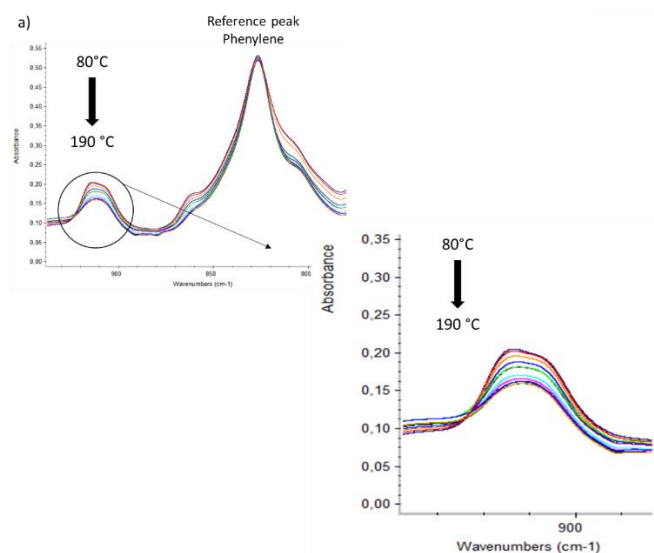


Figure 85. ATR-FTIR spectra of the system epoxy/amine from 80 to $190\text{ }^{\circ}\text{C}$. The direction of the arrow indicates the evolution of the band with increasing temperature

From the spectra, the intensity of the vibration band of the terminal epoxy group (915 cm^{-1}) decreases during the curing reaction up to $150\text{ }^{\circ}\text{C}$, and stabilized after then. The difference in intensity however is very low which makes the method not enough accurate to allow calculating a percentage of conversion. As the intensity is measured in live, the system has probably not enough time to properly crosslinked. Nevertheless, some conclusions can be drawn: from 40 to $80\text{ }^{\circ}\text{C}$, the formation of crosslinkage induced by the curing agent is not evidenced (overlapping of the spectra). From 80 to $150\text{ }^{\circ}\text{C}$, a decrease of the peak is observed, and up to $150\text{ }^{\circ}\text{C}$, a stabilization is logged meaning that the formation of the crosslinked network is almost completed. Accordingly, the onset temperature of the curing reaction is estimated at $80\text{ }^{\circ}\text{C}$, and the offset temperature around $150\text{ }^{\circ}\text{C}$. The method derived from the Beer's law that was based on the ratio of the height of the characteristic to reference absorbance peak was used, however the difference is not enough significant to obtain reliable results. In addition, integration of such peak could be sensitive to baseline bias.

Appendix 4 MLC curves of PC and coated PC with two self-stratifying composition at 35 kW/m²

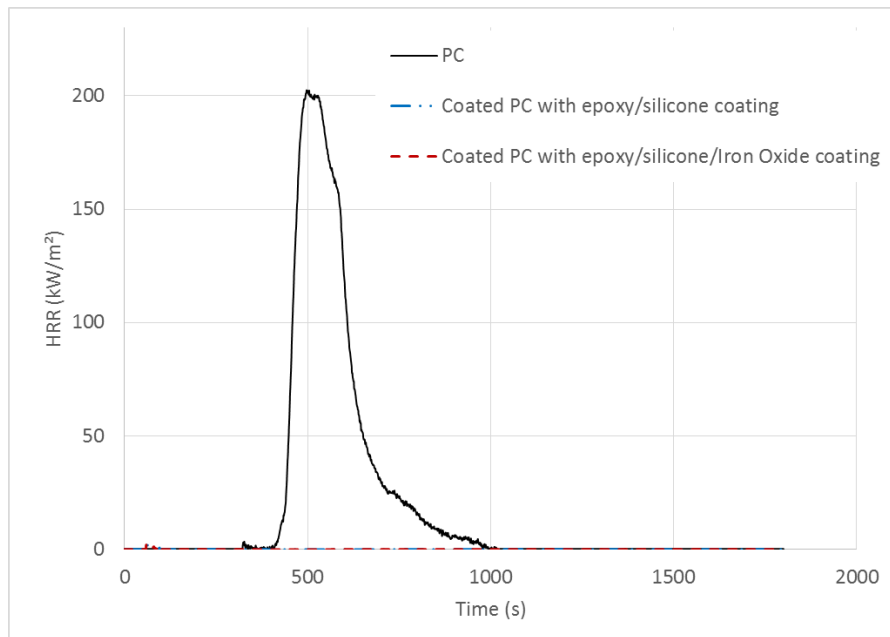


Figure 86. MLC curves of polycarbonate and coated PCs with the epoxy/silicone and epoxy/silicone/iron oxide system (35 kW/m², 35 mm)

Table 41. MLC values of virgin PC, epoxy/silicone and epoxy/silicone/iron oxide coated PC (35 kW/m², 35 mm)

	Virgin PC	Epoxy/Silicone coated PC	Epoxy/Silicone/IO coated PC
TTI (s)	319 ± 10	No ignition	No ignition
pHRR (kW/m ²)	202 ± 24	-	-
THR (MJ/m ²)	35 ± 1	-	-
TFO (s)	1070 ± 110	-	-

Appendix 5: Hansen Solubility Sphere data

Table 42. Coordinates of the junction between the Hansen sphere of the epoxy resin and the silicone and fluoropolymer spheres, their C and overlap factor when diluted at 10 wt.%

Target polymer : Epoxy resin DGEBA	D _j	P _j	H _j	C (MPa ^{3/2})	Overlap factor (%)
Silicone S217	17.9	17.6	3.9	17778	112
Lumiflon LF200	18.8	11.3	7.8	4361	36

Table 43. Coordinates of the junction between the Hansen sphere of the epoxy resin and the silicone and fluoropolymer, their C and overlap factor when diluted at 30 wt.% after 7 days

Target polymer : Epoxy resin DGEBA	D _j	P _j	H _j	C (MPa ^{3/2})	Overlap factor (%)
Silicone S217	19.4	11.1	8.5	4865	116
Lumiflon LF200	16.9	8.9	8	4569	63

Table 44. Coordinates of the junction between the Hansen sphere of the silicone resin and the fluoropolymer spheres, their C and overlap factor when diluted at 10 wt.%

Target polymer : Silicone S217	D _j	P _j	H _j	C (MPa ^{3/2})	Overlap factor (%)
Lumiflon LF200	18.6	9.9	9.5	3802	37

Appendix 6: Choice of resins: Screening based on Hansen Solubility Spheres

The following results gathers the experiments carried out with additional three resin: Acrylic BR106 (*Dianal America, INC.*) and B875 (*IMCD*), and silicone 3055 from *Dow Corning*. The silicone 217 resin was also used as a thermosetting system in combination with a particular resin modifier (7081 resin modifier provided by *Dow Corning*). Similarly, the Silicone 3055 was crosslinked with a large excess of methyltrimethoxysilane (MTM) and a titanium (Ti) catalyst.

Table 45. Hansen Solubility Parameters of the selected resins diluted at 10 wt.%

Resins	δ_d (J.cm ⁻³) ^{1/2}	δ_p (J.cm ⁻³) ^{1/2}	δ_h (J.cm ⁻³) ^{1/2}	δ_{tot} (J.cm ⁻³) ^{1/2}	Radius (MPa ^{1/2})
Acrylic BR106	18.9	6.9	6.9	21.3	10.0
Silicone 3055	22.9	5.5	10.7	25.8	18.2
Acrylic B875	21.0	2.8	10.4	23.6	13.9

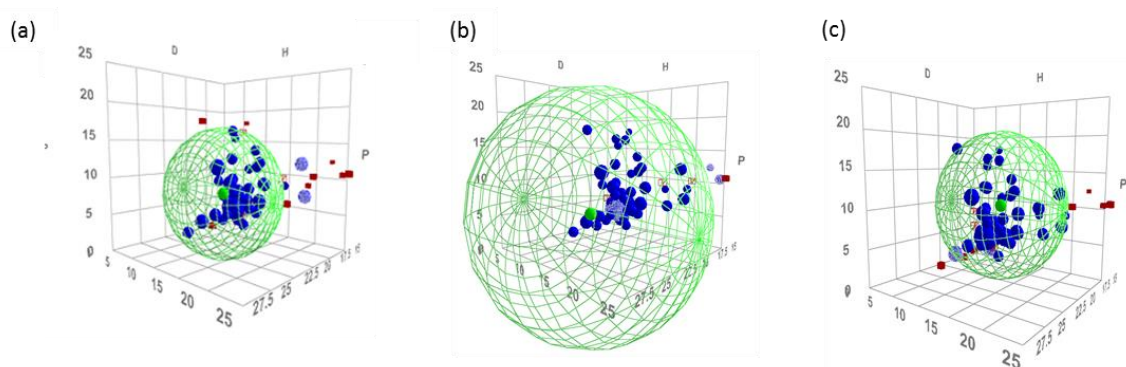


Figure 87. Hansen solubility spheres of (a) acrylic BR106, (b) Silicone 3055 and (c) Acrylic B875 diluted at 10 wt.%

Table 46. Overlap factors between the epoxy DGEBA, Silicone 3055 and 217 and various thermoplastic resins when diluted at 10 wt.%, after 7 days

Target polymer : Epoxy resin DGEBA	V(DGEBA)*/V(X)**	Overlap factor (%)
Acrylic BR106	13 %/ 85 %	94
Silicone 3055	29 %/ 35 %	44
Neocryl B875	14 %/ 39 %	44
Target polymer : Silicone 3055	V(DGEBA)*/V(X)**	Overlap factor (%)
Acrylic BR106	17 %/ 99 %	>100
Neocryl B875	44 %/ 100 %	>100
Lumiflon LF200	38 %/ 93 %	>100
Target polymer : Silicone S217	V(DGEBA)*/V(X)**	Overlap factor (%)
Acrylic BR106	23 %/ 80 %	82

*V(DGEBA) = percentage (by volume) of the crosslinkable resin solubility sphere that is occupied by the sphere of other polymer, **V(X) = percentage (by volume) of the second polymer solubility sphere that is occupied by the crosslinkable resin solubility sphere.

Appendix 7: Interfacial energy data for the prediction of stratification based on the surface energy model

Table 47. Interfacial energy between the epoxy, silicone or fluoropolymer resin on PC

Resin systems		γ_{12} (mN.m ⁻¹)	γ_{s1} (mN.m ⁻¹)	γ_{s2} (mN.m ⁻¹)
Pure resins	Epoxide/ Fluoropolymer	4.13	1.45	8.12
	Epoxide/ Silicone	5.06	1.45	7.88
Xylene	Epoxide/ Fluoropolymer	8.15	11.29	2.23
	Epoxide/ Silicone	9.70	11.29	0.92
BuAc: xylene (1:1)	Epoxide/ Fluoropolymer	0.16	1.81	1.80
	Epoxide/ Silicone	1.60	1.81	3.24
MIBK: xylene (1:1)	Epoxide/ Fluoropolymer	17.19	20.06	0.95
	Epoxide/ Silicone	16.90	20.06	0.95
MIBK: xylene: 1- methoxy-2- propanol (5: 3: 2)	Epoxide/ Fluoropolymer	0.30	1.69	1.82
	Epoxide/ Silicone	0.18	1.69	0.91

Appendix 8: Influence of the level of pigment and percentage of resin solid in the epoxy/silicone self-stratified system

Influence of the level of pigment

The self-stratification of epoxy/silicone films containing Fe_2O_3 or CaCO_3 introduced at different level (2.5, 5 and 10 %PVC) were designed and characterized. The fillers were initially dispersed in the epoxy phase. The appearance of the coatings, their adhesion on PC, their thickness, stratification pattern and the location of the filler in the solid film are detailed in Table 48.

Table 48. Pigments location, appearance of the coating, adhesion rating and stratification pattern resulted from the epoxy/silicone coatings filled with Fe_2O_3 and CaCO_3 at 2.5, 5 and 10 %PVC

Additive	PVC (%) ¹	Filler location after film formation	Appearance of the coating	Thickness (μm)	Cross hatch testing	Stratification pattern
No filler	0	-	Slightly rough. glossy	55	5B	I
Fe_2O_3	2.5	Silicone layer	Smooth. good pigments dispersion	32	5B	I
	5			42	5B	I
	10			30	4B	I
CaCO_3	2.5	Interface epoxy/silicone & silicone layer	Rough. good pigments dispersion	32	5B	I
	5	In both phases		45	4B	I
	10	Silicone layer		55	4B	I

¹ PVC = Pigment Volume Concentration

When the formulation contains Fe_2O_3 , stratified films with nice visual appearance were obtained in all the cases, whatever the amount of filler introduced. At the highest %PVC, adhesion begins to be slightly constrained: 4B rating is obtained, compared to 5B with 2.5 and 5 %PVC. In all cases, iron oxide migrates in the silicone layer during curing, as observed in the Figure 88 a. With CaCO_3 , it was less easy to thoroughly disperse the filler in the epoxy resin and to properly adjust the parameters of the spray gun so that to obtain a nice coating. If the time of grinding is too short, settling is well noticeable even before the mixing with the second resin. However, after these adjustments, coatings with a nice visual appearance and with type

I stratification patterns were obtained in all the cases. Adhesion is slightly reduced with 5 and 10 %PVC: a 4B rating is obtained compared to 5B with a lower amount of fillers. The distribution of calcium carbonate through the thickness after the formation of the film does not however follow any rational according to the amount of fillers incorporated: depending on the PVC, this filler can be present at the interface of both layers (2.5 %PVC), in both phases (5 %PVC) or in the silicone layer only (10 %PVC) (Figure 88 b).

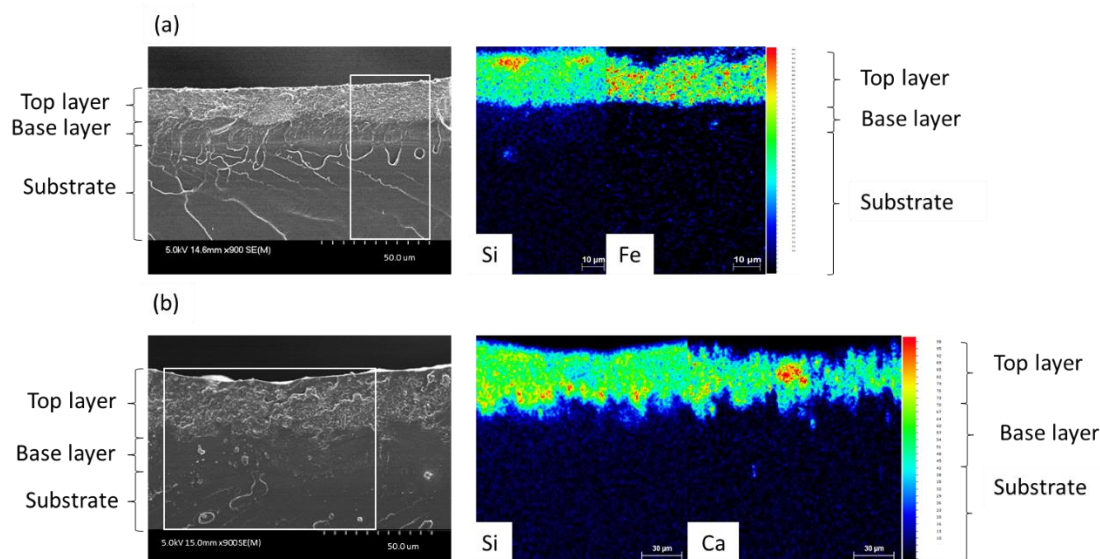


Figure 88. EDX X-ray mappings of a) Silicon and iron and b) Silicon and Calcium on cross-sections of an epoxy/silicone coating filled with 10 %PVC of a) iron oxide and b) calcium carbonate

To conclude, iron oxide and calcium carbonate do not affect the layering when incorporated up to 10 %PVC: they mostly migrate, with a concentration gradient more or less pronounced to the air interface with the silicone resin. The distribution of CaCO_3 through the thickness is more contrasted however it does not impact the quality of the layering: fillers are not well wetted by the resins but this does not modify the equilibrium between the two phases.

Effect of the percentage of solid of the resins

Type I stratification pattern was observed from percentage solid comprises between 30 and 50 wt.%, and for film thicknesses inferior to 130 μm (Figure 89). Some inhomogeneity are discernable between the thickness of the epoxy and silicone phase in some area of the film

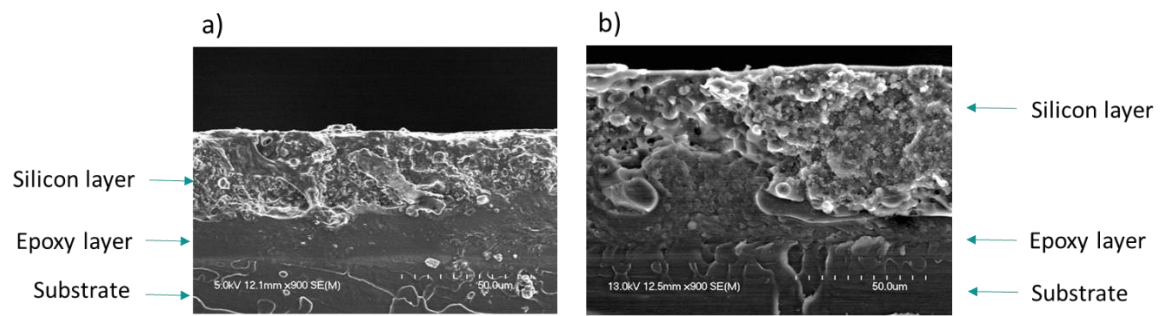


Figure 89. SEM images of epoxy/silicone self-layered system at a) 40 wt.% and b) 50 wt.% of resins sprayed on PC

Appendix 9: MLR curves of PC, and coated PC with iron oxide particle or not

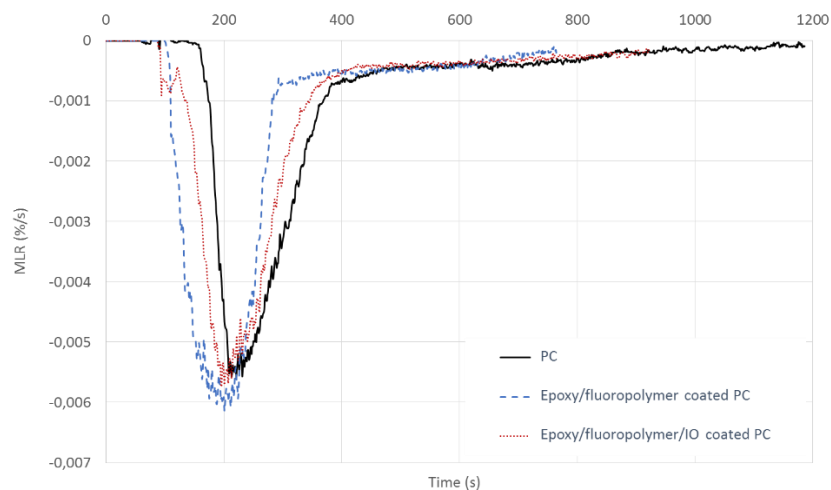


Figure 90. MLR curves of PC, and coated PC with and without IO particles

Table 49. MLC data obtained for PC, and coated PC with unfilled and filled formulations

	PC	Coated PC (no Fe ₂ O ₃)	Coated PC (with Fe ₂ O ₃)
TTI (s)	92 ± 6	26 ± 2	20 ± 3
pHRR (kW/m²)	231 ± 6	250 ± 2 (+8 %) ¹	191 ± 23 (-17 %)
THR (MJ/m²)	52 ± 1	46 ± 3 (-12 %)	29 ± 4 (-44 %)
TFO (s)	1077 ± 47	735 ± 30	735 ± 67
SMLR (g/m².s)	3.1 ± 0.1	4.8 ± 0.3	4.1 ± 0.1

¹Percentage are calculated according the difference with the virgin PC

Résumé

L'objectif de ce travail de thèse consiste à élaborer des revêtements auto-stratifiants pour ignifuger du polycarbonate (PC). La nouveauté réside dans le développement de procédés répondant intelligemment aux enjeux écologiques et économiques actuels. Deux revêtements à base d'une résine thermodurcissable (époxyde) et thermoplastique (silicone ou fluoropolymère) ont été développés. Une stratification parfaite a été mise en évidence par différentes techniques d'analyses, pour des épaisseurs de film allant jusqu'à 130 µm. L'influence du solvant, de l'agent durcisseur, des conditions de séchage, des additifs et de leur phase d'incorporation a été étudiée. Finalement, un système dilué dans un mélange acétate de butyle : xylène (1:1) offre les meilleures propriétés (stratification, adhésion, aspect esthétique), avec la résine thermoplastique constituant la partie supérieure du film. De plus, il a été démontré que la vitesse d'évaporation du solvant influence très fortement le degré de stratification, et que l'ajout d'additifs (oxyde de fer, carbonate de calcium et deux agents phosphorés) jusqu'à 10% en masse n'influence pas la stratification. Leur dispersion peut cependant être affectée par leur phase d'incorporation et par le solvant. L'oxyde de fer introduit à 10% s'est révélé être le meilleur candidat, conservant les propriétés du film (aspect, adhésion, gloss) et améliorant sa tenue au feu et au vieillissement (température, UV et humidité). Il en découle une réduction de l'inflammabilité du PC revêtu, de la propagation de flammes et de l'apparition de gouttes enflammées lorsque le système est soumis à une flamme. La formation d'une couche protectrice limitant les transferts de masse entre le substrat et la flamme a ainsi été valorisée. Une modification de la structure du réseau de silice formé dû à l'ajout des particules de fer apparaît comme le scénario le plus vraisemblable, permettant ainsi l'amélioration de l'effet barrière. La carbonisation du système n'est cependant pas favorisée, bien qu'il soit très probable que les propriétés mécaniques de la couche protectrice soient augmentées. Au contraire, bien que l'oxyde de fer catalyse la dégradation de la résine fluorée, la carbonisation augmente légèrement. Finalement, une bonne résistance au vieillissement des deux systèmes a été évaluée tant en termes de propriétés feu que d'adhésion et d'aspect esthétique.

Mots clés : revêtement auto-stratifiants, séparation de phase, incompatibilité, époxyde, silicone, fluoropolymère, oxyde de fer, résistance au feu, vieillissement accéléré

Abstract

This PhD work is a proof of concept on the design of flame retardant (FR) self-stratifying coatings for polycarbonate (PC). This "one pot" process allows an eco- and smart-development of new products while reducing cost, processing time and solvent emission. In this work, two original self-layering coatings based on epoxy/silicone and epoxy/fluoropolymer blends were developed. Their perfect stratification on PC was evidenced using different techniques, in a thickness range up to 130 µm. The influence of solvents characteristics, hardener, curing conditions, fillers and their incorporation phase was studied. Finally, the system diluted in butylacetate: xylene (at a 1:1 ratio) leads to the best layering and adhesion, with the thermoplastic phase (silicone or fluoropolymer) located on the top of the film. The solvent evaporation rate strongly influences the stratification, and the fillers tested (iron oxide, calcium carbonate and two phosphorus based additives) do not affect the layering when introduced up to 10 wt.%. However, visual appearance and adhesion are strongly dependent on the phase in which the fillers are dispersed and on the solvent used. The best improvements in terms of FR properties, adhesion, visual appearance and weatherability (temperature, UV and humidity) were obtained by incorporating micrometric Fe₂O₃ particles: it allows the formation of a protective barrier which limits substrate/flame mass transfers, and prevents from the yellowing of the system under UV rays. It therefore results a delay in the ignition, the inhibition of the flame spread and dripping when submitted to a flame, and a drastic reduction of the combustibility of the two coatings. When added to the silicone-based system, a modification of the structure of the silica network formed by the particles which enhances the barrier effect of the silicone-based layer would be the most probable assumption. The formation of additional carbonaceous char is not promoted by the iron oxide, although it is very likely that additional mechanical properties are brought to the system, which consequently strengthened the barrier layer formed. Although the particles catalyzes the thermal degradation of the fluorinated resin, the coating slightly promotes the formation of a carbonaceous char. Finally, the FR properties, adhesion and visual appearance are relatively maintained after 8 weeks of ageing.

Key words: Self-stratifying coating, Phase separation, Incompatibility, epoxy, silicone, fluoropolymer, iron oxide, flame retardancy, thermal degradation, ageing resistance